Winter 1986

Tidal Circulation in Chesapeake Bay

Carl W. Fisher
Old Dominion University

TIDAL CIRCULATION IN CHESAPEAKE BAY

by

Carl W. Fisher
B.S. June 1965, State University of New York
M.S. September 1969, Oregon State University

A Dissertation Submitted to the Faculty of
Old Dominion University in Partial Fulfillment of the
Requirements for the Degree of

DOCTOR OF PHILOSOPHY

OCEANOGRAPHY

OLD DOMINION UNIVERSITY
December, 1986

Approved by:

Ronald E. Johnson (Chairman)

ABSTRACT

TIDAL CIRCULATION OF CHESAPEAKE BAY

Carl W. Fisher
Old Dominion University, 1986
Director: Dr. Ronald E. Johnson

This study is a comprehensive examination of the tidal circulation of Chesapeake Bay and its major tributaries. Tide and current data, which were observed in Chesapeake Bay by the National Ocean Service during the period from 1972 to 1983, are analyzed and used to construct charts that describe the tide and tidal current. Frictionally damped analytic models are used to: explain the tidal hydrodynamics of the observed tides, determine the location of the quasinodes and antinodes of the M_2 and K_1 tidal waves, explain the relationship of the tides and tidal currents, and determine if the tide in lower Chesapeake Bay is a Kelvin wave with an amphidromic pattern of cotidal lines. The amplification of constituents as the tide circulates throughout the bay and tributaries is also described and explained.

Tide data from 108 locations throughout the bay and major tributaries, and current meter data from 124 locations in the bay have been analyzed using nonharmonic and harmonic analysis techniques. Cotidal and corange charts have been constructed based on the results of the nonharmonic analysis. Comparable coamplitude and cophase charts for the M_2 and K_1 tidal constituents have been constructed using the harmonic constants determined during this study. Similarly, the

harmonic constants for the M_2 tidal current constituent are used to construct cophase and cospeed charts which serve as an approximate description of the tidal current at Maximum Flood.

A one dimensional analytic model of a frictionally damped reflected tidal wave is used to determine whether reflection actually occurs in each basin, where it occurs, and how much the tide is attenuated. Frictional damping coefficients ranging from 2.1 to 3.0 have been determined for the major tributaries and upper bay. It is shown that the tide in the lower bay cannot be modeled properly using a one dimensional analytic model because of its width. A two dimensional analytic model of a reflected Kelvin wave is considered. This model, as well as the charts constructed during this study, indicates the tidal circulation in the lower bay may be an amphidromic system with a virtual amphidrome located onshore to the west of the bay.

The amplification of shallow water constituents is observed to be fairly large near the limit of tide in the major tributaries, but is relatively insignificant elsewhere. This amplification has been shown to be caused by the nonlinear effect of friction on the tide.

ACKNOWLEDGMENTS

I wish to express my gratitude to the many people who provided guidance and assistance throughout the course of this study. My dissertation director and advisor, Dr. Ronald Johnson encouraged me to continue advanced studies in tides and currents, and kept me "on target" for completion of the Ph.D. program.

I am indebted to a number of personnel in the National Ocean Service for their assistance and support, and particularly want to recognize Dr. Bruce Parker, Steacy Hicks and William (Sonny) Richardson for their guidance and criticism. I also want to thank David Browne, Leonard Hickman, and Gary Soneira for their assistance. In addition, I thank all the NOAA personnel and ODU students who helped me maintain the current meter station in Chesapeake Bay Entrance for two years. I offer a special thanks to the officers and crew of the NOAA ship FERREL who conducted the tide and current survey of Chesapeake Bay. The outstanding quality of the tide gauge and current meter data made this study possible.

Finally, I want to express my appreciation to the National Ocean Service managers and supervisors who sponsored this research and provided me the opportunity to continue work on this dissertation during assignments after I had attended Old Dominion University.

TABLE OF CONTENTS

TABLE OF CONTENTS (CONTINUED)

LIST OF TABLES

LIST OF FIGURES

LIST OF FIGURES (CONTINUED)

LIST OF FIGURES (CONTINUED)

FIGURE PAGE

LIST OF FIGURES (CONTINUED)

FIGURE PAGE

LIST OF SYMBOLS

a_o = Amplitude of a tidal constituent at $x = 0$.

a_n = Speed of a tidal constituent; the rate of change in phase of a constituent, usually expressed in degrees per hour.

A_i, B_i = Component speeds of the tidal current, referenced to Cartesian coordinates ($i = 1,2$).

b = Width of canal or basin.

C = Wave celerity or phase speed.

C_o = Frictionless wave celerity or phase speed.

f = Coriolis parameter.

f_n = Node factor of a particular tidal constituent.

F = Form number.

g = Acceleration of gravity.

h = Mean water depth.

h_{CR} = Critical depth.

H_o = Mean value of tide observations; corresponds to height of mean sea level above adopted datum.

H_n = Mean amplitude (height) of a particular tidal constituent.

J_1 = Smaller lunar elliptic diurnal constituent which, with M_1, modulates the amplitude of the declinational K_1 for the effect of the Moon's elliptical orbit.

k = Wave number.

k_o = Frictionless wave number.

K_1 = Lunisolar diurnal constituent which, with O_1, expresses the effect of the Moon's declination. They account for diurnal inequality and, at extremes, diurnal tides.

K_2 = Lunisolar semidiurnal constituent which modulates the amplitude and frequency of M_2 and S_2 for the declinational effect of the Moon and Sun, respectively.

ℓ = Length of canal or basin.

L = Wavelength.

L_o = Frictionless wavelength.

L_2 = Smaller lunar elliptic semidiurnal constituent which, with N_2, modulates the amplitude and frequency of M_2 for the effect of variation in the Moon's orbital speed due to its elliptical orbit.

M_1 = Smaller lunar elliptic diurnal constituent which, with J_1, modulates the amplitude of the declinational K_1 for the effect of the Moon's elliptical orbit. A slightly slower constituent designated (M_1), with Q_1, modulates the amplitude and frequency of the declinational O_1 for the same effect.

M_2 = Principal lunar semidiurnal constituent which represents the rotation of the Earth with respect to the Moon.

M_3 = Lunar terdiurnal compound constituent caused by the interaction of (M_1) and M_2 in shallow water.

M_4, M_6, M_8 = Shallow water overtides (harmonics) of M_2.

Mf = Lunar fortnightly constituent which expresses the effect of departure from a sinusoidal declinational motion.

MK_3 = Terdiurnal compound constituent caused by the interaction of M_2 and K_1 in shallow water.

Mm = Lunar monthly constituent which expresses the effect of irregularities in the Moon's rate of change of distance and speed in orbit.

MN_4 = Quarterdiurnal compound constituent caused by the interaction of M_2 and N_2 in shallow water.

MS_4 = Quarterdiurnal compound constituent caused by the interaction of M_2 and S_2 in shallow water.

MSf = Lunisolar synodic fortnightly constituent.

N = Linearized frictional resistance coefficient.

N_2 = Larger lunar elliptic semidiurnal constituent (see L_1).

O_1 = Lunar diurnal constituent (see K_1).

OO_1 = Lunar diurnal (second order) constituent.

P_1 = Solar diurnal constituent (see K_1).

Q_1 = Larger lunar elliptic diurnal constituent (see M_1).

R = Rossby Radius of Deformation.

R_2 = Smaller solar elliptic constituent which, with T_2, modulates the amplitude and frequency of S_2 for the effect of variation in the Earth's orbital speed due to its elliptical orbit.

S_n = Exponential coefficient which describes a Poincare wave of mode n.

S_1 = Solar diurnal constituent.

S_2 = Principal solar semidiurnal constituent which represents the rotation of the Earth with respect to the Sun.

S_4, S_6 = Shallow water overtides (harmonics) of S_2.

Sa = Solar annual constituent which, with Ssa, accounts for the nonuniform changes in the Sun's declination and distance. In actuality, they mostly represent yearly meteorological variations influencing sea level.

Ssa = Solar semiannual constituent (see Sa).

t = Time.

T = Wave period; period of tidal constituent.

T_2 = Larger solar elliptic constituent (see R_2).

u, v = Current velocity referenced to Cartesian coordinates (u in the +x direction and v in the +y direction).

u_i = Current velocity of the incident wave (oriented to the x axis).

u_m = Maximum velocity of flood current (oriented to the x axis).

u_r = Current velocity of the reflected wave (oriented to the x axis).

$(V_o+u)_n$ = Argument of a particular tidal constituent at $t = 0$.

w_1 = Maximum speed of an ellipse for a particular tidal current constituent.

w_2 = Minimum speed of an ellipse for a particular tidal current constituent.

x, y = Horizontal Cartesian coordinates.

$2MK_3$ = Terdiurnal compound constituent caused by the interaction of M_2 and K_1 in shallow water.

$2MN_2$ = Semidiurnal compound constituent caused by the interaction of M_2 and N_2 in shallow water.

$2MS_2$ = Semidiurnal compound constituent caused by the interaction of M_2 and S_2 in shallow water.

$2N_2$ = Lunar elliptic semidiurnal (second order) constituent.

$2NM_2$ = Semidiurnal compound constituent caused by the interaction of N_2 and M_2 in shallow water.

$2Q_1$ = Lunar elliptic diurnal (second order) constituent.

$2SM_2$ = Semidiurnal compound constituent caused by the interaction of S_2 and M_2 in shallow water.

α = Phase difference between time of maximum tidal elevation and time of maximum flood tidal current.

η = Tidal elevation at any time and location.

η_o = Tidal elevation at $x = 0$.

η_H = High water tidal elevation at any location.

η_i = Tidal elevation of the incident wave at any time and location.

η_r = Tidal elevation of the reflected wave at any time and location.

κ = Epoch (phase) of a particular constituent at $t = 0$.

λ_2 = Smaller lunar evectional constituent which, with ν_2, μ_2, and S_2, modulates the amplitude and frequency of M_2 for the effects of variation in solar attraction of the Moon.

μ = Frictional damping coefficient (also called the damping modulus).

μ_2 = Variational constituent (see λ_2).

ν_2 = Larger lunar evectional constituent (see λ_2).

π = 3.14159265

ϕ = Latitude.

σ = Wave frequency.

σ_{CR} = Critical frequency.

σt = Phase of constituent wave at any time t.

σt_H = Phase difference between high water at any location in a basin and high water at the point of reflection.

σt_m = Phase difference between maximum flood current at any location in a basin and the phase at the point of reflection.

σt_s = Phase difference between slack water at any location in a basin and the phase at the point of reflection.

ρ_1 = Larger lunar evectional diurnal constituent.

θ_1 = Orientation of the maximum axis of an ellipse for a particular tidal current constituent.

θ_2 = Orientation of the minimum axis of an ellipse for a particular tidal current constituent.

ω_e = Rate of Earth's rotation.

ξ = Exponential coefficient representing the Coriolis effect on tidal amplitude or current speed in a relatively wide basin.

$\frac{\partial}{\partial t}$ = Partial derivative with respect to time.

$\frac{\partial}{\partial x}, \frac{\partial}{\partial y}$ = Partial derivatives with respect to Cartesian coordinates.

CHAPTER 1

INTRODUCTION

Chesapeake Bay is a valuable resource which provides enjoyment and livelihood for a large portion of the nation's population. It is a highly productive marine habitat and is the breeding ground for numerous estuarine and oceanic organisms. Therefore, many commercial and recreational fishermen are dependent upon its productivity. It also serves as a major waterway for marine transportation, naval operations, and recreational boating. In addition, the population residing along its shores is increasing rapidly, and it is a popular vacation attraction for many others.

These uses sometimes conflict and may even jeopardize the health of the estuary and its inhabitants. For example, the dredging of navigable channels may increase siltation or change circulation patterns, which could prove harmful to marine life. Hazardous materials might be discharged into its waters without knowing where they would be transported or their eventual impact on the environment. Therefore, it is important that we understand the processes taking place in Chesapeake Bay and how they are affected by man's activities.

PURPOSE OF STUDY

One of the first processes that needs better understanding is the circulation of waters throughout Chesapeake Bay and its tributaries. It is important because it is interrelated to many of the other processes taking place in the bay. Basically, this estuarine circulation is the combined effect of tidal action, fresh water inflow, and wind-driven currents. Due to the periodic nature of the tides, the tidal circulation can be separated from other circulation processes during analysis. Once the tidal circulation is adequately described and modeled, these other processes can be addressed as modifications of the basic tidal circulation.

The purpose of this study is to provide a more comprehensive understanding of the tidal circulation throughout Chesapeake Bay and its major tributaries, and to explain the tidal hydrodynamics through analysis of observed data and application of analytical models.

THE STUDY AREA

The area encompassed by this study is shown in Figure 1. It includes Chesapeake Bay and its tributaries, which comprise an estuarine system with a surface area of about 3,324 square nautical miles (11,400 square kilometers) and a shoreline of approximately 6,318 nautical miles (11,700 kilometers). For purposes of this study, this area has been subdivided into two regions which have significantly different dimensional characteristics. The largest region, called the Bay Proper, extends from Chesapeake Bay Entrance to the head of bay near the mouth of the Susquehanna River, a distance of about 170 nautical miles (315 kilometers).

Figure 1. The study area - Chesapeake Bay and its tributaries. Depth contours are expressed in feet.

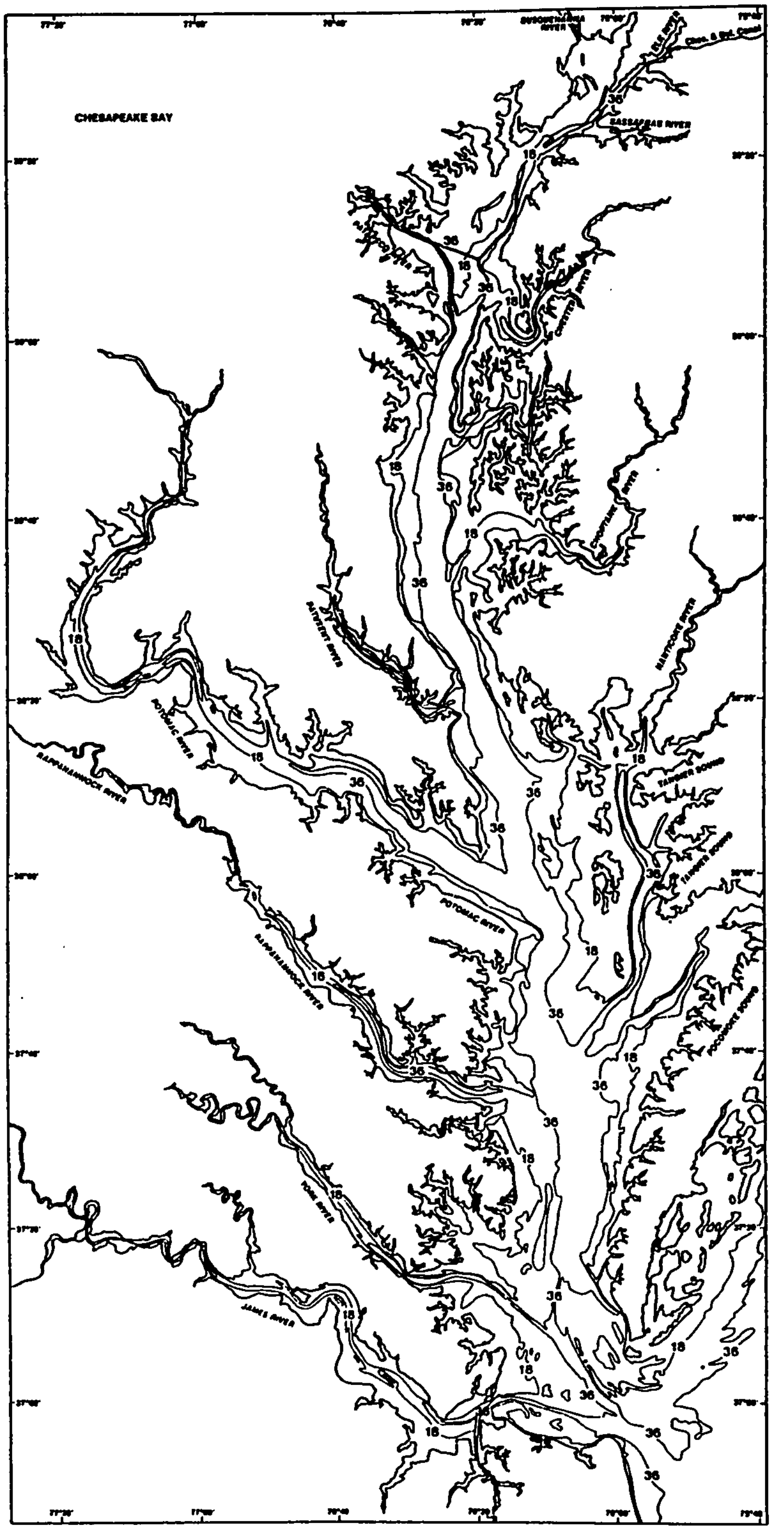
CHESAPEAKE BAY
POTOMAC RIVER
RAPPAHANNOCK RIVER
YORK RIVER
JAMES RIVER
18
36

The second region collectively addresses the major tributaries of Chesapeake Bay. There are actually over 50 tributaries and the bay receives freshwater runoff from a drainage basin of about 48,400 square nautical miles (166,000 square kilometers). The major tributaries are the Susquehanna, Potomac, Rappahannock, York, and James rivers. The Susquehanna River drains 42 percent of this drainage basin, and the Potomac River drains 22 percent. The Rappahannock, York, and James rivers combined drain about 24 percent of the basin (Ruzecki, 1976).

The Bay Proper widens from 10 nautical miles (18.5 km) at Chesapeake Bay Entrance to about 19 nautical miles (35 km) near the mouth of the Potomac River, and then narrows to about 3.25 nautical miles (6 km) near the mouth of the Severn River. The length to width ratio for the lower bay, that portion of the Bay Proper south of the mouth of the Patuxent River, is about 8 to 1. In comparison, the length to width ratio for the upper bay, from the mouth of the Patuxent River northward to the head of bay, is approximately 20 to 1. The average ratio for the tidal portions of the major tributaries is greater than 20 to 1, except for the lower Potomac River which is approximately 10 to 1.

The mean depth of the Bay Proper is about 26 ft (8 m), and the maximum depth is nearly 175 ft (53 m) off Kent Island. The 18 ft (5.5 m) and 36 ft (11 m) depth contours are indicated on Figure 1. These contours show that there is a complicated system of channels in Chesapeake Bay from which smaller channels branch off into the tributaries and sounds. The 36 ft contour shows that there are two main channels and a third narrower channel located in Chesapeake Bay Entrance. The southernmost channel in the entrance extends westward as Thimble Shoal Channel through Hampton Roads where a secondary channel then branches off up the James River. Another main channel is located immediately to the north of the southernmost channel in Chesapeake Bay Entrance. It extends northward up the Bay Proper and is called the Chesapeake Channel. A third channel is located on the north side of Chesapeake Bay Entrance. It is relatively deep and narrow, and extends northward along the eastern shore into Pocomoke Sound. In the entrance to the bay it is called the North Channel.

There are also extensive shoals in Chesapeake Bay Entrance which lie between these channels, but most of the lower bay has depths greater than 30 ft (9.1 m). The 36 ft contour in Figure 1 indicates there is a narrow, five nautical mile (9.3 km) long channel through a shoal area located about 12 nautical miles (22.2 km) up the bay from the entrance. North of this point, this channel widens considerably and continues up the bay to the narrows located just north of the mouth of the Severn River. This channel has many side channels which branch off into the tributaries and sounds along the sides of the lower bay.

The bay is relatively shallow north of the narrows with depths of about 12 ft (3.7 m), except for narrow channels which have been dredged to approximately 36 ft. The main dredged channel extends up the upper bay through its eastern reach to the Chesapeake and Delaware Canal. A shorter dredged channel extends northwestward up the Patapsco River to Baltimore, MD. The western upper reach of the bay is a shallow embayment that is commonly called the head of bay. It is about six nautical miles (11.1 km) long by six nautical miles wide, and is about six feet (1.8 m) deep. A small ten feet (3.0 m) deep channel extends northwestward across this embayment into the mouth of the Susquehanna River.

Salinities in Chesapeake Bay range from nearly 35 parts per thousand at the entrance of the bay to almost zero at the upper limit of tide in the tributaries. The spatial and temporal salinity variations observed in the bay and its tributaries are the result of fluctuations in river discharge and the tide. The lower bay is classified as a type D estuary during normal runoff conditions (Pritchard, 1952 and Dyer, 1973). It is nearly vertically homogeneous with lateral variations in salinity, and the tidal flow is dominant. The upper bay and the major tributaries may be classified as type B estuaries during normal runoff conditions. River discharge and the tide cause a two layered circulation system, which results in a net seaward flow of fresh water in the upper layer and an upchannel flow of saline water in the lower layer.

Primary tidal forcing is through Chesapeake Bay Entrance, but a second tide enters the bay through the Chesapeake and Delaware Canal. The canal is a sealevel, manmade waterway which connects the Delaware River and Chesapeake Bay near the head of bay. The mean range of tide in the Bay Proper is relatively small (U. S. National Ocean Survey, 1983a), generally between 1.0 ft (0.3 m) and 2.0 ft (0.6 m). The mean range in the tributaries may be amplified as the tide progresses from the mouth to the limit of tide. The average tidal currents vary from about 0.5 knot (25 cm sec^{-1}) to slightly over 2.0 knots (103 cm sec^{-1}) in the Bay Proper (U. S. National Ocean Survey, 1983b).

The tide in Chesapeake Bay derives its energy from the ocean tide outside the entrance to the bay rather than from the direct influence of lunar and solar gravitational forces on the waters of the bay. It is a cooscillating system in which the periods of oscillation are determined by the ocean tide, but other characteristics of the tide in the bay and its tributaries depend on the dimensions of the basins.

The tidal hydrodynamics of Chesapeake Bay are especially interesting to study because the Bay Proper is of sufficient length to contain one complete wavelength of the semidiurnal tide. In addition, the lower bay is of sufficient width that the Coriolis effect cannot be considered negligible. Therefore, the tide in this region may be a Kelvin wave. If this Kelvin wave is reflected, the resultant pattern of cotidal and corange lines would be amphidromic. Since the lower bay is relatively shallow, frictional resistance would significantly alter this amphidromic pattern, and the amphidrome (if one exists) would be displaced westward. It might even become a virtual amphidrome, if displaced beyond the bay's shores.

The tributaries are generally narrow enough that tidal motion is not noticeably affected by Coriolis force, so it is assumed there are no cross channel tidal variations. This may also be true for the upper bay. The tidal portions of the major tributaries are also of sufficient length that resonance occurs causing amplification of the tide's amplitude. In addition, the shallow depth of the upper tidal regions of these tributaries causes the growth of shallow water tides which distort the observed tidal wave.

TECHNIQUES FOR ANALYSIS

The tidal circulation of an estuary can be represented by analytical, numerical, or physical models. However, some of the tidal hydrodynamics of estuaries, such as bottom friction, are nonlinear and difficult to model. Therefore, models often simplify or neglect certain processes depending on the intended use of the model.

An analytical technique has been selected for this study because it greatly simplifies modeling the geographic complexity of Chesapeake Bay yet clearly describes the tidal hydrodynamics taking place. Simplifying assumptions and approximations are still required, but analytic models have proven fairly useful for describing the characteristics of the observed tidal waves and for explaining the relationship of the tide and tidal current observed in the Bay Proper. A one dimensional frictionally damped analytical model is applied to the tidal portions of the major tributaries and the upper bay. A two dimensional frictionally damped Kelvin wave analytical model is described which might be used to model the lower bay.

CHAPTER 2

BACKGROUND

Tides and tidal currents have been observed routinely in Chesapeake Bay for nearly 150 years, reportedly since the first systematic tide measurements commenced at Annapolis, MD on June 6, 1844 (Haight et al., 1930 and Hicks, 1964). Prior to 1964, a total of 241 tide stations and 115 near-surface current stations were occupied in the bay and its tributaries by the Coast and Geodetic Survey, a predecessor name of the National Ocean Service. However, these stations were not usually deployed for long periods or at the same time. Only 26 of the tide stations were deployed for periods long enough to allow harmonic analysis to determine the amplitudes and phases of tidal constituents, commonly called harmonic constants. Of these, 16 stations were occupied for a minimum of one year and 10 were occupied for a minimum of 29 days. The data from the remaining tide stations had to be analyzed by nonharmonic techniques which determined high and low water mean lunitidal intervals, mean ranges, and tidal datums referenced to longer duration stations.

Current measurements at each station were limited to approximately 100 hours duration. They were originally obtained with drift poles and surface drogues, but current meters have been used since 1950 (USC&GS, 1950). The majority of the pre-1964 current stations were concentrated in the lower bay, and due to the short duration of these records, none could be analyzed by harmonic analysis techniques. Therefore, non-harmonic techniques were used to determine mean lunitidal intervals for maximum flood, maximum ebb, and slack water, as well as the speed and direction of maximum flood and maximum ebb current.

The National Ocean Service routinely determines harmonic constants for 37 tidal constituents through harmonic analysis of a year-long time series of tide observations (Harris et al., 1963). These 37 constituents and their periods are listed in Table 1. This list actually totals 40 tidal constituents because three compound tidal constituents have the same periods as three astronomical constituents listed earlier.

The list of constituents is divided into three main groups based on their origin or predominate cause. The first group of 25 constituents are caused by the tide producing forces of the Moon and Sun, and are referred to as elementary constituents. This group is further divided into species depending on the number of cycles each has per day. There are 10 constituents listed in the diurnal species, which have periods of about 24 hours (approximately one cycle per day). The semidiurnal species list includes 11 constituents, which have periods of about 12 hours (approximately two cycles per day). There is one terdiurnal constituent listed, which has a period of about eight hours (approximately three cycles per day). The last three constituents of this group are referred to as long period constituents, meaning they have periods of a fortnight or longer. These constituents are not totally caused by the tide producing forces of the Moon and Sun, but may be augmented by meteorological phenomena of the same periodicity.

TABLE 1

NAMES AND PERIODS OF TIDAL CONSTITUENTS

Group 1 - Elementary Constituents

Symbol	Name	Period (solar hours)
	Diurnal Species	
K_1	Lunisolar	23.93
O_1	Principal lunar	25.82
P_1	Principal solar	24.07
Q_1	Larger lunar elliptic	26.87
M_1	Smaller lunar elliptic	24.84
J_1	Small lunar elliptic	23.10
S_1	Solar	24.00
rho_1	Larger lunar evectional	26.72
OO_1	Lunar diurnal, second order	22.31
$2Q_1$	Lunar elliptic diurnal, second order	28.01
	Semidiurnal Species	
M_2	Principal lunar	12.42
S_2	Principal solar	12.00
N_2	Larger lunar elliptic	12.66
K_2	Lunisolar	11.97
T_2	Larger solar elliptic	12.01
L_2	Smaller lunar elliptic	12.19
$2N_2$	Lunar elliptic semidiurnal, second order	12.91
nu_2	Larger lunar evectional	12.63
$lamda_2$	Smaller lunar evectional	12.22
mu_2	Variational	12.87
R_2	Smaller solar elliptic	11.98
	Terdiurnal Species	
M_3	Lunar	8.28
	Long Period Constituents	
Mm	Lunar monthly	661.30
MSf	Lunisolar synodic fortnightly	354.37
Mf	Lunar fortnightly	327.86

TABLE 1 (CONTINUED)

Group 2 - Meteorological Constituents

Symbol	Name	Period (solar hours)
SSa	Solar semiannual	2,191.43
Sa	Solar annual	4,382.92

Group 3 - Shallow Water Constituents

Symbol	Name	Period (solar hours)
	Overtides	
M_4	harmonic of M_2	6.21
M_6	harmonic of M_2	4.14
M_8	harmonic of M_2	3.11
S_4	harmonic of S_2	6.00
S_6	harmonic of S_2	4.00
	Compound Tides	
MK_3	The sum of the freq. of M_2 and K_1	8.18
$2MK_3$	Twice the freq. of M_2 minus that of K_1	8.39
MS_4	The sum of the freq. of M_2 and S_2	6.10
MN_4	The sum of the freq. of M_2 and N_2	6.27
$2MN_2$	Twice the freq. of M_2 minus that of N_2	12.19
$2MS_2$	Twice the freq. of M_2 minus that of S_2	12.87
$2NM_2$	Twice the freq. of N_2 minus that of M_2	12.91
$2SM_2$	Twice the freq. of S_2 minus that of M_2	11.61

The second group in Table 1 includes two long period constituents that are predominantly caused by periodic meteorological phenomena, but their periodicity can be represented by terms in the mathematical developement of the tide producing force of the Sun. Therefore, these tides are commonly referred to as meteorological tides.

The third group includes 13 constituents commonly referred to as shallow water tides. Shallow water effects, such as friction, can cause the transfer of tidal energy to other constituents which have periods that are different from the original elementary constituent. The combined effect of these shallow water constituents is to distort the form of the tidal wave.

There are two types of shallow water tides: overtides and compound tides. Overtides are the result of transferring tidal energy to higher harmonics of an elementary constituent. Therefore, an overtide has a speed (rate of change in phase) that is an exact multiple of the speed of an elementary constituent. The first three constituents in this group are overtides of the principal lunar semidiurnal constituent, and the next two are overtides of the principal solar semidiurnal constituent.

Compound tides have speeds that are equal to the sum or difference of the speeds of two or more elementary constituents. The last six constituents in this group are compound tides. Note that the periods for three of these compound constituents are the same as the periods of three elementary constituents in the first group. This does not cause much confusion during analysis because the compound tides would only be expected to occur in shallow water, and would probably dominate the elementary constituents of the same periods.

Van Der Stok (1897), Courtier (1938), and Dietrich (1944) have developed criteria to classify the type of tide at any location, based on the relationship of major diurnal and semidiurnal tidal constituents. These criteria all use the ratio of the sum of the amplitudes of the major diurnal constituents, K_1 and O_1, to the sum of the amplitudes of the major semidiurnal constituents, M_2 and S_2, to quantitatively determine the type of tide. This ratio is called the form number, F, because it indicates the form of the tide on any given day (Defant, 1961, Dietrich, 1966, and Amin, 1986). Dietrich's criterion is presented in Table 2. It was used to classify the type of tide observed in Chesapeake Bay during this study because it provides more detail as to whether a mixed tide is mainly semidiurnal or diurnal.

TABLE 2

TIDE CLASSIFICATION CRITERION

FORM NUMBER	TYPE
$F \leq 0.25$	Semidiurnal
$F > 0.25$ and ≤ 1.50	Mixed, mainly semidiurnal
$F > 1.50$ and ≤ 3.00	Mixed, mainly diurnal
$F > 3.00$	Diurnal

A criterion is also required to determine whether the Coriolis effect in an embayment can be considered negligible. If it can be, then the tidal wave may be considered in simple one dimensional terms.

However, if the Coriolis effect is not negligible, the tidal wave may be a Kelvin wave and must be considered in two dimensional terms.

The Rossby Radius of Deformation (R) is a measure of Coriolis effectiveness. It is a scale length comparing gravitational force to Coriolis force (Pedlosky, 1979), and can be expressed as:

$$R \equiv \frac{C}{f} \approx \frac{C_o}{f} \tag{1}$$

where, C = wave celerity or phase speed

C_o = the frictionless wave celerity = $\sqrt{gh}$

g = acceleration of gravity

h = mean water depth

f = Coriolis parameter = $2\omega_e \sin\phi$

ω_e = earth's rotation = 0.727×10^{-4} radians $\sec^{-1}$

ϕ = latitude

The frictionless celerity is generally used to approximate the actual wave celerity, resulting in a slightly high estimate of the Rossby Radius of Deformation. Assuming an average depth of 26 ft (8 m) and a midlatitude of 38° N. for lower Chesapeake Bay, R would be slightly less than 54 nautical miles (100 km). Since the width of the lower bay at this latitude is approximately 19 nautical miles (35 km), it is more than one third the length of R. Therefore, the Coriolis effect should not be considered negligible. However, it can be considered negligible in the upper bay and tributaries because their widths are much less than that of the lower bay. For example, the widest part of the James River (near Burwell Bay) is about 4.6 nautical miles (8.5 km) and that of the Rappahannock River (near its mouth) is about 3.0 nautical miles (5.6 km). In comparison, the lower portion of the Potomac River is much wider, about 6.5 nautical miles (12.0 km), and upper Chesapeake Bay varies in width from 3.0 to 6.0 nautical miles (5.6 to 11.1 km). However, these widths are still significantly smaller than the Rossby Radius of Deformation.

PRIOR DESCRIPTIVE STUDIES

Harris (1907) and Hicks (1964) constructed cotidal and cocurrent charts to describe the tidal circulation of Chesapeake Bay. The cotidal chart is a plot of cotidal hour contours throughout a basin. The cotidal hour of the tide at any location is defined as the average time interval between the Moon's transit over the Greenwich meridian and the time of the following high water at the specified location (Hicks, 1984). The corange chart is a similar set of contours or corange lines which represent the distribution of mean ranges throughout a basin.

Similarly, current hour is defined as the mean time interval between the transit of the Moon over the Greenwich meridian and the time of maximum flood current, modified by the times of slack water (or minimum current) and the maximum ebb current at the specified location (Hicks, 1984). The cocurrent chart is a plot of cocurrent hour contours throughout a basin. The cospeed chart is a similar set of contours or cospeed lines which represent the distribution of maximum flood (or maximum ebb) current speeds.

Prior investigators have expressed these time intervals in lunar hours, based on the assumption that the tide in Chesapeake Bay is predominantly semidiurnal and can be represented solely by the period of the principal lunar semidiurnal constituent, M_2. Therefore, one complete cycle of the tide would be exactly 12 lunar hours, and the cotidal lines could all be expressed as integers.

Harris (1907) published a cotidal chart of the Chesapeake Bay, based on observations from only 47 tide stations, and a cocurrent chart which was based on only 34 current stations. These charts were not very definitive due to the sparceness of stations and the short duration of the time series. Haight (1934) published a very thorough compilation of harmonic constants for only a few long term tide and current stations occupied in Chesapeake Bay prior to 1930. He graphed the high water lunitidal intervals and mean ranges for stations along the main axes of the bay and its major tributaries, but did not construct any cotidal or cocurrent charts.

Hicks (1964) constructed more definitive cotidal and cocurrent charts of Chesapeake Bay. His cotidal charts were based on tide data observed by the U. S. Coast and Geodetic Survey at 241 locations throughout Chesapeake Bay and its tributaries from 1897 to 1963. These tide records varied in length from 29 days to a year or longer, and most were observed during hydrographic surveys which progressed slowly throughout the bay. Therefore, few of these tide stations were deployed simultaneously. Hicks' cocurrent chart was based on currents observed by the Coast and Geodetic Survey at 115 locations in Chesapeake Bay. Most of this current data was observed after 1950 using current meters at stations that were concentrated in lower Chesapeake Bay. These current meters were deployed for periods of 100 hours each at depths of four to seven feet (1.2 to 2.1 m) below the surface.

The observed high water on Hicks' cotidal chart travels from Chesapeake Bay Entrance to the head of bay in 13.75 lunar hours (14.23 solar hours). This shows that Chesapeake Bay is able to contain one complete semidiurnal wavelength of the tide. For example, if the incident tidal wave has a period of 12 lunar hours (12.42 solar hours) and travels with the speed of a shallow water wave, the wave crest will not quite traverse the entire length of the bay before the next crest enters Chesapeake Bay Entrance. In addition, his cocurrent chart indicates the time of maximum flood current becomes progressively later by about 11 lunar hours (11.39 solar hours) as the tidal wave progresses from Chesapeake Bay Entrance to the head of bay. However, Hicks questioned the validity of this observation because of the uneven areal distribution of current stations.

Hicks' corange chart shows that the mean range decreases from 3.0 ft (0.91 m) at the entrance to the bay to about 1.3 ft (0.40 m) off the mouth of the Potomac River. Continuing up the bay, the range increases slightly to 1.4 ft (0.43 m) off the mouth of the Patuxent River, then decreases to about 1.0 ft (0.30) off the mouth of the Severn River, and finally increases to 2.3 ft (0.70 m) at the head of bay. He observed that the range is significantly larger on the east side of the lower bay than on the west side, directly opposite. The difference is as much as 0.5 ft (0.15 m) just north of the mouth of the Rappahannock River, but averages about 0.2 ft (0.06 m) overall.

Hicks provided an explanation for the observed changes in the time of high water and mean range throughout the Bay Proper, based on simple reflected tidal wave theory. He explained that the observed tidal wave in an embayment is usually composed of two damped progressive waves traveling in opposite directions. An incident wave enters from the open ocean and progresses toward the head of bay. It is reflected there and travels back toward the open end as a reflected wave.

Without friction, the observed tidal wave would be a perfect standing wave with a range increasing from zero at the nodes to a maximum at the antinodes. When it is high water at the point of reflection, it is also high water everywhere between the node and the point of reflection. Low water occurs simultaneously everywhere on the other side of the node. The opposite relationship will occur when it is low water at the point of reflection. Maximum current will occur at half tide. However, if the incident wave is completely attenuated before reaching the head of bay, hence no reflected wave, the observed wave will be a pure progressive wave whose range decreases from the entrance to the head of bay. Maximum current would occur at the times of both high and low water.

If the incident wave is not completely attenuated, there will be a reflected wave. The incident and reflected waves will both have the same amplitude at the reflecting barrier, and the difference between the ranges of the incident and reflected waves will be the most at the entrance to the bay. Therefore, the progressive nature of the observed wave increases when approaching the entrance of the bay. Hicks' cotidal and cocurrent charts indicate that the observed tidal wave is actually intermediate between a purely progressive and a purely standing wave, tending to be more progressive near the entrance of the bay and more of a standing wave near the head of bay.

Hicks also described the spatial distribution of tidal characteristics throughout Chesapeake Bay, based on the criterion for tidal classification. Since he was only able to determine harmonic constants for tidal constituents at 26 locations throughout the bay and its tributaries, the change in the type of tide was not well defined. His chart shows the tide is predominantly semidiurnal throughout most of the lower bay and portions of the James, York, Patuxent and Potomac rivers. The tide in the remaining areas is classified as mixed, mainly semidiurnal.

Hicks' classification chart indicates both semidiurnal and diurnal constituent tidal waves are present in Chesapeake Bay, but is not detailed enough to use to describe their interaction throughout the bay and tributaries. However, he does provide the following explanation of their interaction, based on simple reflected tidal wave theory. If the diurnal and semidiurnal waves were both pure standing waves and in phase at the point of reflection, the node of the diurnal wave would coincide with the antinode of the semidiurnal wave. In addition, the amplitude of the diurnal wave would be nearly maximum at the location of the nodes of the semidiurnal wave. Therefore, the ratio of the amplitudes of the diurnal and semidiurnal waves would be zero at the diurnal node and infinite at the semidiurnal node. If the diurnal and semidiurnal constituents were both pure progressive waves, these ratios would be constant. Since the observed tidal wave actually lies intermediate between a purely progressive wave and a pure standing wave, the amplitude ratio should be greatest at the northernmost node of the semidiurnal wave and a lesser maximum should occur near the entrance of the bay, at the central antinode, and at the head of bay.

Hicks also observed that the maximum flood current in the lower bay occurs near the time of high water and maximum ebb occurs near low water which indicates the tidal wave is nearly progressive. If the Coriolis effect is not negligible, this tide and current relationship will cause an increase in the elevation of high water and a decrease in elevation of low water to the right of the direction of propagation of the wave. Both the incident and reflected waves will be affected similarly. However, the increase in range to the right of the incident wave will be greater because the incident wave is not as attenuated as the reflected wave. Hicks' corange chart shows that the tidal range is significantly greater along the east side of lower Chesapeake Bay.

Hilder (1980) observed clockwise rotary currents in the lower bay, which he suggested were possible evidence of Kelvin or Poincare waves. He proposed that an amphidrome might exist in lower Chesapeake Bay and recommended additional studies, such as simultaneous recording of tidal heights which could be used to construct cotidal and corange charts.

Finally, Hicks observed that shallow water tides cause distortion of the observed tide in the upper reaches of the Potomac and James rivers. He indicated that distortion by M_4 becomes significant when the amplitude ratio M_4/M_2 is 0.1 or greater. Based on pre-1964 data, the ratios for Washington, DC and Richmond, VA were 0.094 and 0.122, respectively. The ratios were less than 0.05 throughout the rest of the bay. Similarly, distortion by M_6 becomes significant when the ratio M_6/M_2 is 0.04 or greater. The ratio was 0.052 at Richmond, VA. Hicks suggested that distortion might also occur in the upper tidal reaches of other tributaries.

ONE DIMENSIONAL ANALYTICAL MODEL

It does not appear that the tidal circulation in Chesapeake Bay or its major tributaries has been modeled previously using analytical techniques, mainly because of the bay's relatively shallow depths, irregular boundaries, and the width of the lower bay. Analytical models of tidal motion in canals and simple embayments have been developed which account for frictional resistance through linearizing the friction term in the equations of motion. However, the problem in applying a frictionally damped model to a real embayment is that the coefficient in the exponential damping term is unknown and difficult to determine directly.

Redfield (1950) developed a one dimensional frictionally damped analytical model of a reflected tidal wave in a canal or embayment, which is closed at one end and connected to the ocean at the other. He linearized the friction term in the equations of motion in a manner similar to that used by Fjeldstad (1929) in his development of a two dimensional frictionally damped analytical model of a progressive wave in a canal of infinite length. Fjeldstad's model will be described in more detail in the next section during the development of a two dimensional frictionally damped model of a reflected Kelvin wave.

Redfield eliminated the geographic complexity of modeling a real embayment by expressing the characteristics of the incident and reflected tidal waves in a form in which the wave period represents a unit of time, and the phase change (relative to the point of reflection) represents distance. He defined a model of a frictionally damped tidal wave entering a canal of finite length with a reflecting end as shown in Figure 2.

Figure 2. One dimensional model of the tide in a canal of finite length with a reflecting end.

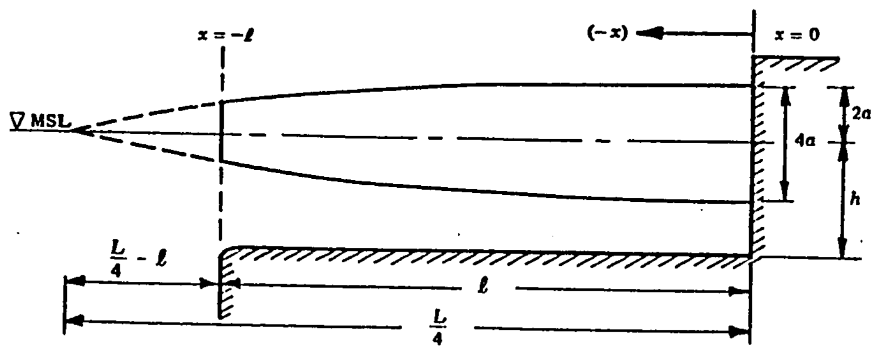

From Ippen (1966)

ONE-DIMENSIONAL MODEL OF THE TIDE
IN A CANAL CLOSED AT ONE END

The model is oriented so that the major axis of the canal is aligned parallel to the x axis, with the reflecting end of the canal located at $x = 0$ and the open end located at $x = -\ell$. A tide of wavelength L enters the canal as the incident wave, is reflected at the closed end, and travels back to the open end as the reflected wave with the same period, T. In Figure 2 the canal length is slightly less than one quarter wavelength of the tide and there is no frictional damping. Because of the orientation of the model, an antinode of both the incident and reflected waves is located at the reflecting end and a node is located just beyond the open end. Nodal points will occur at $x = L/4$ and at odd multiples thereof. If the incident and reflected waves are superimposed, the result will be a pure standing wave as shown in Figure 2 whose amplitude at the reflecting end of the canal is twice the amplitude of the incident wave at this point.

If frictional damping is also considered, the amplitude of the incident wave will decrease as it travels up the canal toward the reflecting end. Similarly, the amplitude of the reflected wave will decrease as it travels in the opposite direction. The amplitudes of the incident and reflected waves will only be equal at the closed end. The x-axis convention used in Figure 2 will cause the frictional damping term in the model to behave in this manner. Depending on the extent of frictional damping, the resultant wave will be more like a progressive wave when these waves are superimposed.

Redfield applied the following assumptions and simplifications to this model.

1. Tide wavelength > canal length >> width >> depth >> wave amplitude.
2. Canal width and mean depth are constant.

3. Canal width is small, therefore Coriolis effect is negligible.
4. Since water depth is constant, current velocity is assumed uniform over depth.
5. Tidal system in the canal is driven only by the ocean tide at the entrance, which is periodic with a single frequency.
6. Amplitude of incident and reflected waves are the same at the point of reflection.
7. All the energy of the reflected wave remains in the same frequency as that of the incident wave.
8. Resistance force is applied uniformly per unit mass.
9. Friction is linearized so that frictional resistance is proportional to the velocity of the current.

Although the resistance force acts only on the bottom and sides of the canal, it is assumed that it is applied uniformly per unit mass. Also, frictional resistance is actually proportional to the square of the velocity, as expressed in the quadratic resistance law. However, the friction term is usually linearized and resistance is assumed proportional to the velocity. Ippen (1966) explains that the friction term may be linearized on the basis that the work done by friction over a tidal cycle must be the same, whether determined by the quadratic resistance law or by a substitute linear approximation.

For the conditions described, the equation of motion and the continuity equation (in the x direction) are:

$$\frac{\partial u}{\partial t} + Nu = -g\frac{\partial \eta}{\partial x} \qquad (2)$$

$$\frac{\partial \eta}{\partial t} = -h\frac{\partial u}{\partial x} \qquad (3)$$

where: u = uniform current velocity in the x direction

η = tidal elevation

h = mean depth of canal

g = acceleration due to gravity

t = time

N = linearized frictional resistance coefficient

Since the incident progressive wave is periodic in time and travels in the positive x direction, the solution for the elevation of the incident tidal wave is:

$$\eta_i = a_o e^{-\mu x} \cos(\sigma t - kx) \tag{4}$$

In a similar manner, the solution for the reflected wave is:

$$\eta_r = a_o e^{\mu x} \cos(\sigma t + kx) \tag{5}$$

where: η_i = elevation of incident wave at any x and t

η_r = elevation of reflected wave at any x and t

a_o = amplitude of wave at x = 0

μ = frictional damping coefficient (per tidal cycle or per wavelength); also called the damping modulus

σ = wave frequency = $\frac{2\pi}{T}$

T = wave period

k = wave number = $\frac{2\pi}{L}$

L = wave length

kx = phase difference (relative to the point of reflection)

t = phase of constituent at any time t

The frictionless wave celerity or phase speed is:

$$C_o = \frac{L_o}{T} = \frac{\sigma}{K_o} = \sqrt{gh} \tag{6}$$

where: L_o = frictionless wave length

k_o = frictionless wave number

h = water depth

The wave celerity or phase speed with friction is:

$$C = \frac{L}{T} = \frac{\sigma}{K} < \sqrt{gh} \tag{7}$$

The linearized resistance coefficient can be expressed as:

$$N = 2\mu C \frac{K}{K_o} \tag{8}$$

For the boundary conditions at x = 0 and t = 0:

$$\eta = a_o \quad \text{and} \quad K_o^2 = K^2 - \mu^2 \tag{9}$$

This indicates the wave number increases with increasing friction, hence the wavelength decreases with increasing friction. Since the frequency remains constant, the wave celerity must also decrease with increasing friction.

These relationships can be expressed as:

$$\frac{K_o}{K} = \frac{L}{L_o} = \frac{C}{C_o} = \frac{1}{\sqrt{1 + \left(\frac{\mu}{K}\right)^2}} \tag{10}$$

Therefore, the wavelength can be expressed as:

$$L = \frac{2\pi}{\sqrt{\frac{\sigma^2}{gh} + \mu^2}} \tag{11}$$

The solution for the current velocity of the incident wave is:

$$u_i = a_o \frac{C_o}{h} e^{-\mu x} \frac{K_o}{\sqrt{\mu^2 + K^2}} \cos(\sigma t - Kx + \alpha) \tag{12}$$

Similarly, the solution for the current velocity of the reflected wave is:

$$u_r = -a_o \frac{C_o}{h} e^{\mu x} \frac{K_o}{\sqrt{\mu^2+K^2}} \cos(\sigma t + Kx + \alpha) \tag{13}$$

where: u_i= current velocity of incident wave at any x and t

u_r= current velocity of reflected wave at any x and t

a_o= amplitude of wave at kx = 0

α= the phase difference between the time of high water and the time of maximum flood

Also,

$$\tan\alpha = \frac{\mu}{K} \quad \text{or} \quad \alpha = \tan^{-1}\left(\frac{\mu}{K}\right) \tag{14}$$

The solutions for the tidal elevation and velocity of the incident and reflected waves indicate:

1. the ratio, $\frac{\mu}{K}$, must be constant throughout the canal;
2. the tidal elevation and velocity are reduced by an exponential damping factor: $e^{-\mu x}$ in the positive x direction and $e^{\mu x}$ in the negative x direction;
3. the current velocity is reduced by an additional factor $\frac{K_o}{\sqrt{\mu^2+K^2}}$, which is always less than unity; and
4. the occurrence of the maximum velocity is shifted relative to the maximum amplitude by the time angle, α .

The wave observed in an embayment or a canal that is closed at one end would be the result of the superposition of the incident and reflected waves. Therefore, the elevation at any time and any location is the sum of the elevations of the incident and reflected waves.

$$\eta = \eta_i + \eta_r = a_o e^{-\mu x} \cos(\sigma t - kx) + a_o e^{\mu x} \cos(\sigma t + kx) \tag{15}$$

The local phase angle or difference in phase of high water, σt_H, at location kx (relative to that at the point of reflection) will be:

$$\sigma t_H = \tan^{-1}(-\tan kx \tanh \mu x) \tag{16}$$

Redfield plotted σt_H versus kx for different damping coefficients. He showed that when the damping coefficient is small, indicating little frictional resistance, the local phase angle of high water changes little from the point of reflection, where the phase angle is zero, to a location downstream near kx = -90°. Then the change in phase increases rapidly to -90° at kx = -90°. Continuing down the canal, the phase angle changes rapidly to nearly -180° at a location slightly downstream of kx = -90°, and then changes slowly to -180° at kx = -180°. Therefore, high water occurs at approximately the same time at almost all locations on one side of the location where kx = -90°, and low water occurs nearly simultaneously at almost all locations on the other side. This indicates the wave would be an almost pure standing wave when the damping coefficient is small.

When the damping coefficient is large, the phase angle changes gradually from zero at kx = 0° to -90° at kx = -90°. The phase angle continues to change gradually to -180° at kx = -180°. Therefore, the time or phase of high water gets progressively later as the wave travels up the canal from the open end. This indicates the tide is an almost pure progressive wave.

The solution for the high water elevation at any location, kx, is:

$$\eta_H = 2a_o \sqrt{\tfrac{1}{2}(\cos 2Kx + \cosh 2\mu x)} \tag{17}$$

At the closed end of the canal, the high water elevation, η_o , is:

$$\eta_o = 2a_o \tag{18}$$

Therefore, the high water elevation or amplitude of a single frequency tide at the point of reflection is twice the amplitude of the incident wave at that point.

The ratio of the high water elevation at any location along the canal to high water at the point of reflection can be expressed as:

$$\frac{\eta_H}{\eta_o} = \sqrt{\tfrac{1}{2}(\cos 2Kx + \cosh 2\mu x)} \tag{19}$$

In the frictionless case, the amplitude of the incident and reflected waves would be zero at their nodes which would both be at the same location, kx = -90. When superimposed, the combined wave will also have a zero amplitude node at this location. Frictional damping would cause the amplitude of the incident wave to be attenuated as it travels toward the closed end of the canal. The reflected wave would also be attenuated as it travels toward the open end, but its amplitude will be smaller than the corresponding incident wave amplitude at any location other than the point of reflection. At the location of the reflected wave's node, the incident wave will still have a small amplitude remaining. Therefore, the combined wave will not have a zero amplitude node because a small amplitude will remain. The location where this minimum amplitude occurs is called the quasinode. Redfield has also shown that the location of the quasinode will move up the canal slightly as friction increases. The amplitudes of the incident and reflected waves are both attenuated very rapidly when the damping coefficient is large, and the reflected wave may be totally attenuated before reaching the location where kx = -90. No quasinode would occur in this case. The amplitude would decrease continuously from the entrance to the point of reflection, and an almost pure damped progressive wave would occur.

Redfield also considered the amplification of the tides due to resonance in reflecting canals of different lengths. If the canal length from the entrance to the closed end is equal to or less than one quarter wavelength, the high water elevation (amplitude) will continue to increase as the tide travels toward the closed end, and maximum amplification occurs when the canal length approaches one quarter wavelength. If the canal length is greater than one quarter wavelength, the amplitude will progress through a minimum at the quasinode and then increase as the wave approaches the point of reflection. However, the amplification will be less than that which occurs when the canal length is approximately one quarter wavelength.

Redfield also described the relationship of the damping coefficient to amplification due to resonance. He observed that amplification is very sensitive to damping. For the case where the canal length is approximately one quarter wavelength (therefore maximum amplification of the tide due to resonance) the amplification would not be more than fourfold if the damping coefficient is 1.0, and would decrease to two-fold if it is about 2.0. He suggested that resonance would become insignificant with a damping coefficient greater than 2.0.

Since the observable properties, $\frac{n_H}{n_o}$ and σt_H, are both functions of only kx and μx, Redfield constructed a nomogram with $\frac{n_H}{n_o}$ on the vertical axis and σt_H on the horizontal axis. This nomogram has been reconstructed by Parker (1980) using computerized techniques, and is shown in Figure 3. The desired properties, kx and μ, are represented by two sets of curves which are superimposed on the nomogram.

The harmonic constants, which have been determined from harmonic analysis of tide data observed at locations throughout an embayment, can be used with this nomogram to determine the phase distribution of an incident constituent wave as well as a representative value for the damping coefficient. The same phase distribution, with signs reversed, and the same damping coefficient would apply to the reflected constituent wave.

The procedure for using the nomogram with real data is to observe (or estimate) the amplitude and phase of a tidal constituent at the point of reflection. These values are then used to compute the amplitude ratios and the phase differences between the point of reflection and other locations in the embayment. This data is plotted on the nomogram and compared to the damping coefficient curves to determine whether any points consistently fall along a particular curve. If the amplitude and phase of the tidal wave at the point of reflection are known but the amplitude ratios and phase differences did not plot consistently along any specific curve (or curves), it might be due to: imperfect reflection at the reflecting boundary, partial secondary

Figure 3. The Redfield nomogram.

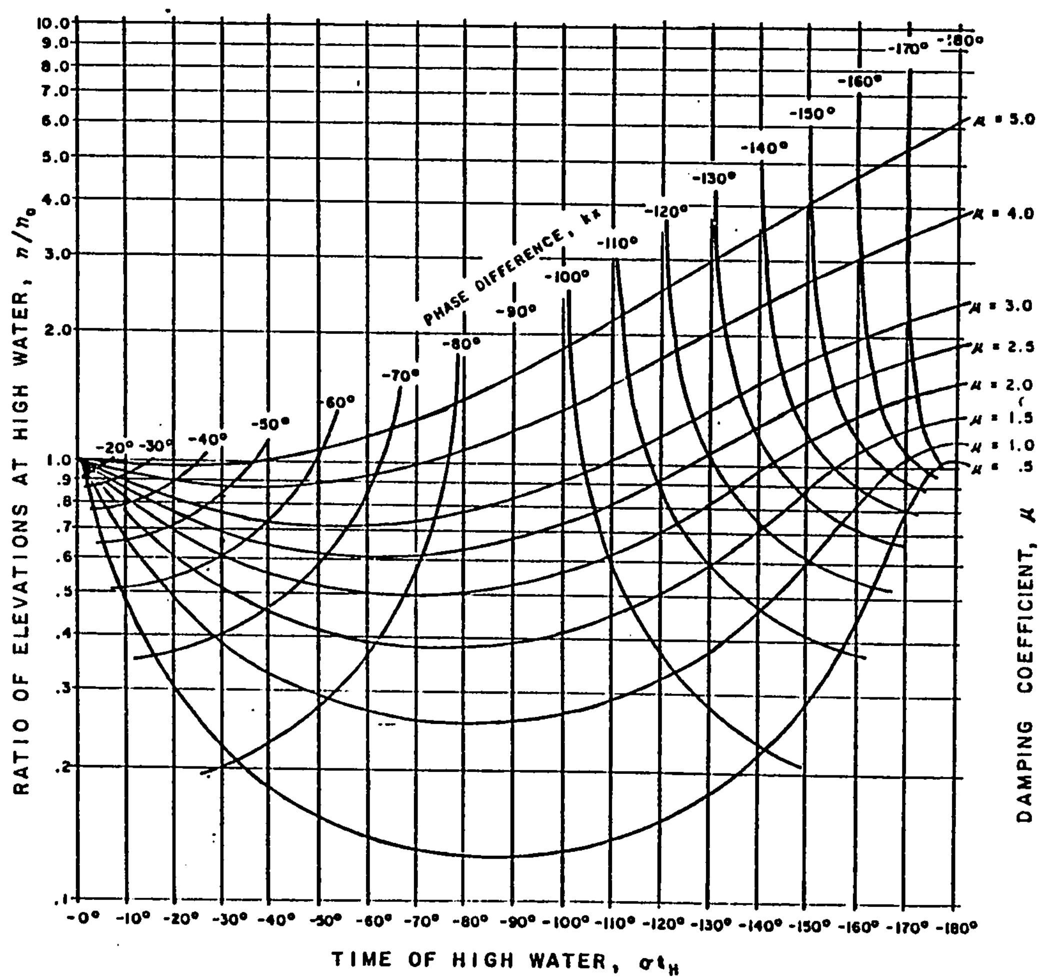

From Parker (1980)

THE REDFIELD NOMOGRAM

reflections, or loss of tidal energy into side channels. If the amplitude and phase at the point of reflection were incorrectly estimated, it would also cause the amplitude ratios and phase differences for downstream locations to plot inconsistently. In this case, the estimated amplitude and phase at the point of reflection could be adjusted slightly and used to compute new amplitude ratios and phase differences that might plot more consistently on the nomogram, assuming that there is total reflection at the boundary and no loss of energy into side channels.

Once the best fit is obtained, values of μ and kx can be determined and used to describe the characteristics of the frictionally damped tidal wave. Since the Redfield model can only be used with a single wave period, separate plots are required to determine the damping coefficient and phase distribution for each tidal constituent.

The tidal current velocity resulting from the superposition of the incident and reflected waves can be determined by adding the solutions for the velocity of each wave.

$$u = a_o \frac{C_o}{h} \frac{K_o}{\sqrt{\mu^2 + k^2}} \left[e^{-\mu x} \cos(\sigma t - kx + \alpha) - e^{\mu x} \cos(\sigma t + kx + \alpha) \right] \quad (20)$$

The slack water phase angle, σt_s, is defined as the phase of slack water at any location along an embayment or canal relative to the phase of slack water at the point of reflection. It can be determined from:

$$\sigma t_s = \tan^{-1}\left(\frac{\tanh \mu x}{\tan kx}\right) - \alpha \quad (21)$$

Redfield plotted a graph of σt_s versus kx for a number of damping coefficients to describe the change in the time or phase of slack water along the longitudinal axis of the canal. His plot shows that when the damping coefficient is small, slack water occurs almost simultaneously from the point of reflection to a point one half wavelength downstream. This indicates the tidal wave is nearly a standing wave. As the damping coefficient increases and the tide becomes a more progressive wave, the local phase angle of slack water gradually decreases from a maximum at the point of reflection to zero at a distance of one quarter wavelength. It then gradually increases to another maximum at one half wavelength from the point of reflection. Therefore, the time of slack water changes progressively with distance.

Since the maximum current precedes or follows slack water by a quarter period of the wave, the relationship of maximum flood current to the phase difference, kx, can be expressed in terms of the local phase angle of maximum flood current σt_m, as follows:

$$\sigma t_m = \tan^{-1}\left(-\tan kx \coth \mu x\right) - \alpha \tag{22}$$

In addition, the maximum flood velocity, u_m, is:

$$u_m = 2a_o \frac{C_o}{h} \frac{k_o}{\sqrt{\mu^2 + k^2}} \sqrt{\frac{1}{2}\left(\cosh 2\mu x - \cos 2kx\right)} \tag{23}$$

Note that equation 23 satisfies the boundary condition that the current velocity must be zero at the closed end of the canal. This solution indicates that, when the damping coefficient is small, the flood current is greatest at or near the quasinode where the high water elevation was shown to be at a minimum. This again shows that an almost pure standing wave occurs when the damping coefficient is small. For large damping coefficients, the solution indicates there is a gradual decrease in the maximum flood velocity as the wave travels from the entrance to the closed end of the canal. Therefore, an almost pure damped progressive wave will occur throughout most of the canal.

Redfield also considered the relationship between the tide and tidal current at any point along a canal. He plotted the difference between the local phase angle of high water, σt_H, and the local phase angle of slack water, σt_s, for selected values of the damping coefficient. For this study it is more useful to consider the relationship between the local phase angle of high water and the local phase angle of maximum flood current, σt_m. This graph is basically the same as Redfield's except the phase angle difference, $\sigma t_H - \sigma t_m$, is graduated from -90° to $+90^{\circ}$ through 0° at mid scale.

Between the point of reflection and the first quasinode, maximum flood current occurs before high water. The phase angle difference is greatest for all damping coefficients at the point of reflection, and is zero at the quasinode indicating maximum flood and high water are in phase. When the damping coefficient is small, the phase angle difference is a maximum at the point of reflection and changes little over most of the quarter wavelength. However, the phase angle difference decreases rapidly near the quasinode and high tide and maximum flood are again in phase at the quasinode.

In the second quarter wavelength, high water occurs before maximum flood current for all values of the damping coefficient, except at the quasinode and antinode where the tide and current will be in phase.

The maximum phase angle difference occurs approximately at the midpoint of the second quarter wavelength. The phase angle again changes the most rapidly when the damping coefficient is small, but the maximum difference in each successive quarter wavelength is slightly less than that observed in the one before. Even though the third and fourth quarter wavelengths were not plotted, it is obvious that maximum flood current and high water will again occur at the same time at the second quasinode where $kx = -270^{\circ}$. In the third quarter wavelength, maximum flood current occurs before high water for all values of the damping coefficient, and high water again precedes maximum flood current in the fourth quarter wavelength. The maximum difference will continue to be less than the maximum observed in the previous quarter wavelength for all values of the damping coefficient. Therefore, the maximum differences in the fourth quarter are much less than those observed in the first quarter. When the damping coefficient is small, the tidal wave is an almost pure standing wave in the first quarter wavelength, and then becomes progressively less of a standing wave in subsequent quarter wavelengths.

When the damping coefficient is large, the phase angle difference at the point of reflection is less than that observed when it is small, and the difference decreases gradually throughout the first quarter wavelength to zero at the quasinode. The difference in the second, third and fourth quarter wavelengths becomes progressively smaller with distance from the point of reflection. This again indicates the tide is becoming a more progressive wave the further it proceeds away from the point of reflection.

The relationships derived for a uniform channel may be applied to a more irregular channel if the following assumptions are made.

1. The effect of irregularities in cross section is to alter the celerity of the incident and reflected waves, therefore distorting the geographical distribution of phase differences.
2. Damping is proportional to the phase change in tidal waves, rather than to the distance traveled.
3. The damping coefficient is constant along the length of the canal or embayment (or sections thereof), if well-defined by the distribution of observed data.

These assumptions may be valid for Chesapeake Bay's tributaries and perhaps for the upper bay also.

Redfield applied his analytical model to three large embayments: Long Island Sound, the Bay of Fundy, and the Strait of Juan de Fuca - Georgia Strait System. The first two embayments were selected because of their relatively regular geometry. They also provide good examples of typical standing wave systems. In contrast, the Strait of Juan de Fuca System is geometrically more complex. The tidal motion in portions of the system departs markedly from that of a typical standing wave, and the type of tide is mixed. This permitted examination of the interaction of semidiurnal and diurnal tides where both components contribute significantly to the behavior of the observed tide.

He determined that the damping coefficient is of the order of 1.0 to 2.0 in these coastal embayments. However, the observed range and time of high water in the shallow regions which frequently occur near the head of tide in many coastal embayments suggest greater damping. Note that a damping coefficient of 2.0 implies an 86 percent reduction in amplitude per tidal cycle. This indicates the tide is rapidly attenuated in shallow waters.

Parker (1977 and 1980) applied Redfield's technique to more recent tide data for the Strait of Juan de Fuca system, which was observed by the National Ocean Service during an extensive tide and current survey from October 1973 through November 1976. He determined the amplitudes and phases of the tidal constituents, and used these harmonic constants to construct cophase and corange charts for the M_2 and K_1 tides. A cophase line for a particular constituent is analogous to a cotidal line for the observed tide, if the tide could be represented by a single tidal frequency. Separate cophase charts are required for each constituent. Since the range of a constituent is actually twice its amplitude, either corange or coamplitude charts can be constructed from the harmonic constants. The corange or coamplitude charts for a tidal constituent are analagous to the corange chart for the observed tide.

Parker plotted the range ratio versus the phase angle (relative to an assumed point of reflection) for the M_2 and K_1 constituents on the Redfield nomograms to determine the best fit of this data to the damping coefficient curves. He observed that the relationship between the plotted data and the curves indicated there might be energy losses in the system which were not accounted for by the Redfield model alone. He suggested these losses were possibly due to imperfect reflection of the incident wave at the head of the embayment, partial secondary reflections caused by irregular topography, and the splitting of portions of the incident wave into side channels. Imperfect reflection at the head of an embayment could be due to the nonexistence or partial existence of a reflecting barrier. Therefore, there would not be any cross section at this location through which there is no current. This would violate a boundary condition of the model. In addition, the embayment may be of sufficient width near the supposed reflecting boundary that the Coriolis effect cannot be considered negligible. In this case, the incident wave may be a Kelvin wave which would have a cross channel slope in elevation at high water. The cross channel elevation of the reflected Kelvin wave would have to be opposite in slope at this location. However, they cannot be simultaneously opposite in slope at the reflecting boundary where the Redfield model assumes the amplitudes of the incident and reflected waves are equal. A possible solution to this problem will be discussed later.

THE TWO DIMENSIONAL ANALYTICAL MODEL

A two dimensional model is needed when an embayment is of sufficient width that the Coriolis effect cannot be considered negligible, and may also be used to explain reflection in a channel where no solid reflecting barrier exits. As indicated previously, Fjeldstad (1929) developed a two dimensional frictionally damped analytical model of a progressive wave in a canal of infinite length and sufficient width that Coriolis force is not negligible. Fjeldstad's model is similar to the model shown in Figure 4 except his model is open at both ends. The major axis of the canal in this model is aligned parallel to the x axis and the tidal wave progresses in the positive x direction. Fjeldstad's assumptions and simplifications are.

1. Canal length > width >> depth > amplitude of tidal wave.
2. Constant water depth and canal width.

Figure 4. Two dimensional model of the tide in an embayment.

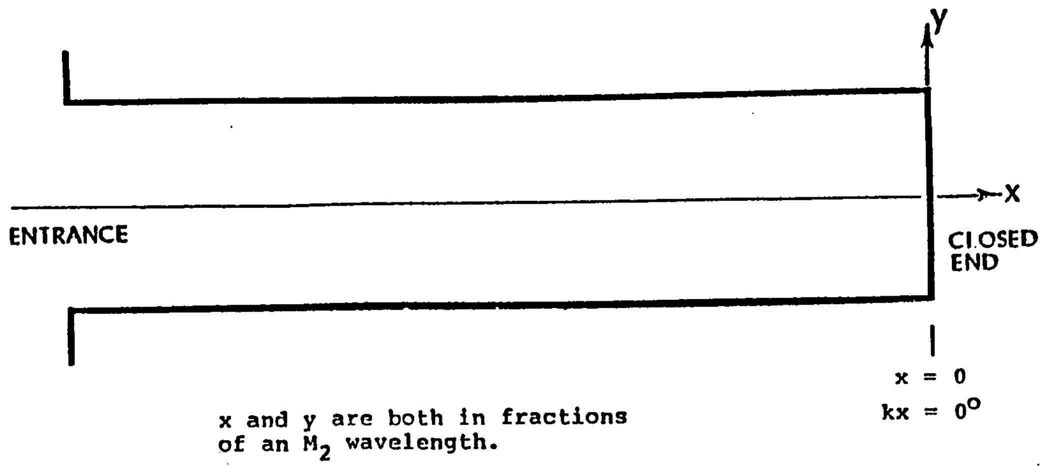

TWO-DIMENSIONAL MODEL
OF THE TIDE IN AN EMBAYMENT

3. Infinite canal length, therefore no reflection in x direction.
4. No cross channel currents.
5. Tidal system in the canal is driven only by the ocean tide at the entrance, which is periodic with a single frequency.
6. Friction is applied uniformly per unit mass.
7. The friction term is linearized and resistance is assumed proportional to the velocity.

The equations of motion (in the x and y direction) and the continuity equation are:

$$\frac{\partial u}{\partial t} = -g\frac{\partial \eta}{\partial x} - Nu \tag{24}$$

$$fu = -g\frac{\partial \eta}{\partial y} \tag{25}$$

$$\frac{\partial \eta}{\partial t} = -h\frac{\partial u}{\partial x} \tag{26}$$

where: u = vertically averaged current velocity

η = tidal elevation relative to mean sea level

N = linear coefficient representing frictional resistance

h = mean water depth

The boundary conditions at the centerline entrance to the canal, where x = 0 and t = 0, are: $\eta = a_o$ and $K_o^2 = K^2 - \mu^2$

The solutions for the tidal elevation and velocity are:

$$\eta = a_o e^{-\mu x - k\beta y} \cos(\sigma t - kx - \mu\beta y) \tag{27}$$

$$u = a_o \frac{c_o}{h} \frac{k_o}{\sqrt{\mu^2 + k^2}} e^{-\mu x - k\beta y} \cos(\sigma t - kx - \mu\beta y + \alpha) \tag{28}$$

where: $\rho = \dfrac{f\sigma}{C_o^2(K^2+\mu^2)} = \dfrac{f}{\sigma}\left(\dfrac{K^2-\mu^2}{K^2+\mu^2}\right)$

$\alpha = \tan^{-1}\left(\dfrac{\mu}{K}\right)$

a_o = amplitude of wave at centerline entrance

σ = wave frequency = $\dfrac{2\pi}{T}$

k = wave number = $\dfrac{2\pi}{L}$

T = wave period

L = wave length

C_o = frictionless wave celerity or phase speed

C = wave celerity

μ = damping coefficient per cycle or per wavelength

α = phase difference between time of maximum tidal elevation and time of maximum tidal current

Note that equation 27 describes a frictionally damped Kelvin wave. Some significant characteristics of equations 27 and 28 are.

1. The ratio, $\frac{\mu}{K}$, must be constant throughout the canal in order to satisfy the equations of motion.
2. The exponential damping factor, $e^{-\mu x}$, causes a reduction in tidal amplitude and current speed.
3. Current speed is reduced by the additional factor, $\dfrac{K_o}{\sqrt{\mu^2+K^2}}$, which is always less than unity;
4. The term $e^{-K\rho y}$ (or $e^{-K\frac{f}{\sigma}\left(\frac{K^2-\mu^2}{K^2+\mu^2}\right)y}$) is the Coriolis effect on tidal amplitude and current speed. The magnitude of this term is always one at the centerline of the channel where y = 0. Looking in the positive x direction, its magnitude is greater than one to the

right of the centerline (negative y) and less than one to the left of the centerline (positive y).

5. The term $\frac{k^2-\mu^2}{k^2+\mu^2}$ is a frictional modification of the Coriolis term that reduces its effect.
6. The Coriolis effect, modified by friction, imposes a phase shift on the tide and tidal current.
7. The occurrence of maximum current velocity is shifted relative to the maximum amplitude by the phase angle, α .
8. At the centerline of the canal (y = 0), the equations for the tidal elevation and current velocity are the same as the equations for the one dimensional model given in equations 4 and 12.

If the canal in Fjeldstad's model is closed at one end (as shown in Figure 4) and reflection of the incident Kelvin wave does occur, the reflected Kelvin wave equations for the tidal elevation and current velocity would be similar to the equations for the incident wave, with appropriate sign changes. As in the case of the one dimensional model, the combined Kelvin wave is simply the sum of the incident and reflected wave equations.

$$\begin{aligned} \eta &= \eta_i + \eta_r \\ &= 2a_0\left[\cos(\sigma t)\cos(kx+\mu \xi y)\cosh(\mu x + k\xi y) \right. \\ &\qquad \left. - \sin(\sigma t)\sin(kx+\mu\xi y)\sinh(\mu x + k\xi y)\right]. \end{aligned} \tag{29}$$

The local phase angle at high water is:

$$\sigma t_H = \tan^{-1}\left[-\tan(kx+\mu\xi y)\tanh(\mu x + k\xi y)\right] \tag{30}$$

The high water elevation is:

$$\eta_H = 2a_o\sqrt{\tfrac{1}{2}\left[\cos 2(kx+\mu\varrho y) + \cosh 2(\mu x + k\varrho y)\right]} \tag{31}$$

Similarly, the current velocity of the combined Kelvin wave is:

$$\begin{aligned} u &= u_i + u_r \\ &= 2a_o \frac{c_o}{h}\frac{k_o}{\sqrt{\mu^2+k^2}}\Big[-\cos(\sigma t)\cos(kx+\mu\varrho y)\sinh(\mu x+k\varrho y) \\ &\qquad + \sin(\sigma t)\sin(kx+\mu\varrho y)\cosh(\mu x+k\varrho y)\Big] \end{aligned} \tag{32}$$

The local phase angle or time of maximum flood is:

$$\sigma t_m = \tan^{-1}\left[-\tan(kx+\mu\varrho y)\coth(\mu x + k\varrho y)\right] \tag{33}$$

The maximum flood velocity is:

$$u_m = 2a_o\frac{c_o}{h}\frac{k_o}{\sqrt{\mu^2+k^2}}\sqrt{\tfrac{1}{2}\left[\cosh 2(\mu x + k\varrho y) - \cos 2(kx+\mu\varrho y)\right]} \tag{34}$$

Again, note there is no value of x for which $u_m = 0$ for all values of y. There cannot be a cross section through which there is no motion, hence there is no solid barrier at which a Kelvin wave can be reflected. Taylor (1920) solved this problem by adding another wave oscillation across the reflecting end of the canal. This wave is also a solution to the same equations of motion expressed in equations 24 through 26 in such a way that $u_m = 0$ for all y at x = 0. This wave is a Poincare wave of the form:

$$\eta \sim e^{s_m x + i\left(\frac{m\pi}{b}\right)y} \tag{35}$$

where: $s_m^2 = \left(\frac{m\pi}{b}\right)^2 - \left(\frac{\sigma^2 - f^2}{gh}\right)$

n = 1,2,3,...,n

b = width of canal

The amplitude of this wave decays exponentially in a narrow canal, in the direction away from the closed end, if:

$$\frac{m\pi}{b} > \frac{\sigma^2 - f^2}{gh} \tag{36}$$

The decay distance of the first mode is approximately one-third the width of the canal. Therefore, its effect will only occur near the boundary where the Kelvin wave is reflected. Hendershott and Speranza (1971) have established criteria to indicate whether a wave is reflected perfectly or if the boundary at the closed end absorbs a portion of the power flux incident upon it. These criteria are:

$$\sigma_{CR} = \sqrt{\frac{f^2 + \pi^2 gh}{b^2}} \tag{37}$$

$$h_{CR} = \frac{(\sigma^2 - f^2)\, b^2}{\pi^2 g} \tag{38}$$

where: σ_{CR} = critical frequency

h_{CR} = critical depth

Kelvin waves are reflected perfectly if $\sigma < \sigma_{CR}$ or $h > h_{CR}$.

Brown (1972) reformulated the Taylor problem to allow for the possibility of imperfect reflection of Kelvin waves. His model is a frictionless, midlatitude, constant depth canal of semi-infinite length. He determined that the mode just below the critical frequency at which Poincare mode propagation becomes possible is the principal energy reflection mechanism.

Brown also considered two limiting cases of interest. First was the case of a narrow canal, where he determined the end effect or cross channel oscillation was virtually absent and tidal behavior was similar to that expected without Coriolis force. In the second case, the period of oscillation was significantly shortened, and he determined the amplitude of the cross channel oscillation and the incident Kelvin wave were of similar magnitude and cannot be ignored.

Parker (1980) modified Redfield's one dimensional model to account for energy loss at the reflecting boundary and constructed a modified nomogram which he used to redetermine damping coefficients and wave numbers for the M_2 and K_1 tidal constituents. He obtained better agreement between the tide data, which was observed in the Strait of Juan de Fuca - Georgia Strait System, and the damping coefficient curves on the modified nomogram.

Parker also investigated applying damping coefficients, which were determined through use of the one dimensional model, to the equations describing the two dimensional frictionally damped reflected Kelvin wave model. This may be feasible because the equations derived for the two dimensional model at the centerline of the canal are the same equations that were derived for the one dimensional model, and the basic assumptions of each model are the same.

The application of damping coefficients, which were determined for the midchannel of a real embayment, to the entire width of the embayment may present problems. However, the midchannel values for $\frac{\eta}{\eta_o}$ and σt_H actually represent average values across the embayment because they were interpolated from tide observations at alongshore stations. If the bottom topography across the embayment isn't too irregular, these midchannel values can be used in the two dimensional model to provide a reasonable description of the observed Kelvin wave.

Parker applied different values for the damping coefficient to the frictionally damped reflected Kelvin wave equations for a semidiurnal tide, and plotted the results as cotidal and corange lines in order to investigate the effect of the damping coefficient on a Kelvin wave in an embayment. These plots are shown in Figure 5. Figure 5a is the frictionless case where the damping coefficient is zero. An amphidrome, which is a two dimensional node, is located midchannel at half the length of the embayment. The corange lines are nearly concentric circles, or portions thereof, which are centered on this amphidrome. The cotidal lines all originate at the amphidrome and radiate outwards with a counterclockwise rotation about the amphidrome. The six and twelve hour cotidal lines are coincident with the centerline of the bay, with the twelve hour cotidal line directed toward the closed end.

When friction is included as in 5b, 5c and 5d, the amphidrome shifts toward the left side of the bay (looking toward the closed end) and the six and twelve hour cotidal lines become skewed with respect to the centerline of the bay. The corange lines are also somewhat distorted but are still concentric to the amphidrome. The location of the amphidrome continues to move down the bay slightly toward the entrance.

When the damping coefficient is 1.0 as in Figure 5c, the amphidrome is located just beyond the left side of the bay. Since it is not located in the waterway anymore, it is called a virtual amphidrome. Now only the right half of the amphidromic pattern is located in the waterway (looking toward the closed end of the basin). The corange lines are even more distorted but are still concentric to the

Figure 5. The effect of changing the damping coefficient on a two dimensional model of a Kelvin wave in an embayment.

a. $\mu = 0$

b. $\mu = 0.5$

c. $\mu = 1.0$

d. $\mu = 1.5$

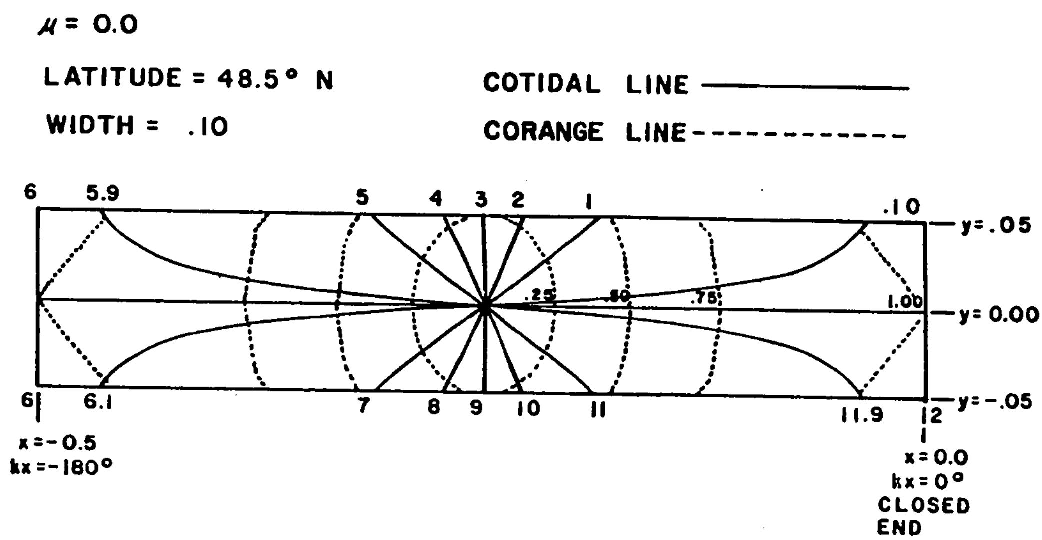

μ = 0.0
LATITUDE = 48.5° N
WIDTH = .10
COTIDAL LINE
CORANGE LINE
6
5.9
5
4
3
2
1
.10
y = .05
.25
.50
.75
1.00
y = 0.00
y = -.05
6
6.1
7
8
9
10
11
11.9
12
x = -0.5
kx = -180°
x = 0.0
kx = 0°
CLOSED
END

a

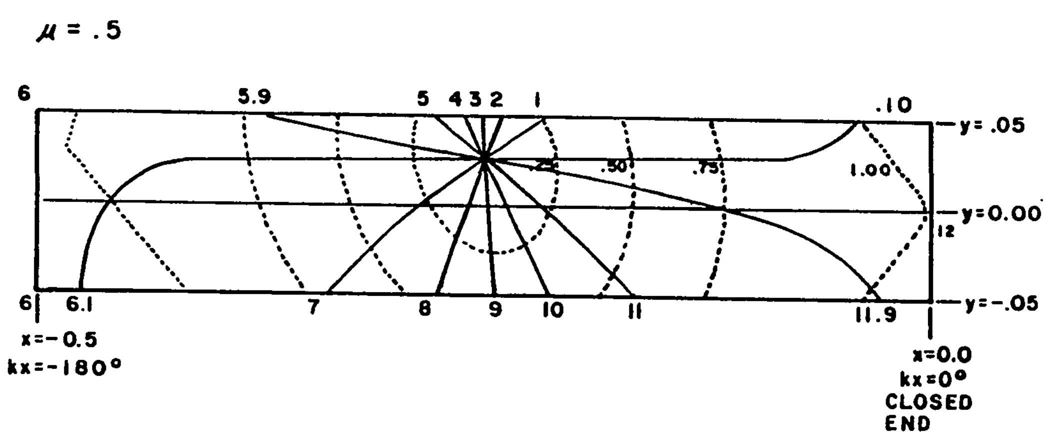

μ = .5
6
5.9
5 4 3 2
1
.10
y = .05
.25
.50
.75
1.00
y = 0.00
12
y = -.05
6
6.1
7
8
9
10
11
11.9
x = -0.5
kx = -180°
x = 0.0
kx = 0°
CLOSED
END

b

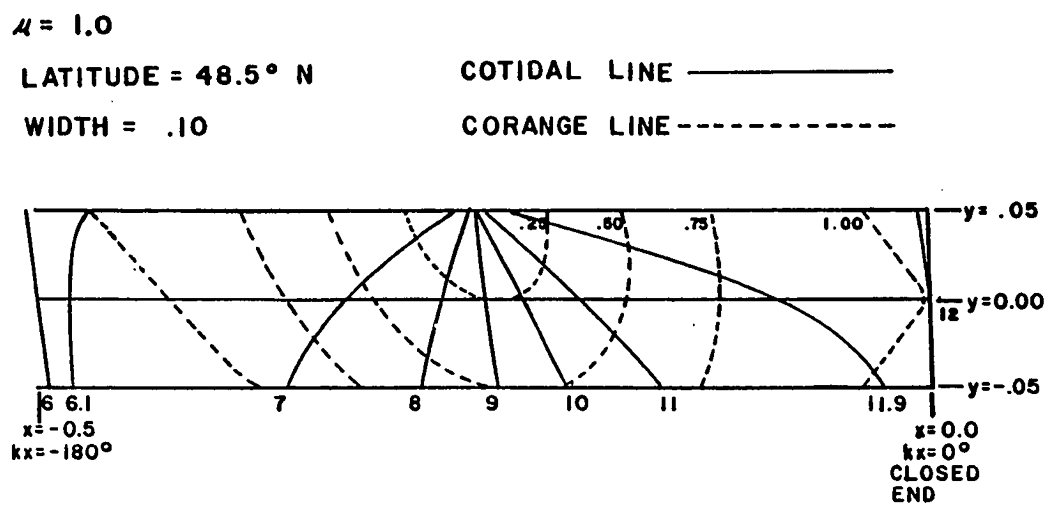

μ = 1.0
LATITUDE = 48.5° N
WIDTH = .10
COTIDAL LINE
CORANGE LINE
.25
.50
.75
1.00
y = .05
y = 0.00
y = -.05
12
6
6.1
7
8
9
10
11
11.9
x = -0.5
kx = -180°
x = 0.0
kx = 0°
CLOSED END

c

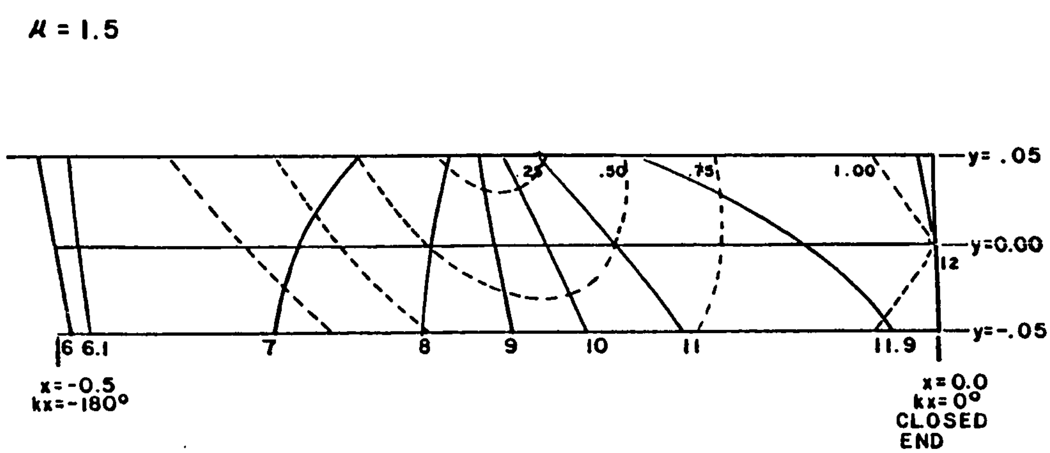

μ = 1.5
.25
.50
.75
1.00
y = .05
y = 0.00
y = -.05
12
6
6.1
7
8
9
10
11
11.9
x = -0.5
kx = -180°
x = 0.0
kx = 0°
CLOSED END

d

amphidrome. When the damping coefficient is 1.5 as in Figure 5d, the virtual amphidrome is located well outside the left boundary, and the 0.25 ft corange line is barely visible within the bay. Only a portion of the right side of the amphidromic pattern lies within the waterway, and the cotidal and corange lines are more distorted. However, the corange lines still appear to be concentric to the virtual amphidrome. The projected position of this amphidrome on the centerline of the bay indicates the amphidrome has moved further toward the entrance as it has moved off to the left (looking toward the closed end of the basin).

The amphidromic pattern when the damping coefficient is 1.5 bears some similarity to the cotidal and corange patterns observed in lower Chesapeake Bay. Even though it may not be possible to pose an exact analytical solution for a relatively wide embayment that is very irregular with numerous side channels such as Chesapeake Bay, the observed cotidal and corange patterns can be visually compared with the results of this model and inferences can be made from its similarity or lack thereof.

AMPLIFICATION OF TIDAL CONSTITUENTS IN SHALLOW WATERS

Parker (1984) also investigated the role of friction in determining the tidal characteristics of a shallow estuary, and in providing a mechanism for coupling tidal and nontidal phenomena. Using the Delaware River and Bay as an example and scaling the equations of motion, he determined that friction plays a dominant role in the tidal dynamics of a shallow estuary because of the low frequencies of motion involved. He showed that frictional effects increase with: a decrease in depth, an increase in tidal amplitude, or a decrease in frequency.

Nonlinear frictional effects were shown to be important in the transfer of energy and momentum among the tidal frequencies, and in the interaction of the tide with river flow and low frequency storm surge. These nonlinear mechanisms are accounted for in the hydrodynamic equations by the quadratic term representing frictional momentum loss, the term representing the variation in frictional effect due to changing elevation, and by first order frictional effects via the nonlinear continuity term.

These nonlinear effects are shown to be at least as important as the effect of the shallow water terms of the hydrodynamic equations, which include the nonlinear continuity term and the inertial (convective) term (Gallagher and Munk, 1971, LeBlond, 1978, Kabbaj and LeProvost, 1980, and Parker, 1984). The nonlinear term in the continuity equation and the inertial term generate mean effects, such as tidally induced changes in mean sea level, and generate even harmonics of tidal constituents. However, it is shown that the term representing the elevation effect on frictional momentum loss can generate these same effects. The nonlinear term in the continuity equation is also shown to depend on first order (linear) frictional effects. The importance of the inertial term is reduced in the upchannel direction due to friction, decreasing channel width, and reflection, which cause the tide to become more like a standing wave.

The quadratic frictional resistance term is shown to generate odd harmonic overtides, semidiurnal tides, terdiurnal tides, fifth diurnal tides, and higher frequency compound tides; provide the mechanism whereby the presence of a larger elementary constituent causes the reduction in amplification of smaller elementary constituents; and provides the mechanism whereby river flow reduces the tide range and generates even harmonic overtides.

The nonlinear continuity term and the elevation effect on the frictional momentum loss term are shown to generate even harmonic overtides, terdiurnal tides, quarterdiurnal tides and very low frequency compound tides; generate tidally induced changes in mean sea level, provide a coupling mechanism whereby low frequency storm surge and local wind setup or setdown affect the amplitude and phase of the tidal constituents; and provide a mechanism for the smearing of tidal spectral lines by low frequency storm surges.

Parker constructed coamplitude and cophase charts of the Delaware River and Bay for 14 tidal constituents, based on tide data observed at 21 locations along the estuary. He also prepared graphs of the variation in amplitude and phase of tidal constituents along the Delaware River and Bay, and explained the amplification of these constituents as the tidal wave travels up the waterway to the point of reflection.

He determined first order solutions of the linearized equations of motion for simple basin geometries, and developed a linear friction, exponential width analytical model of the Delaware River and Bay. The data analysis results for the M_2 and K_1 waves fit the model very well, considering the shallowness of the estuary.

It was observed that the tidal dynamics of the dominant M_2 tidal constituent were fairly accurately reproduced using a linearized friction term. However, as in the case of the Redfield model, the damping coefficient cannot be determined _a priori_, and must be determined by fitting observed data to the model.

The analytical model demonstrated a number of first order effects of friction on the tidal dynamics of the estuary. Friction decreases the wave propagation speed of the tidal wave and its wavelength. In comparison, the exponential decrease in width causes the opposite effect. However, friction and the exponential decrease in width both cause the damping coefficient to increase. Friction also causes attenuation of tidal amplitude as the wave proceeds from the entrance to the point of reflection.

For small damping coefficients, amplification depends on the wavelengths of the tidal constituents relative to the length of the basin. Friction also affects how rapidly the phase of high water changes along the basin. If the damping coefficient is small, the phase changes little with distance except near the quasinode, and the tide is nearly a pure standing wave. Increased friction will cause larger phase changes with distance until the wave eventually becomes a pure damped progressive wave.

Since a linear friction model cannot describe the nonlinear interaction effects resulting from the true quadratic nature of frictional momentum loss, Parker used a finite difference technique to solve the nonlinear forms of the continuity and momentum equations. The resulting numerical model was then used to demonstrate the effects of these nonlinear terms in the Delaware River and Bay, the relative importance of each in causing the generation of compound tides and overtides, the effect of river discharge on the tide, and the effect of low frequency storm surge on the tide.

The numerical model was tested by reproducing the linearized solutions which were obtained with the analytical model. The numerical model was also run on several ideal constant width and constant depth cases to demonstrate that the frictional effects predicted in the theoretical analysis were also produced by the numerical solution. The model was then applied to the Delaware River and Bay, and used to produce the same nonlinear effects seen in the observed data. It was also used to quantify these nonlinear effects, and determine the relative importance of several mechanisms that can have the same effects.

CHAPTER 3

THE FIELD PROGRAM

DESIGN OF THE FIELD PROGRAM

The tide and current data used in this study to describe the tidal circulation of Chesapeake Bay and its major tributaries were obtained during an extensive tide and current survey of Chesapeake Bay by the National Ocean Service from August 1981 through December 1983. These data were supplemented by tide data which was collected during a cooperative project between the National Ocean Survey (National Ocean Service) and the U. S. Army Corps of Engineers in the early 1970s. This project obtained tidal information for use in construction of the Corps of Engineers' physical model of Chesapeake Bay. The National Ocean Survey installed approximately 60 tide gauges at locations in Chesapeake Bay and its tributaries for periods of one year or longer. Some of these tide stations were added to the National Tide and Water Level Observation Network and have been in continuous operation since installation. The National Ocean Survey analyzed this tide data and provided the results to the Corps of Engineers.

The 1981-1983 tide and current survey of Chesapeake Bay was conducted to update tide and tidal current predictions, provide estuarine and navigational information, and to define tidal datums for shoreline boundary determination. Most of the field work was accomplished by the NOAA Ship

FERREL, an estuarine research vessel whose home port is Norfolk, VA. It is 133 ft long and 32 ft wide, has a maximum draft of 8 ft, a displacement of 360 tons, and a personnel complement of five commissioned officers and 14 crew. The arrangement of cranes, A-frames, and winches on a large, open afterdeck, along with twin screw propulsion and a bowthruster, provide an excellent platform for deploying and retrieving current meter moorings and conducting other oceanographic operations in estuaries.

This tide and current survey was designed by the Ocean Requirements and Data Analysis Division of the National Ocean Service in coordination with personnel from the FERREL and the Operations Division of the NOAA Atlantic Marine Center in Norfolk, VA. Planning for this survey was also guided by a working group which consisted of representatives from various universities, agencies, environmental groups, and individual citizens who are interested in the bay. Old Dominion University participated in this working group. The survey was also planned in cooperation with other Federal and state agencies who were conducting studies in the bay at the same time. For example, field operations in 1981 were coordinated with the U S Geological Survey which was conducting a multiyear current measurement program in the Potomac River.

The working group recommended that the tide and current should be continuously observed at key locations throughout the bay during the two and a half year survey. These observations were needed to describe seasonal changes and other long term variations in the circulation. For many years, the National Ocean Service has been able to operate tide gauges for long periods of time at shoreside installations, but has had to limit current meter station deployments to the availability of a support vessel.

The National Ocean Service used a new approach to obtain long term current meter observations during this survey. Cooperative agreements were established with Old Dominion University (Houlder and Dunston, 1982), the Virginia Institute of Marine Sciences, and the Maryland Department of Natural Resources to maintain four key long term current meter stations while the FERREL was occupied elsewhere in the bay. The location of these long term stations are indicated by large circles in Figure 6. Personnel from Old Dominion University and the NOAA Atlantic Marine Center maintained a current meter station in Chesapeake Bay Entrance throughout the entire survey, except for the period when the FERREL maintained it while working in the area. The current meters were changed by divers every month and acoustically monitored every other week to ensure proper operation. The Atlantic Marine Center provided the current meters, acoustic monitoring equipment and a Divemaster, and Old Dominion University provided a dive boat and students who were NOAA qualified divers. This operation proved very successful.

In addition to the aforementioned long term current meter stations, approximately 120 shorter term current meter stations were deployed throughout the Bay Proper and the Chesapeake and Delaware Canal during this survey. These stations were deployed for periods ranging from a minimum of 7.5 days up to a half year. Site selection was based on navigational requirements, potential application to future modeling, and to satisfy requirements of non-NOS participants in the survey where possible within the resources available. The locations of these shorter term current meter stations are indicated by smaller circles in Figure 6.

Figure 6. Location of tide and current meter stations deployed by the National Ocean Service in Chesapeake Bay and its tributaries during the past decade.

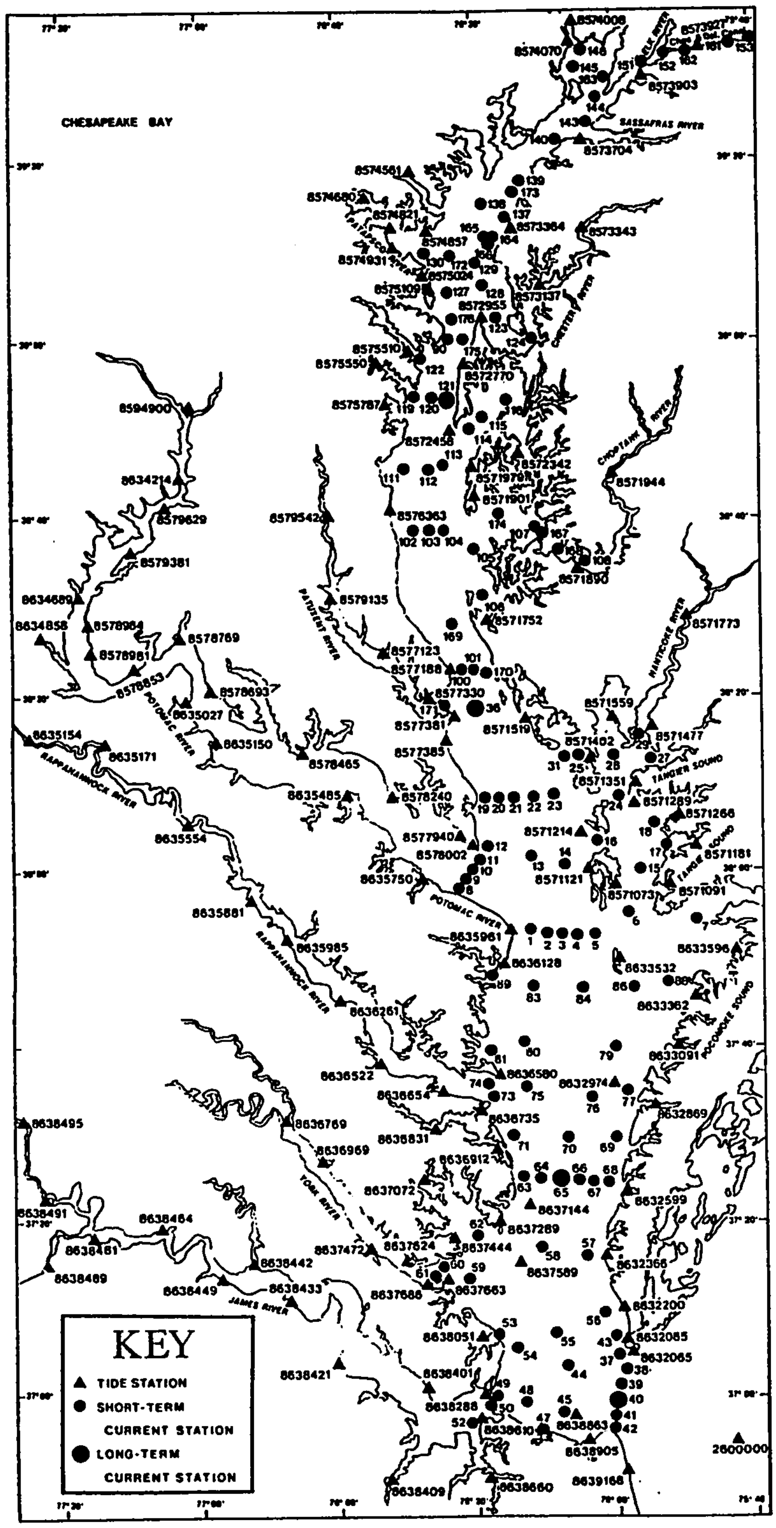
CHESAPEAKE BAY
KEY
TIDE STATION
SHORT-TERM CURRENT STATION
LONG-TERM CURRENT STATION

There are 12 tide stations in Chesapeake Bay and its tributaries which are part of the National Tide and Water Level Observation Network. These primary tide stations are permanent installations and have been continuously in operation for years. Approximately 35 shorter term tide stations were installed during the tide and current survey for periods of 30 to 180 days to provide data to update tide predictions and to provide simultaneous tide and current observations for analysis. These tide stations, along with the tide stations deployed during the Corps of Engineers cooperative project, obtained tide observations at 129 locations throughout the bay and major tributaries. The locations of these tide stations are indicated by triangles in Figure 6.

The FERREL also deployed six portable meteorological stations at sites onshore and on offshore structures in the Bay Proper. These stations, in addition to selected National Weather Service meteorological stations, provide data to assist in analyzing the tide and current observations and to correlate with observed nontidal effects.

Water temperature and conductivity versus depth measurements were also observed at approximately 270 hydrographic stations which were part of a system of longitudinal and transverse sections throughout the Bay Proper. In addition, time series were obtained for at least one semidiurnal cycle at 18 key locations. This data is used to describe estuarine effects and to assist in analyzing the tide and current data.

The author participated in most phases of planning and conducting this survey. While Chief of the Operations Division at the NOAA Atlantic Marine Center, he was involved in planning the survey and served as liaison between the NOAA ship FERREL and the National Ocean Service's Ocean Requirements and Data Analysis Division in Rockville, MD. He also served later as liaison with Old Dominion University while attending full time university training, and coordinated maintenance of the long term current meter station in Chesapeake Bay Entrance. The author has also participated in the National Ocean Service's processing of the current meter data, and performed the analyses described in this study. In addition, he has served as Executive Officer of the FERREL during similar projects.

DATA COLLECTION

Tide observations were obtained using either Fischer-Porter analog to digital recording (ADR) gauges, which record movement of a float in a stilling well, or with Metercraft "bubbler" gauges, which record hydrostatic pressure fluctuations due to changes in water elevation above an oriface and produce an analog record. The National Ocean Service's procedures for installation and operation of these gauges are documented in the U. S. Coast and Geodetic Survey Manual of Tide Observations (1965). Sketches of a typical tide station and a "bubbler" gauge and record are shown in Figures 7 and 8, respectively. The ADR gauges recorded the water level every six minutes and were mounted on six or twelve inch stilling wells which damped out most of the wave action by means of the size of the oriface in the well. This gauge required installation on a pier or offshore structure in order to support the well and tide staff.

The "bubbler" gauge purges nitrogen gas through a flexible hose and oriface. Hydrostatic pressure is sensed as back pressure on the gas at the oriface, and these pressure fluctuations are converted mechanically to an analog record called a marigram. Most wave action was damped mechanically by means of a valve in the gas line. This gauge did not

Figure 7. A typical National Ocean Service primary tide station.

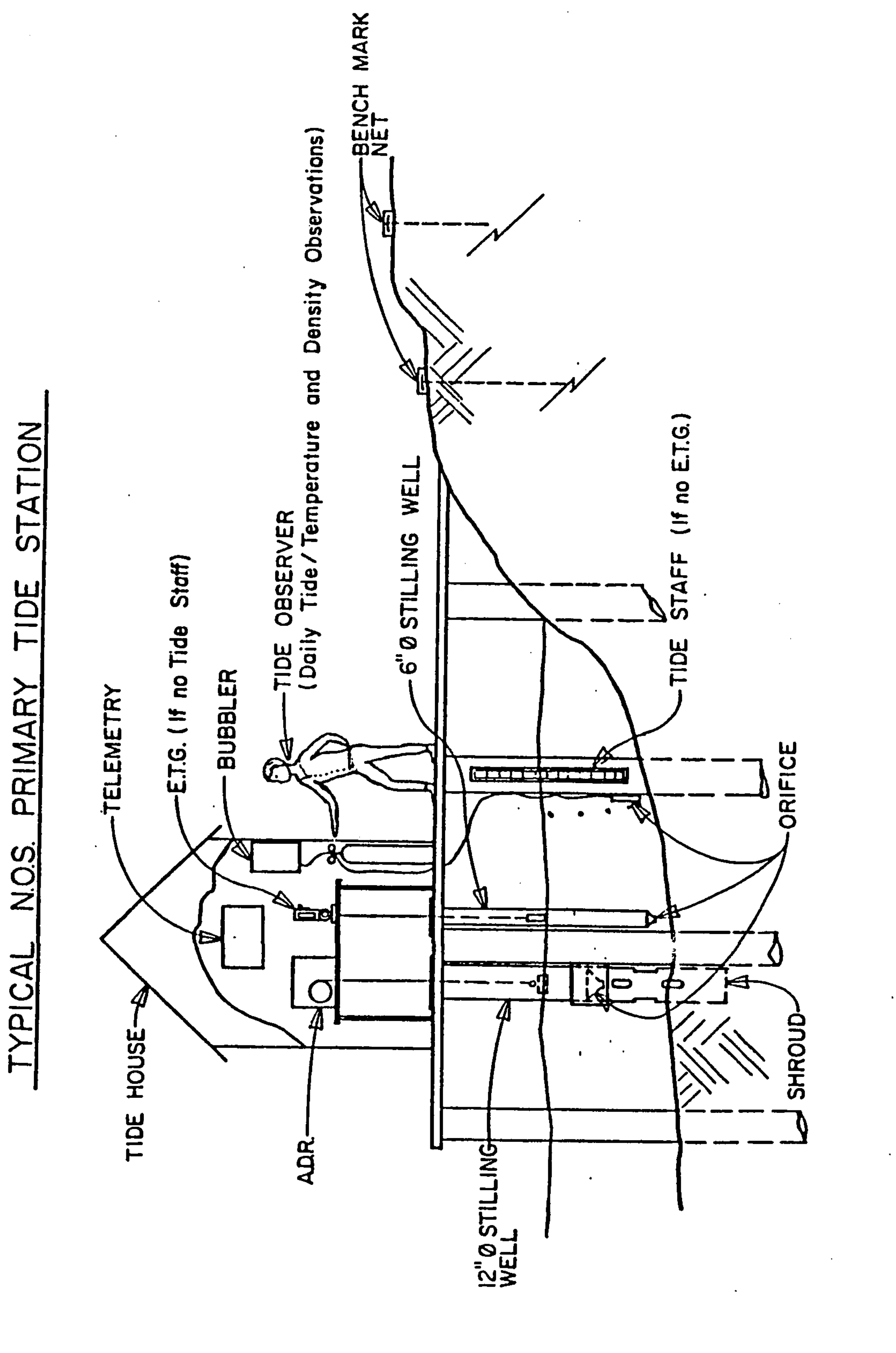
TYPICAL N.O.S. PRIMARY TIDE STATION
TIDE HOUSE
TELEMETRY
E.T.G. (If no Tide Staff)
BUBBLER
TIDE OBSERVER
(Daily Tide / Temperature and Density Observations)
BENCH MARK
NET
6"Ø STILLING WELL
TIDE STAFF (If no E.T.G.)
ORIFICE
SHROUD
A.D.R.
12"Ø STILLING
WELL

Figure 8. A pressure operated tide gage.

PRESSURE OPERATED TIDE GAGE

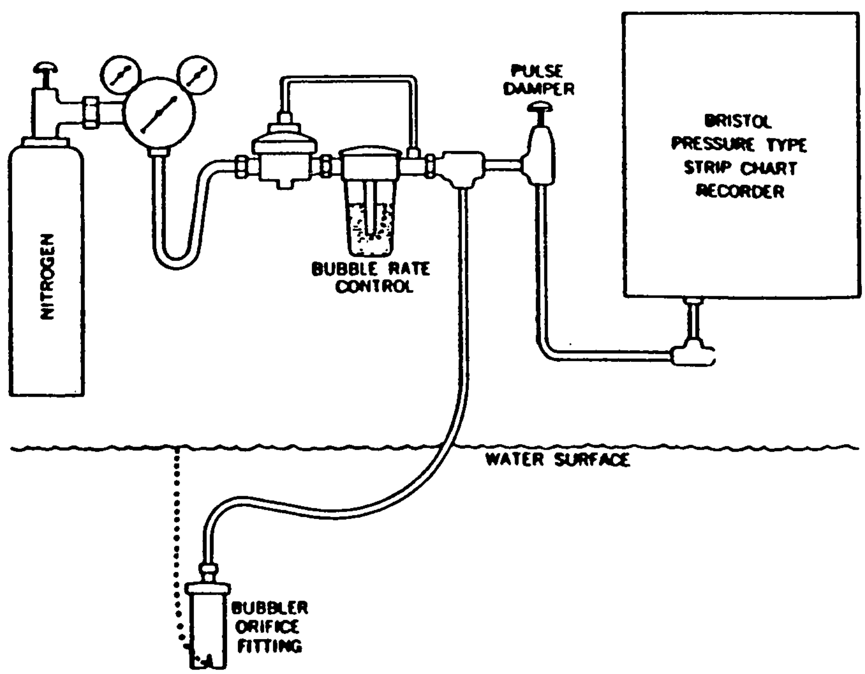

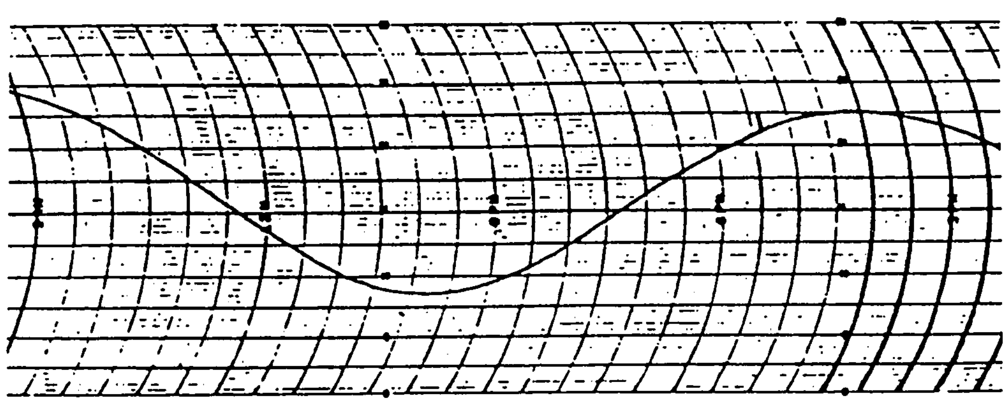

require a major structure for installation, and was typically used where shoal areas extended offshore or no offshore structure was available.

A tide staff reading was compared to the gauge value daily (when possible) to determine proper operation of the gauge and to provide a mathematical relationship to the staff. The zero mark on the staff was related by differential leveling techniques to a set of tidal benchmarks which were located onshore in stable foundations. This was done at installation and removal of the station to determine any station instability, such as subsidence of a pier, and to provide the relationship necessary to transfer tidal datums, once computed from gauge data, to absolute elevations referenced to the benchmarks.

The current meter data was obtained using Grundy model 9021 current meters which measured current speed and direction, water temperature, and conductivity. Some of the meters also measured hydrostatic pressure which was primarily used to indicate the depth of deployment of the meter. The meters sampled every ten minutes, and data was recorded internally on magnetic tape. Timing was determined by comparing the number of sequential samples observed to both the start/stop and the in-water/out-of-water times.

The current meters were deployed at preselected depths on taut-wire subsurface moorings. A sketch of a typical taut-wire mooring is shown in Figure 9. Usually the near surface current meter was deployed about 15 feet below the surface at Mean Low Water (water depth permitting) to avoid the influence of surface wave action. The near bottom current meter was deployed five to eight feet above the bottom to clear the anchor and avoid fouling. Intermediate depth meters were deployed when stations were located in deeper waters.

Figure 9. A typical National Ocean Service taut-wire current meter mooring system.

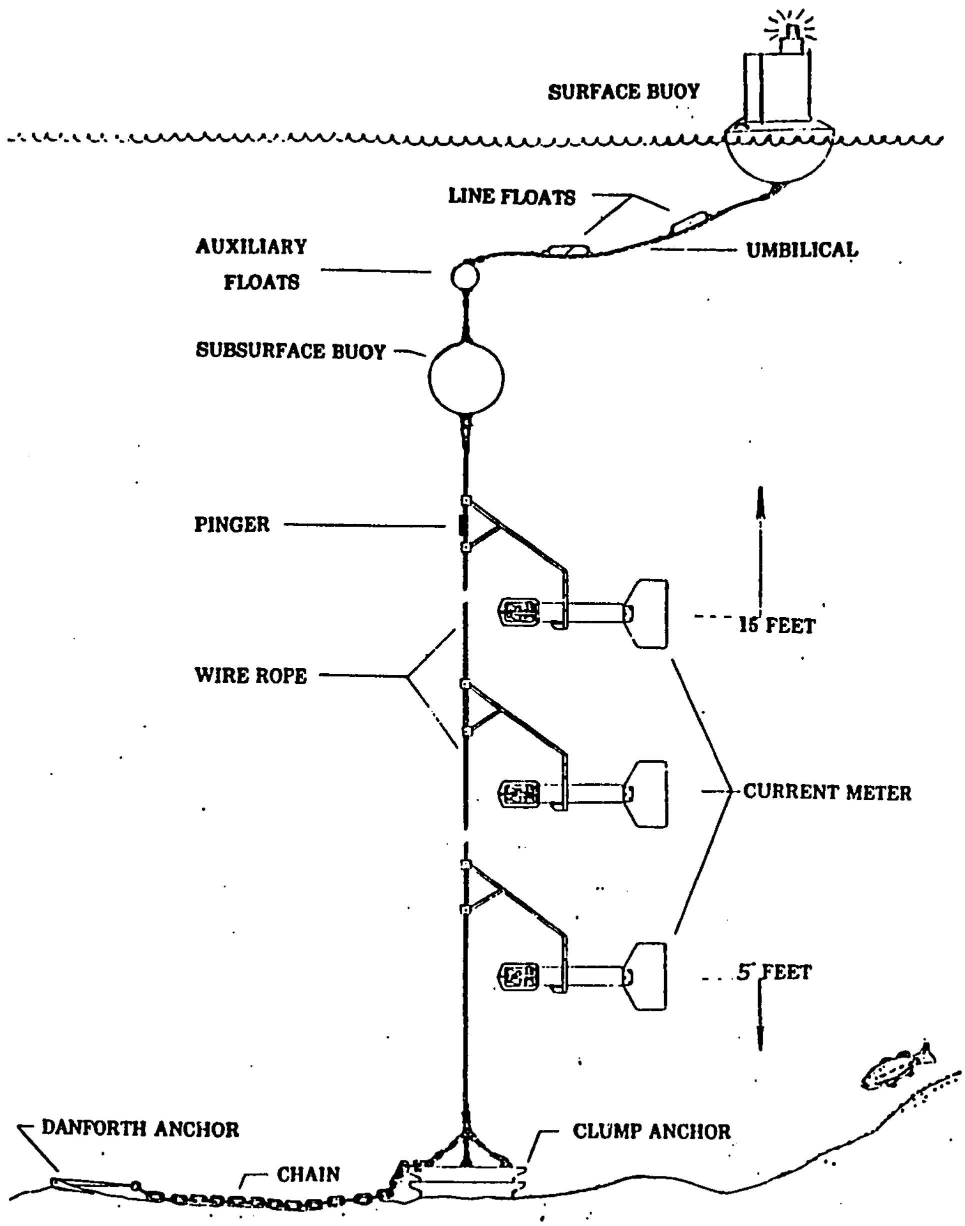
SURFACE BUOY
LINE FLOATS
AUXILIARY FLOATS
UMBILICAL
SUBSURFACE BUOY
PINGER
15 FEET
WIRE ROPE
CURRENT METER
5 FEET
DANFORTH ANCHOR
CLUMP ANCHOR
CHAIN
Not Drawn to Scale

The National Ocean Service has established a data quality assurance program for its oceanographic instrumentation. Current meters are calibrated before and after each field season, and checked out prior to each deployment. The control of data quality in the field is prerequisite to obtaining calibration constants for use in data processing.

Water temperature and conductivity measurements versus depth were obtained using a Grundy model 9400 Conductivity-Temperature-Depth (CTD) system, and a Beckman model RS-5 CTD system was used for backup. The Grundy system measures conductivity, temperature and depth (pressure) in situ, and digitally records the data on deck or is interfaced directly to the FERREL's PDP 11/34 computer. The Beckman system also measures conductivity and temperature in situ, but only has an on-deck readout. Depth is determined by the amount of cable lowered.

Temperature, conductivity, and pressure sensor field checks of these instruments were performed aboard ship using temperature baths, wire loop conductivity cells, a pressure generating system, and a Paroscientific field standard. Niskin casts were taken in conjunction with a limited number of CTD casts to check the performance of the systems. Comparative temperatures were obtained with reversing thermometers, and the conductivity of the Niskin water samples was obtained using a Guideline model 8400 AutoSal. Standardization of the AutoSal was performed at the beginning, midpoint, and completion of the survey.

Meteorological data was obtained using Aanderaa meteorological stations which record wind speed and direction, air temperature, and barometric pressure every six minutes on magnetic tape. The Aanderaa sensors were calibrated before and after each field season, in accordance with the data quality assurance program.

CHAPTER 4

DATA PROCESSING

TIDE DATA

Tide (water level) data from all stations observed by the National Ocean Service in Chesapeake Bay and its major tributaries during the past 20 years were reviewed to determine which unbroken time series were of sufficient length for analysis, yet would also provide the best spatial coverage. The name, station number, location, and date of installation and removal for each tide station are summarized in Appendix A.

The Analog to Digital Recording (ADR) tide gauge data was transcribed and processed by the Tides and Water Levels Branch of the National Ocean Service using automated techniques. Analog "bubbler" tide gauge records were manually digitized. Water level heights were tabulated from both types of record at hourly intervals. The times and heights of high and low water were recorded as a separate table.

The tidal component of this water level data has been determined using both nonharmonic and harmonic analysis techniques. Nonharmonic techniques were used to determine mean values for Greenwich high water and low water lunitidal intervals, tidal datums, and mean range of tide for all tide stations (Marmer, 1951). The results are summarized in Appendix A. These results are also used to compile the "Table of Tidal

Differences and Other Constants" which is published in the annual tide prediction tables (U. S. National Ocean Survey, 1983a).

Harmonic analysis, whether by Fourier or least squares techniques, involves separation of tidal constituents of known periods from the data, orientation of the constituent tides with their astronomic elements, and elimination of effects from tidal constituents other than the constituent sought (Dennis and Long, 1971). The amplitudes and phases of the tidal constituents are referred to as harmonic constants. An equation describing the height of tide at any time can be expressed as:

$$h = H_0 + \sum_{n}^{m} f_n H_n \cos\left[a_n t + (V_0 + u)_n - \kappa_n\right] \tag{39}$$

and:

$$H_0 = \frac{1}{N} \sum_{i=0}^{N-1} h_i \tag{40}$$

where:

h = height of tide at any time t

H_0 = mean value of tide observations; corresponds to the height of mean sea level above an adopted datum

t = time reckoned from some arbitrary point

f_n = node factor of constituent

H_n = mean amplitude of constituent

a_n = speed of constituent

κ_n = epoch (phase) of constituent at t=0, for period of observation

$(V_0+u)_n$ = argument of constituent at t=0, for period of observation

n = particular constituent being computed = 1,..., m

m = total number of constituents computed

N = total number of data values being used in the analysis

The National Ocean Service generally uses computerized least squares harmonic analysis techniques to analyze a 365 day time series of tide observations to determine harmonic constants for 37 tidal constituents. This program was developed by Harris et al. (1963), based on equations from Schureman (1958). This program can also be used to analyze shorter time series if one reduces the number of tidal constituents sought to only those that can be separated in that time series. The National Ocean Service also uses a Fourier harmonic analysis technique developed by Schureman (1958) and programmed by Dennis and Long (1971) to analyze any 29 day portion thereof to determine harmonic constants for 15 tidal constituents. Only harmonic constants for five major tidal constituents and overtides are actually computed by this technique. The remaining constituents are inferred using equilibrium tide theory (Schureman, 1958 and U. S. Coast and Geodetic Survey, 1952).

When the 29 day Fourier technique was used on repeated time series at the same station, it was observed that there was too much temporal variability in the harmonic constants to be able to select representative values for construction of cotidal lines for specific constituents. Parker (1984) used the least squares harmonic analysis technique of Harris et al. (1963) with tide data time series of all lengths. The node factors for the midpoint of each time series and equilibrium arguments were calculated using a program by Long (1983) to provide input for the harmonic analysis program.

Table 3, reproduced from Parker (1984), lists the 37 tidal constituents routinely determined from a one year time series by the National Ocean Service in an order that reflects the length of the data series needed to separate each constituent from a previous one. The angular speed (frequency) of each constituent, expressed in degrees per solar hour, is shown in the second column. One constituent cycle (360°) divided by the angular speed gives the period of the constituent in solar hours. The origin of the constituent is indicated in the third column. The cause of the tide may be either lunar, solar, lunisolar, or shallow water in origin. The first three causes represent astronomical effects, which result from periodic variations in the tide producing forces due to movement of the sun and moon relative to the Earth. The tidal constituents caused by astronomical effects are called elementary constituents. A shallow water constituent is caused by the nonlinear interaction of two elementary constituents that occurs in shallow water.

In some cases, an elementary constituent and a shallow water constituent may have exactly the same frequency. For example, the smaller lunar elliptic semidiurnal constituent, L_2, has the same frequency as the semidiurnal compound constituent $2MN_2$, whose angular speed is twice the speed of M_2 minus the speed of N_2. Also, the semidiurnal variational constituent, μ_2, has the same frequency as the semidiurnal compound constituent $2MS_2$, whose angular speed is twice the speed of M_2 minus the speed of S_2. According to Schureman (1958), there is no practical way of separating an elementary constituent from the compound constituent of the same speed. In these cases, the depth of water should be considered when interpreting whether a constituent with

TABLE 3

ORDERING OF TIDAL CONSTITUENTS

Constituent	Speed Deg/Hour)	Origin	Days Needed to Separate	From:	Amplitude at Trenton	Amplitude at Wash. DC
M_2	28.984104	Lunar	---	---	3.547	1.302
M_4	57.968208	Shallow-water	0.5	M_2	.517	.143
M_6	86.952313	Shallow-water	0.5	M_4	.266	.040
M_8	115.936417	Shallow-water	0.5	M_6	.120	.013
K_1	15.041069	Lunisolar	1.1	M_2	.349	.149
O_1	13.943036	Lunar	13.7	K_1	.288	.089
MK_3	44.025173	Shallow-water	13.7	$2MK_3$	.120	.013
$2MK_3$	42.927140	Shallow-water	13.7	MK_3	.116	.042
OO_1	16.139102	Lunar	13.7	K_1	.030	.013
$2Q_1$	12.854286	Lunar	13.8	O_1	.028	.011
S_2	30.000000	Solar	14.8	M_2	.461	.174
S_4	60.000000	Shallow-water	7.4	M_4	.005	.001
S_6	90.000000	Shallow-water	4.9	M_6	.005	.001
MS_4	58.984104	Shallow-water	14.8	M_4	.148	.039
$2SM_2$	31.015896	Shallow-water	14.8	S_2	.025	.019
M_3	43.476156	Lunar	27.3	MK_3	.034	.013
M_1	14.492052	Lunar	27.3	K_1	.027	.004
N_2	28.439730	Lunar	27.6	M_2	.553	.242
MN_4	57.423834	Shallow-water	27.6	M_4	.176	.055
Mm	0.544375	Lunar*	27.6	---	.124	.112
Q_1	13.398661	Lunar	27.6	O_1	.022	.006
J_1	15.585443	Lunar	27.6	K_1	.016	.012
$2MN_2/L_2$	29.528479	Shallow/lunisolar	31.8	S_2	.409	.107
$2MS_2/mu_2$	27.968208	Shallow/Lunar	31.8	N_2	.219	.031
MSf	1.015896	Lunar*	182.6	Mf	.186	.063
Mf	1.098033	Lunar*	182.6	MSf	.132	.025
P_1	14.958931	Solar	182.6	K_1	.110	.040
K_2	30.082137	Lunisolar	182.6	S_2	.094	.041
nu_2	28.512583	Lunar	205.9	N_2	.210	.048
$lamda_2$	29.455625	Lunar	205.9	$2MN_2$	.102	.033
$2MN_2/2N_2$	27.895355	Shallow/Lunar	205.9	$2MS_2$	.042	.026
rho_1	13.471514	Lunar	205.9	Q_1	.013	---
Sa	0.041069	Solar*	365.2	SSa	.430	
Ssa	0.082137	Solar*	365.2	Sa	.169	
S_1	15.000000	Solar	365.2	K_1	.062	.054
T_2	29.958933	Solar	365.3	S_2	.056	.017
R_2	30.041067	Solar	365.3	S_2	.028	.009

*Values are determined predominantly by long term meteorological effects and thus vary from year to year.

one of these frequencies is mainly of astronomical or shallow water origin.

The number of days required to separate a constituent from its largest neighbor constituent, that is one with nearly the same frequency, is indicated in the fourth column, and the name of this neighbor constituent is given in the fifth column. The amplitude of each constituent which was determined from a 365 day least squares harmonic analysis of tide observations from January 1 to December 31, 1981 at Trenton, NJ is shown in the sixth column.

A seventh column has been added to this table which shows the constituent amplitudes for tides observed at Washington, DC in order to compare Parker's results to tide characteristics observed at a location near the limit of tide in a major tributary of Chesapeake Bay. These amplitudes were determined by the same least squares technique from a 366 day series of tide observations at Washington, DC which commenced on September 1, 1979. If the amplitudes of constituents at Trenton and Washington, DC are scaled to the same ratio as their respective M_2 amplitudes, it is shown that the relative sizes of the amplitudes at each location are similar. This suggests that the ordering of constituents and criteria for separation of neighbor constituents expressed in Table 3 can be applied to tidal constituents in Chesapeake Bay and its major tributaries also.

The order begins with M_2, which is by far the largest constituent observed in either the Delaware River and Bay or Chesapeake Bay and its major tributaries. The remaining constituents continue to be arranged according to both the increased length of time series required to separate a constituent from a previously determined neighbor constituent and by decreasing size of amplitude.

Those constituents arranged near the top of the list can be calculated from shorter time series than those located further down the list. However, longer time series are desired, not only to determine more constituents, but also because constituents can be determined more accurately with a longer series. Harmonic constants determined from shorter time series still contain errors due to the effect of neighbor constituents which could not be separated out. In addition, the effect of an unresolved constituent will depend on the astronomical conditions at the time the data was observed.

However, the effect of these unknown errors can be accounted for by determining the harmonic constants for a nearby long term station that has similar tidal characteristics for the same short period and a year-long series of observations which encompasses this period. This station can then serve as a reference station for adjusting the harmonic constants which were determined for the short term station. Amplitude ratios and phase differences can be determined for the same constituents at the reference station using the harmonic constants determined for both the long period and the short period time series. These ratios and differences can be applied to the harmonic constants calculated from the shorter time series, resulting in the determination of equivalent long term values. This technique was tested and used by Parker in 1977 and 1984, and has proven successful for use in constructing accurate coamplitude and cophase charts for tidal constituents.

Therefore, Parker's techniques were used during all harmonic analysis of tide data during this study. The least squares harmonic analysis of a year-long time series was preferred, since harmonic constants for all 37 tidal consituents could be determined. The harmonic constants for the long term meteorological constituents Sa and SSa may vary significantly from year to year. However, the magnitude of their amplitudes, compared to M_2, may be relatively large, especially in estuaries. Mean values for these long term constituents, based on harmonic constants which have been determined for a number of consecutive 365 day series, are required before they can be used for tide prediction. Such repetitive time series were not generally available in the Chesapeake Bay tide data. Therefore, harmonic constants for these constituents have been rejected, since they might bias the results in any given year.

For time series shorter than 365 days, the results shown in Table 3 indicate that 34 constituents might be determined from a time series of at least 205 days. In fact, 34 constituents were occasionally determined from time series as short as 150 days during this study. Parker (1984) suggested this least squares technique appears to be more "forgiving", relative to the 205 day requirement, than the Fourier harmonic analysis technique. During his study of the Delaware River and Bay, acceptable results were obtained for 34 constituents when as few as 154 days of data were analyzed using this technique. Therefore, the number of days required to separate neighbor constituents indicated in Table 3 are a general criterion, and occasionally separation can be accomplished with a shorter series of tide observations.

If a time series was not of sufficient length for an analysis to determine 34 constituents, only the 15 major constituents were determined by the least squares technique. The harmonic constants were reduced to 365-day equivalent values using the technique which has been described.

The harmonic constants for 108 locations throughout Chesapeake Bay and its major tributaries were determined during this study and are presented in Appendix B. Included for each location are: station name and identification number, location, beginning date of series, length of series, reference station identification number (if correction to long term series was required), and the amplitudes and phases of whichever constituents could be determined depending on the length of the time series.

Figures 10 and 11 are amplitude spectral line plots of the tidal constituents for tide stations located in Chesapeake Bay Entrance and at Washington, DC. The amplitude of each constituent has been plotted on a four cycle logarithmic scale so that the smaller amplitude constituents can also be seen. The Chesapeake Bay Entrance site was selected to represent the tide before it becomes significantly affected by the characteristics of the bay. In comparison, the Washington, DC site was selected to represent the tide in the upper tidal region of a major tributary where shallow water effects are expected to occur. These plots show that the shallow water constituents are much larger in amplitude at Washington, DC. The amplitudes of the elementary constituents aren't significantly different at either location.

CURRENT METER DATA

Data from all current meters deployed within 15 ft of the surface (at Mean Low Water) during the tide and current survey was also evaluated to determine which unbroken time series were of sufficient length

Figure 10. Amplitude of tidal constituents at Chesapeake Bay Entrance.

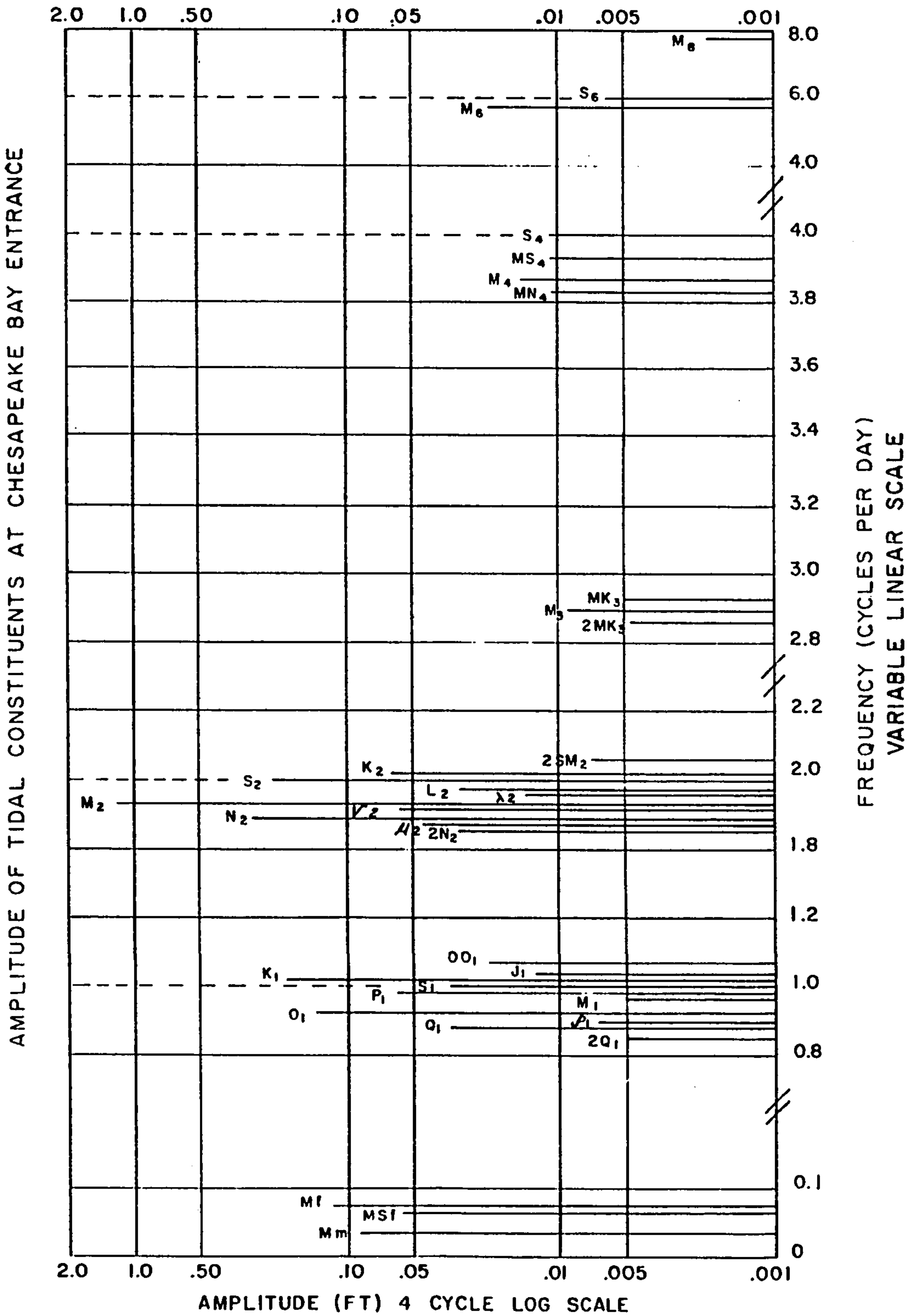
AMPLITUDE OF TIDAL CONSTITUENTS AT CHESAPEAKE BAY ENTRANCE
FREQUENCY (CYCLES PER DAY)
VARIABLE LINEAR SCALE
AMPLITUDE (FT) 4 CYCLE LOG SCALE
2.0
1.0
.50
.10
.05
.01
.005
.001
8.0
6.0
4.0
4.0
3.8
3.6
3.4
3.2
3.0
2.8
2.2
2.0
1.8
1.2
1.0
0.8
0.1
0
M8
S6
M6
S4
MS4
M4
MN4
MK3
M3
2MK3
2SM2
K2
S2
L2
λ2
M2
N2
ν2
μ2
2N2
OO1
J1
K1
P1
S1
M1
O1
Q1
ρ1
2Q1
Mf
MSf
Mm

Figure 11. Amplitude of tidal constituents at Washington, DC.

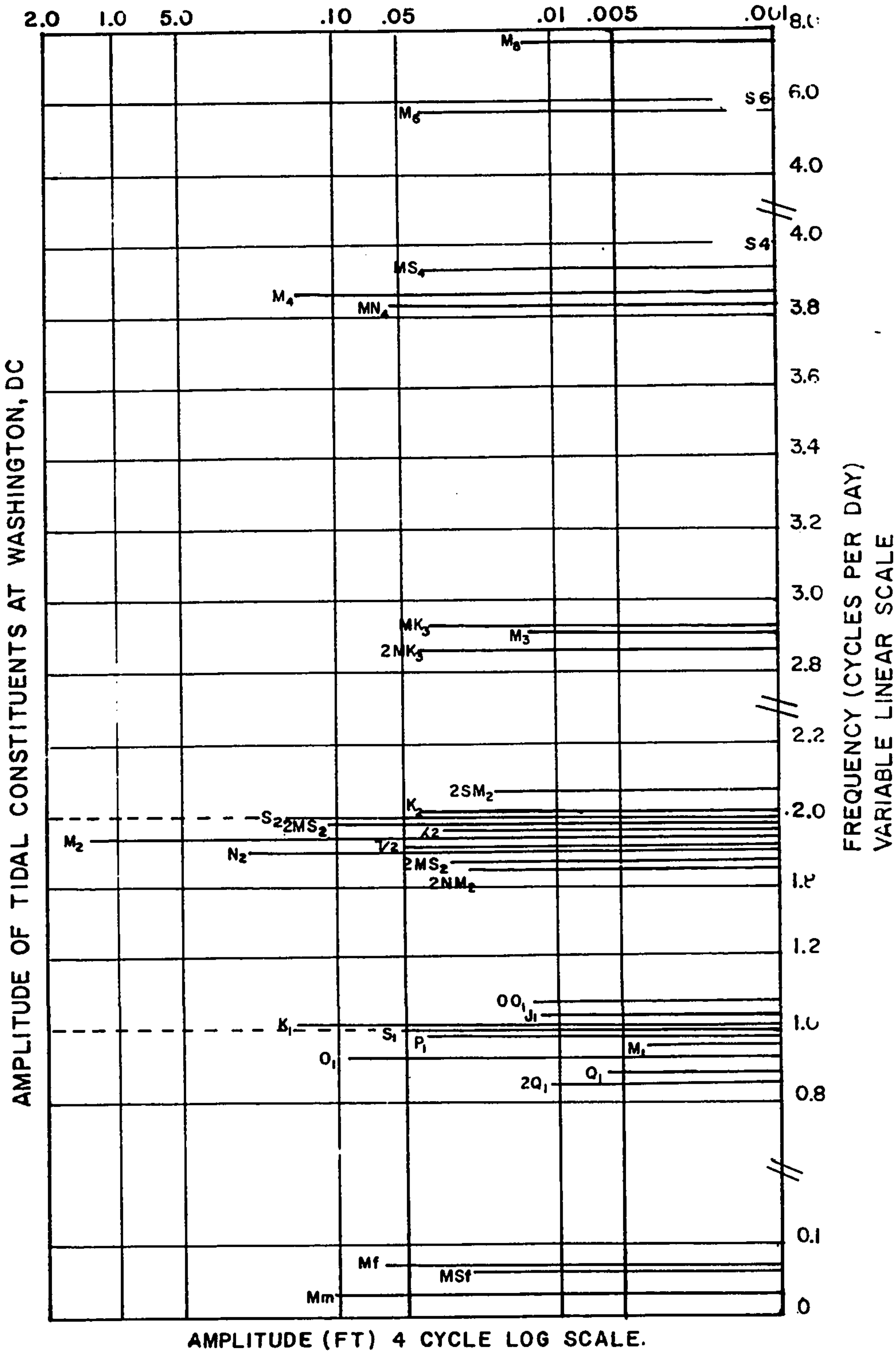
AMPLITUDE OF TIDAL CONSTITUENTS AT WASHINGTON, DC
2.0
1.0
5.0
.10
.05
.01
.005
.001
8.0
6.0
4.0
4.0
3.8
3.6
3.4
3.2
3.0
2.8
2.2
2.0
1.8
1.2
1.0
0.8
0.1
0
FREQUENCY (CYCLES PER DAY)
VARIABLE LINEAR SCALE
M8
S6
M6
S4
MS4
M4
MN4
MK3
M3
2NK3
2SM2
S2
2MS2
K2
M2
N2
2MS2
2NM2
OO1
J1
K1
S1
P1
M1
O1
Q1
2Q1
Mf
MSf
Mm
AMPLITUDE (FT) 4 CYCLE LOG SCALE.

for analysis, as well as provide the best spatial coverage of the bay. The 15 ft current meter depth was selected as a common depth for comparing tidal current information from various stations deployed throughout the bay. It is the current meter depth least affected by bottom influence, yet deep enough to minimize wave effects. Even though additional current meters were deployed at deeper depths during the tide and current survey, their data was not incorporated into this study. The station identification number, location, depth of water, height of meter above bottom, beginning of time series and duration for each station analyzed are summarized in Appendix C.

The digital current meter records were transcribed and preprocessed on a PDP 11/34 computer aboard the NOAA Ship FERREL before being transmitted to the Circulation Surveys Section of the National Ocean Service on nine track magnetic tape. During preprocessing, vessel personnel used automated data processing procedures to correct format errors, compare sequential record counts to elapsed time, and apply calibration constants. If a sensor failed, the meter stopped, or the rotor fouled, the FERREL often redeployed the station. Therefore, the required time series was successfully observed at most stations. Since the National Ocean Service expresses current speeds in metric units, current speeds are stated throughout this study in centimeters per second (cm sec^{-1}).

Upon receipt at the Circulation Surveys Section, the current meter data was processed on NOAA's Univac Series 1100 computer. The FERREL's preprocessing was verified and invalid data was rejected. The tidal current component is usually extracted from the total observed current by either harmonic or nonharmonic analysis techniques. The harmonic analysis of current meter data, whether by Fourier or least squares technique, separates the tidal current into periodic constituents using a procedure similar to that used in the harmonic analysis of tide data (Schureman, 1958). Since the current is expressed in terms of velocity and direction, each observation has to be separated into vector components before harmonic analysis. The results are therefore expressed relative to the major and minor axes used in the separation process. These results may also be recombined as tidal current constituent ellipses. For example, ellipses for the six major constituents of the tidal current which was observed at Station 40 in Chesapeake Bay Entrance are shown in Figure 12. These ellipses were constructed using a program by Patchen (1975), based on a procedure developed by Doodson and Warburg (1941) and modified by Swanson (1971). The procedure is to let the major (U) and minor (V) components of the tidal current constituent's velocity be represented by:

$$u = A_1 \cos \sigma t + B_1 \sin \sigma t \tag{41}$$

$$V = A_2 \cos \sigma t + B_2 \sin \sigma t \tag{42}$$

where: Amplitude $= (A_i^2 + B_i^2)^{1/2}$

Phase $= \tan^{-1}\left(\frac{B_i}{A_i}\right)$

Squaring and summing Equations 40 and 41 yields the square of the velocity at any moment.

$$\begin{aligned} w^2 &= [A_1 \cos \sigma t + B_1 \sin \sigma t]^2 + [A_2 \cos \sigma t + B_2 \sin \sigma t]^2 \\ &= [A_1^2 + A_2^2] \cos^2 \sigma t + [B_1^2 + B_2^2] \sin^2 \sigma t \\ &\quad + [A_1 B_1 + A_2 B_2] \cos \sigma t \sin \sigma t \end{aligned} \tag{43}$$

Figure 12. Ellipses for major tidal current constituents at Chesapeake Bay Entrance.

LONG - TERM CURRENT STATION 40

PRINCIPAL TIDAL CURRENT CONSTITUENTS

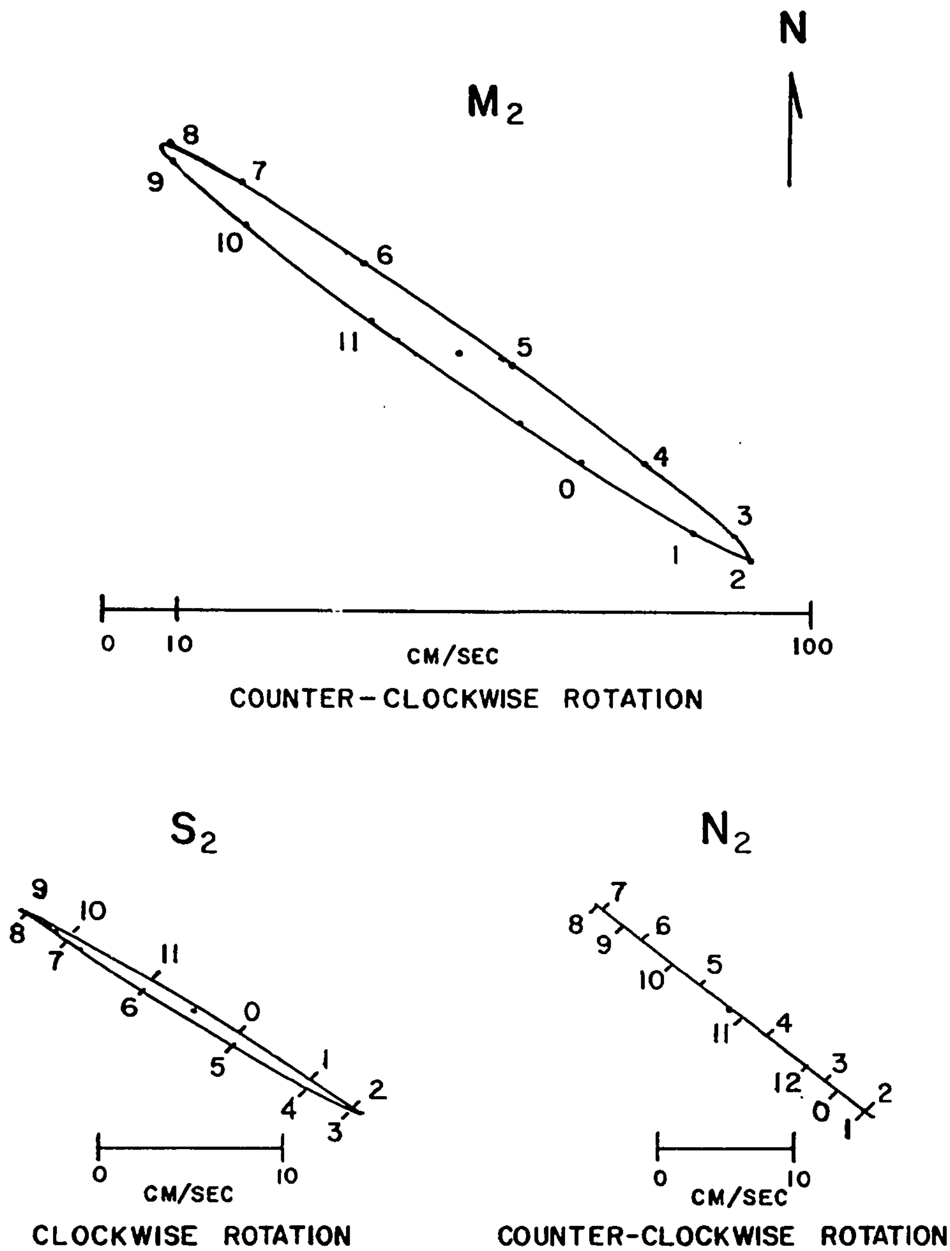

a

LONG - TERM CURRENT STATION 40

PRINCIPAL TIDAL CURRENT CONSTITUENTS
(CONTINUED)

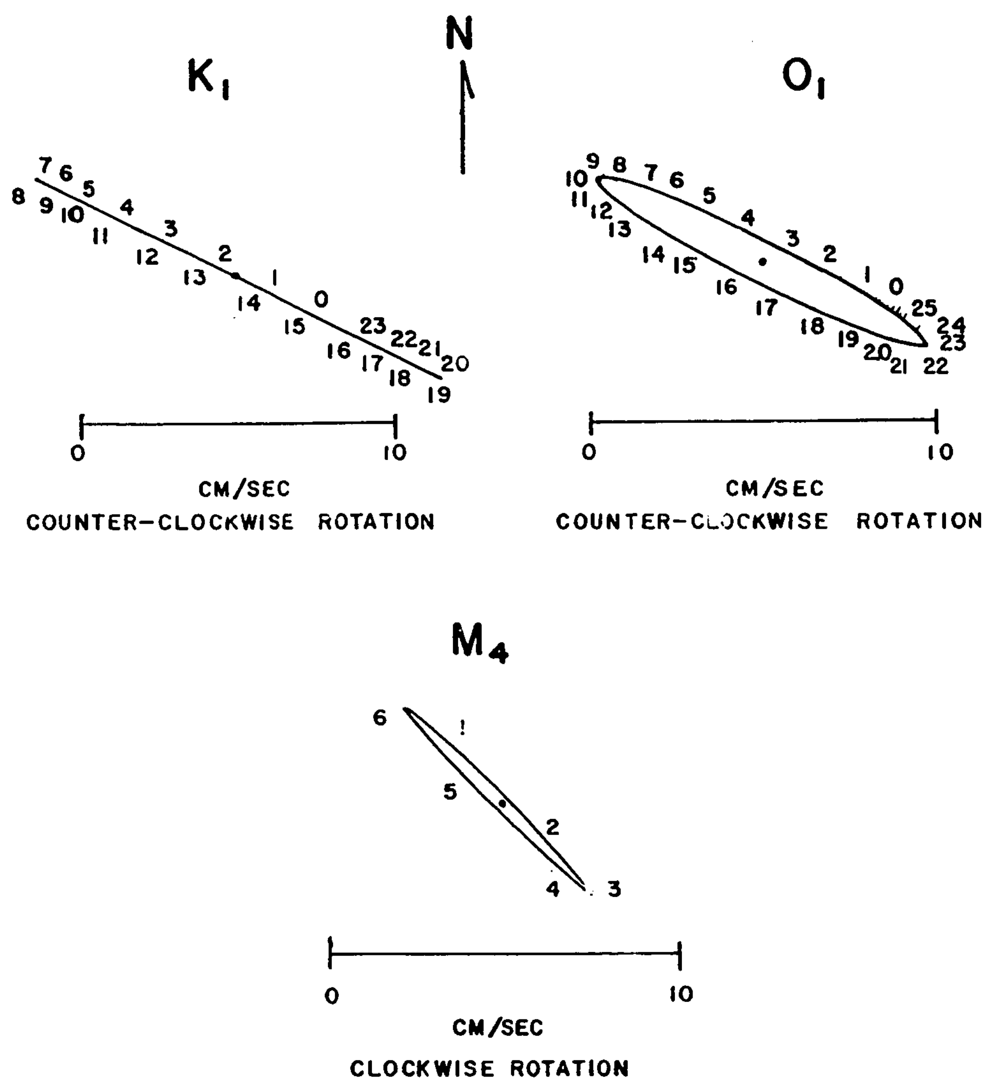

b

Manipulation of this expression, using trigonmetric identities, produces expressions for W_1 and W_2, the maximum and minimum speeds of the tidal current ellipse. Doodson and Warburg related W_1 and W_2 to angles θ_1 and θ_2. These angles, measured clockwise from the East, give the orientation of the maximum and minimum axes of the ellipse. The direction of rotation of the ellipse is clockwise if:

$$\theta_2 = \theta_1 - 90^\circ \tag{44}$$

and is counterclockwise if:

$$\theta_2 = \theta_1 + 90^\circ \tag{45}$$

According to Doodson and Warburg, the direction of rotation of the tidal current ellipse can be the result of direct response to tide generating astronomical forces, the effect of Earth's rotation, the effect of shelving coasts, and bottom friction. For semidiurnal constituents, the result of the direct response to the tide generating forces and rotation of a frictionless Earth is a clockwise rotation in the northern hemisphere. Defant (1961) stated that the influence of friction on a constituent ellipse results in a decrease in W_1 and an increase in the ratio, W_2/W_1, causing a retardation of phase and a reversal of rotation. For diurnal constituents, the direct response to the tide generating forces is a counterclockwise rotation of the ellipse between Latitudes 0° and 45° N. However, the effect of the rotation of a frictionless Earth is a clockwise rotation of the ellipse in the Northern Hemisphere. Friction affects diurnal constituents in the same manner as semidiurnal constituents.

During the tide and current survey, three current meter stations were deployed for two years or longer and a fourth was deployed for over a year. These long term stations were intended to serve as reference stations during analysis of data from shorter term stations which were deployed in their vicinity. In addition, a harmonic analysis of a long term series of current meter data is required to separate constituents having very close frequencies. Like the harmonic analysis of tide data, this would improve accuracy as well as determine harmonic constants for long period constituents, heretofore not determinable because current meter data previously observed by the National Ocean Service in Chesapeake Bay was not of sufficient duration.

Current meters were usually retrieved and redeployed every 30 days at these long term stations during the survey. The records for each deployment were processed sequentially and transmitted separately to the Circulation Surveys Section of the National Ocean Service. Each transmittal was stored as a separate computer file. This required joining files by station during this study, in order to assemble for each station the longest continuous time series possible for analysis. Due to intermittant sensor failure and fouling of the rotors, there were occasional breaks in the time series which could not be filled.

The velocity and direction data recorded at the 15 ft current meter depth at each of the long term stations was inspected to determine the longest unbroken time series available for harmonic analysis. There were 330 days available at Station 40 (in Chesapeake Bay Entrance), 171 days at Station 36 (near the mouth of the Patuxent River), 286 days at Station 65 (east of Wolf Trap Light), and 198 days at Station 121 (southeast of Annapolis, MD).

There were also 120 current meter stations deployed for shorter periods throughout the bay which recorded time series of sufficient length for limited harmonic analysis. The National Ocean Service's standard Fourier harmonic analysis programs were used to analyze both 29 day and 15 day portions of the time series observed at these short term stations because they are well documented and readily available. The least squares harmonic analysis program has not been adapted for efficient use with current meter data and requires extensive data manipulation. This manipulation was well justified to analyze the long term station data, but the large number of short term stations occupied required techniques that were efficient and readily available.

The use of relatively short time series from different times of year for harmonic analysis, the inability to separate neighbor constituents, and the steering effect of bottom topography might lead to errors which would cause the harmonic constants to vary too much from station to station for any interpretation, such as contouring tidal current cophase or cospeed lines. A preliminary review of the harmonic constants for various stations throughout the bay indicated the M_2 tidal current speeds and phases were fairly consistent. However, the phases for K_1 were not very consistent, possibly due to its relatively small speeds.

The results of the Fourier harmonic analysis of current meter data are summarized in Appendix D. This information includes: the station identification number, the ratio of meter height above bottom to total water depth at Mean Low Water, length of series analyzed, harmonic analysis technique, orientation of the major axis, the speeds and phases of tidal current constituents referenced to their major and minor axes, and the direction of rotation of the ellipse. The results of the least squares harmonic analysis of current meter data from long term Station 40 are given in Appendix E.

The tidal current can also be extracted from the shorter series of current meter data by using a nonharmonic comparison technique since current data observed at two nearby locations will have similar harmonic characteristics, differing only due to bottom topography and nontidal effects. If the current meter data time se [illegible] one of the stations is of sufficient length to analyze harmonically, so that the harmonic constants can be used to generate predictions for the period of short term observations, the data from the other station can be compared to these predictions. The results of this comparison are time differences and velocity ratios which can be applied to predictions for any time period at the reference station resulting in prediction of tidal currents at the subordinate locations.

Nonharmonic analysis of tidal current data has traditionally been done by either the reversing reduction method or the rotary reduction method. The reversing reduction method (U. S. Coast and Geodetic Survey, 1950) is used primarily with data obtained in a fairly constricted area where the current floods in one direction, slows to slack water, and then ebbs in the reverse direction. A reversing reduction determines the times and strengths of maximum floods and ebbs, and times of slack waters. The times and velocities for these phases are then compared to the observed or predicted velocities of the corresponding phases at the nearest reference station. The time differences determined for each phase are also translated to Greenwich lunitidal intervals. The mean maximum flood and ebb velocities are corrected for the time of year, a seasonal effect, using the corresponding values for the reference station.

However, most tidal currents are not purely reversing, but are somewhat rotary, where the direction of flow of a rotary tidal current continuously changes direction (clockwise or counterclockwise) around the compass. There are no slack waters but two times of minimum flow, usually in directions perpendicular to the direction of maximum flow. If the current is perfectly rotary, current speeds will be the same in all directions. However, the more constricted the area, the more predominant the flood and ebb directions will be.

The results of the reversing and rotary analyses of current meter data are used to compile the "Table of Current Differences and Other Constants" which is published in the annual tidal current prediction tables (U. S. National Ocean Survey, 1983b).

CHAPTER 5

DISCUSSION

THE OBSERVED TIDE

The cotidal and corange charts shown in Figures 13 and 14 describe the tide in terms of cotidal hours and mean ranges as it progresses throughout Chesapeake Bay and its major tributaries. It is a standard procedure of the National Ocean Service to express lunitidal intervals in solar time and tidal heights in English units. Therefore, all tidal characteristics referred to in this study have been expressed in these units, with the exception of tidal current speeds which are expressed in cm sec^{-1}.

Hicks (1964) and prior investigators of the tide in Chesapeake Bay expressed lunitidal intervals in lunar time, based on the assumption that the tide in Chesapeake Bay is dominated by the principal lunar semidiurnal constituent, M_2. However, harmonic analysis of tidal data observed throughout the bay and its tributaries indicates the amplitudes of tidal constituents other than M_2 can also be relatively large, especially in the upper reaches of the bay and tributaries, and these constituents often have periods significantly different from that of M_2. Since there appears to be little reason to adjust the time

Figure 13. Cotidal chart of Chesapeake Bay and its major tributaries. Cotidal lines are expressed in solar hours.

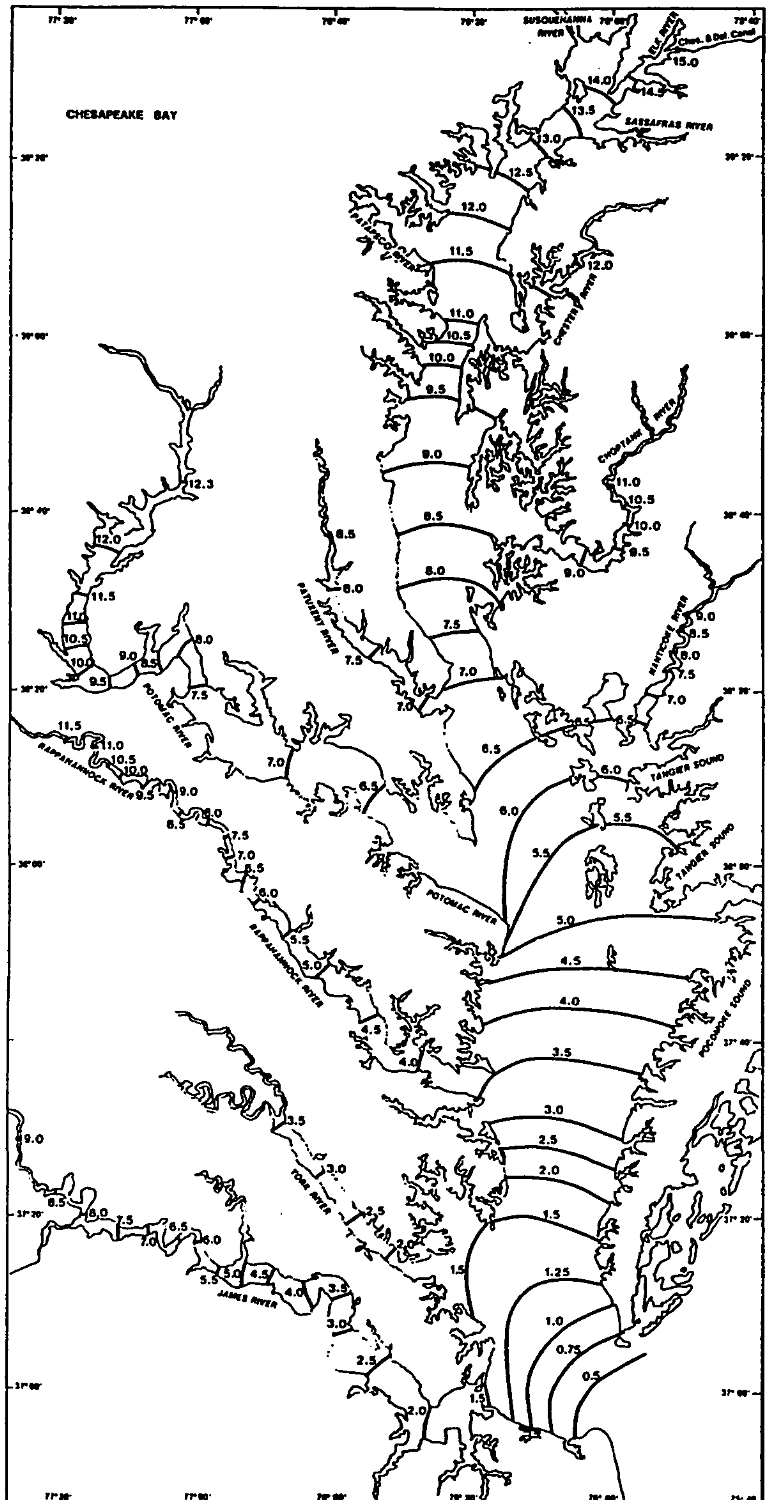
CHESAPEAKE BAY
SUSQUEHANNA RIVER
SASSAFRAS RIVER
CHESTER RIVER
CHOPTANK RIVER
NANTICOKE RIVER
PATUXENT RIVER
POTOMAC RIVER
RAPPAHANNOCK RIVER
YORK RIVER
JAMES RIVER
TANGIER SOUND
POCOMOKE SOUND

Figure 14. Corange chart of Chesapeake Bay and its major tributaries. Corange lines are expressed in feet.

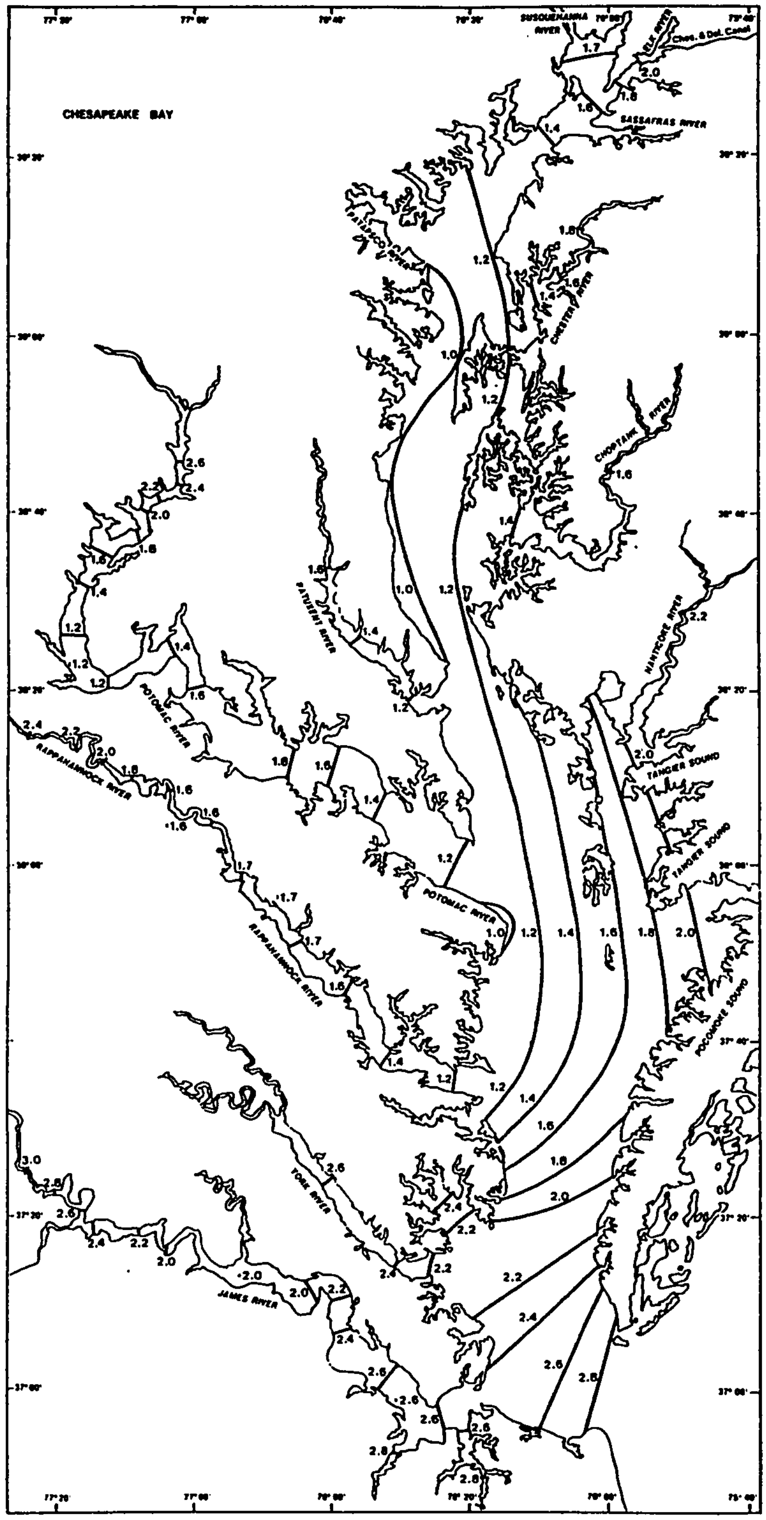
CHESAPEAKE BAY
SUSQUEHANNA RIVER
SASSAFRAS RIVER
CHESTER RIVER
CHOPTANK RIVER
PATUXENT RIVER
POTOMAC RIVER
RAPPAHANNOCK RIVER
NANTICOKE RIVER
TANGIER SOUND
POCOMOKE SOUND
YORK RIVER
JAMES RIVER

reference to the period of M_2, all cotidal charts prepared during this study have been expressed in solar time.

The cotidal hour is nearly 0.5 at Cape Henry, slightly greater than 0.5 at Cape Charles, and 0.68 at the Chesapeake Bay Bridge Tunnel tide station. Therefore, the 0.5 hour cotidal line curves into the bay across Chesapeake Bay Entrance. This indicates the tidal wave travels faster in the deeper waters offshore between the capes than it does in the shoaler waters nearshore. The tide data from offshore tide stations in the lower bay such as New Point Comfort Shoal, Wolf Trap Lighthouse, Holland Bar Light, and Rappahannock Shoal suggest all the cotidal lines in the lower bay should curve up the bay. There weren't any offshore tide stations in the upper bay or tributaries that would indicate how to draw these lines, so straight lines have been drawn across the narrower regions.

The tidal characteristics at Chesapeake Light Tower, an offshore structure located approximately 15 nautical miles outside Chesapeake Bay Entrance, have also been determined in order to describe the tide outside the bay's immediate influence. The cotidal hour at Chesapeake Light Tower is 0.04, significantly less than observed at the Chesapeake Bay Bridge Tunnel.

The cotidal lines indicate that, after entering the bay, the tide rapidly travels both westward and northward apparently following the deeper channels of the lower bay. The tide's progress slows somewhat in the region north of the mouth of the York River and Mobjack Bay, possibly due to shoaling and a slight narrowing of the lower bay. North of this region, the bay begins to widen significantly. If Tangier and Pocomoke sounds are included in the determination of the effective width of the bay, then Chesapeake Bay's total width can be considered much greater in this region.

The cotidal lines appear to be compressed just south of the mouth of the Potomac River in the vicinity of a shoal that extends nearly two nautical miles eastward from Smith Point. North of Smith Point, the cotidal lines tend to bend northward across the mouth of the Potomac River. This compression and bending of the cotidal lines may be due to the shoal retarding the tidal wave along the west side of the bay and the influence of the Potomac River basin.

The 6.0 hour cotidal line is oriented northward across the mouth of the Potomac River and then bends northeastward across the bay. North of Point No Point, which is located on the western shore approximately six nautical miles north of the mouth of the Potomac River, the cotidal lines are again oriented directly across the bay. The tide's progress is reduced in the narrow part of the bay north of the mouth of the Patuxent River and in the narrows north of the mouth of the Severn River. The tide then travels more uniformly northward to where the upper bay is divided into two reaches at Turkey Point. The western reach extends northward to Havre de Grace, MD near the head of bay, and the eastern reach extends northeastward toward the Chesapeake and Delaware Canal. The cotidal hour at Havre de Grace is 14.46 hours. Therefore, the tide takes nearly 14 hours to travel from Chesapeake Bay Entrance to the head of bay.

The cotidal chart also describes the tide in the major tributaries of Chesapeake Bay. In the James River, the tide takes about 7.5 hours to travel from the mouth to Richmond, VA near the limit of tide. Similarly, the tide requires about 8.5 hours to travel from the mouth of the Rappahannock River to the rapids near Fredericksburg, MD which are most likely the limit of tide. In comparison, the tide only takes about 6.4 hours to travel from the mouth of the Potomac River to Washington, DC. The limit of tide is most likely located at Great Falls, about 12 nautical miles upriver from Washington, DC. However, there weren't any tide stations installed in this region that would indicate the point of reflection. Since the tidal hour does not appear to change appreciably between Alexandria, VA and Washington, DC, little change is expected upriver. It wasn't possible to describe the tide adequately in the York, Patuxent, Chester, Choptank, and Nanticoke rivers, since there were only a few tide stations located in each of these tributaries.

The corange chart shown in Figure 14 describes the change in mean tide range throughout the bay and its major tributaries. The mean range at all stations has been adjusted to the 1960 to 1978 tidal epoch, which is the epoch of reference presently used by the National Ocean Service. The mean range at Chesapeake Light Tower is 3.55 ft compared to about 2.8 ft at Cape Henry and 3.0 ft at Cape Charles. The mean range generally tends to be greater along the eastern shore of the Bay Proper than on the western shore, directly opposite.

The corange lines pivot clockwise on Cape Charles and the southernmost eastern shore as the tide travels toward the mouths of the James and York rivers, and northward up the bay. The mean range decreases in a somewhat orderly manner, from slightly over 2.8 ft at Chesapeake Bay Entrance to less than 2.2 ft off the mouth of the York River. The cross bay difference in mean range varies from 0.2 ft to 0.4 ft, with the greater mean range observed on the eastern side of the bay.

The corange lines then pivot counterclockwise along the western shore between the mouths of the York and Rappahannock rivers, becoming oriented nearly parallel to the longitudinal axis of the bay in the region extending from below the mouth of the Potomac River to north of the mouth of the Patuxent River. The mean range increases from slightly less than one foot at Smith Point to over two feet on the eastern shore, crossing the bay at its widest point. The corange chart clearly shows that the mean range is greater along the eastern shore of the bay in this region than on the western shore, directly opposite.

Along the western shore between Cove Point (located about four nautical miles north of the mouth of the Patuxent River) and North Point (located approximately 50 nautical miles further north), the mean range varies slightly about a value of one foot with a cross channel variation of about one tenth foot. Since many of the tide stations were located in the small bays along the eastern shore in this region, they do not accurately represent open bay conditions. In addition, there wasn't adequate tide station coverage along the western shore between North Point and Havre de Grace, MD. Therefore, the change in mean range is not well defined in this region, especially across the bay. Continuing northward along the eastern shore from opposite North Point to Town Point near the western end of the Chesapeake and Delaware Canal, the mean range changes from 1.18 ft to 2.06 ft. In comparison, the mean range changes along the western shore from 1.11 ft at North Point to 1.77 ft at Havre de Grace. This indicates there is a significant increase in mean range as the tide approaches the upper reaches of the bay. However, there isn't sufficient information available to construct accurate corange lines in this region.

The distribution of tide stations in the major tributaries isn't sufficient to define any cross channel variation in mean range, but this change can be considered insignificant since the tributaries are usually relatively narrow. However, the change in mean range along the longitudinal axis of the tributaries is well defined.

In the James River, the mean range is about 2.6 ft at the mouth, but decreases to a minimum of 1.84 ft at Claremont, VA. It then increases to 3.15 ft at Richmond, VA. The mean range in the Rappahannock River increases from about 1.2 ft at its mouth to 1.75 ft at Wares Wharf, VA. It then decreases to 1.52 ft at Saunders Wharf, VA and finally increases to about 2.5 ft at Fredericksburg, VA. In comparison, the mean range in the Potomac River increases from about 1.2 ft at its mouth to 1.8 ft at Colton Point, MD. It then decreases to 1.24 ft at Riverside, MD and increases to 2.77 ft at Washington, DC.

The mean range in the York River increases about 0.6 ft from its mouth to West Point, VA where it divides to form the Pamunkey and Mattaponi rivers. Similarly, the mean range in the Patuxent River increases about 0.6 ft from its mouth to Upper Marlboro, MD. However, there weren't any tide stations located further upriver in either tributary which would help determine the location of the limit of tide.

Comparison of these cotidal and corange charts with those constructed by Hicks (1964) indicates general agreement, even though derived from different data sets. The cotidal lines on Hick's chart have to be converted to solar hours for comparison with the new chart, which requires a slight adjustment in line position. The 14 hours required for the tide to travel from Chesapeake Bay Entrance to Havre de Grace, MD agrees well with Hicks' observation of 14.23 solar hours. However, the charts prepared during this study show more definition of the tide as it travels through the lower bay and as it approaches the mouth of the Potomac River.

The mean ranges observed throughout the bay are generally about 0.1 ft less than those observed by Hicks at similar locations. This is possibly due to a change in sea level between the times when the different data sets were observed, combined with the effect of any local sedimentation or dredging.

This corange chart confirms Hicks' observation that the mean range is significantly larger along the eastern shore of the Bay Proper than on the western shore, directly opposite, but the difference now appears to be slightly greater. He also observed that the corange lines become aligned parallel to the longitudinal axis of the bay in the region north of the mouth of the Rappahannock River, and then tend to be poorly defined north of the mouth of the Patuxent River. His corange lines in the upper reaches of the bay are more uniform than those constructed on this chart. However, his results were not based on any greater density of tide stations.

In the James, Rappahannock and Potomac rivers, both corange charts indicate that the mean range increases gradually, proceeding up each river from its mouth, decreases significantly in the midregion, and then increases again before reaching the limit of tide. This is most likely due to the interaction of tidal constituent waves and to the length of the tidal portion of each river which will be discussed later.

The harmonic constants, which are summarized in Appendix B, can be used to construct cophase and coamplitude charts for any desired tidal constituent. The interaction of the semidiurnal and diurnal tides will be explained by describing the interaction of representative tidal constituents of each species. Cophase and coamplitude charts have been constructed for both the principal lunar semiannual constituent, M_2, and the principal lunisolar diurnal constituent, K_1.

THE M_2 TIDE

The cophase chart for the M_2 tidal constituent shown in Figure 15 indicates the phase of M_2 is slightly less than 230° at Chesapeake Bay Entrance, and the cophase lines curve into the bay in this region, similar to the cotidal lines in Figure 13. In the region which extends from north of New Point Comfort to south of Smith Point, the cophase lines are oriented across the bay with the phase progressing more rapidly along the western shore. The spacing of the cophase lines is fairly uniform, even where the bay widens to include Pocomoke Sound and Tangier Sound.

The cophase lines, like the cotidal lines, appear to be compressed near Smith Point and pivot counterclockwise so that the 30° cophase line becomes oriented northward across the mouth of the Potomac River. This cophase line then bends eastward so that it is oriented across the bay in the vicinity of Point No Point. There is a definite decrease in the spacing of the cophase lines through the narrow portion of the bay north of the mouth of the Patuxent River indicating the phase speed of the M_2 wave has decreased. North of the narrows, the spacing widens significantly indicating an increase in speed. The cophase lines

Figure 15. Cophase chart for the M_2 tide in Chesapeake Bay and its major tributaries. Cophase lines are expressed in degrees.

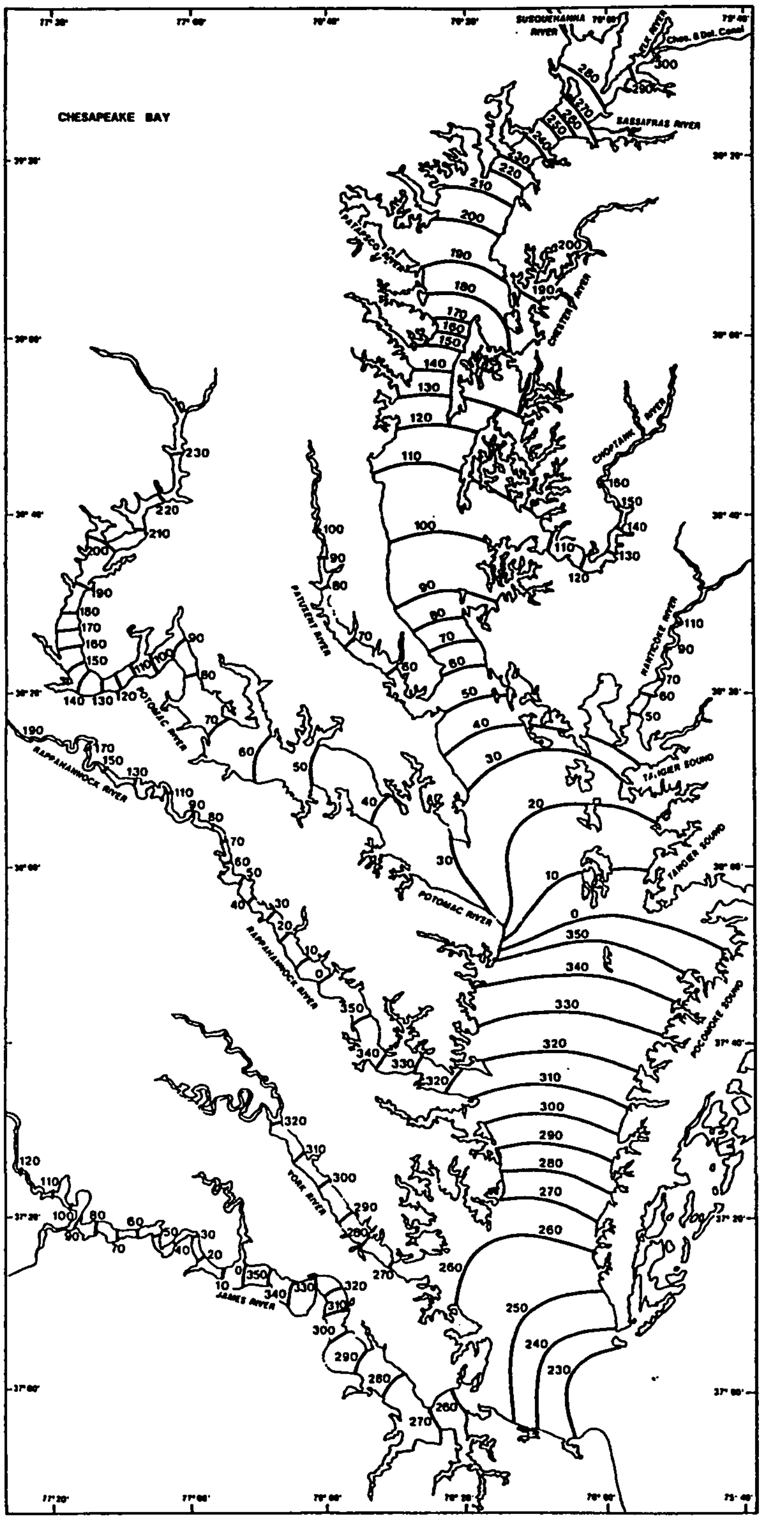
CHESAPEAKE BAY
SUSQUEHANNA RIVER
SASSAFRAS RIVER
PATAPSCO RIVER
CHESTER RIVER
CHOPTANK RIVER
PATUXENT RIVER
NANTICOKE RIVER
POTOMAC RIVER
RAPPAHANNOCK RIVER
TANGIER SOUND
POCOMOKE SOUND
YORK RIVER
JAMES RIVER

continue to be oriented across the bay throughout this region.

The spacing decreases again in the narrow region just north of the mouth of the Severn River, then increases in the wider region to the north, and decreases again in the upper reaches of the bay. The M_2 wave divides at Turkey Point, where the phase is 280°, and travels up each reach. In the eastern reach, the M_2 wave travels towards the Chesapeake and Delaware Canal and the phase is 306° at Chesapeake City, MD. In the western reach, the wave travels towards the mouth of the Susquehanna River where the phase is 286° at Havre de Grace, MD and is 288° upriver at Port Deposit, MD. Therefore, the change in phase of M_2 from Chesapeake Bay Entrance to Havre de Grace is 416°, more than one cycle of the M_2 tide. In fact, one complete cycle, measured from Chesapeake Bay Entrance, is completed at the narrows south of Turkey Point, a distance of 145 nautical miles.

The phase of the M_2 tide is very well defined in the major tributaries. The phase at the mouth of the James River is 270° and is 123° at Richmond, VA; a total change of 213°. The phase at the mouth of the Rappahannock River is about 320° and is 190° near Fredericksburg, VA; a total change of 230°. The phase at the mouth of the Potomac River is about 30° and is nearly 234° at Washington, DC; a total change of 204°.

This phase change agrees well with reflected tidal wave theory which indicates the M_2 tide should become more like a standing wave near the point of reflection. Therefore, the phase should change very little with distance near the limit of tide in each tributary if the tidal wave is reflected. Since the wave should become more progressive as it travels further from the point of reflection, the change in phase should be much greater with distance. It is observed that the phase change in the James River from Willcox Wharf, VA to Hopewell, VA (a distance of about nine nautical miles) is 31.1°. However, the phase change in the upper tidal region (over a distance of ten nautical miles) from Chester, VA to Richmond, VA is only 6°. Similarly, the change in the Rappahannock River from Tappahannock, VA to Saunders Wharf, VA (a distance of about 16 nautical miles) is 58.6°. In comparison, the change in the upper tidal Rappahannock River from Hopyard Landing, VA to a location near Fredericksburg, VA (a distance of about 12 nautical miles) is 12°. Finally, the change in the Potomac River from Quantico, VA to Indian Head, MD (a distance of about eight nautical miles) is 11° but the change from Alexandria, VA to Washington, DC (a distance of about five nautical miles) is 3.7°.

The small change in phase observed over a substantial distance in the upper tidal regions of these tributaries indicates the M_2 wave does become more like a standing wave as the point of reflection is approached. If there is sufficient water depth so that the attenuation of the incident and reflected waves isn't too severe, near-standing wave conditions could exist over a considerable distance from the point of reflection. Note that a 16 ft channel is maintained in the upper James River as far as Richmond. The channels in the upper reaches of the Rappahannock and Potomac rivers are not dredged to any extent, but may be of sufficient depth that standing wave characteristics can be observed further from the point of reflection than expected.

In comparison, the change in phase of M_2 in the upper reaches of Chesapeake Bay is not as clearly defined. The phase of M_2 changes about 25° in the western reach between Betterton, MD and Havre de Grace, MD but changes only 2° in the short distance upriver to Port Deposit, MD. In the eastern reach, the phase increases 30° from Betterton to Town Point and then increases about 16° as it travels toward Chesapeake City, MD. Therefore, the M_2 tide appears to be more like a standing wave in the western reach than in the eastern reach. This suggests the M_2 tide may be reflected near the head of bay. A comparison of the phases of the M_2 tide and tidal current later in this study will help determine whether the tide is more like a standing wave in this region.

The coamplitude chart for M_2 is presented in Figure 16. The amplitude of M_2 at Chesapeake Light Tower is 1.651 ft compared to an amplitude of about 1.40 ft at Chesapeake Bay Entrance. The amplitude continues to decrease as the M_2 wave travels simultaneously toward the mouth of the James River and up the bay. The coamplitude lines appear to pivot clockwise, changing slowly along the eastern shore and more rapidly along the western shore. The M_2 amplitudes along the eastern shore are approximately 0.2 ft greater in magnitude than amplitudes on the western shore, directly opposite, indicating an increase in mean range eastward across the bay similar to that seen on the corange chart.

There is a marked change in the coamplitude line pattern near New Point Comfort Shoal. The 1.1 ft coamplitude line is nearly straight and is oriented northeastward from a location on the western shore south of the mouth of the York River. Beginning with the 1.0 ft coamplitude line, these lines are curved toward the entrance of the

Figure 16. Coamplitude chart for the M_2 tide in Chesapeake Bay and its major tributaries. Coamplitude lines are expressed in feet.

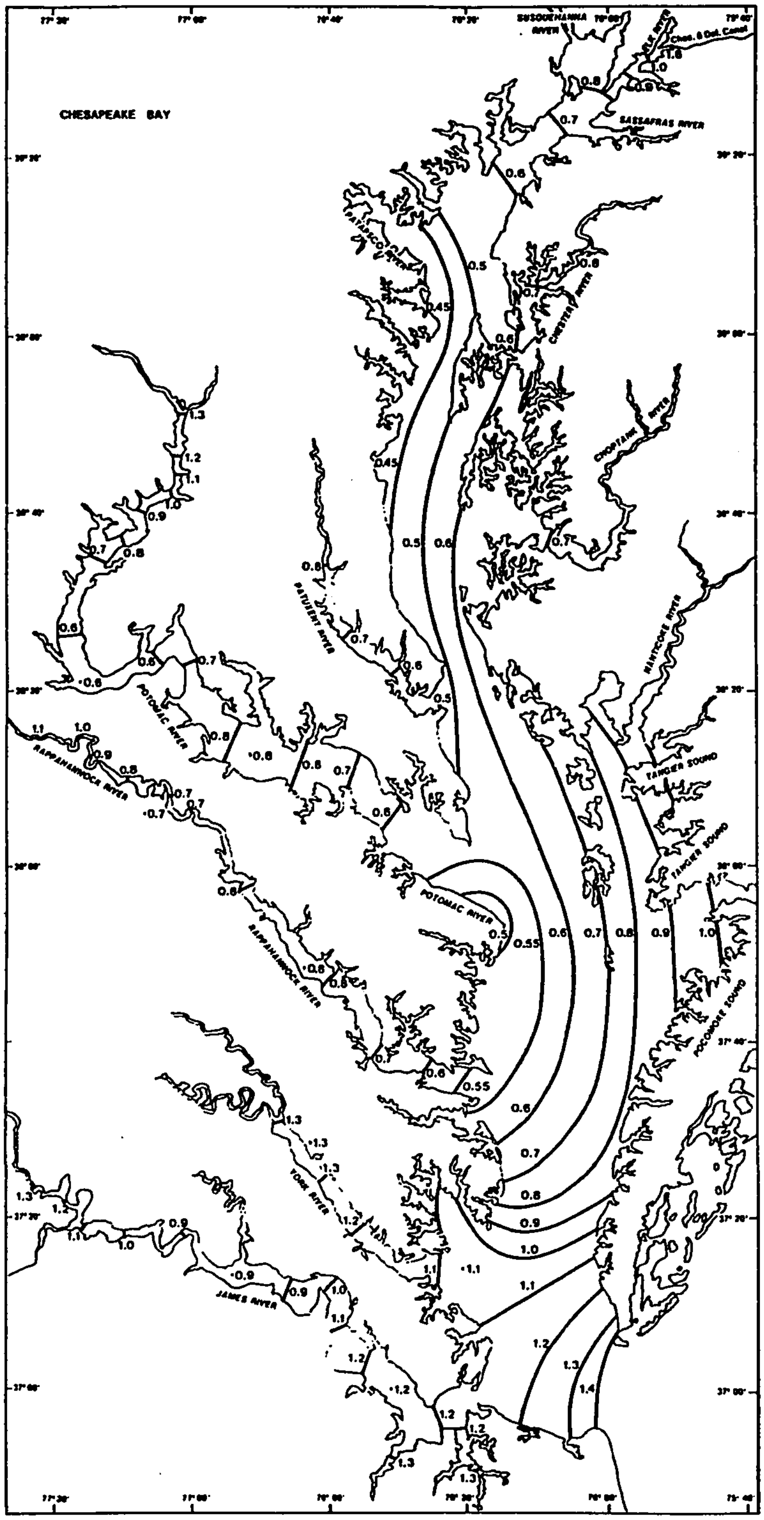

bay, and their western ends appear to pivot on New Point Comfort. These lines tend eastward across the bay and then bend northward so that most eventually align themselves parallel to the longitudinal axis of the bay.

The amplitude of M_2 decreases fairly rapidly along the western shore from New Point Comfort Shoal to the vicinity of Wolf Trap Light, which is located approximately 12 nautical miles southeast of the mouth of the Rappahannock River. Then it decreases gradually from this point northward to the mouth of the Rappahannock River. Smith Point Shoal is enclosed within the 0.5 ft coamplitude line, and the amplitude at Smith Point is 0.40 ft; the smallest M_2 amplitude observed in Chesapeake Bay during this study. The supplemental 0.55 ft coamplitude line encompasses all the nearshore waters off the western shore between the mouths of the Potomac and Rappahannock rivers.

The 0.6 ft coamplitude line commences south of the mouth of the Rappahannock River and also bends northward up the bay. It continues northward, uninterrupted for nearly 80 nautical miles, until it intersects the eastern shore at Tilghman Island. These northward oriented coamplitude lines are spaced fairly uniformly across the bay, which in this region includes the Bay Proper, Tangier Sound, and Pocomoke Sound. The amplitude increases from 0.40 ft at Smith Point to 1.06 ft on the eastern shore directly across the bay.

About three nautical miles north of Point No Point, the 0.5 ft coamplitude line again extends northward from the western shore and nearly longitudinally bisects the main channel until it terminates on the eastern shore at Kent Point, which is located approximately 42 nautical miles north of Point No Point. The 0.5 ft coamplitude line recommences approximately 12 nautical miles to the north, and extends northward until it crosses the bay to the western shore, about three nautical miles north of North Point.

In the upper reaches of the bay, the coamplitude lines become oriented more cross channel and increase in magnitude from 0.6 ft approximately 15 nautical miles southwest of Turkey Point to 0.8 ft at Turkey Point. The amplitude continues to increase rapidly in the eastern reach as the wave approaches the Chesapeake and Delaware Canal, and the amplitude is 1.373 ft at Chesapeake City, MD. The amplitude does not increase as much in the western reach and is only 0.850 ft at Havre de Grace, MD.

Note that the M_2 cophase and coamplitude lines are oriented somewhat parallel to each other in the region which entends from Chesapeake Bay Entrance to the vicinity of New Point Comfort Shoal. From this region northward, the coamplitude lines bend northward becoming nearly orthogonal to the cophase lines. This pattern continues until the upper reaches of the bay where the coamplitude lines bend westward to become more parallel to the cophase lines again. The pattern of orthogonally-oriented coamplitude and cophase lines in the lower bay suggests the M_2 tide may be a Kelvin wave in this region. However, the amphidromic pattern appears to be displaced westward, and a virtual amphidrome may be located somewhere inland on the peninsula between the Rappahannock and Potomac rivers.

The M_2 coamplitude lines in the major tributaries tend to be oriented cross channel, and are nearly parallel to the cophase lines. The M_2 coamplitude line patterns in the James, Rappahannock, and Potomac rivers are similar to the corange lines shown in Figure 14, indicating the predominant influence of this semidiurnal constituent on the observed tide. Proceeding upriver from the mouth of each of these tributaries, the M_2 amplitude first increases to a maximum value and then decreases to a minimum before increasing again as it approaches the limit of tide. It will be shown later that these maximum and minimum amplitudes are located about where the antinodes and quasinodes of the M_2 tidal wave occur.

Since the pattern of M_2 coamplitude and cophase lines in the upper reaches of the bay is similar to that in the major tributaries, it may be possible to apply simple one dimensional reflected wave theory to this area also. The maxima and minima in M_2 amplitude, if observed, would again be the antinodes and quasinodes of the M_2 tidal wave. However, the point of reflection is not clearly defined. The one dimensional analytical model will be used to determine whether the observed M_2 tide behaves like a reflected wave and to estimate the phase and amplitude at the point of reflection, if one exists.

THE K_1 TIDE

The cophase chart for the K_1 tidal constituent shown in Figure 17 indicates the phase of K_1 is nearly 110° at Chesapeake Bay Entrance, and the cophase lines in the lower bay curve up the bay similar to the pattern for M_2. In the region which extends from New Point Comfort to south of Smith Point, the K_1 wave travels more rapidly northward along the western shore causing the cophase lines to be oriented southeastward toward the eastern shore. These cophase lines exhibit some curvature up the bay too.

Figure 17. Cophase chart for the K_1 tide in Chesapeake Bay and its major tributaries. Cophase lines are expressed in degrees.

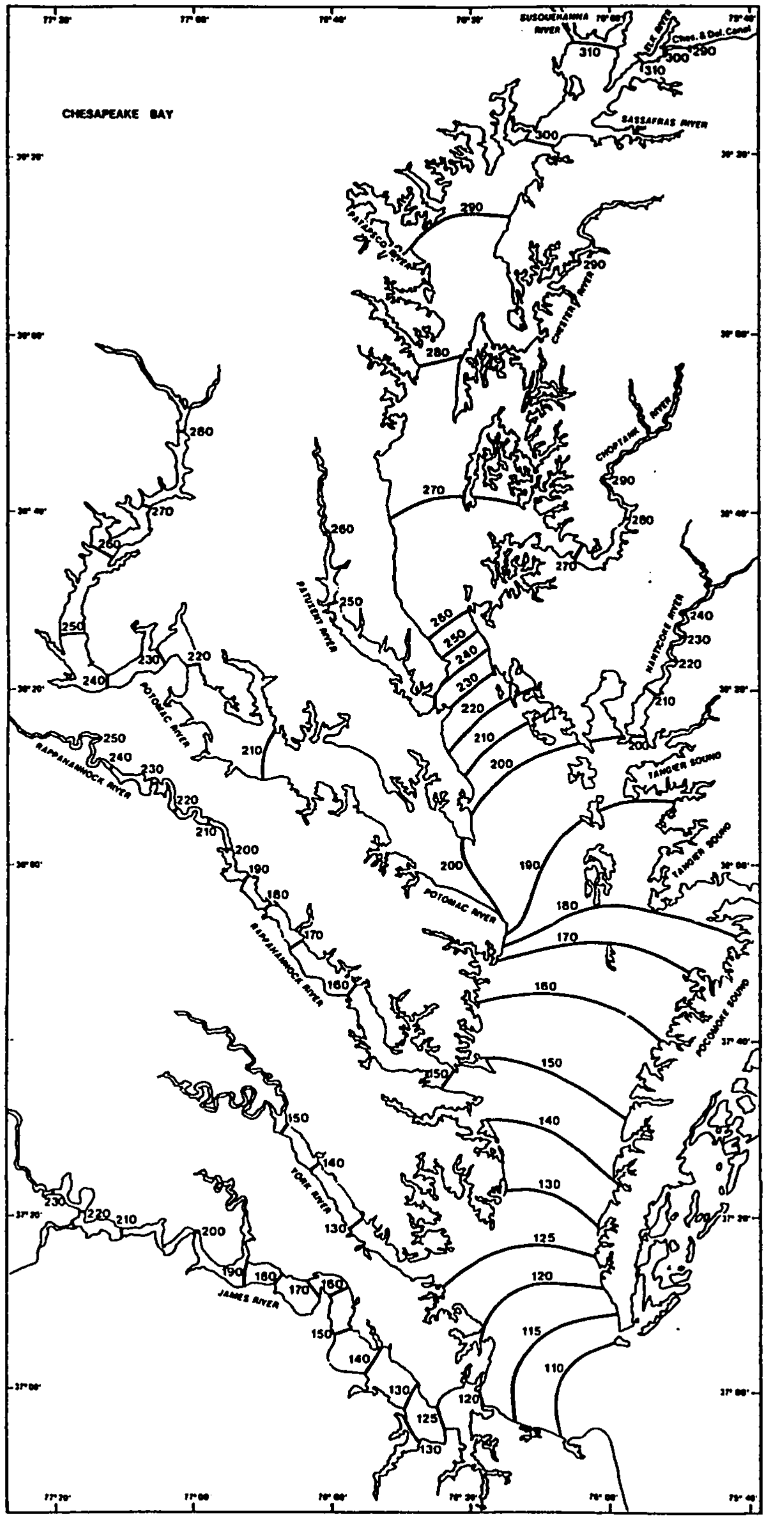

The K_1 cophase lines are also compressed along the western shore in the vicinity of Smith Point, similar to the pattern of the M_2 cophase lines. The K_1 cophase lines in this region also bend northward sweeping across the Bay Proper, Tangier Sound, and Pocomoke Sound. This results in a very rapid change in phase along the eastern shore. The 200° cophase line is oriented northward across the mouth of the Potomac River, and then bends eastward from Point Lookout at the north side of the river mouth to become oriented cross channel in the Bay Proper.

The spacing of the K_1 cophase lines in the narrower regions of the bay north of the mouth of the Patuxent River is compressed similar to the M_2 cophase lines, and the spacing increases significantly in the wider regions. The cophase lines are oriented nearly cross channel throughout the upper bay. The K_1 wave also divides at Turkey Point where the phase is nearly 310°. In the eastern reach, the phase increases to 311.2° at Town Point, but then decreases to 288.9° at Chesapeake City. In the western reach, the phase is 311.7° at Havre de Grace, and increases to 318.9° upriver at Port Deposit. Therefore, the change in phase from Chesapeake Bay Entrance to Havre de Grace is about 200°, slightly over one half cycle of the K_1 tidal wave. Actually, one half cycle is completed in the vicinity of North Point (a distance of approximately 140 nautical miles from Chesapeake Bay Entrance).

The phase of the K_1 tide is also well defined in the major tributaries. The phase at the mouth of the James River is nearly 130° and at Richmond is 239°; a total change of about 110°. The phase at the mouth of the Potomac River is about 200° and at Washington, DC is nearly 282°; a total change of only 82°. The phase at the mouth of the Rappahannock River is nearly 150° and at Hopyard Landing is 250°; a total change of 100°. However, the computed phase near Fredericksburg is about 77°. Either the phase of K_1 changes more than a half cycle over a distance of approximately 12 nautical miles or there is a 180° ambiguity in the results of the harmonic analysis. This large a phase change in such a relatively short distance seems unreasonable compared to the change observed in other major tributaries. Therefore, it is suspected that the harmonic analysis program output for the K_1 phase was out of cycle by 180°, and the phase near Fredericksburg should be 257°. This would make the total change in phase from the mouth of the river to the assumed point of reflection 107°, which seems more reasonable.

The behavior of the K_1 tidal wave in these tributaries is very similar to that of M_2. The phase in the lower regions of these rivers increases fairly rapidly, but the phase changes very little with distance in the upper reaches near the limit of tide. This indicates the K_1 wave is more progressive in the lower regions of these tributaries, but becomes more like a standing wave in the upper reaches.

The change in phase of K_1 in the upper reaches of Chesapeake Bay is not as clearly defined. The phase in the western reach increases about nine degrees between Betterton and Havre de Grace, and then increases another seven degrees continuing upriver to Port Deposit. In the eastern reach, the phase increases nearly nine degrees from

Betterton to Town Point, but then appears to decrease as it enters the Chesapeake and Delaware Canal. This suggests the K_1 wave is reflected in the western reach, but reflection of the K_1 wave in the eastern reach may be complicated by tidal interaction from Delaware Bay through the Chesapeake and Delaware Canal.

The coamplitude chart for K_1 is presented in Figure 18. The coamplitude line pattern in the lower bay, from the entrance northward to the vicinity of Cove Point, is similar to that of the M_2 tide. However, the K_1 amplitudes are significantly smaller than those of M_2 indicating the dominance of M_2 in the lower bay. The amplitude of K_1 at Chesapeake Bay Light Tower is 0.234 ft, which is about 36 percent of that of M_2. At Chesapeake Bay Entrance, the K_1 amplitude is about 0.20 ft or 14 percent of M_2. The amplitude of K_1 continues to decrease as the wave travels westward and northward throughout the lower bay. Due to the orientation of the coamplitude lines in this region, the amplitude of K_1 is 0.03 to 0.05 ft larger on the eastern shore than on the western shore, directly opposite.

There is a marked change in the orientation of the K_1 coamplitude lines north of New Point Comfort Shoal, similar to the pattern seen on the M_2 coamplitude chart in Figure 16. The K_1 coamplitude lines also bend northward from the western shore in the region that extends from New Point Comfort to Smith Point. They then become aligned nearly parallel to the longitudinal axis of the bay in the region extending from the mouth of the Potomac River to the mouth of the Patuxent River. North of this region the coamplitude lines appear to bend northwestward and intersect the western shore. This did not occur with the M_2 coamplitude lines.

Figure 18. Coamplitude chart for the K_1 tide in Chesapeake Bay and its major tributaries. Coamplitude lines are expressed in feet.

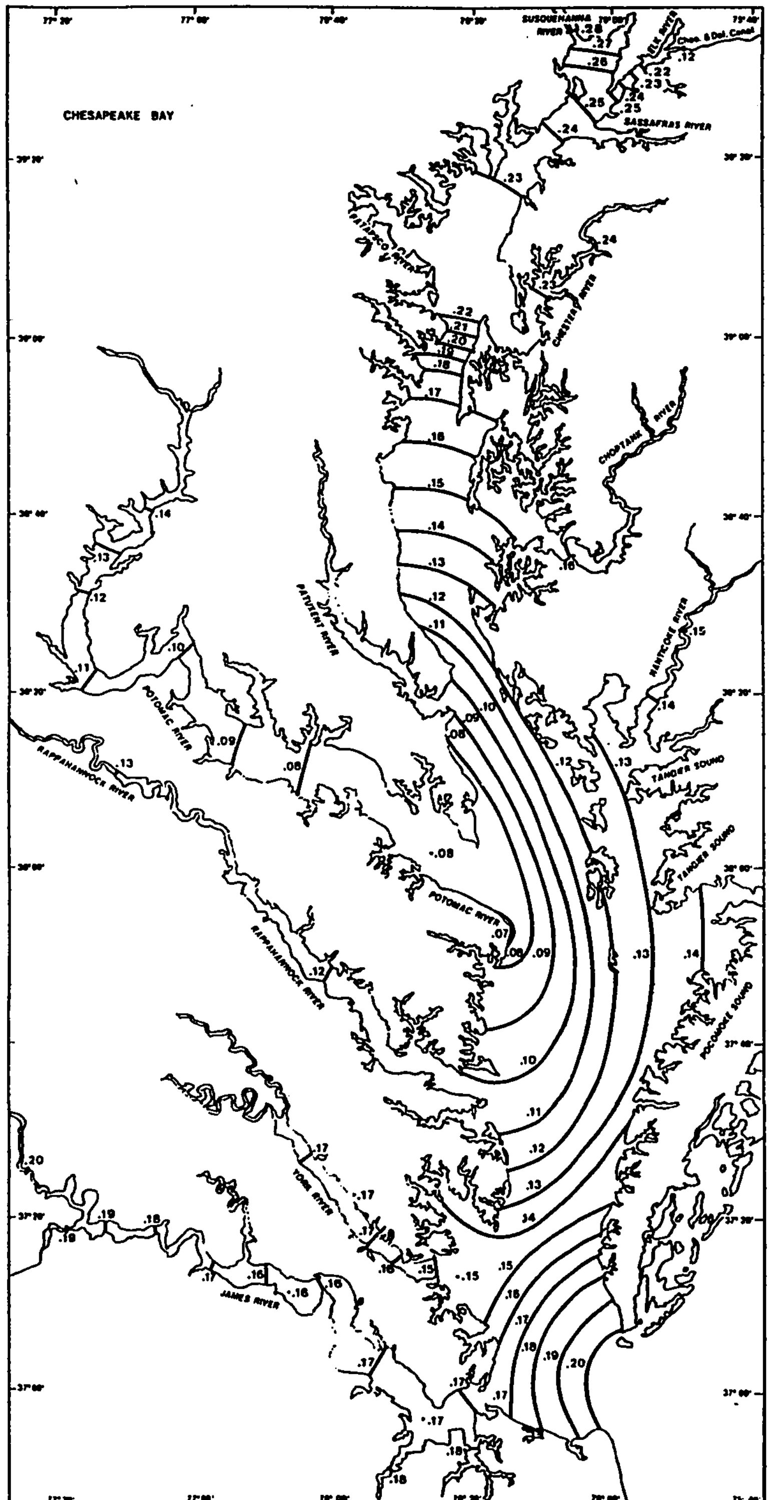
CHESAPEAKE BAY
SUSQUEHANNA RIVER
SASSAFRAS RIVER
CHESTER RIVER
CHOPTANK RIVER
PATUXENT RIVER
POTOMAC RIVER
RAPPAHANNOCK RIVER
TANGIER SOUND
POCOMOKE SOUND
YORK RIVER
JAMES RIVER

The amplitude of K_1 at Smith Point is 0.062 ft, the smallest K_1 amplitude observed in Chesapeake Bay. This was also the location of the minimum amplitude of the M_2 tide. The amplitude of K_1 is 15.5 percent that of M_2 at Smith Point, and the K_1 coamplitude lines also tend to be orthogonally-oriented to the K_1 cophase lines in this region. This again suggests an amphidromic pattern with a virtual amphidrome located inland to the west.

North of Cove Point, the K_1 coamplitude lines are uniformly oriented across the bay. In comparison, the M_2 coamplitude lines continue to be aligned nearly parallel to the longitudinal axis of the bay as far northward as North Point. No reason is readily apparent for this difference, except that the relatively small change in M_2 amplitude observed in this region didn't provide much detail for contouring coamplitude lines.

The K_1 coamplitude lines then increase in magnitude, continuing northward from Smith Point to the head of bay. The amplitude increases to a maximum of 0.291 ft at Port Deposit. Therefore, the K_1 amplitude at Port Deposit is nearly 35 percent of that of M_2 indicating the relative effect of K_1 is greater near the head of bay than in the lower bay, perhaps because M_2 is less dominant near the head of the bay. Continuing northward in the eastern reach, the K_1 amplitude increases to about 0.25 ft in the vicinity of Turkey Point, and then decreases rapidly to 0.116 ft at Chesapeake City. This decrease in amplitude as the K_1 wave approaches the Chesapeake and Delaware Canal was not exhibited by the M_2 wave in this region.

The pattern of K_1 coamplitude lines in the major tributaries is similar to that of the M_2 tide, but it is observed that the regions of maximum and minimum amplitudes in each tributary are at different locations than were observed for M_2. It will be shown that these maximum and minimum amplitudes are located approximately where the quasinodes and antinodes of the K_1 wave occur. The analytical model will be applied to the major tributaries and the upper bay to determine whether the observed K_1 wave behaves like a reflected wave, and to estimate the phase and amplitude at the point of reflection.

INTERACTION OF THE M_2 AND K_1 TIDAL WAVES

The result of interaction of the semidiurnal and diurnal tides in Chesapeake Bay and its tributaries can be indicated by classifying the observed tide according to the criterion (form number) described in Table 2. This classification criterion was also used by Hicks (1964) to describe the tide observed in Chesapeake Bay and its tributaries. However, his analysis was based on harmonic constants for only 26 locations, whereas this study is based on harmonic constants for 108 locations.

The tide classification chart shown in Figure 19 indicates a somewhat different and more detailed description of the change in type of tide than that presented by Hicks. The type of tide has also been determined outside Chesapeake Bay Entrance for comparison with the tide in the bay. The tide is predominantly semidiurnal outside the entrance with form numbers of 0.216 and 0.224 at Chesapeake Light Tower and Virginia Beach, VA, respectively. The tide is also predominantly semidiurnal throughout the lower bay, including the mouths of the James and York rivers. The tide continues to be semidiurnal as it travels

Figure 19. Type of tide in Chesapeake Bay and its major tributaries, and the location of quasinodes and antinodes of the M_2 and K_1 tidal waves.

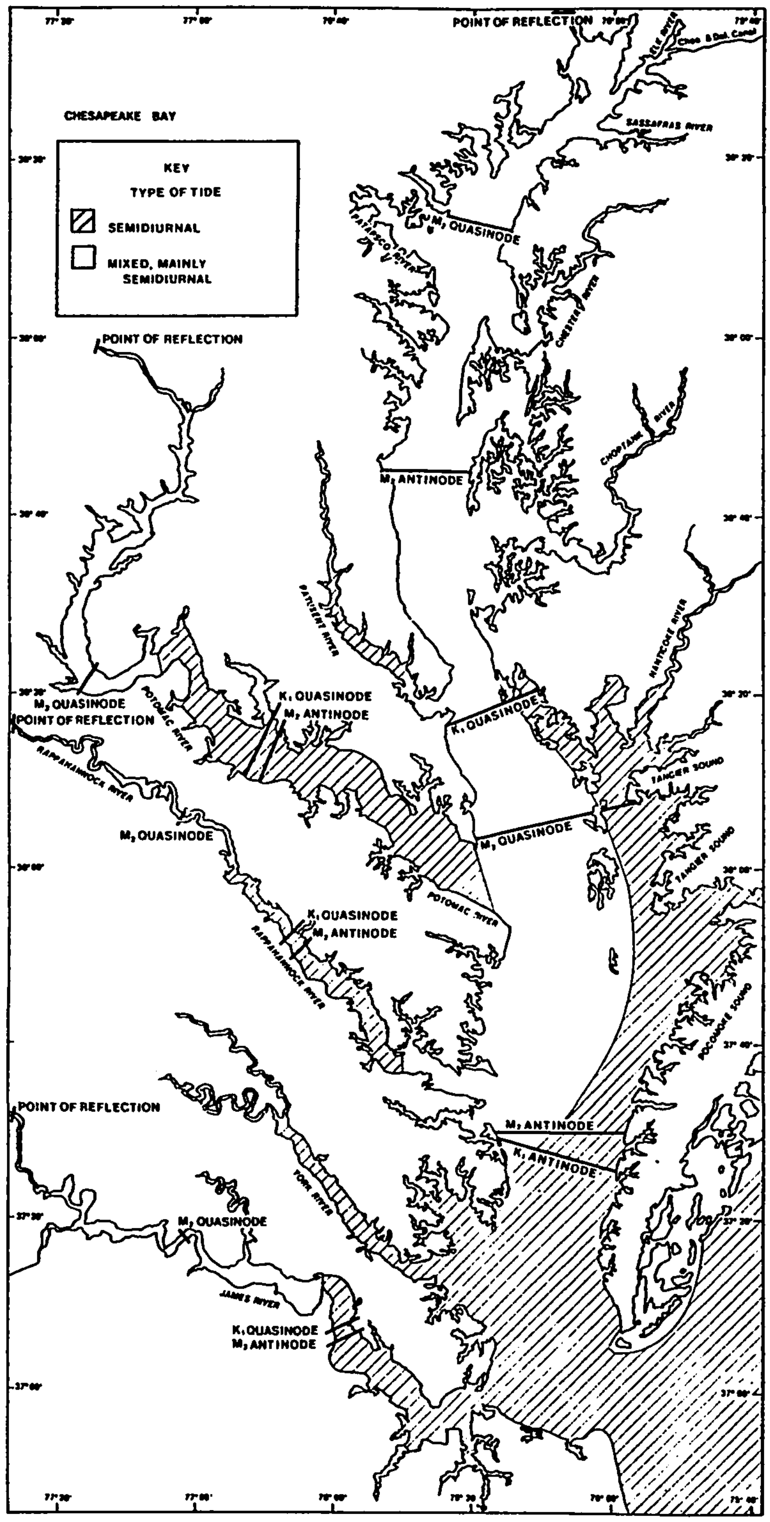
CHESAPEAKE BAY
KEY
TYPE OF TIDE
SEMIDIURNAL
MIXED, MAINLY SEMIDIURNAL
POINT OF REFLECTION
SASSAFRAS RIVER
M₂ QUASINODE
PATAPSCO RIVER
CHESTER RIVER
POINT OF REFLECTION
M₂ ANTINODE
CHOPTANK RIVER
PATUXENT RIVER
NANTICOKE RIVER
M₂ QUASINODE
POINT OF REFLECTION
POTOMAC RIVER
K₁ QUASINODE
M₂ ANTINODE
K₁ QUASINODE
RAPPAHANNOCK RIVER
TANGIER SOUND
M₂ QUASINODE
M₂ QUASINODE
POTOMAC RIVER
K₁ QUASINODE
M₂ ANTINODE
RAPPAHANNOCK RIVER
POCOMOKE SOUND
POINT OF REFLECTION
M₂ ANTINODE
K₁ ANTINODE
YORK RIVER
M₂ QUASINODE
JAMES RIVER
K₁ QUASINODE
M₂ ANTINODE

northward along the eastern shore and through the eastern regions of Pocomoke and Tangier Sounds into the Nanticoke River.

The tide is mixed, mainly semidiurnal throughout the remainder of the Bay Proper. This indicates the influence of the diurnal tide in the upper bay has increased resulting in a decreased dominance of the semidiurnal tide. The highest form numbers are located in the upper bay between the mouth of the Severn River and the mouth of the Patapsco River. In comparison, the lowest form numbers are located in the lower bay near Chesapeake Bay Entrance reflecting the influence of the semi-diurnal tide outside the entrance.

The type of tide often changes two or three times throughout the tidal length of each of the major tributaries. The tide is classified predominantly semidiurnal in the James River from its mouth to 20 nautical miles upriver; a continuation of the semidiurnal tide observed outside the mouth in the lower bay. The tide becomes mixed, mainly semidiurnal upriver of this region, but appears to become predominantly semidiurnal again in the vicinity of Richmond. However, the form number at Richmond is 0.243, which isn't significantly different from the classification criterion of 0.25. This indicates the tide isn't clearly one type or the other. The semidiurnal tide of the lower bay also continues up the York River to West Point, which is the furthest upriver that the tide was observed.

The tide in the mouth and lower region of the Rappahannock River is mixed, mainly semidiurnal, the same as in the bay outside the mouth of the river. Approximately five nautical miles upriver, the tide becomes predominantly semidiurnal and remains so for 35 nautical miles. Then the tide becomes mixed, mainly semidiurnal again over a short distance. However this mixed, mainly semidiurnal classification is based on tide observations at only one location in this region. Upriver, the tide once again becomes predominantly semidiurnal and remains so to the vicinity of Fredericksburg.

The change in type of tide in the Potomac River appears to be more complicated. The tide is strongly semidiurnal in the region which extends from its mouth to approximately 50 nautical miles upriver, even though the tide in the adjacent bay is classified as mixed, mainly semidiurnal. The form numbers at a number of locations in both the river and bay confirm this observation. Upriver, beyond the semidiurnal region, the tide becomes mixed, mainly diurnal for a distance of about 30 nautical miles, beyond which it becomes semidiurnal again for a distance of about 16 nautical miles upriver to Washington, DC.

The tide is mixed, mainly semidiurnal in the region which extends from the mouth of the Patuxent River to about five nautical miles upriver, a continuation of the tide in the Bay Proper. The tide is predominantly semidiurnal upriver of this region to Upper Marlboro, MD which was the limit of tide observations.

The interaction of the diurnal and semidiurnal tides in these relatively narrow tributaries is much simpler to explain than that in the Bay Proper. Therefore, it is addressed first. The interaction of the M_2 and K_1 tidal waves is used to represent how the diurnal and semidiurnal tides interact in the major tributaries.

The one dimensional analytical model can be used to determine whether reflection actually occurs in a particular tributary and to determine the best estimate of the amplitudes and phases of M_2 and

K_1 at the point of reflection. According to this model, the point of reflection is an antinode of the constituent wave, and a quasisnode is located one quarter wavelength downriver from the point of reflection. Another antinode is located a half wavelength downriver from the point of reflection, and so on. Because of friction, the locations of the observed minimum and maximum amplitudes will not be at the same locations as these quasinodes and antinodes. As previously explained in Chapter 2, an increase in the damping coefficient causes the minimum amplitude to occur slightly upriver of the quasinode. The maximum amplitude located further downriver will similarly occur slightly upriver from the antinode. However, the spatial coverage of tide stations used during this study wasn't dense enough to detect the difference.

Separate Redfield nomograms were plotted for the M_2 and K_1 tidal waves in the James, Rappahannock, and Potomac rivers. The amplitude ratio for each tide station is the observed M_2 or K_1 amplitude at a particular location along the tributary divided by the estimated amplitude at the point of reflection. This ratio was plotted on the nomogram relative to the difference in phase between the point of reflection and the selected location. The M_2 and K_1 nomogram plots for the James River are presented in Figures 20 and 21, respectively, and the change in amplitude of M_2 and K_1 with distance is shown in Figure 22.

The point of reflection in the James River is most likely located in the vicinity of the river locks and rapids in Richmond. The best fit of M_2 amplitude ratios and differences in phase on the nomogram

Figure 20. James River M_2 tide data plotted on the Redfield nomogram.

JAMES RIVER

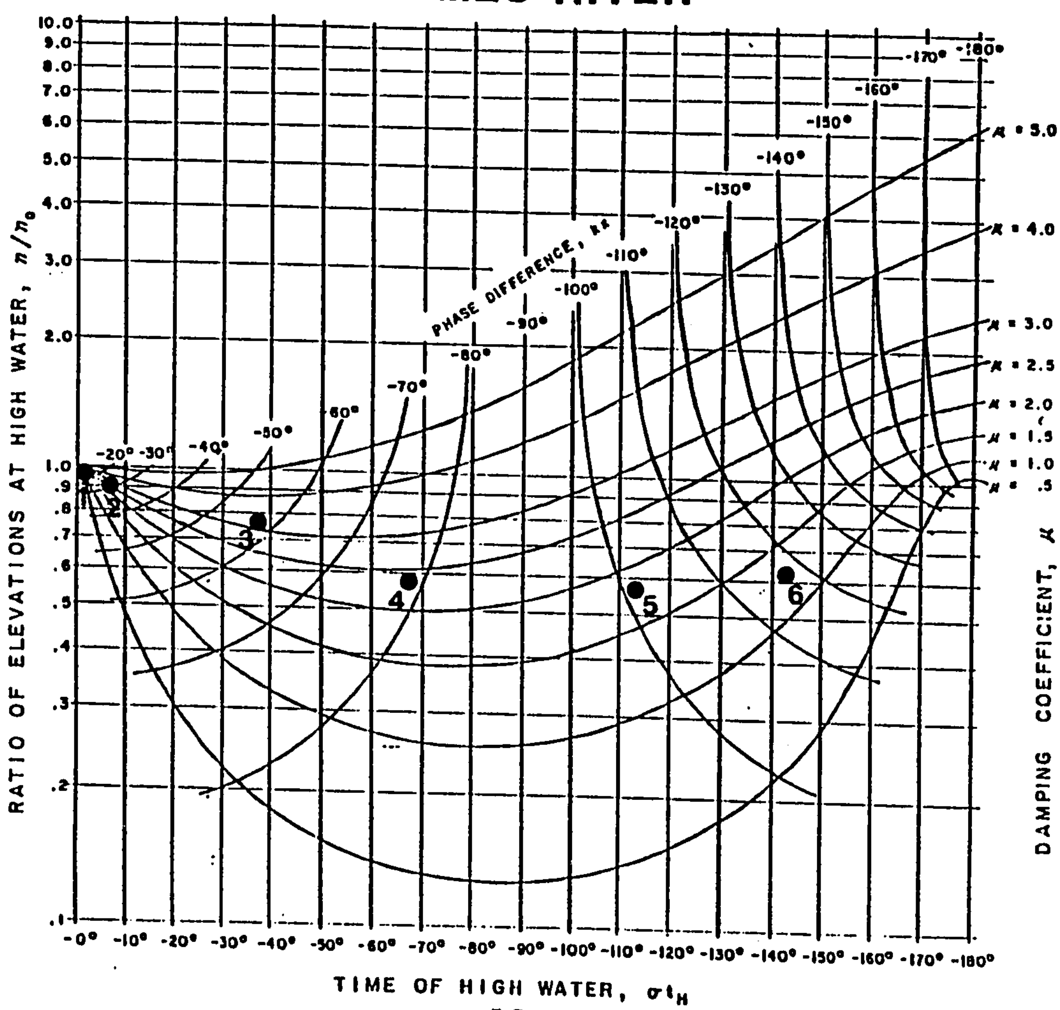

M_2

1. Richmond
2. Chester
3. Hopewell
4. Wilcox Wharf
5. Claremont
6. Scotland

Figure 21. James River K_1 tide data plotted on the Redfield nomogram.

JAMES RIVER

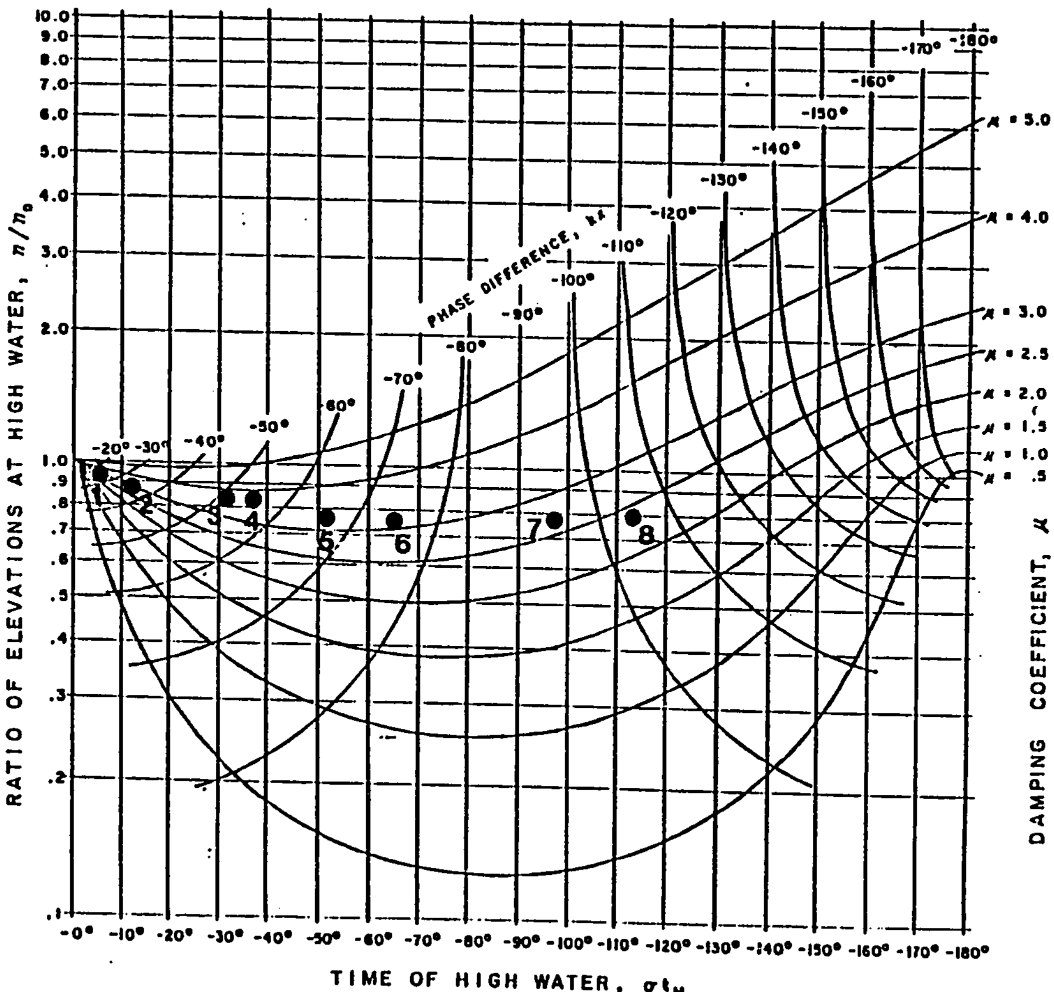

K_1

1. Richmond
2. Chester
3. Hopewell
4. Wilcox Wharf
5. Claremont
6. Scotland
7. Burewell Bay
8. Huntington Park

Figure 22. Amplitude of the M_2 and K_1 tides in the James River.

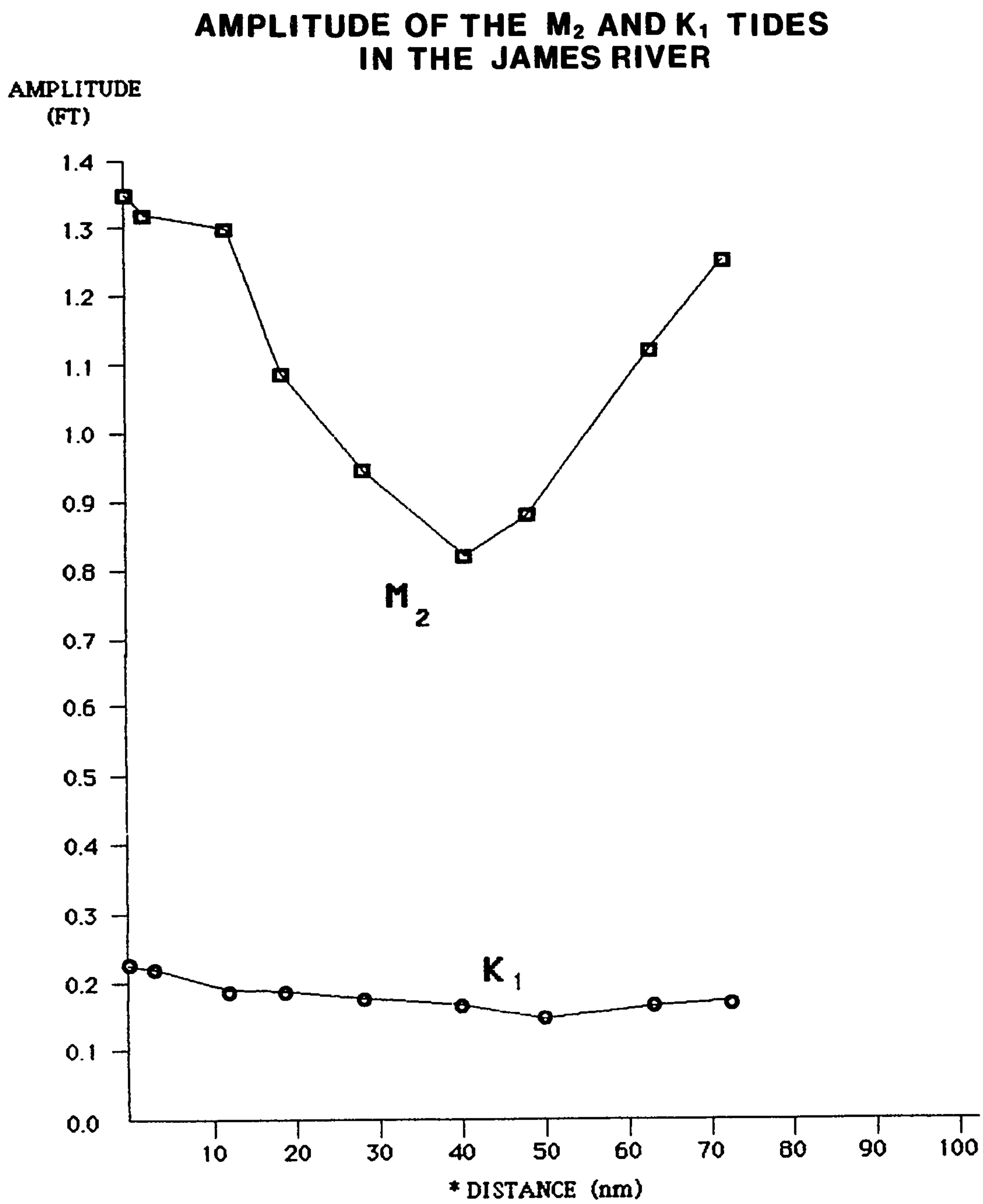

*Measured from point of reflection

in Figure 20 is shown to occur when the amplitude and phase at the point of reflection are estimated to be 1.40 ft and 125°, respectively. Therefore, the M_2 quasinode should be located approximately where the phase is observed to be 35° (about 35 nautical miles downriver from Richmond), which agrees fairly well with Figure 22. An antinode is located approximately where the phase is 305° (about 63 nautical miles below Richmond). The best fit of K_1 data on the nomogram in Figure 21 is shown to occur when the K_1 amplitude and phase at the point of reflection are estimated to be 0.220 ft and 245°, respectively. Therefore, the K_1 quasinode would be located where the phase is about 155° (approximately 60 nautical miles downriver from Richmond). There is no antinode located further downriver because the K_1 phase difference at the mouth is only 115°. The locations of the M_2 and K_1 quasinodes and antinodes are also indicated on Figure 19.

According to the one dimensional model, both the M_2 and K_1 tidal waves will have an antinode at the point of reflection, and each wave will be at maximum amplitude at this point. If the M_2 and K_1 waves are also in phase at the point of reflection, these maximum amplitudes will occur at the same time. However, the M_2 and K_1 waves will not be in phase downriver due to the different frequencies of K_1 and M_2. It was observed that the amplitudes of the K_1 and M_2 waves at Richmond are 0.207 ft and 1.323 ft, respectively. The ratio of these amplitudes is 0.156 compared to a form number of 0.243. Therefore, both ratios indicate the tide is predominantly semidiurnal.

Figure 22 shows that, in the James River, the M_2 quasinode is encountered downriver from the point of reflection well before the K_1

quasinode. Even though the amplitude of K_1 at Richmond was only 15.6 percent of that of M_2, the amplitude of M_2 drops off much faster than K_1 with distance. At the M_2 quasinode, the effect of the diurnal tide becomes more pronounced as the amplitude of M_2 rapidly decreases, and the tide becomes mixed, mainly semidiurnal throughout a considerable region around the location of the M_2 quasinode.

Note that the K_1 quasinode is located at approximately the same location as the M_2 antinode. As the amplitude of K_1 approaches its minimum, the absolute value of the M_2 amplitude approaches its maximum, and the semidiurnal tide strongly dominates. Therefore, the tide is classified predominantly semidiurnal throughout the remainder of the James River to its mouth.

The M_2 and K_1 nomogram plots for the Rappahannock River are presented in Figures 23 and 24, respectively, and the change in amplitude of the M_2 and K_1 waves with distance is shown in Figure 25. The point of reflection in the Rappahannock River is most likely located at the shoals near Fredericksburg. The best fit of M_2 amplitude ratios and differences in phase on the nomogram in Figure 23 is shown to occur when the amplitude and phase at the point of reflection are estimated to be 1.20 ft and 195^o, respectively. Therefore, the M_2 quasinode should be located approximately where the phase is observed to be 105^o (about 30 nautical miles downriver from the point of reflection). An antinode would be located where the phase is 15^o (about 55 nautical miles downriver from the reflection point). Therefore, the observed locations of the minimum and maximum amplitudes of the M_2 wave agree fairly well with the locations of the quasinode and antinode.

Figure 23. Rappahannock River M_2 tide data plotted on the Redfield nomogram.

RAPPAHANNOCK RIVER

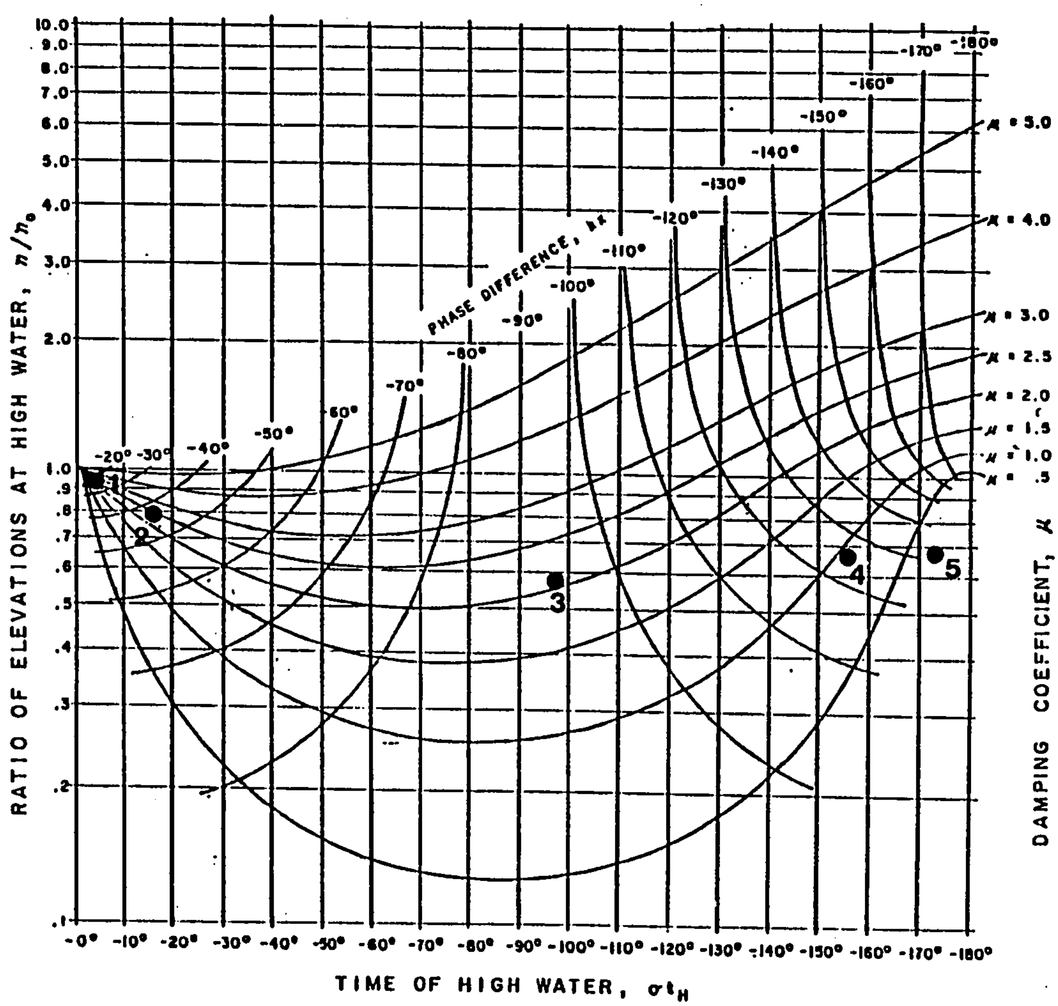

M_2

1. Massaponax
2. Hopyard Landing
3. Saunders Wharf
4. Tappahannock
5. Wares Wharf

Figure 24. Rappahannock River K_1 tide data plotted on the Redfield nomogram.

RAPPAHANNOCK RIVER

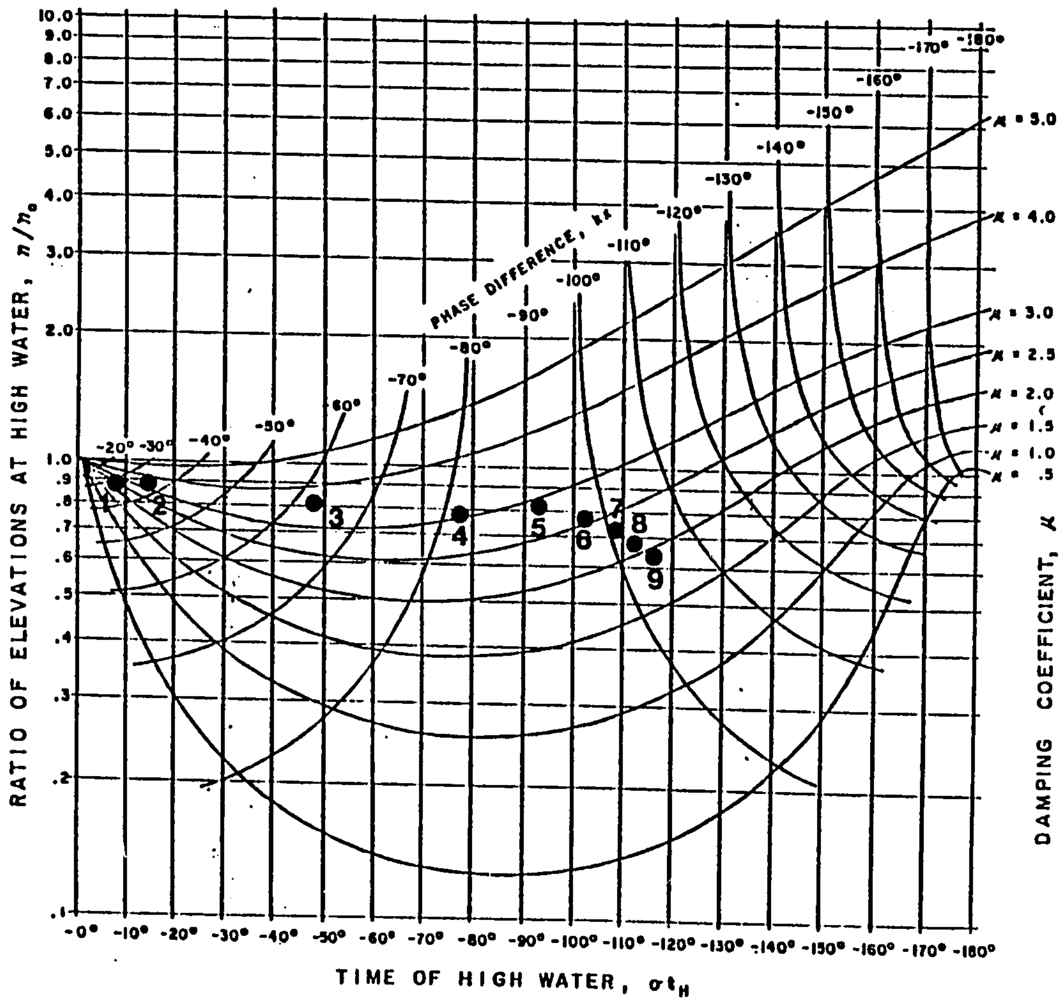

K_1

1. Massaponax
2. Hopyard Landing
3. Saunders Wharf
4. Tappahannock
5. Wares Wharf
6. Bayport
7. Unbanna
8. New Mill Creek
9. Windmill Point

Figure 25. Amplitude of the M_2 and K_1 tides in the Rappahannock River.

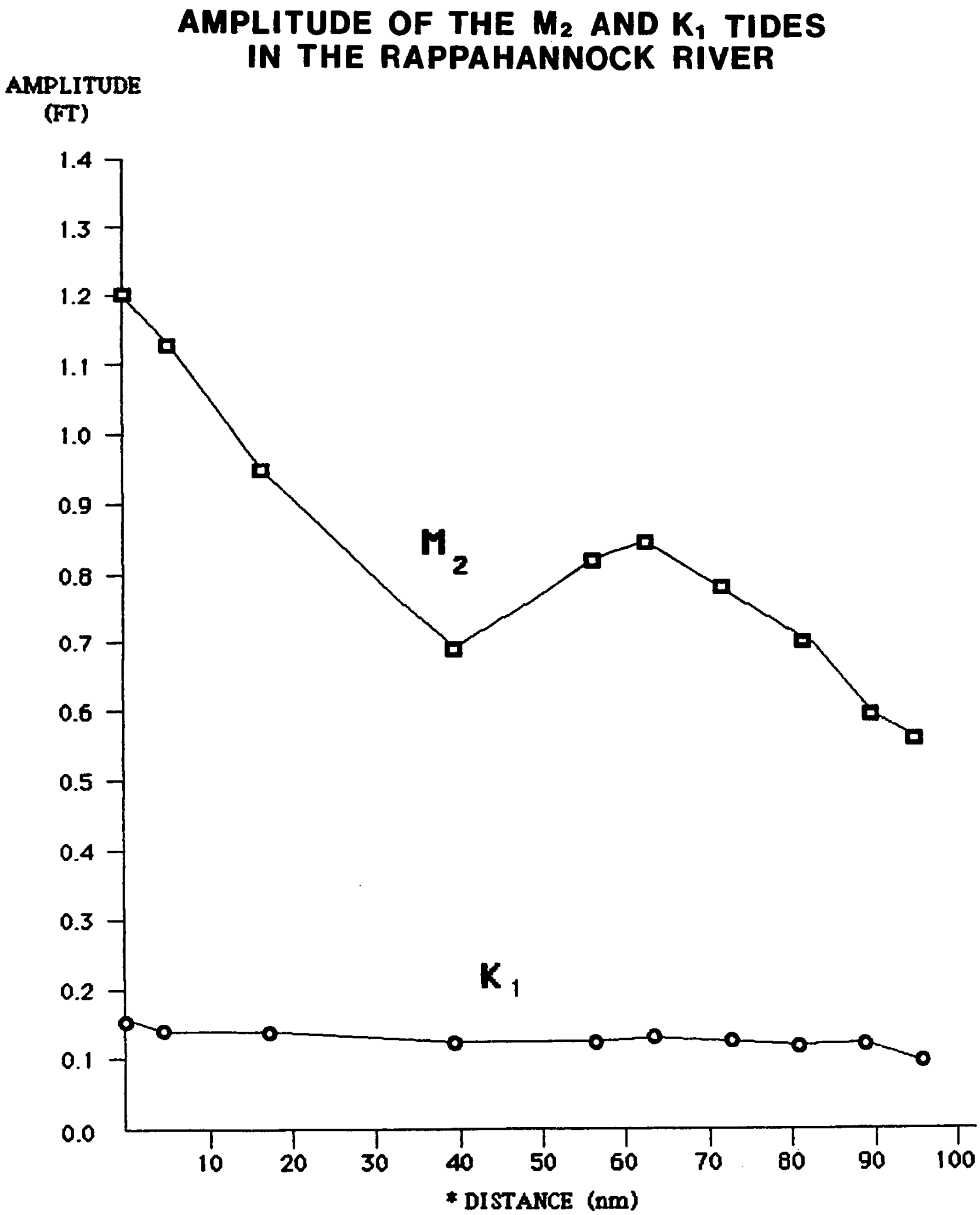

*Measured from point of reflection

The best fit of K_1 data on the nomogram in Figure 24 is shown to occur when the amplitude and phase at the point of reflection are estimated to be 0.150 ft and 265°, respectively. Therefore, the K_1 quasinode should be located approximately where the phase is 175° (about 50 nautical miles downriver from the point of reflection), and there is no antinode further downriver. The location of the minimum K_1 amplitude isn't very distinct in Figure 25. The locations of the M_2 and K_1 quasinodes and antinodes in the Rappahannock River are indicated on Figure 19.

Near the point of reflection, the ratio of the K_1 and M_2 amplitudes is 0.117 compared to a form number of 0.173. Both indicate the semidiurnal tide dominates near the point of relection. Proceeding downriver, the observed tide continues to be semidiurnal until, in the vicinity of the M_2 quasinode, it becomes mixed, mainly semidiurnal. Then the tide becomes predominantly semidiurnal again approximately five nautical miles downriver from this quasinode. This semidiurnal region spans both the K_1 quasinode and the M_2 antinode which are located about five nautical miles apart. Downriver from this region, the M_2 amplitude decreases while the K_1 amplitude simultaneously increases. These changes are sufficient that the observed tide is classified as mixed, mainly semidiurnal throughout the remainder of the Rappahannock River to its mouth.

The M_2 and K_1 nomogram plots for the Potomac River are presented in Figures 26 and 27, respectively, and the change in amplitude of the M_2 and K_1 waves is shown in Figure 28. The point of reflection in the Potomac River is most likely located at Great Falls, approximately 12 nautical miles upriver from Washington, DC. The best fit of M_2

Figure 26. Potomac River M_2 tide data plotted on the Redfield nomogram.

POTOMAC RIVER

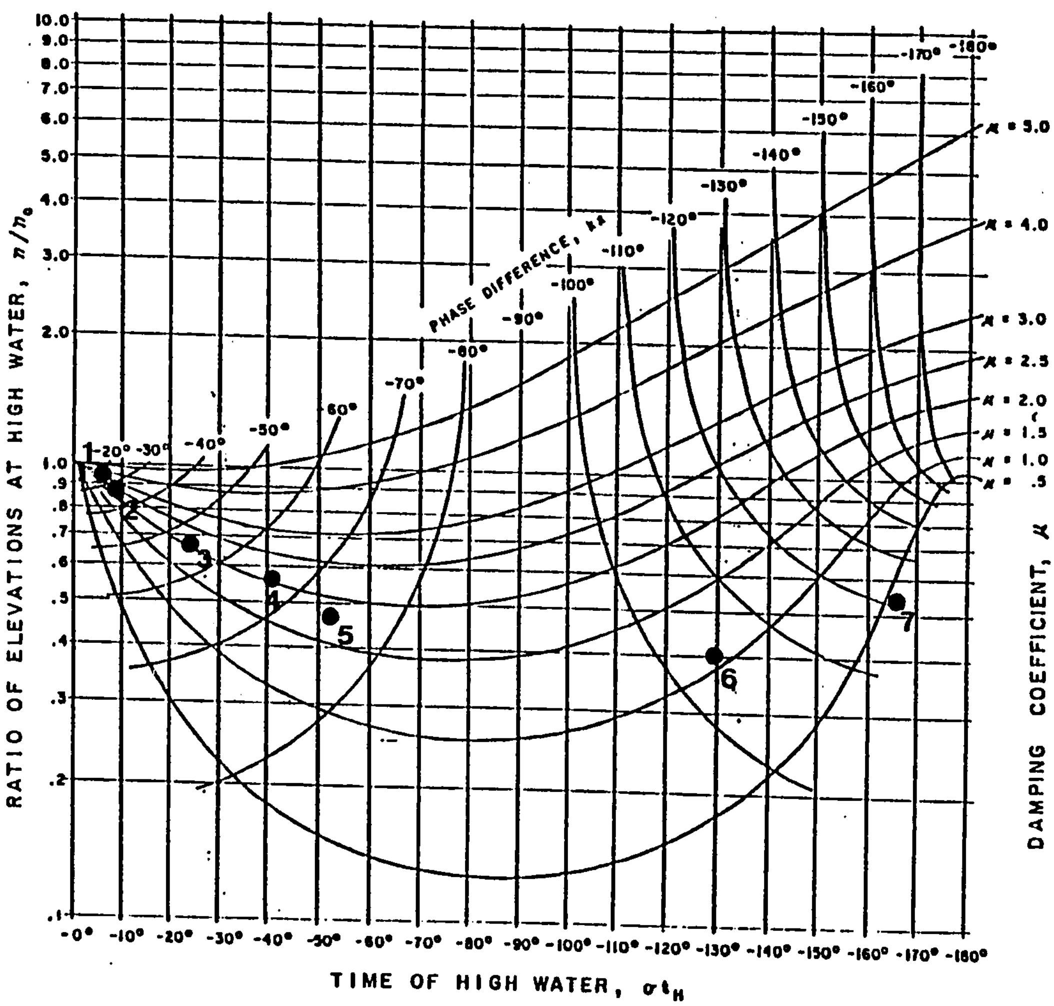

M_2

1. Washington, D.C.
2. Alexandria
3. Marshall Hall
4. Indian Head
5. Quantico
6. Riverside
7. Dahlgren

Figure 27. Potomac River K_1 tide data plotted on the Redfield nomogram.

POTOMAC RIVER

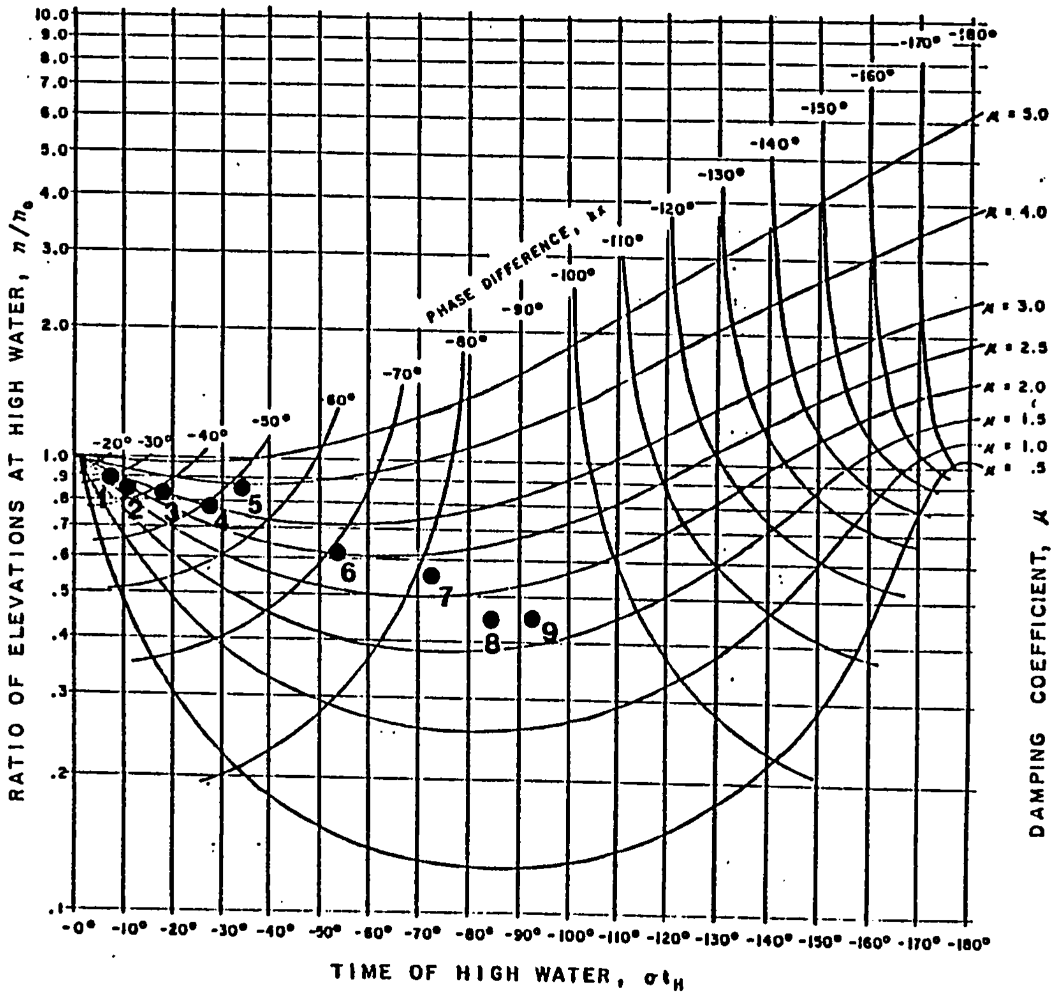

K$_1$

1. Washington, D.C.
2. Alexandria
3. Marshall Hall
4. Indian Head
5. Quantico
6. Riverside
7. Dahlgren
8. Piney Point
9. Point Lookout

Figure 28. Amplitude of the M_2 and K_1 tides in the Potomac River.

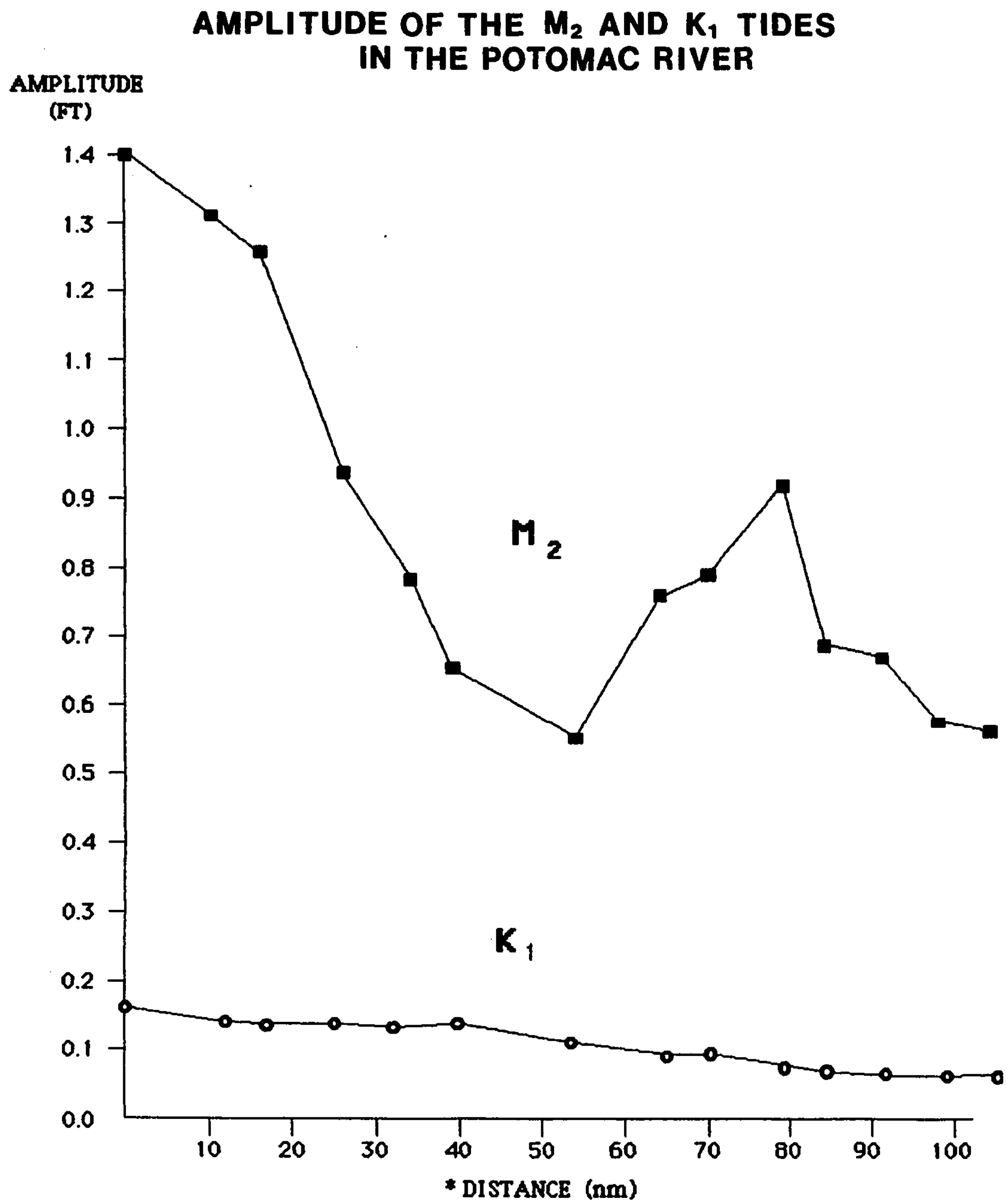

*Measured from point of reflection

amplitude ratios and differences in phase on the nomogram in Figure 26 is shown to occur when the amplitude and phase at the point of reflection are estimated to be 1.40 ft and 240°, respectively. Therefore, the M_2 quasinode should be located approximately where the phase is 150° (about 45 nautical miles downriver from the point of reflection). An antinode would be located where the phase is 60° (about 75 nautical miles downriver from Great Falls).

The best fit of K_1 data on the nomogram in Figure 27 is shown to occur when the amplitude and phase at the point of reflection are estimated to be 0.170 ft and 300°, respectively. The K_1 quasinode should be located approximately where the phase is 210° (about 72 nautical miles downriver from the point of reflection). The minimum amplitude of the K_1 wave isn't very distinct in Figure 28. The locations of the M_2 and K_1 quasinodes and antinodes in the Potomac River are indicated in Figure 19.

The location nearest the point of reflection where the tide has been observed is Washington, DC. The ratio of the K_1 and M_2 amplitudes at Washington, DC is 0.114 compared to a form number of 0.161. Both indicate the semidiurnal tide dominates at this location. The observed tide is classified predominately semidiurnal until approximately 30 nautical miles downriver from Great Falls where the decrease in amplitude of M_2, in the vicinity of the M_2 quasinode, allows the K_1 tide to become more pronounced. The observed tide is classified mixed, mainly semidiurnal for the next 28 nautical miles downriver. Then the tide becomes semidiurnal in a region which extends for nearly 50 nautical miles further downriver to its mouth. The M_2 antinode and K_1 quasinode are both located in the middle of this region.

Therefore, the M_2 amplitude is reaching its maximum as that of K_1 is passing through its minimum. The ratio of K_1 to M_2 remains relatively small, indicating that the semidiurnal tide dominates throughout the entire region. Immediately bayward of the river's mouth, the semidiurnal tide of the Potomac River appears to have little effect on the tide in the bay, which is classified mixed, mainly semidiurnal, and vice versa.

The interaction of the semidiurnal and diurnal tides in the Bay Proper is more complicated than that observed in the tributaries. This is due to the greater width of the lower bay and possibly due to imperfect reflection of the incident tidal constituent waves. The one dimensional model is applied to the upper bay to determine whether reflection actually occurs and to estimate the amplitudes and phases of M_2 and K_1 at the point of reflection.

The fit of the M_2 amplitude ratios and differences in phase on the nomogram in Figure 29 was not as good as was observed for the major tributaries, because of the small number of locations of observed tide data which are included within a half wavelength of M_2. However, the data does suggest the M_2 tide is reflected at the head of bay, and the amplitude and phase at the point of reflection are estimated to be 0.90 ft and 290°, respectively. Figure 30 shows the observed change in amplitude of the M_2 and K_1 tidal waves as they travel along the east and west sides of the Bay Proper.

Assuming a one dimensional model of the entire Bay Proper for illustrative purposes only, the first M_2 quasinode would be located where the observed phase is 200° (about 25 nautical miles down the

Figure 29. M_2 tide data for the east and west sides of Chesapeake Bay Proper plotted on the Redfield nomogram.

CHESAPEAKE BAY PROPER

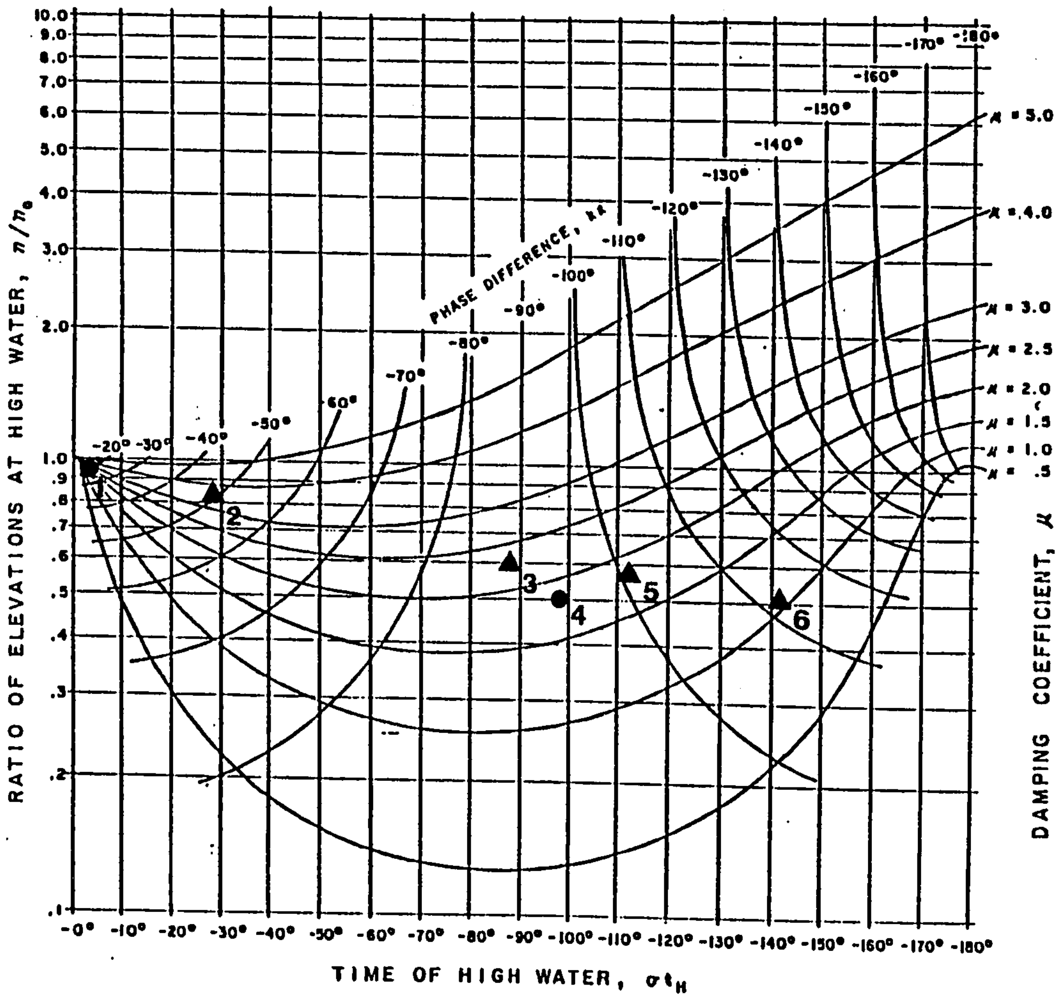

M_2

▲ East Side ● West Side

1. Havre de Grace
2. Betterton
3. Tolchester Beach
4. North Point
5. Love Point
6. Matapeake

Figure 30. Amplitude of the M_2 and K_1 tides in Chesapeake Bay Proper.

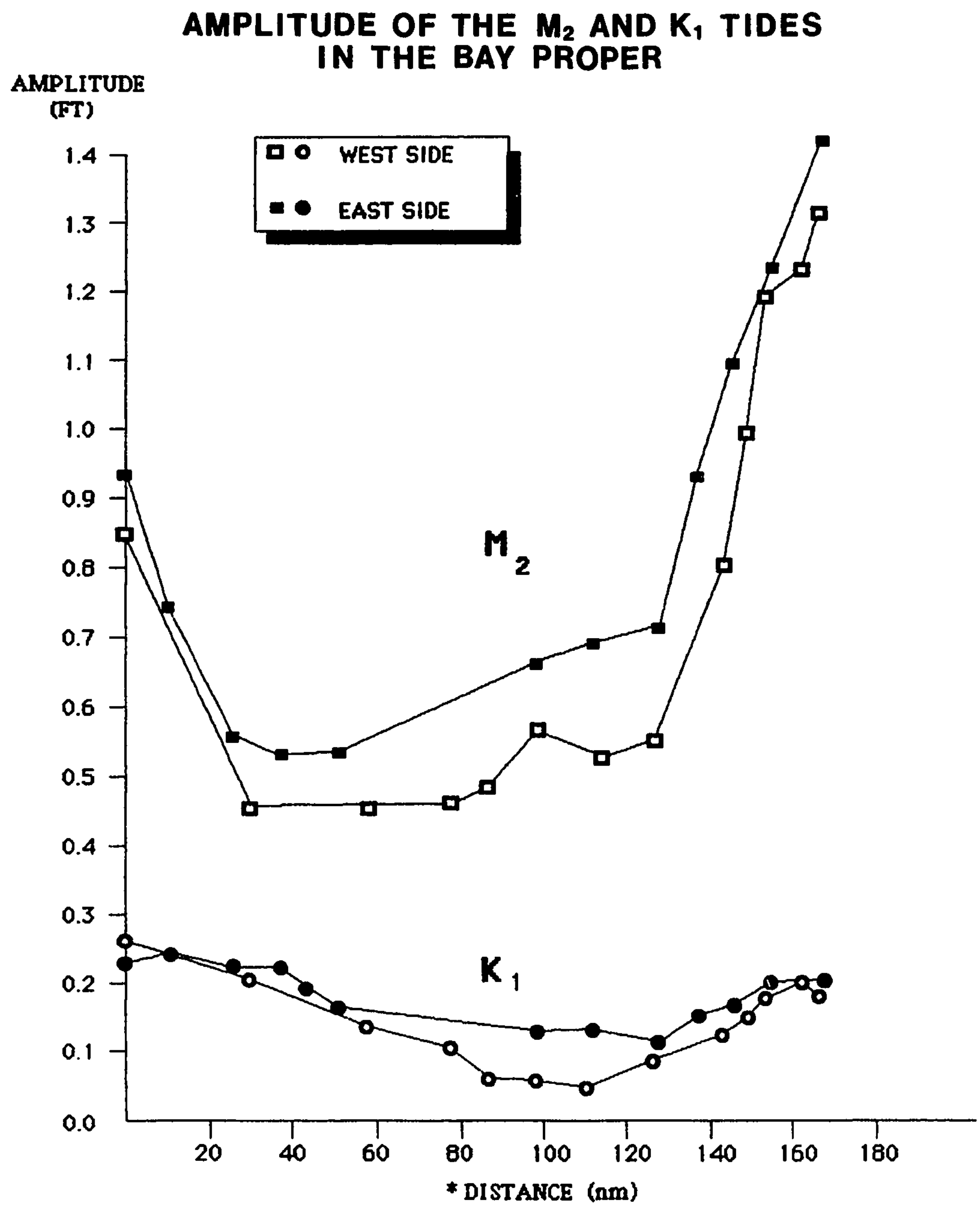

*Measured from Head of Bay (near point of reflection) bay from Havre de Grace). An antinode would be located approximately where the phase is 110° (about 30 nautical miles further down the bay), and a second quasinode would be located approximately where the phase is 20° (about 40 nautical miles further down the bay in the vicinity of the mouth of the Potomac River).

The location of the remaining antinode is estimated to be where the M_2 phase is observed to be 290° (approximately 30 nautical miles from Chesapeake Bay Entrance). This location is in the lower bay where use of the one dimensional model is not recommended, but might be considered as describing the location of the antinode along the centerline of the main channel. Since the phase is approximatly 230° at the entrance, there should not be another quasinode. Counting from the antinode at the point of reflection, the modeled locations of the first and second quasinodes and the third antinode of the M_2 tidal wave agree fairly well with the locations of the observed minimum and maximum amplitudes shown in Figure 30. However, no increase in amplitude is observed in the vicinity of the second antinode.

The fit of the K_1 amplitude ratios and differences in phase on the nomogram in Figure 31 was somewhat better than that for M_2, possibly because more locations where tide data has been observed are included within the half wavelength of K_1. There is a clear indication that the K_1 tide is reflected, and the amplitude and phase at the point of reflection are estimated to be 0.30 ft and 320°, respectively.

Assuming a one dimensional model of the entire Bay Proper again, the K_1 quasinode would be located approximately where the phase is 230°, about 80 nautical miles down the bay from Havre de Grace. A

Figure 31. K_1 tide data for the east and west sides of Chesapeake Bay Proper plotted on the Redfield nomogram.

CHESAPEAKE BAY PROPER

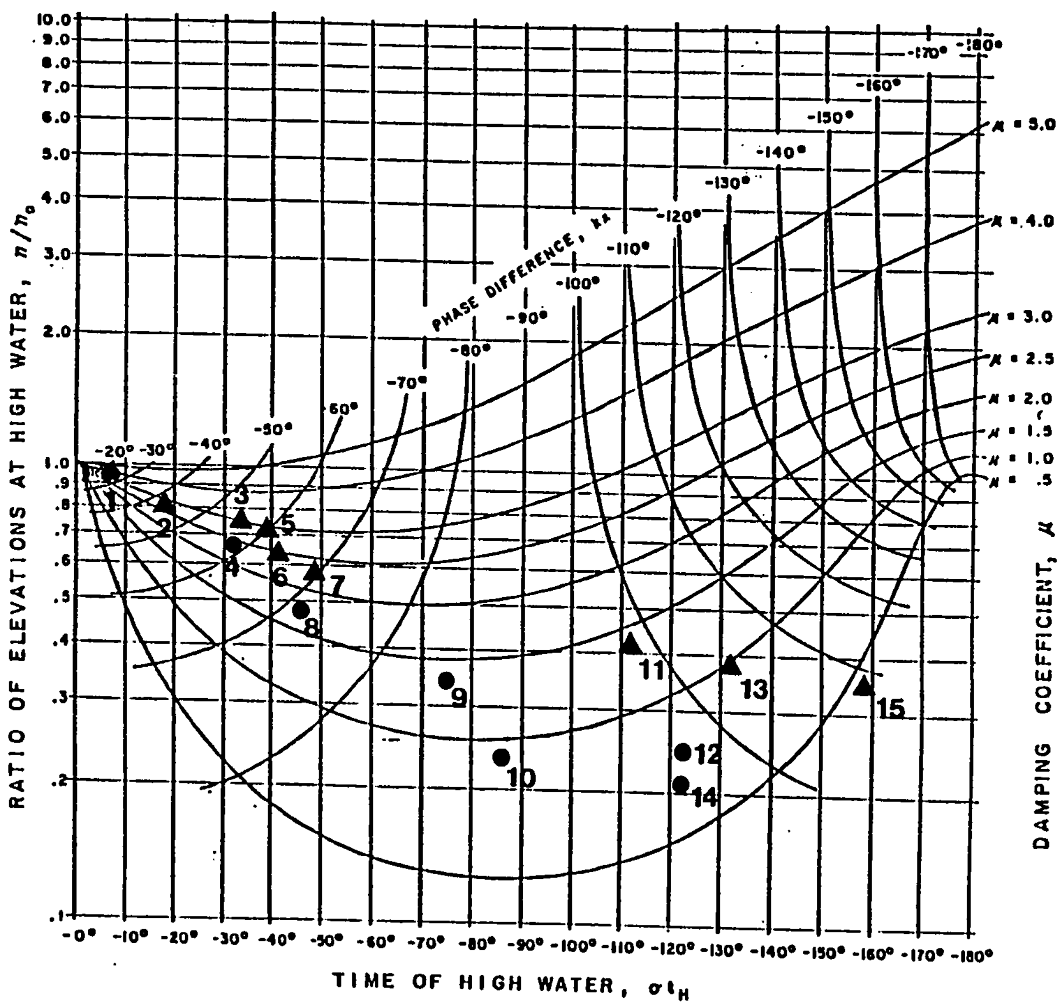

K_1

▲ East Side ● West Side

1. Havre de Grace
2. Betterton
3. Tolchester Beach
4. North Point
5. Love Point
6. Matapeake
7. Ferry Cove
8. Chesapeake Beach
9. Cove Point
10. Lexington Park
11. Hooper Is.
12. Point Lookout
13. Holland Bar Light
14. Smith Point
15. Rappahannock Shoal

second antinode would be located approximately where the phase is 140°, about 55 nautical miles further down the bay or 30 nautical miles up the bay from the entrance. The modeled locations of the K_1 quasinode and antinode only roughly agree with the locations of the observed minimum and maximum amplitudes shown in Figure 30.

The ratio of the amplitudes of K_1 and M_2 at Port Deposit is 0.346 compared to a form number of 0.466. Both indicate a strong influence of the diurnal tide in this area. In fact, the tide in the entire upper bay, with the exception of portions of Pocomoke Sound and Tangier Sound, is classified as mixed, mainly semidiurnal. This region spans the first M_2 quasinode, the second M_2 antinode, a second M_2 quasinode, the K_1 quasinode, and is bounded on its southern end by both the third M_2 antinode and the second K_1 antinode.

The decrease in M_2 amplitude in the vicinity of the first M_2 quasinode allows the effect of K_1 to become more pronounced, and the ratios of K_1 to M_2 are the largest observed in the Bay Proper. Continuing down the bay, it is surprising that the form number remains greater than 0.25 in the vicinity of the M_2 antinode which is located approximately 25 nautical miles south of North Point and in the vicinity of the K_1 quasinode which is located just south of the mouth of the Patuxent River. It appears that the amplitude of K_1 remains large enough in the vicinity of the M_2 antinode, compared to the increasing amplitude of M_2, that the ratio stays slightly larger than 0.25. This suggests the K_1 tide, and perhaps all diurnal tides, have a strong effect in this region of the bay compared to a more moderate effect of the semidiurnal constituents.

In the vicinity of the K_1 quasinode, the ratios are noticeably smaller than those observed to the north, but remain slightly larger than 0.25. This indicates the observed tide is still mixed, mainly semidiurnal though not as strongly so. This may be due to the proximity of the K_1 quasinode and the second M_2 quasinode.

The type of tide changes to predominantly semidiurnal just south of the mouth of the Rappahannock River where the M_2 and K_1 antinodes occur in nearly the same location, and remains predominantly semidiurnal throughout the lower bay. Even though the amplitudes of both constituents are at a maximum in the region where their antinodes are colocated, the amplitude of M_2 is sufficiently larger than that of K_1 to cause their ratio to be less than 0.25. This relationship also holds true for the form number.

It has been observed in this study and by Hicks (1964) that the semidiurnal tide extends further northward along the eastern shore than along the western shore. In addition, the amplitudes of the M_2 and K_1 tides are larger along the eastern shore of the bay than on the western shore, directly opposite. However, the magnitude of the increase of M_2 is greater than that of K_1. This will cause the ratio of the amplitude of K_1 divided by M_2, as well as the form number, to be proportionately smaller along the eastern shore. Therefore, ratios of 0.25 or smaller, hence a predominantly semidiurnal tide, will extend further north along the eastern shore than on the west side of the bay, directly opposite.

The nomogram plots for each basin can also be used to determine representative values for the damping coefficient, μ , and the wave number, k. Values for μ and kx have been determined for the James, Rappahannock, and Potomac rivers from the M_2 and K_1 nomograms for the regions where the best fit of the amplitude ratios and phase angles occurred. These values are listed in Table 4. The wavelengths and phase speeds of the M_2 and K_1 waves in the applicable portions of each tributary have been computed, based on the wave numbers and periods of these constituents. In addition, the average depth of each region has been calculated using equation 11 and information obtained from the M_2 and K_1 nomograms.

Comparison of the two depths computed for a particular region provides a means for assessing confidence in the results. Each pair of depths agree fairly well. Surprisingly, the best agreement occurs in the upper bay, which is where some of the shoalest average depths occur. In addition, comparison of each pair of computed average depths for a particular region with the average charted depth provides another assessment of the validity of applying the Redfield model to these regions. The computed depths for the upper tidal region of the James River appear to be three to four feet less than the average charted depth. This may be due to the relatively small width of the dredged channel in the upper James River, or perhaps the depth of the channel has actually shoaled since it was charted. The computed depths for the Rappahannock River agree well with the average charted depth.

It is difficult to compare the computed depths for the Potomac River to the average charted depth because the charted depths change considerably in the vicinity of Washington, DC. There is a 24 ft (7.32 m) dredged channel from Alexandria, VA to Washington, DC whereas the average charted depth from Washington, DC to Great Falls, VA is

TABLE 4

CHARACTERISTICS OF FRICTIONALLY DAMPED REFLECTED WAVES

Tributary or Embayment	Charted Depth (ft)	M_2 Tidal Wave μ	kx (deg)	κ (deg/nm)	L (nm)	C (kt)	h (ft)	K_1 Tidal Wave μ	kx (deg)	κ (deg/nm)	L (nm)	C (kt)	h (ft)
James River	16*	3.0	77	2.7018	133.25	10.73	13.27	3.0	75	1.5244	236.16	9.87	11.23
Rappahannock River	12	2.5	43	2.4855	144.84	11.66	14.38	3.0	92	1.4744	244.17	10.20	12.00
Potomac River	24**	2.1	66	2.1086	170.73	13.75	18.94	2.75	71	1.3124	277.31	11.46	14.47
Upper Bay	10***	3.5	50	3.3333	108.00	8.70	9.76	3.0	60	1.6216	222.00	9.28	9.92
Lower Bay		---	--	-----	-----	----	----	1.0	105	1.0000	360.00	15.04	20.67

* There is a 16 ft dredged channel to Richmond, VA. Continuing upriver to the limit of tide, the average depth is six feet.

** There is a 24 ft dredged channel from Alexandria, VA to Washington, DC. Continuing upriver to the limit of tide, the average depth is 12 ft.

*** There is a 10 ft dredged channel from Sandy Point to Havre de Grace, MD. The average depth for the rest of the head of bay is 6 ft.

about 12 ft (3.66 m). Therefore, the computed depths of 18.94 ft (5.77 m) and 14.47 ft (4.41 m) most likely relate to where this transition in depth occurs.

The M_2 and K_1 tidal wave characteristics summarized in Table 4 indicate the upper tidal regions of the James and Rappahannock rivers are very similar in terms of frictional resistance and their respective wavelengths and phase speeds. The damping coefficient is 3.0 for the K_1 wave in both rivers, and is 3.0 and 2.5 for the M_2 wave in the James River and Rappahannock River, respectively. A damping coefficient of 3.0 implies a reduction in amplitude of a tidal wave of 95 percent per tidal cycle. The tidal portions of the James and Rappahannock rivers are about 75 and 95 nautical miles long, respectively, and the M_2 wavelength is about 150 nautical miles long in the upper tidal region of each. Therefore, the reflected M_2 tide in each should be almost totally attenuated before reaching the mouth of each river. The K_1 wavelength in the upper tidal region of the James and Rappahannock rivers is about 250 nautical miles long. Therefore, the reflected K_1 tide will not be completely attenuated. However, the K_1 amplitudes are generally so small, compared to the M_2 amplitudes, that little tidal energy is returned from these rivers to the bay by the K_1 tide.

Table 4 also shows that the characteristics of the M_2 and K_1 tidal waves in the Potomac River are somewhat different than those observed in the James and Rappahannock rivers. The pair of damping coefficients are smaller in magnitude, 2.1 for the M_2 tide and 2.75 for the K_1 tide. This reduction is most likely due to the deeper depths and wider channels in the upper tidal waters of the Potomac

River. The damping coefficients determined for the M_2 and K_1 waves in the Potomac River do not agree as well as was observed for the James and Rappahannock rivers. However, 2.5 may be assumed to represent an average damping coefficient for both the M_2 and K_1 waves in this region. This implies a reduction in amplitude of a tidal wave of about 92 percent per tidal cycle. Since the tidal portion of the Potomac River is about 100 nautical miles long and the M_2 wavelength in the upper tidal region is about 170 nautical miles, most of the reflected M_2 tide will be attenuated before reaching the river's mouth. However, the K_1 wavelength is approximately 275 nautical miles. Therefore, the reflected K_1 tide will not be as attenuated, but its small amplitude (compared to that of M_2) indicates little tidal energy will be returned from the Potomac River to the bay by the K_1 tide.

The M_2 and K_1 characteristics in Table 4 indicate the largest damping coefficients, shortest wavelengths, and shoalest computed depths occur in the upper reach near the head of bay. The damping coefficients for the M_2 and K_1 tidal waves are 3.5 and 3.0, respectively. This implies a reduction of amplitude of the M_2 and K_1 tides in this region of 97 and 95 percent per tidal cycle, respectively, which indicates the tide is very rapidly attenuated.

This evaluation indicates the Redfield model can be used to represent the tidal circulation of the upper tidal regions of these tributaries and the upper bay. The damping coefficients and wave numbers listed in Table 4 can be used with equation 15 to compute the amplitudes of the M_2 and K_1 tides for any time at any location in the applicable waterway. They can also be used with equation 20 to compute the velocity of the M_2 and K_1 tidal currents.

THE M_2 TIDAL CURRENT

It was intended to construct cocurrent charts of Chesapeake Bay, based on current meter data obtained during this study, which would have been compared to the cocurrent charts constructed by Hicks in 1964. However, the Greenwich lunitidal intervals and mean maximum flood speeds required to construct these new cocurrent charts have not yet been determined. This will require extensive harmonic analysis of data from the long term current meter stations and rotary analysis of data from all the other stations. The National Ocean Service is doing these analyses at this time in order to prepare daily predictions for new reference stations and compute relationships to subordinate stations for publication in future tidal current prediction tables. However, it was possible to construct cospeed and cophase charts for the M_2 tidal current constituent which are presented in Figures 32 and 33, respectively. These charts were constructed using the harmonic constants which have been determined from data observed at 124 locations throughout the Bay Proper during this study.

The harmonic analysis program resolves the observed current velocity and direction into speeds for each constituent, oriented to predetermined major and minor axes. It has been observed during this study that the major axis speeds are much larger than the minor axis speeds at most current stations throughout the bay, indicating the tidal current tends to be reversing at most locations. Most likely this is due to the effect of bottom topography. For example, the ellipses in Figure 12 show that the major simidiurnal tidal current constituents at Chesapeake Bay Entrance are nearly reversing currents.

Figure 32. Cospeed chart for the M_2 tidal current in Chesapeake Bay Proper. Cospeed lines are expressed in centimeters per second.

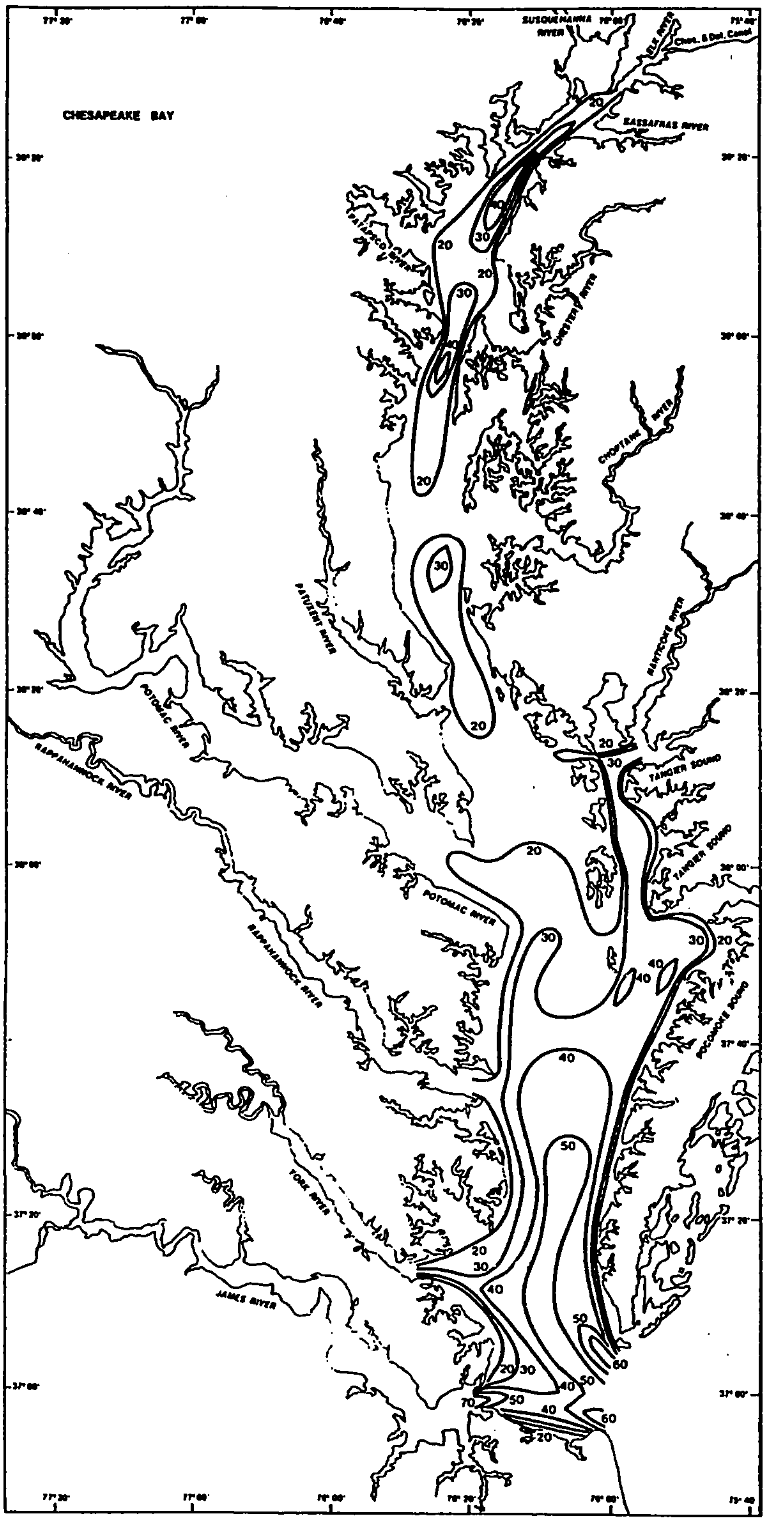
CHESAPEAKE BAY
SUSQUEHANNA RIVER
SASSAFRAS RIVER
CHESTER RIVER
CHOPTANK RIVER
PATUXENT RIVER
NANTICOKE RIVER
POTOMAC RIVER
RAPPAHANNOCK RIVER
TANGIER SOUND
POCOMOKE SOUND
YORK RIVER
JAMES RIVER

Figure 33. Cophase chart for the M_2 tidal current in Chesapeake Bay Proper. Cophase lines are expressed in degrees.

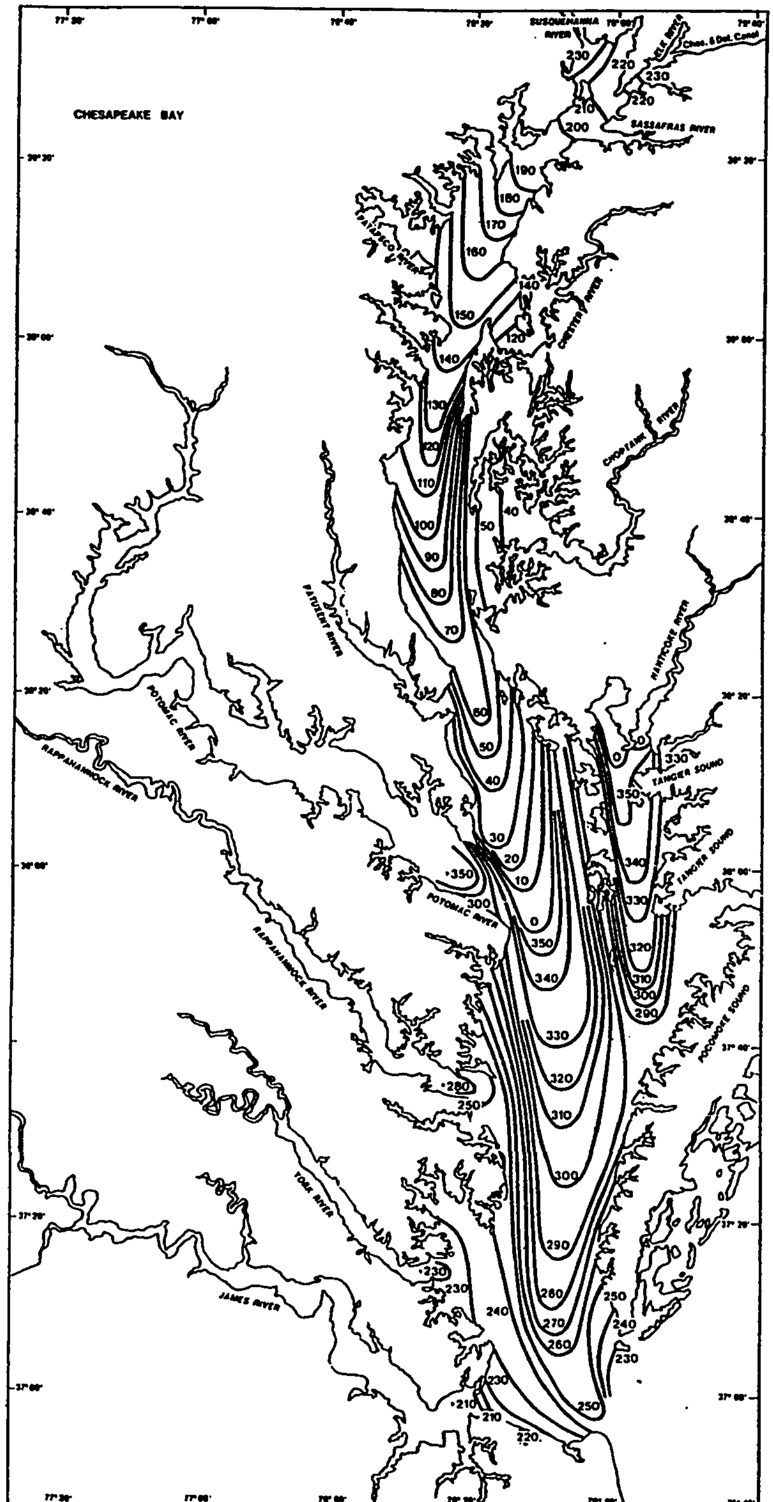
CHESAPEAKE BAY
SUSQUEHANNA RIVER
SASSAFRAS RIVER
CHOPTANK RIVER
NANTICOKE RIVER
PATUXENT RIVER
POTOMAC RIVER
RAPPAHANNOCK RIVER
YORK RIVER
JAMES RIVER
TANGIER SOUND
POCOMOKE SOUND

Therefore, only the major axis phases and speeds of the M_2 tidal current constituent were used to construct cophase and cospeed charts representing the maximum flood current. The phases and speeds of M_2 were consistent enough from station to station to allow contouring cospeed and cophase lines. The major axis speeds of K_1 were much smaller and the phases varied too much from station to station for contouring.

The major axis phase of M_2 was surprisingly consistent in its progress throughout the bay, and contours were drawn with a high degree of confidence. The major axis speed of M_2 was consistent enough for contouring cospeed lines, however the confidence level of these contours is not as high as for the cophase lines for the M_2 tidal current or the comparable coamplitude lines for the M_2 tidal constituent.

A ratio, consisting of the height that each current meter was deployed above bottom divided by the total depth (at Mean Low Water), was used to recognize where current meters may have been deployed so close to the bottom that friction might cause distortion of the phases and speeds determined for this study. Current meter data was not considered significantly affected by bottom friction when the depth ratio was 0.5 or greater. For example, the depth ratio for the top meter at station 40 in Chesapeake Bay Entrance is 0.64 (27 ft height of current meter above bottom divided by 42 ft total depth of water). Therefore, the current data from this meter was not considered significantly affected by bottom friction. The depth ratio for each current meter is indicated in Appendix C.

The major axis speed of the K_1 tidal current constituent is similarly used during this study to approximate the maximum flood speed of the diurnal tidal current. The ratio of the major axis speed of K_1 to the major axis speed of M_2 has been used to roughly indicate the type of tidal current, much like using the ratio of the amplitudes of the K_1 and M_2 tidal constituents to indicate the type of tide. Similarly, this speed ratio is an approximation of a tidal current classification ratio. The observed tidal current is considered predominately semidiurnal if the speed ratio is less than 0.25, and is considered mixed, mainly semidiurnal if the speed ratio is equal to or greater than 0.25 but does not exceed 1.50.

The results of this classification of the observed tidal current are presented in Figure 34. The tidal current is also predominantly semidiurnal in the lower bay, extending up the west side from Chesapeake Bay Entrance to the mouth of the Potomac River and up the east side to the mouth of the Nanticoke River. It then becomes mixed, mainly semidiurnal from these locations northward to the vicinity of North Point. The remainder of the upper bay is classified predominantly semidiurnal, except for the region near the mouth of the Chesapeake and Delaware Canal where the tidal current once again becomes mixed, mainly semidiurnal.

Since the M_2 tidal current constituent appears to dominate throughout the bay, an analysis of the M_2 tidal current cospeed and cophase charts alone should provide a basic description of the dominant tidal current circulation. In addition, the phase relationship of the M_2 tide and M_2 tidal current at various locations throughout the bay can be described through comparison of the M_2 tide cophase chart

Figure 34. Types of tidal current in Chesapeake Bay Proper.

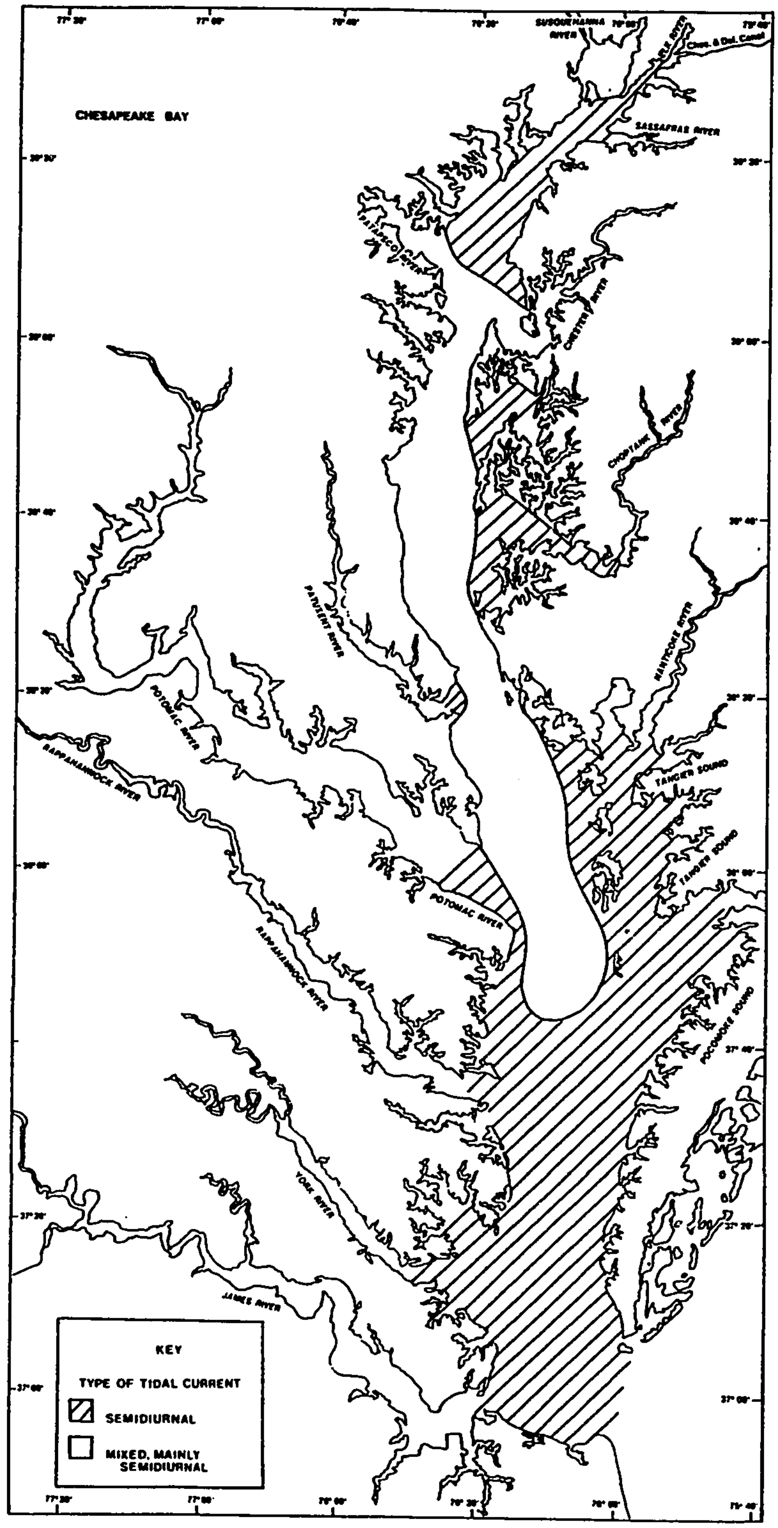
CHESAPEAKE BAY
SUSQUEHANNA RIVER
SASSAFRAS RIVER
PATAPSCO RIVER
CHESTER RIVER
CHOPTANK RIVER
PATUXENT RIVER
NANTICOKE RIVER
POTOMAC RIVER
RAPPAHANNOCK RIVER
TANGIER SOUND
POTOMAC RIVER
RAPPAHANNOCK RIVER
TANGIER SOUND
POCOMOKE SOUND
YORK RIVER
JAMES RIVER
KEY
TYPE OF TIDAL CURRENT
SEMIDIURNAL
MIXED, MAINLY SEMIDIURNAL

shown in Figure 15 with the M_2 tidal current cophase chart shown in Figure 33.

The M_2 tidal current cospeed chart shown in Figure 32 roughly approximates the maximum flood speed of the tidal current throughout the bay, and the cospeed lines may be considered isotachs. The shape and orientation of these cospeed lines indicate various circulation patterns in the bay. This cospeed chart indicates two distinct flood currents in Chesapeake Bay Entrance which have also been described by Boicourt (1981). The main current is located in the channel directly north of Cape Henry. It has a maximum speed of more than 68 cm sec^{-1} (1.32 kt) near the Cape, and divides into two separate currents in the vicinity of the Chesapeake Bay Bridge Tunnel. The larger of these currents proceeds northward up the bay, and the smaller is directed westward toward Hampton Roads. The 50 cm sec^{-1} (0.97 kt) isotach extends northward from Chesapeake Bay Entrance for approximately 33 nautical miles. Within this flow is a 30 cm sec^{-1} (0.58 kt) isotach which also appears to divide into two currents; one of which extends northward up the main channel of the Bay Proper and a second that extends northward up Pocomoke Sound and Tangier Sound. There is a 20 cm sec^{-1} (0.39 kt) isotach also located within this flow. This isotach extends up the west side of the bay from Chesapeake Bay Entrance to the mouth of the Potomac River and to the upper reaches of Tangier Sound on the east side. Note that most of the reduction in the speed of the M_2 tidal current in the Bay Proper appears to take place just south of Smith Point.

The second current in Chesapeake Bay Entrance is located in the North Channel. It's major axis flood speed is over 60 cm sec^{-1}

(1.17 kt), but the speed rapidly decreases with distance up the bay. Therefore, this feature is of little significance beyond the entrance.

North of the mouth of the Patuxent River, the cospeed lines appear to be closed contours which strongly reflect the effect of bottom topography. Immediately north of the mouth of the Patuxent River, the maximum speed along the major axis is 30 cm sec^{-1} (0.58 kt). Speeds greater than 40 cm sec^{-1} (0.78 kt) were observed in the narrows near the mouth of the Severn River and near the mouth of the Patapsco River.

Moving up the western reach of the upper bay, the major axis speed of the M_2 tidal current decreases rapidly. It is 16.1 cm sec^{-1} (0.31 kt) at current station 145, approximately two nautical miles south of Havre de Grace, but is only 3.5 cm sec^{-1} (0.07 kt) at current station 146 near Havre de Grace. This rapid decrease in speed agrees well with reflected wave theory, which indicates the current speed should go to zero at the point of reflection. Since the point of reflection was not well defined in the observed tidal data, it was not expected that the current speed would so clearly approach zero at the head of bay.

A similar decrease in current speed was not observed in the eastern upper reach of the bay. At current station 151 (approximately 5.5 nautical miles west of Chesapeake City), the major axis speed is 53.0 cm sec^{-1} (1.03 kt) and at station 152 (approximately three nautical miles west of Chesapeake City), the speed is 65.6 cm sec^{-1} (1.28 kt). The flood speed of the M_2 tidal current actually appears to be increasing in this region.

The major axis phase of the M_2 tidal current varies from 223° to nearly 258° in Chesapeake Bay Entrance. The higher phases are located in the channel directly north of Cape Henry and in Chesapeake Channel which is located in the middle of the entrance. The average major axis phase of the M_2 tidal current across the entrance is estimated to be 230°.

The M_2 tidal current cophase pattern differs significantly from that of the M_2 tide throughout the Bay Proper. The M_2 tidal current cophase lines have a definite curvature toward the entrance, whereas the M_2 tide cophase lines in the lower bay were shown to be slightly curved toward the head of bay.

There are a few cocurrent lines on Hicks' current hours chart that suggest a similar tidal current phase pattern, but the lines north of the 3.0 current hour line indicate little curvature in either direction, except for the 10.5 hour line. In comparison, the M_2 tidal current cophase lines in this study indicate a definite seaward curvature throughout most of the Bay Proper. This seaward curvature is most pronounced in the deeper channels. In addition, the tidal current classification chart shown in Figure 34 indicates the boundary between the region of mixed, mainly semidiurnal tidal current and the region of predominately semidiurnal tidal current in the lower bay also has a definite seaward curvature.

This can be explained as follows. When proceeding up the bay, a particular phase of the M_2 tidal current is encountered in deeper water before it is reached in shoaler water nearshore. For example, the 300° cophase line is encountered in the main channel approximately 22 nautical miles north of the entrance. This same cophase line appears to intersect the western shore near Smith Point (approximately

55 nautical miles north of the entrance), and nearly longitudinally bisects Pocomoke Sound on the east side of the bay.

Since the phases of the M_2 tide and tidal current are both about 230° at Chesapeake Bay Entrance, the M_2 tidal wave must be nearly a pure progressive wave at this location. In comparison, the phase of the M_2 tide is 286° at Havre de Grace near the head of bay and the phase of the M_2 tidal current is 238° at nearby station 146. Therefore, the M_2 tide lags the tidal current by approximately 48° indicating the M_2 tidal wave is more like a standing wave at this location. The phase of the M_2 tide is about 300° in the eastern reach, approximately five nautical miles west of Chesapeake City, and the phase of the tidal current is about 195° at nearby station 152. Therefore, the M_2 tide lags the tidal current by over 100° at this location.

Since the M_2 tidal wave is nearly a pure standing wave at the head of bay and nearly a pure progressive wave at Chesapeake Bay Entrance, the reflected M_2 tidal wave must be almost totally attenuated before reaching the entrance. In addition, the change from a near standing wave to a more progressive wave should occur further down the bay in the channels than in shoaler water near the sides of the bay because the reflected wave would be attenuated less in deeper water. This would explain why the M_2 tide still precedes the tidal current slightly in the deeper channels in Chesapeake Bay Entrance.

Therefore, the phases of the M_2 tide and tidal current have been compared at offshore locations in the Bay Proper where the progression of the tidal current appears to be more uniform rather than near the sides of the bay where the phase changes rapidly and sometimes erratically, possibly because of distortion of the tidal current due to bottom effects. In addition, the meter height/depth ratios for the nearshore current meter stations are usually small compared to those deployed in offshore waters, which also indicates the nearshore data might be significantly affected by bottom friction.

Proceeding down the bay from the upper reaches to a location approximately nine nautical miles south of Havre de Grace, the phases of the M_2 tide and tidal current are about 260° and 210°, respectively. Therefore, the M_2 tide lags the tidal current by about 50° at this location. In the narrows 40 nautical miles down the bay from Havre de Grace, the phase of the M_2 tide is about 155° and the phase of the M_2 tidal current at nearby station 175 is 154°. Therefore, the M_2 tide and tidal current are nearly in phase at this location. Approximately seven nautical miles further down the bay at current station 121, the phase of the M_2 tide is approximately 130° and that of the M_2 tidal current is 138°. The M_2 tide now precedes the tidal current by 8°. This relationship is confirmed at current station 112, another 10 nautical miles down the bay. The phase of the M_2 tide is about 110° and that of the M_2 tidal current is 119° Therefore, the M_2 tide precedes the tidal current by 9° at this location.

Redfield's model of the relationship of the phases of high water and maximum flood current, which has been described in Chapter 2, can be used to explain the observed change in the M_2 tide and tidal current throughout the Bay Proper. Since the damping coefficient for the upper bay has been determined to be about 3.5 (which is fairly large), the M_2 tide should be greatly attenuated in the the upper bay. The model indicates the tide should lag the tidal current in the region between the point of reflection and the first quasinode, and the amount of lag at the point of reflection should be about 60°. In fact, the observed lag of 48° at Havre de Grace agrees very well with the model. However, the lag of about 100° in the eastern reach may not be totally due to reflection of Chesapeake Bay's M_2 wave. It may be partially due to interaction with the tide in Delaware Bay, through the Chesapeake and Delaware Canal.

It has been shown that the M_2 tide and tidal current are in phase at the narrows located about 40 nautical miles down the bay from Havre de Grace. This is fairly close to the location of the first quasinode of the M_2 tide. The Redfield model indicates that the amount the tide lags the tidal current should decrease from a maximum at the point of reflection to zero at the quasinode. Seaward of the quasinode, the phase of the tide should begin to precede that of the tidal current, increasing to a maximum approximately midway through the second quarter wavelength. It should then decrease to zero again at the second antinode. Therefore, the observed relationship of the M_2 tide and tidal current agrees fairly well with the model.

Continuing this comparison of the phases of the M_2 tide and tidal current seaward along the longitudinal axis of the bay, the phase of the M_2 tide is about 50° approximately five nautical miles east of the mouth of the Patuxent River, and that of the M_2 tidal current at nearby station 36 is about 65°. Therefore, the tide precedes the tidal current by about 15^{o} at this location. Approximately five nautical miles east of Smith Point at current station 2, the M_2 tide and tidal current again appear to be in phase at about 360^{o}.

The phase of the M_2 tide is about 280^{o} approximately 25 miles up the bay from the entrance at the site of current station 65, and that of the M_2 tidal current is 308^{o}. Therefore, the M_2 tide again precedes the tidal current by about 28^{o}. Finally, the M_2 tide and tidal current are nearly in phase at Chesapeake Bay Entrance, as indicated before.

The observed relationship of the M_2 tide and tidal current beyond a half wavelength from the point of reflection does not appear to agree well with the Redfield model. Seaward of the narrows near the mouth of the Patuxent River, the tide either precedes the tidal current or is in phase. Theoretically, the tide should again lag the tidal current in the third quarter wavelength. This disagreement may be due to a number of causes. The most likely explanation is that the Redfield model is a one dimensional model and unable to adequately model the tidal circulation of the lower bay.

Some of the disagreement may also be due to errors involved in contouring the tidal current phase information determined during this study. The current meter stations were not all deployed simultaneously and the water depth was not constant, as assumed in the model. In addition, the variations in the phase of the tidal current due to seasonal variability in the harmonic constants and the steering effect of bottom topography may lead to misinterpretation during contouring. Since the agreement between the observed relationship of the M_2 tide and tidal current and the modeled relationship for the upper bay is very good, the use of a one dimensional frictionally damped analytical model in this region is well justified. Conversely, the poor agreement in the lower bay indicates a one dimensional model isn't adequate.

MODELING THE BAY PROPER

The M_2 and K_1 nomograms in Figures 29 and 31 indicate the damping coefficients are not constant but decrease significantly when proceeding seaward from the upper region of the bay. Redfield (1950) and Parker (1980) have shown that the plots of amplitude ratios versus phase angles are often clustered in groups which define regions that have different frictional resistance characteristics.

These regions are not well defined on the M_2 nomogram, perhaps because fewer tide stations are included in a half wavelength of the M_2 tide. The size of the damping coefficient decreases from 3.5 near the head of bay to approximately 2.4 at the first M_2 quasinode. It then decreases to 1.8 at North Point on the western shore and at Love Point on the eastern shore. These stations are both located in a region off the mouth of the Patapsco River where the bay widens considerably. The last location plottable on the M_2 nomogram is Matapeake, MD which is located on the eastern shore opposite the mouth of the Severn River. This station is located in a region which is separated from the previous one by the narrows just north of the mouth of the Severn River. The damping coefficient is about 1.1 at this location, the lowest observed on the nomogram. However, the reduction in the size of the damping coefficient at these latter stations may be due to energy losses into the small tributaries of the upper bay and secondary reflections at constrictions in the channels.

The K_1 nomogram provides greater detail about the change in the value of the damping coefficient in the upper bay since more stations are included in a half wavelength of K_1. The damping coefficient remains fairly constant at 3.0 from the point of reflection to Love Point. Continuing seaward, it decreases significantly but appears to decrease more rapidly along the western shore. First, there is a gradual decrease along the western shore from about 2.5 at North Point to 1.4 at Cove Point located just north of the mouth of the Patuxent River. However, there isn't any discernable region where it is fairly constant. Seaward of Cove Point, the damping coefficient decreases rapidly to slightly less than 1.0 at Lexington Park, and then decreases more gradually to about 0.8 at Point Lookout on the north side of the mouth of the Potomac River. This rapid decrease may be partially due to a loss of energy into the Patuxent River and secondary reflection below Cove Point.

The damping coefficient decreases more gradually along the eastern shore, from 3.0 at Matapeake to about 2.6 at Love Point and approximately 2.4 at Ferry Cove. Unfortunately, there weren't any tide stations located between Ferry Cove and Hooper Island. The damping coefficient is about 1.4 at Hooper Island, a significant decrease from that at Ferry Cove. Note that this region encompasses the mouth of the Choptank River, and the bay narrows considerably just north of the mouth of the Patuxent River. The damping coefficient decreases rapidly south of Hooper Island to about 1.0 at Holland Bar Light and less than 0.5 at Rappahannock Shoal, which are both offshore locations. These stations are located in a region where considerable tidal energy may be lost into Pocomoke Sound, Tangier Sound, and the Nanticoke River along the eastern shore, as well as into the Potomac River on the western shore.

This data suggests a damping coefficient ranging from 1.0 to 1.5 might be appropriate for the lower bay, which would indicate a reduction in amplitude of 63 and 78 percent per tidal cycle, respectively. If the damping coefficient of 1.0 at Holland Bar Light is selected as representative of the lower bay, then kx at this location would be approximately 105°. Since Holland Bar Light is approximately 105 nautical miles from the assumed point of reflection, the wave number, k, is about one degree per nautical mile. This would indicate the wavelength of the K_1 tide in the lower bay is 360 nautical miles, and the computed average depth is 20.67 ft (6.30 m). Comparison with the wavelengths for the K_1 tide listed in Table 4 indicates this wavelength for the lower bay is not unreasonable. However, the computed average depth appears to be too shallow. Perhaps the shoals and islands located in the lower bay cause the effective depth to be shallower than expected.

If the energy loss to the tributaries south of the narrows and side reflections from constrictions and islands are ignored, the lower bay might be considered a simple rectangular basin that is of sufficient width for Coriolis force to affect the tidal circulation. Then the two dimensional frictionally damped analytical model could be applied to this basin. The damping coefficient and wave number which have been suggested for the lower bay could be applied to the two dimensional equations for the high water elevation (Equation 30) and phase angle of a single frequency tidal wave (Equation 31). If these equations were solved for all x and y and plotted as coamplitude and cophase lines, the result would be very similar to the corange and cotidal line patterns produced by Parker (1980), which are shown in Figure 5. The difference is that he modeled the Strait of Juan de Fuca - Georgia Strait system, which has a midlatitude of 48.5° N. and a length to width ratio of 10 to 1. In comparison, lower Chesapeake Bay has a midlatitude of about 37.5° N. and a length to width ratio of 8 to 1. There will be a smaller Coriolis effect in lower Chesapeake Bay, which will slightly reduce the exponential damping term and phase of the incident and reflected Kelvin waves. This will cause very small differences in the cotidal and corange line patterns. The amphidrome will be in approximately the same location, but the magnitude of the coamplitude lines will be less in the lower bay. The location of some of the cophase lines will shift slightly. However, the differences are so small that Figure 5c can be considered representative of the tide in lower Chesapeake Bay also.

It has already been observed that there is a general similarity between the pattern of corange and cotidal lines in Figure 5c and the M_2 and K_1 patterns in the lower bay described in Figures 15 through 18. This suggests very strongly that the tidal circulation of the lower bay is amphidromic with a virtual amphidrome located to the west of the bay.

If there is no reflection of the incident wave near the upper limit of the lower bay, the Kelvin wave would have to become more like a one dimensional wave as the bay narrows. This simple tidal wave would travel to the head of bay where reflection is known to occur. Then the reflected wave would travel seaward as a simple tidal wave also, but it would have to transform again into a Kelvin wave upon reaching the lower bay. When superimposed, this would result in a simple one dimensional tidal wave in the upper bay and a Kelvin wave in the lower bay that would have an amphidromic pattern of cotidal lines.

A less likely possibility might be that the incident Kelvin wave would be reflected by an added oscillation across the Bay Proper in the narrows located just north of the mouth of the Patuxent River. This added oscillation would be of the form described in Chapter 2. If such reflection does occur at the narrows, it's likely that it would only be a partial reflection, and a portion of the incident tidal energy would continue up the bay to be reflected at the head of bay. This would be very complicated and difficult to model. However, no reflection of the incident Kelvin wave at the narrows was observed during this study. The current meter data from stations located in this region did not indicate any cross channel oscillations at tidal frequencies, but such oscillations might be present at other frequencies.

AMPLIFICATION OF TIDAL CONSTITUENTS

This study has focused primarily on the tidal constituents M_2 and K_1 as representatives of the semidiurnal and diurnal types of tides. However, the observed tide is actually comprised of many constituents whose interaction can significantly affect its shape and amplitude.

The constituents normally considered by the National Ocean Service in its analysis and prediction of tides have been listed in Tables 1 and 2. The harmonic constants presented in Appendix B indicate M_2 is by far the largest amplitude tidal constituent in the bay or its major tributaries. If the solar semiannual constituent, SSa, and the solar annual constituent, Sa, are not considered because they are really meteorological tides, the next two largest constituents are the larger lunar elliptic semidiurnal constituent, N_2, and the principal solar semidiurnal constituent, S_2. However, the amplitudes of N_2 and S_2 are often an order of magnitude smaller than that of M_2 as shown in Figures 10 and 11.

The lunisolar diurnal constituent, K_1, is usually the next largest in amplitude in the bay and tributaries. Its amplitude is of the same order of magnitude as N_2 and S_2, and therefore an order of magnitude smaller than M_2 also. The principal lunar diurnal constituent, O_1, is usually the second largest diurnal constituent, though often of the same magnitude as K_1.

The lunar fortnightly and lunar monthly tidal constituents, Mm and Mf, may be of the same magnitude as K_1 and O_1. However, this relationship varies somewhat during the year because the size of these constituents may be augmented by meteorological phenomena of the same periodicity.

The remaining tidal constituents include a number of smaller elementary and shallow water constituents. Since a large portion of the bay and its tributaries is relatively shallow, there may be considerable amplification of the shallow water constituents as well as more moderate amplification of some elementary constituents. Parker (1984) has shown that this amplification is primarily due to the nonlinear effects of friction as the tide progresses through shallow waters. These effects were explained in Chapter 2 of this study. He showed that these frictional effects increased with a decrease in depth, an increase in tidal amplitude, or a decrease in frequency.

Hicks (1964) observed that shallow water tides cause distortion of the observed tide in the upper reaches of the Potomac and James rivers, which he attributed was mainly due to the overtides of M_2. He suggested that similar distortion might also occur near the limit of tide in other tributaries of Chesapeake Bay. Distortion of the tide due to M_4 becomes significant when the amplitude ratio, M_4/M_2, is 0.1 or greater, and distortion due to M_6 becomes significant when the amplitude ratio, M_6/M_2, is 0.04 or greater (Schureman, 1958). Amplitude ratios have been computed, based on the harmonic constants determined during this study, for tide stations located along the major tributaries and along the east and west sides of the Bay Proper. These ratios have been plotted versus distance in each tributary and in the Bay Proper, as shown in Figures 35 through 38.

The plot in Figure 35 shows that the M_4/M_2 ratio in the James River increases from 0.018 at the mouth to 0.156 at Richmond, VA (near the limit of tide). In fact, the ratio reaches 0.1 somewhere between Hopewell, VA and Chester, VA. Therefore, distortion of the tide due to M_4 significantly affects about 15 nautical miles of the upper James River. In comparison, Hicks determined an M_4/M_2 ratio of 0.122 for Richmond, but could not define the extent of river over which the distortion occurred. In the Rappahannock River, the M_4/M_2 ratio increases from 0.051 at the mouth to 0.136 at Massaponax, VA (approximately four nautical miles downstream from the limit of tide). Therefore, distortion due to M_4 may affect about 15 to 20 nautical miles of the upper Rappahannock River.

Figure 35. Ratio of the amplitudes of the M_4 to M_2 tidal constituents in the James River, Rappahannock River and Potomac River.

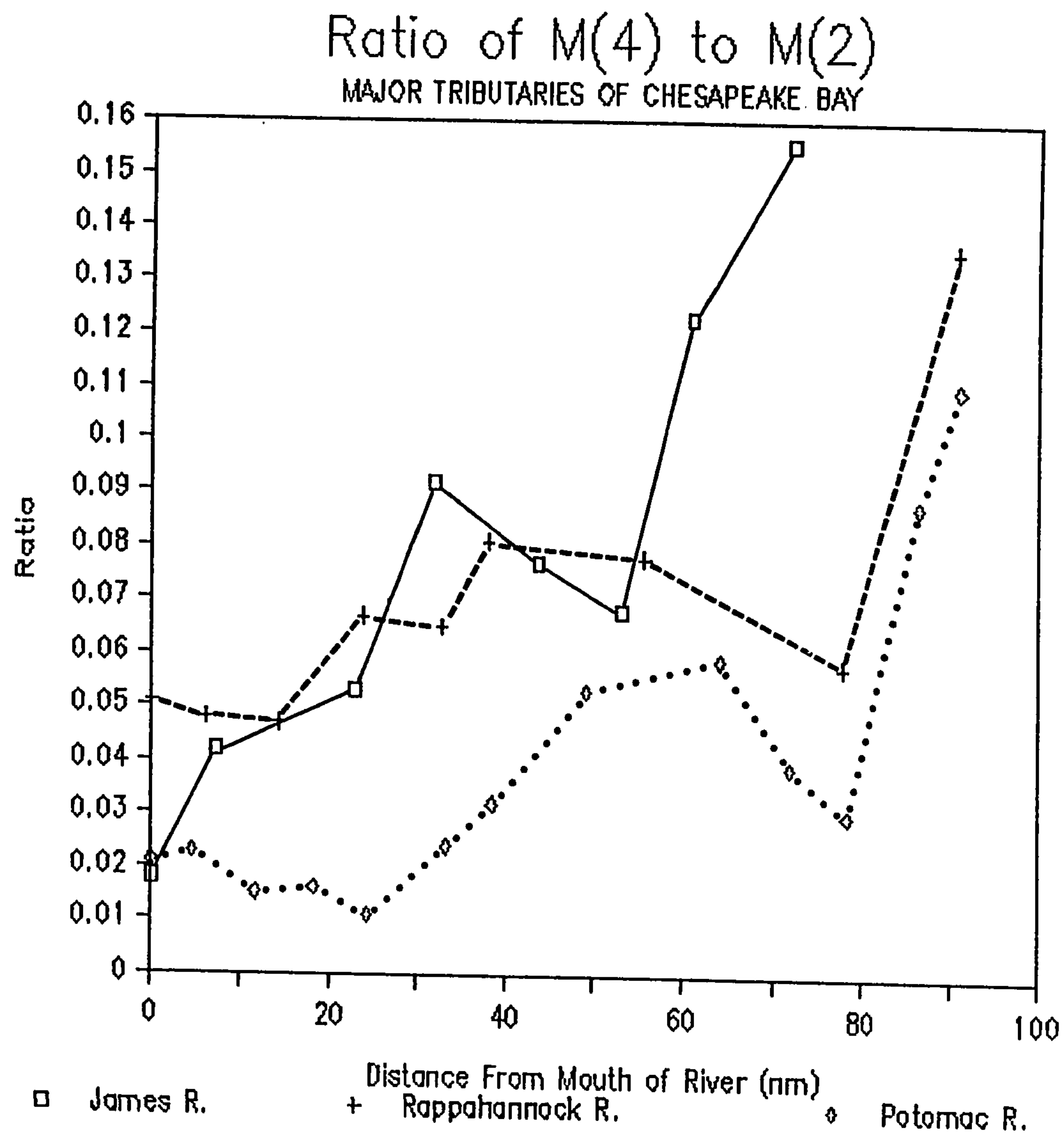

Ratio of M(4) to M(2)
MAJOR TRIBUTARIES OF CHESAPEAKE BAY
Ratio
0.16
0.15
0.14
0.13
0.12
0.11
0.1
0.09
0.08
0.07
0.06
0.05
0.04
0.03
0.02
0.01
0
0
20
40
60
80
100
Distance From Mouth of River (nm)
James R.
Rappahannock R.
Potomac R.

Figure 36. Ratio of the amplitudes of the M_4 to M_2 tidal constituents in Chesapeake Bay Proper.

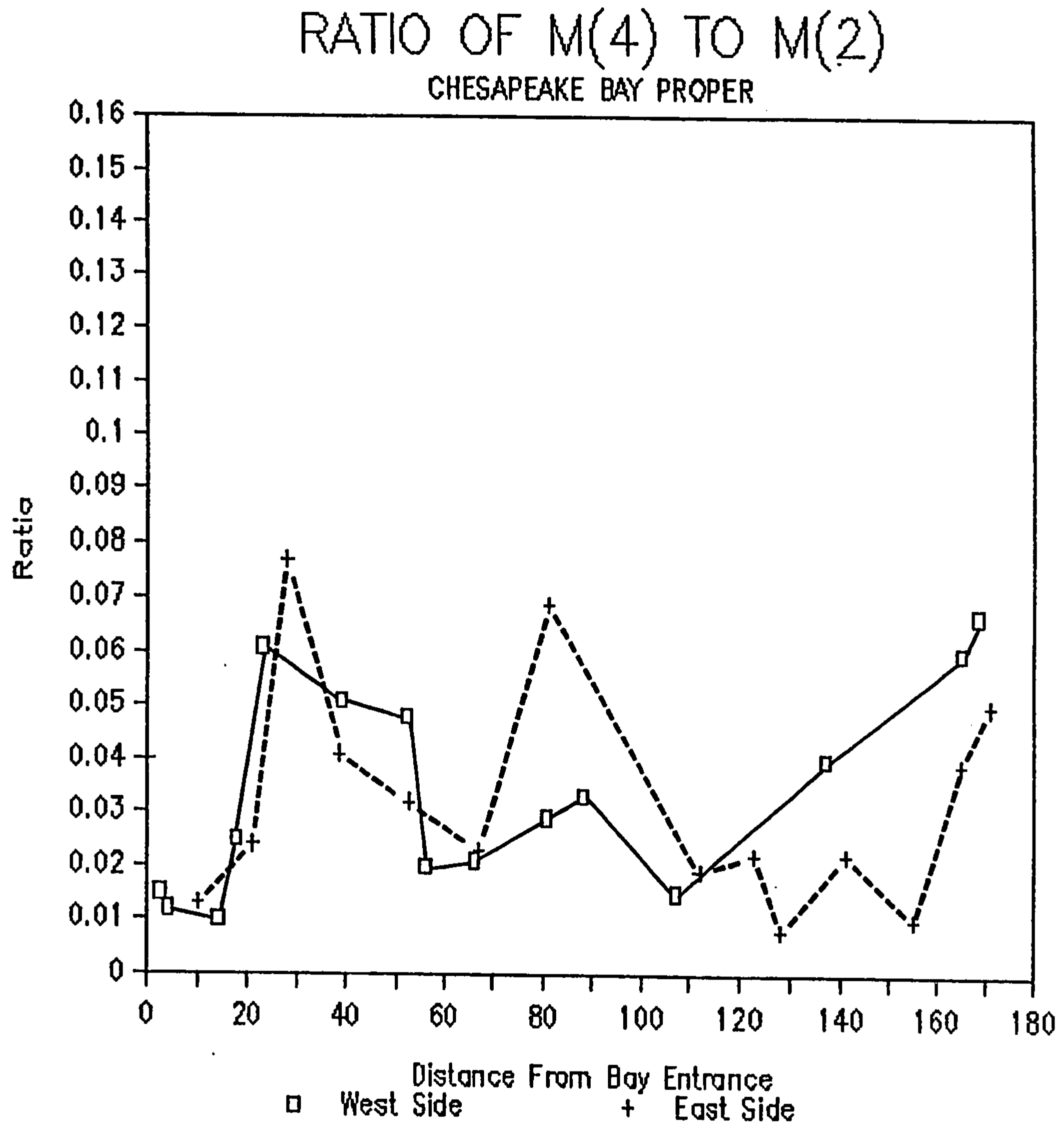
RATIO OF M(4) TO M(2)
CHESAPEAKE BAY PROPER
Ratio
0.16
0.15
0.14
0.13
0.12
0.11
0.1
0.09
0.08
0.07
0.06
0.05
0.04
0.03
0.02
0.01
0
0
20
40
60
80
100
120
140
160
180
Distance From Bay Entrance
West Side
East Side

Figure 37. Ratio of the amplitudes of the M_6 to M_2 tidal constituents in the James River, Rappahannock River and Potomac River.

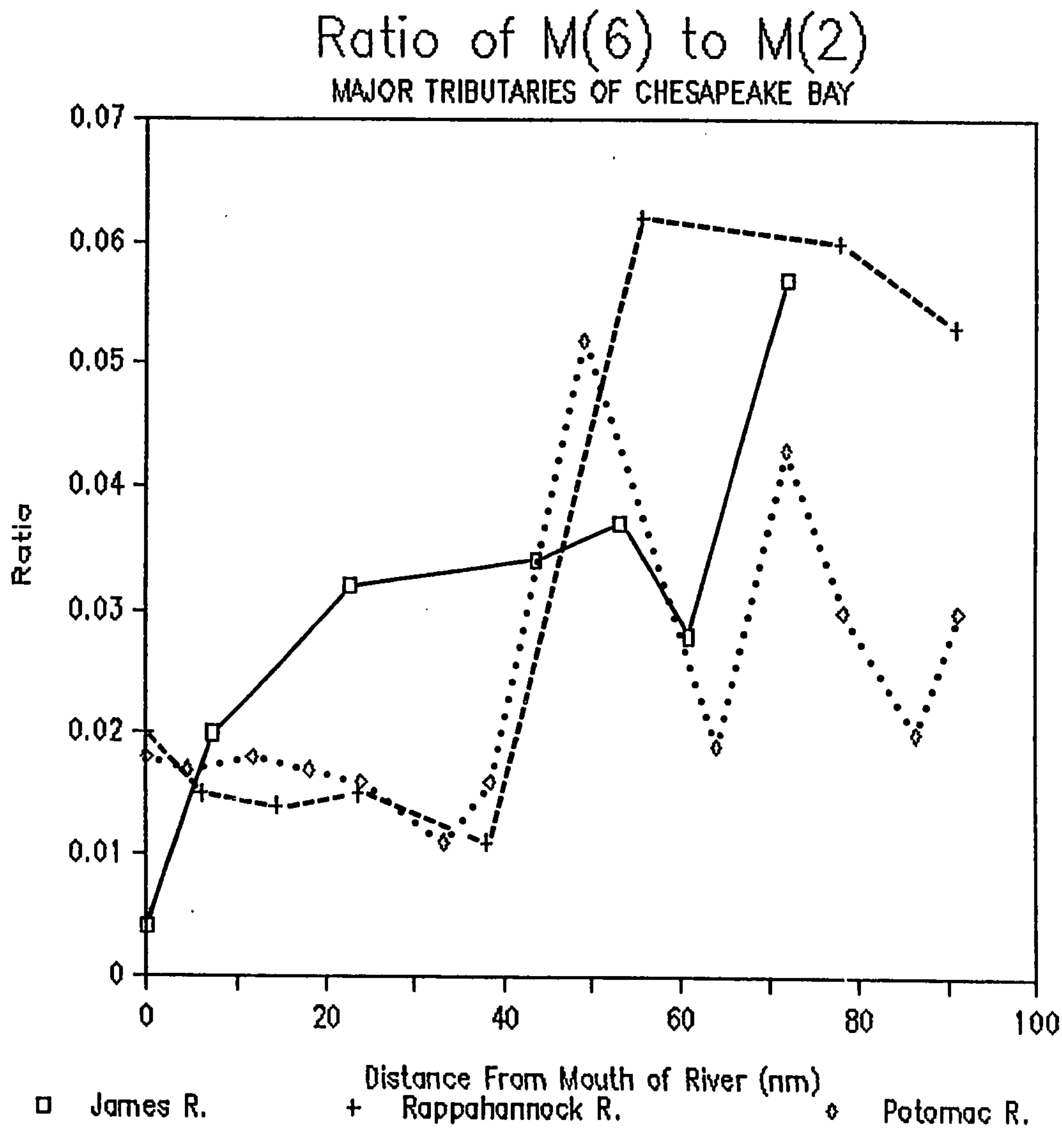
Ratio of M(6) to M(2)
MAJOR TRIBUTARIES OF CHESAPEAKE BAY
0.07
0.06
0.05
0.04
0.03
0.02
0.01
0
Ratio
0
20
40
60
80
100
Distance From Mouth of River (nm)
James R.
Rappahannock R.
Potomac R.

Figure 38. Ratio of the amplitudes of the M_6 to M_2 tidal constituents in Chesapeake Bay Proper.

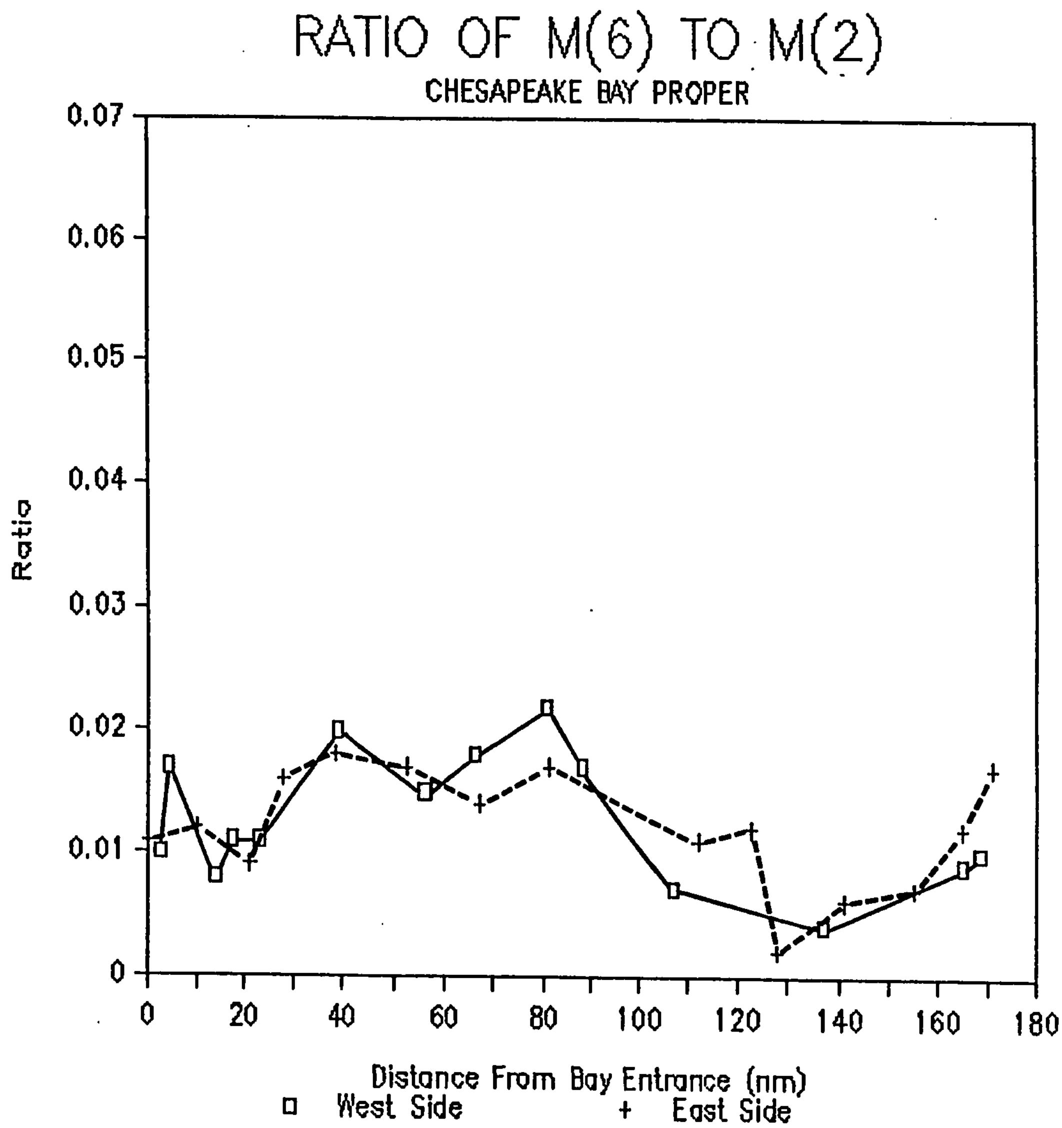
RATIO OF M(6) TO M(2)
CHESAPEAKE BAY PROPER
Ratio
0.07
0.06
0.05
0.04
0.03
0.02
0.01
0
0
20
40
60
80
100
120
140
160
180
Distance From Bay Entrance (nm)
West Side
East Side

The M_4/M_2 ratio in the Potomac River increases from 0.021 at the mouth to 0.088 at Alexandria, VA and 0.110 at Washington, DC (approximately 12 nautical miles downriver from the limit of tide). Hicks determined an M_4/M_2 ratio of 0.094 for Washington, DC. His ratios for Washington and Richmond, which were based on pre1964 data, are slightly smaller than the ratios determined during this study. This may be due to deeper dredging of channels in these rivers, or may be due to the rise in mean sea level since 1964 (Harris, 1981). Figure 35 indicates that the amplification of M_4 in the James and Potomac rivers is quite similar, but there is considerably less amplification of M_4 in the Potomac River. This may be due to the greater width and depth of the Potomac River.

There doesn't appear to be any significant distortion of the tide in the Bay Proper due to M_4. Figure 36 shows that the M_4/M_2 ratio is definitely less than 0.1 at all locations where the tide was observed along the sides of the Bay Proper. It is possible that distortion might become significant in some of the small tributaries and embayments along the sides of the bay, but these features are not included within the boundaries of the Bay Proper. The plots of the M_4/M_2 ratios along each side of the Bay Proper are much noisier than those observed for the major tributaries. Some of this noise might be due to the relatively small values of M_4.

The M_6/M_2 ratio plots for stations along the James, Potomac, and Rappahannock rivers are shown in Figure 37. These plots are much noisier than those plotted for the M_4/M_2 ratio, probably because of the very small amplitudes of M_6. The criterion of 0.04 is exceeded in all three tributaries and possibly further downriver than was observed for M_4.

Hicks observed that the M_6/M_2 ratio at Richmond was 0.052 whereas this study determined that it is 0.057. He also observed that the ratio at Washington was 0.33, but this study determined that the M_6/M_2 ratio is only 0.030 at Washington. In fact, the maximum ratio observed in the Potomac River is 0.052 at Riverside, MD. It does not appear the M_6/M_2 ratio could ever become as large as 0.33 in the Potomac River.

The M_6/M_2 ratio plots for the Bay Proper shown in Figure 38 indicate there isn't any significant distortion of the tide due to M_6 on either the east or west sides of the bay. The ratio at all locations is significantly less than 0.04, and the plots don't appear to be too noisy, considering the small amplitude of M_6.

Figures 39 through 43 describe the amplification of M_2 and its harmonics in Chesapeake Bay and its major tributaries. In this case, the amplification ratio is the amplitude of a particular constituent at any location divided by the amplitude of that constituent at the mouth of the tributary or the entrance to the bay. If the amplitude at the mouth or entrance was so small that it would cause the ratio to be erroneously large, the amplitude from another station further upriver or up the bay was used which was of sufficient size to cause meaningful ratios. Parker (1984) used a similar technique to describe the amplification of tidal constituents in the Delaware River and Bay. It was explained in Chapter 2 that this amplification of tidal constituents is

Figure 39. Amplification of the M_2 tide and its harmonics in the James River.

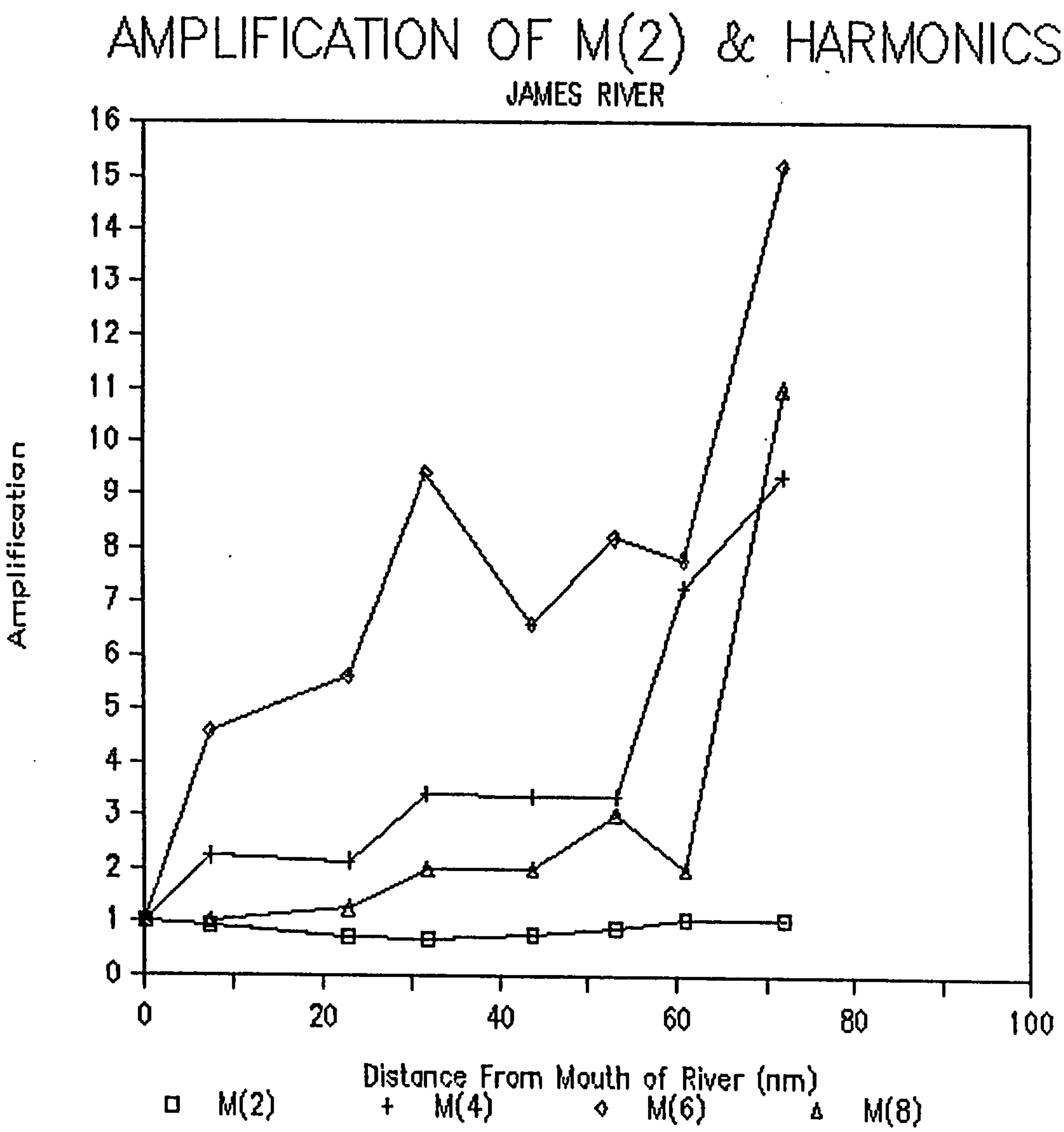
AMPLIFICATION OF M(2) & HARMONICS
JAMES RIVER
Amplification
0
1
2
3
4
5
6
7
8
9
10
11
12
13
14
15
16
0
20
40
60
80
100
Distance From Mouth of River (nm)
M(2)
M(4)
M(6)
M(8)

Figure 40. Amplification of the M_2 tide and its harmonics in the Rappahannock River.

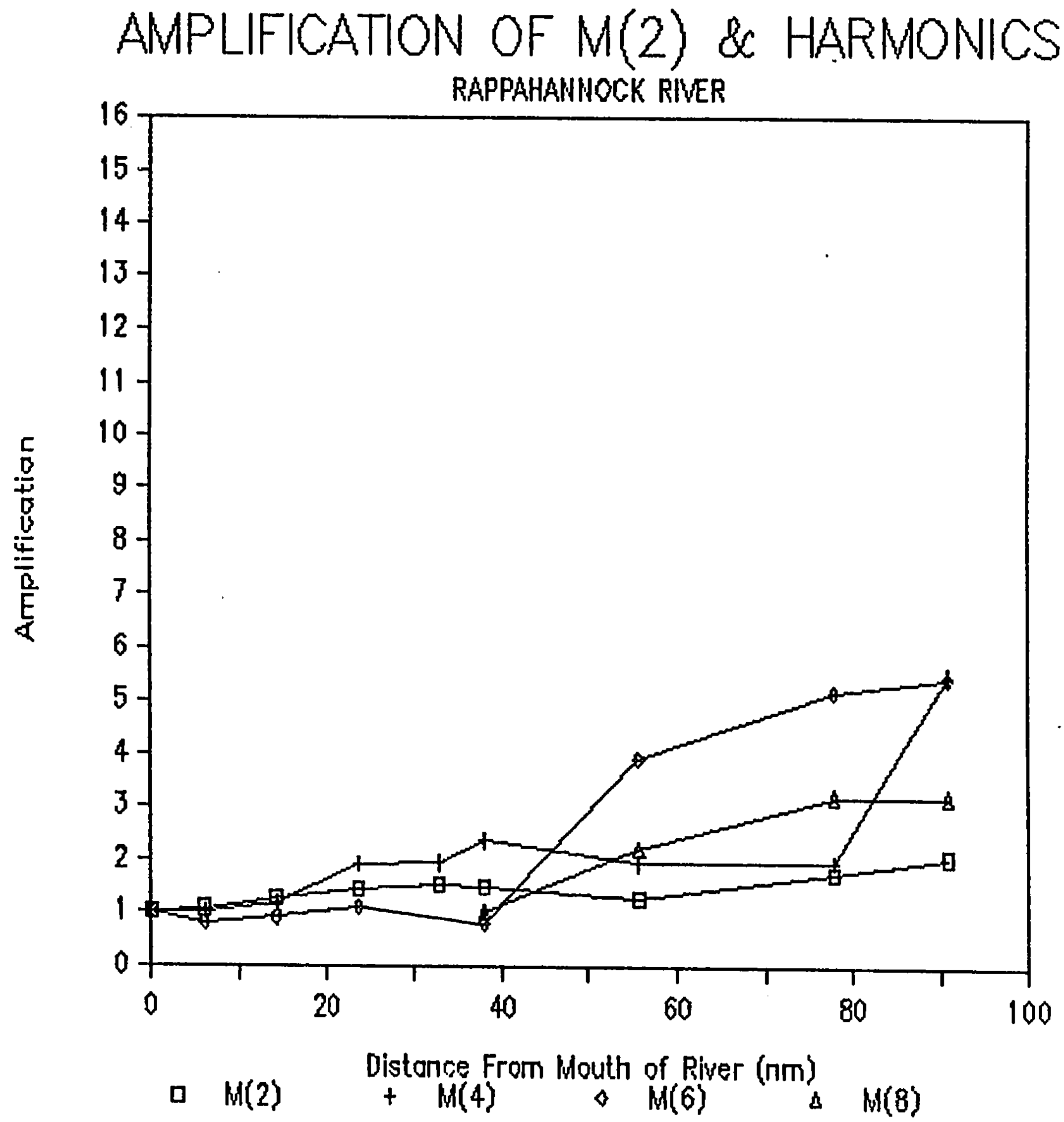
AMPLIFICATION OF M(2) & HARMONICS
RAPPAHANNOCK RIVER
Amplification
16
15
14
13
12
11
10
9
8
7
6
5
4
3
2
1
0
0
20
40
60
80
100
Distance From Mouth of River (nm)
M(2)
M(4)
M(6)
M(8)

Figure 41. Amplification of the M_2 tide and its harmonics in the Potomac River.

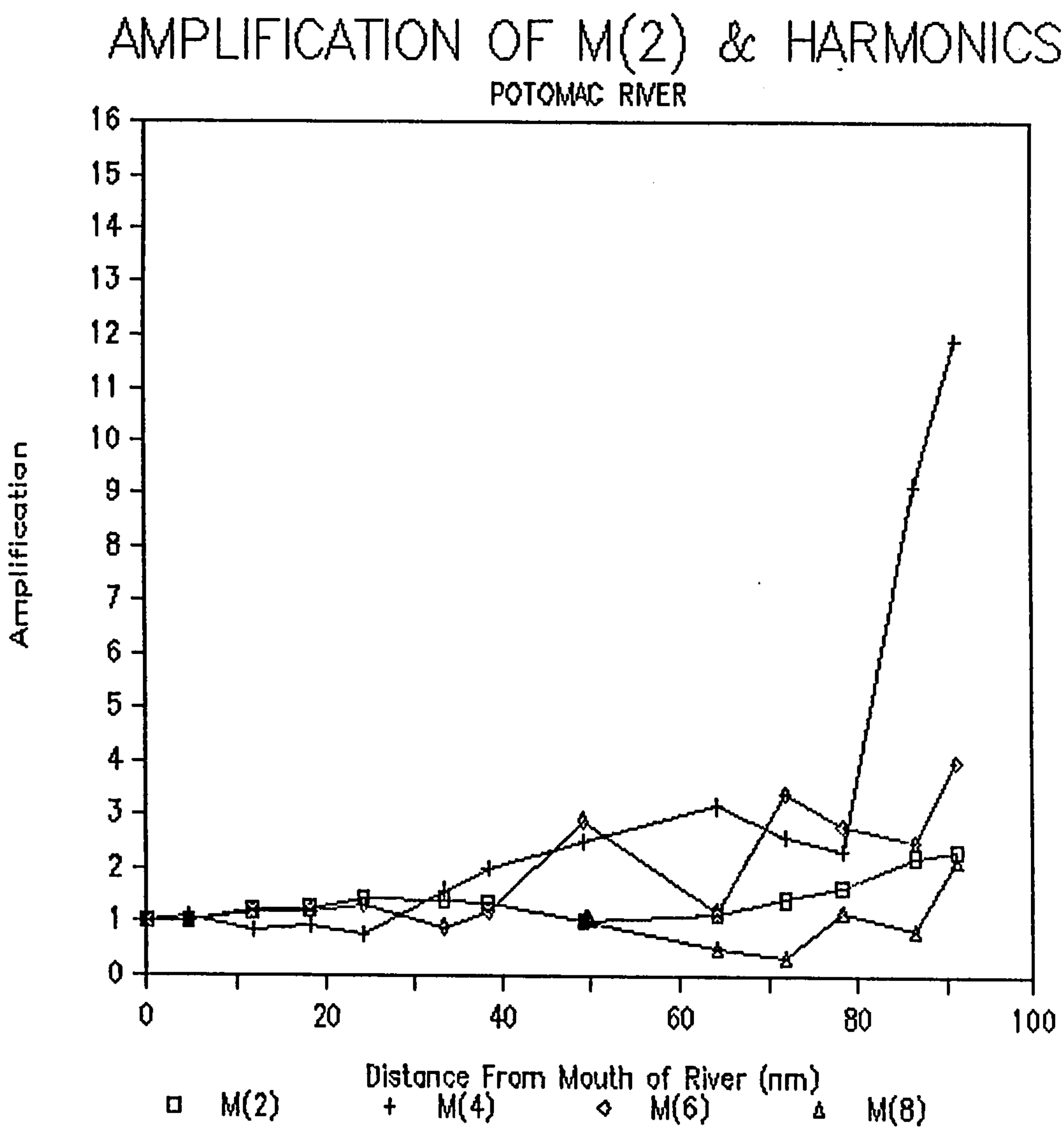
AMPLIFICATION OF M(2) & HARMONICS
POTOMAC RIVER
Amplification
0
1
2
3
4
5
6
7
8
9
10
11
12
13
14
15
16
0
20
40
60
80
100
Distance From Mouth of River (nm)
M(2)
M(4)
M(6)
M(8)

Figure 42. Amplification of the M_2 tide and its harmonics along the west side of Chesapeake Bay Proper.

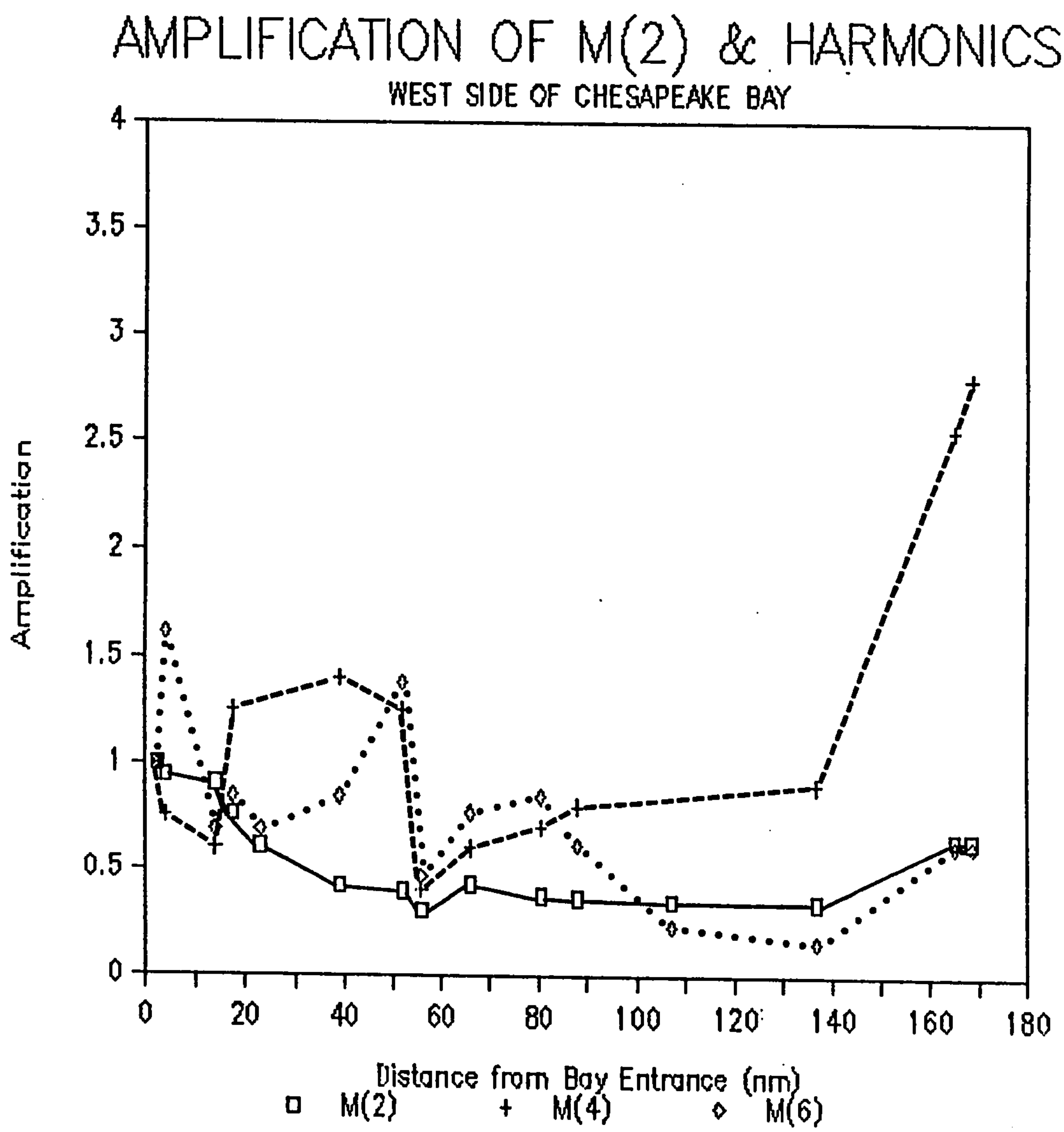
AMPLIFICATION OF M(2) & HARMONICS
WEST SIDE OF CHESAPEAKE BAY
Amplification
4
3.5
3
2.5
2
1.5
1
0.5
0
0
20
40
60
80
100
120
140
160
180
Distance from Bay Entrance (nm)
M(2)
M(4)
M(6)

Figure 43. Amplification of the M_2 tide and its harmonics along the east side of Chesapeake Bay Proper.

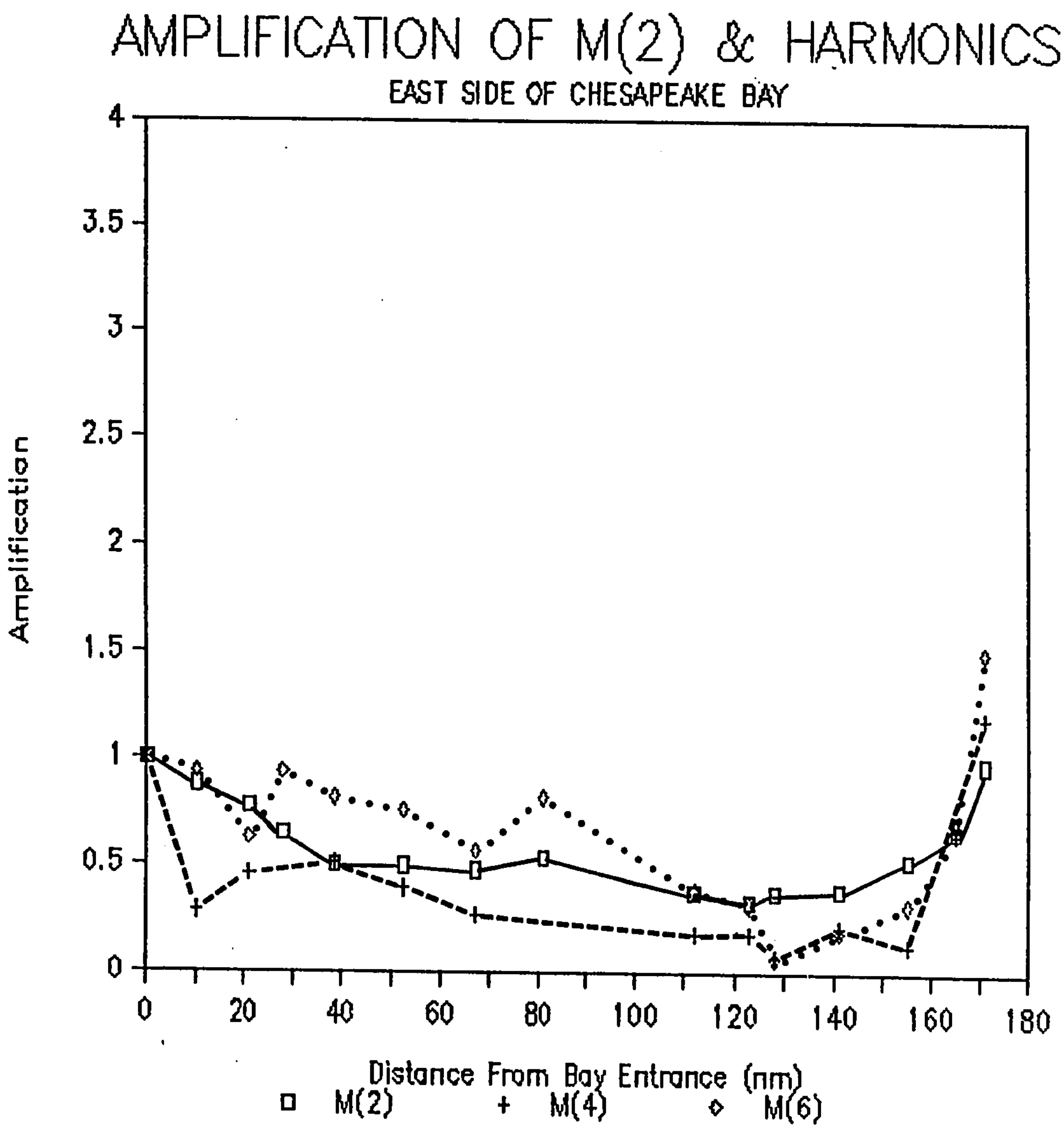
AMPLIFICATION OF M(2) & HARMONICS
EAST SIDE OF CHESAPEAKE BAY
Amplification
4
3.5
3
2.5
2
1.5
1
0.5
0
0
20
40
60
80
100
120
140
160
180
Distance From Bay Entrance (nm)
M(2)
M(4)
M(6)

caused by the transfer of energy and momentum amongst the tidal frequencies, due to nonlinear frictional effects.

Figure 39 shows the amplification of M_2 and its harmonics in the James River. From the mouth of the river, the M_2 amplification ratio decreases to a minimum of 0.66 at Claremont, VA and then increases to 1.06 at Richmond. Therefore, no significant amplification of M_2 occurs in the James River. The location of the minimum ratio corresponds well with the modeled location of the M_2 quasinode.

There is considerable amplification of M_4, M_6, and M_8 in the James River, and the maximum ratios at Richmond are 9.36, 15.20, and 11.00, respectively. The amplification plots for M_4 and M_8 are very similar. The most rapid increase in amplification is located in the upper tidal region of the river over a distance of about 10 nautical miles. The amplification of M_6 is somewhat different. There is a rapid increase in amplification to 4.0 in the region which extends about seven nautical miles upriver from the mouth followed by a more gradual increase up the river to Richmond. The amplification of M_6 is greater than that of the other harmonics of M_2 throughout the tidal length of the river, except in the vicinity of Richmond where the amplification of M_4 and M_8 abruptly become greater.

Figure 40 shows the amplification of M_2 and its harmonics in the Rappahannock River. The amplification of M_2 is relatively small throughout its length and is a maximum of only 2.05 at Massaponax, VA. Minimum amplification occurs about 70 nautical miles from the mouth, which is in the region of the M_2 quasinode, but it is only a single value not confirmed by any other ratios. The plots for M_4 and M_6 are somewhat erratic, and the amplitude of M_8 did not become large enough to use as a denominator in the amplification ratio until almost 40 nautical miles up the river from the mouth. However, there is a general trend indicating moderate amplification of M_4, M_6, and M_8, and the ratios at Massaponax are 5.50, 5.46 and 3.20, respectively.

The amplification of M_2 and its harmonics in the Potomac River is shown in Figure 41. From the mouth of the river, the ratio for M_2 increases slightly to a secondary maximum of 1.45 at a location about 24 nautical miles upriver, and then decreases to a minimum of 1.00 about 49 nautical miles from the mouth. Then the ratio increases gradually to 2.32 at Washington, DC. The locations of this minimum and secondary maximum agree fairly well with the modeled locations of the quasinode and antinode of the M_2 wave. There is a very rapid increase in amplification of M_4 in the region which extends from Marshall Hall, MD where the ratio is 2.33 to Washington, DC where it is 11.92 (a distance of about 12 nautical miles). In comparison, there is only a gradual but somewhat erratic increase in amplitude of M_6 to a maximum of 4.00 at Washington. The amplification shown for M_8 is questionable because its amplitudes are so small.

The amplification of M_2 and its harmonics along the west and east sides of the Bay Proper is shown in Figures 42 and 43. There weren't any plots of M_8 because the amplitudes were too small. Both figures indicate the ratios for M_2, M_4, and M_6 all decrease at first, proceeding up the bay from the entrance, to a minimum located about 120 nautical miles from the entrance. This minimum occurs in the narrows located near the mouth of the Severn River. The location of this minimum is about 15 nautical miles south of the modeled position of the M_2 quasinode. Continuing up the bay along the east side, M_2, M_4 and

M_6 all indicate a rapid increase in amplification, but the magnitude of the change is relatively small. There is a more substantial increase in the amplification of M_4 on the west side of the bay, from 0.90 at North Point to 2.80 at Port Deposit, MD. The amplification of M_2 and M_6 only increases slightly north of the narrows, and not to the levels that occurred at the entrance. It is evident that greater amplification of the harmonics of M_2 occurs in the shallow waters near the limit of tide in the tributaries than in the Bay Proper. Therefore, an examination of the amplification of diurnal, semidiurnal, terdiurnal, and quarterdiurnal constituents has been limited to the James, Rappahannock, and Potomac rivers.

Figures 44, 45, and 46 show the amplification of diurnal constituents K_1 and O_1 in these tributaries. Even though the K_1 and O_1 amplification curves tend to differ from tributary to tributary, the K_1 and O_1 curves in any one tributary are quite similar. This suggests the dimensions of the tributary strongly affect the shape of the amplification curve.

There appear to be K_1 and O_1 quasinodes located about 20 to 30 nautical miles from the mouth of the James River and about 40 nautical miles from the mouth of the Rappahannock River. The locations of the K_1 quasinodes agree well with the locations determined earlier in this study. The amplification of K_1 and O_1 in the Potomac River decreases to a minimum just upriver of the mouth. The modeled location of the K_1 quasinode is about 20 nautical miles further upriver than indicated by this minimum. The amplification of O_1 tends to decrease in the uppermost tidal waters of all three tributaries, but the amplification of K_1 decreases only in this region of the Rappahannock River. Parker

Figure 44. Amplification of the principal diurnal tidal constituents in the James River.

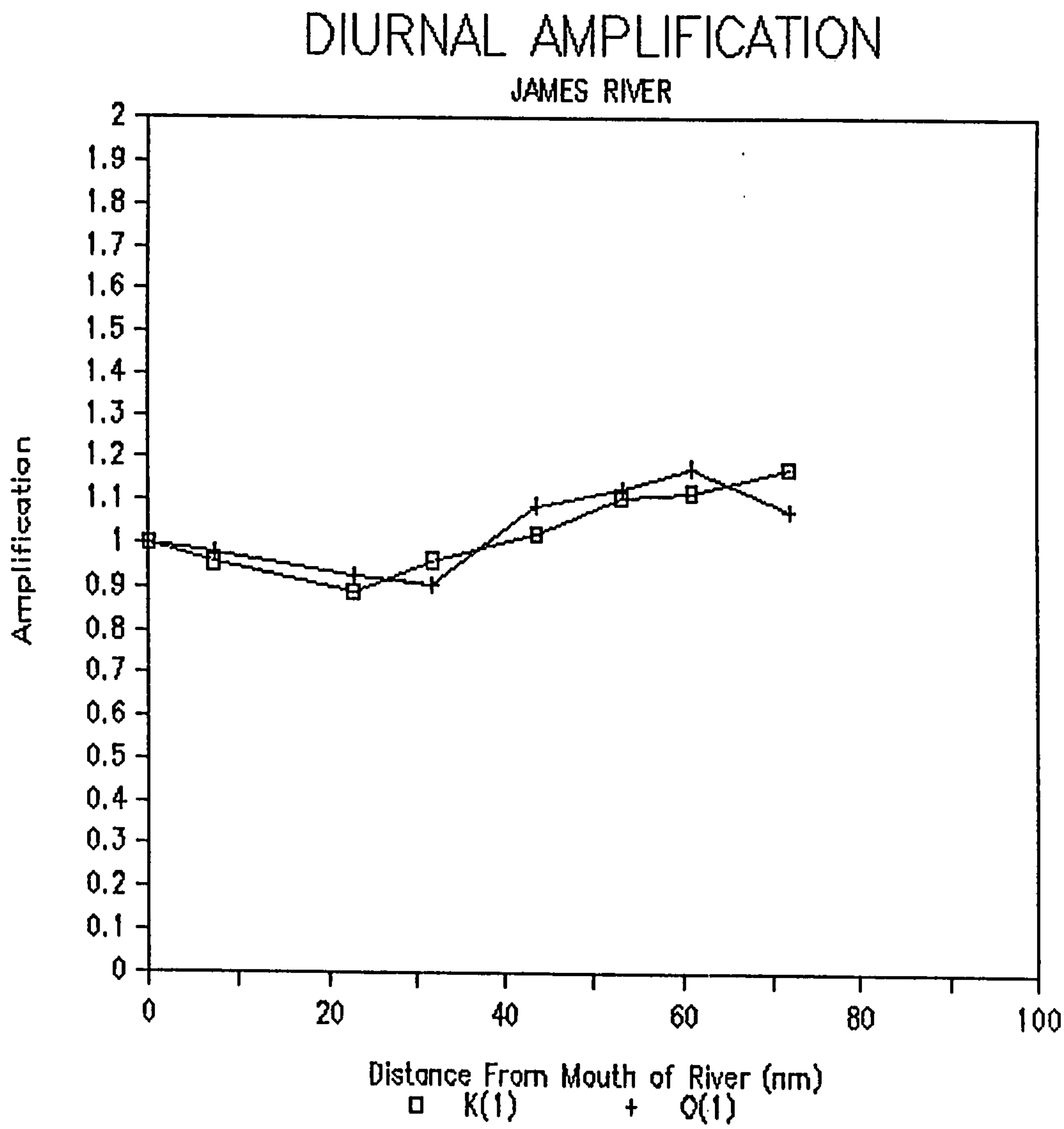
DIURNAL AMPLIFICATION
JAMES RIVER
Amplification
2
1.9
1.8
1.7
1.6
1.5
1.4
1.3
1.2
1.1
1
0.9
0.8
0.7
0.6
0.5
0.4
0.3
0.2
0.1
0
0
20
40
60
80
100
Distance From Mouth of River (nm)
K(1)
O(1)

Figure 45. Amplification of the principal diurnal tidal constituents in the Rappahannock River.

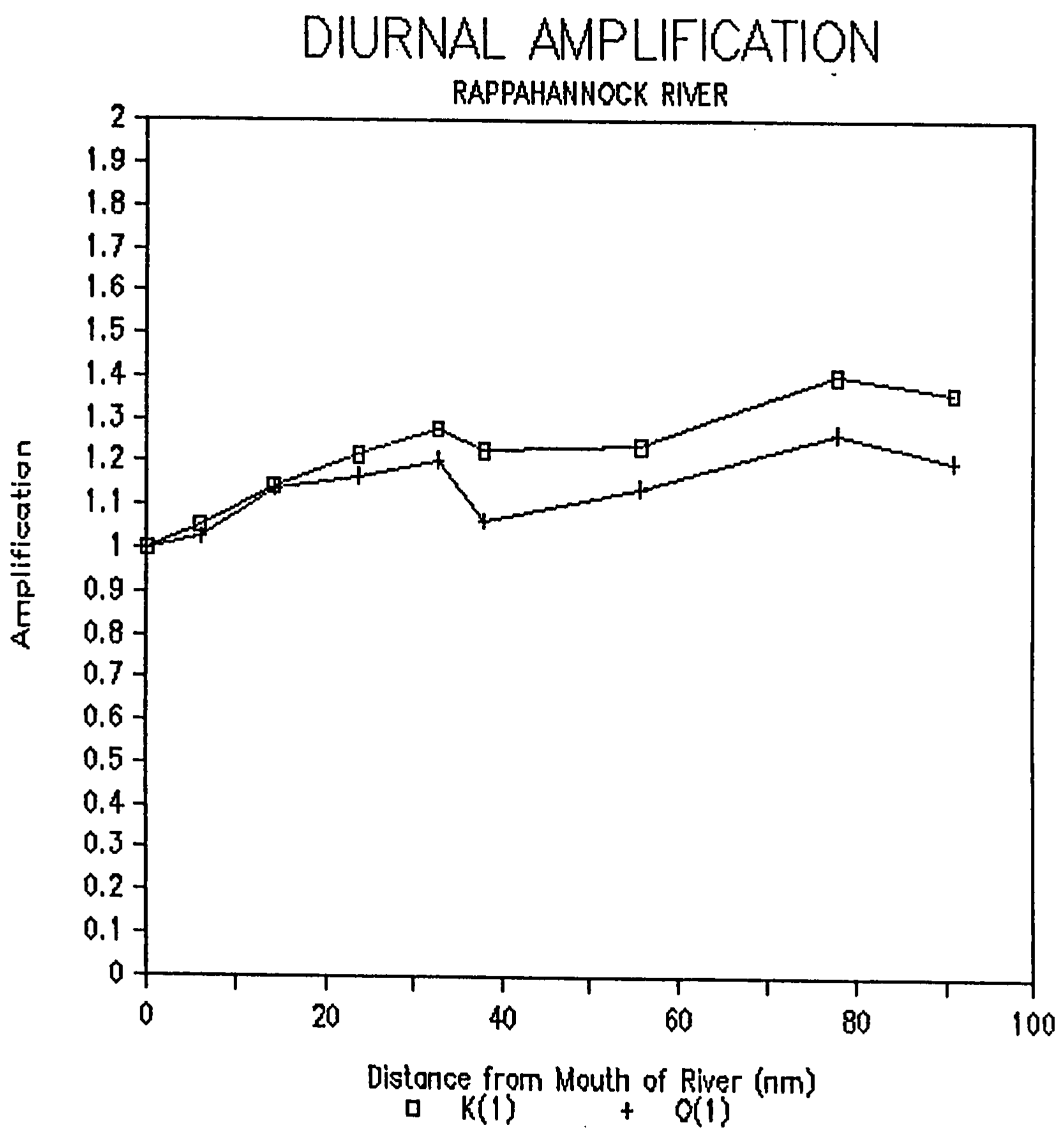
DIURNAL AMPLIFICATION
RAPPAHANNOCK RIVER
Amplification
2
1.9
1.8
1.7
1.6
1.5
1.4
1.3
1.2
1.1
1
0.9
0.8
0.7
0.6
0.5
0.4
0.3
0.2
0.1
0
0
20
40
60
80
100
Distance from Mouth of River (nm)
K(1)
O(1)

Figure 46. Amplification of the principal diurnal tidal constituents in the Potomac River.

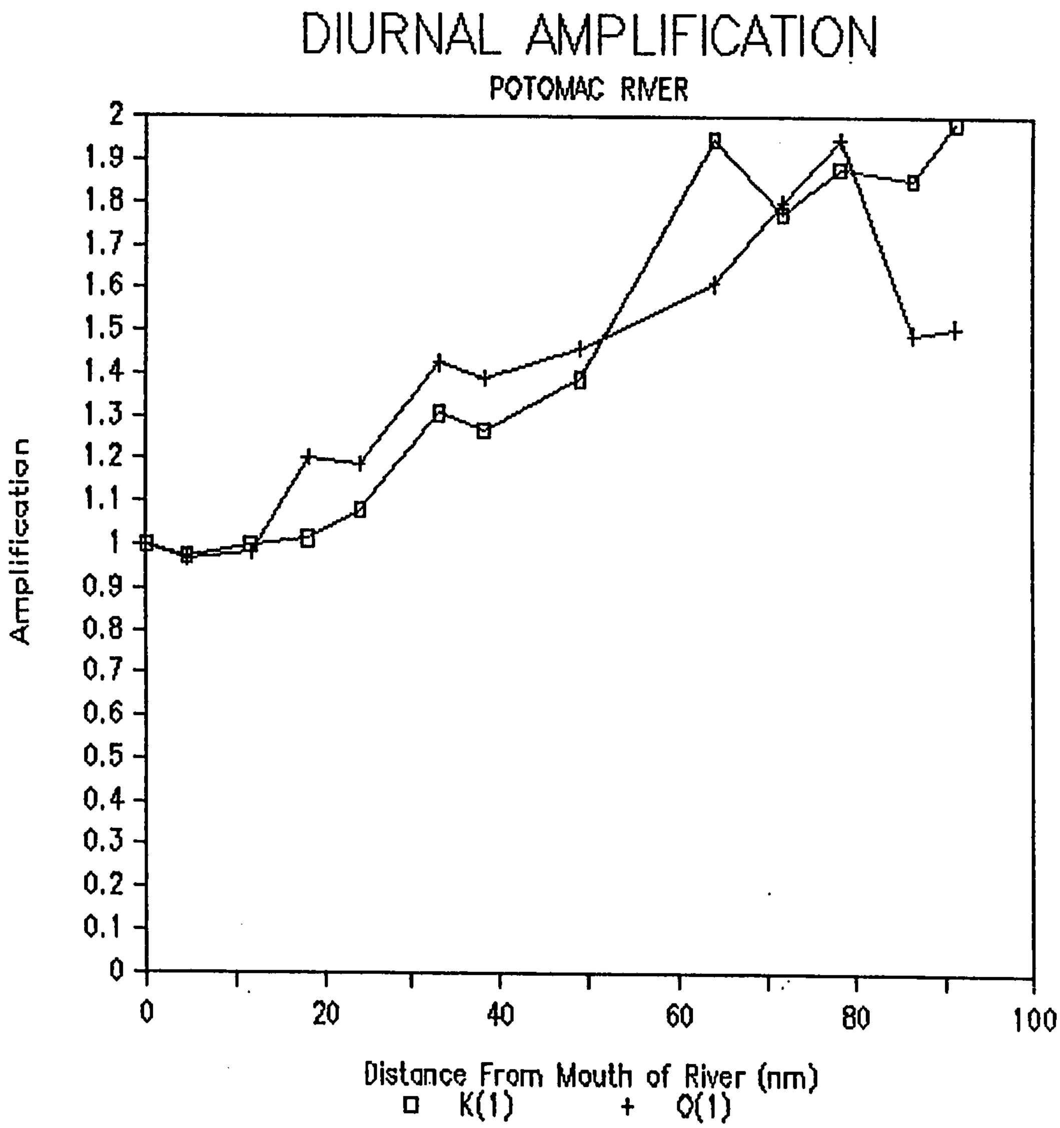
DIURNAL AMPLIFICATION
POTOMAC RIVER
Amplification
2
1.9
1.8
1.7
1.6
1.5
1.4
1.3
1.2
1.1
1
0.9
0.8
0.7
0.6
0.5
0.4
0.3
0.2
0.1
0
0
20
40
60
80
100
Distance From Mouth of River (nm)
K(1)
O(1)

explained that the decrease in amplification of a constituent in the upper tidal region of a basin or embayment is because the importance of the inertial term in the hydrodynamic equations is reduced where the tide becomes more like a standing wave.

Figures 47, 48, and 49 show the amplification of the semidiurnal elementary constituents M_2, N_2, and S_2 as well as the semidiurnal compound constituents $2MS_2$ and $2MN_2$. The amplification of M_2 (or lack thereof) has already been described in Figures 39, 40, and 41. The amplification curves for N_2 and S_2 are very similar to those of M_2 in these tributaries, but their amplification tends to be smaller. This is most evident in the upper tidal portion of the James River where the amplification ratios for M_2, N_2, and S_2 at Richmond are 1.06, 0.905, and 0.784, respectively. Parker explained that the quadratic resistance term in the equations of motion is responsible for reducing the amplification of a smaller elementary constituent when in the presence of a larger elementary constituent of the same species.

It is clearly shown that the semidiurnal compound constituents $2MS_2$ and $2MN_2$ are amplified more than the semidiurnal elementary constituents. The greatest amplification occurs in the Rappahannock River where $2MN_2$ is amplified about 7.3 times its original amplitude near the limit of tide. The compound constituent $2MS_2$ is not amplified much more than the semidiurnal elementary constituents.

Figure 49 shows that the amplificaton of $2MS_2$ throughout the tidal length of the Potomac River is usually much greater than the other semidiurnal constituents. Its amplification rapidly decreases until approximately 50 nautical miles from the mouth where it actually becomes less than the amplification of the other semidiurnal constituents for a

Figure 47. Amplification of the principal semidiurnal tidal constituents in the James River.

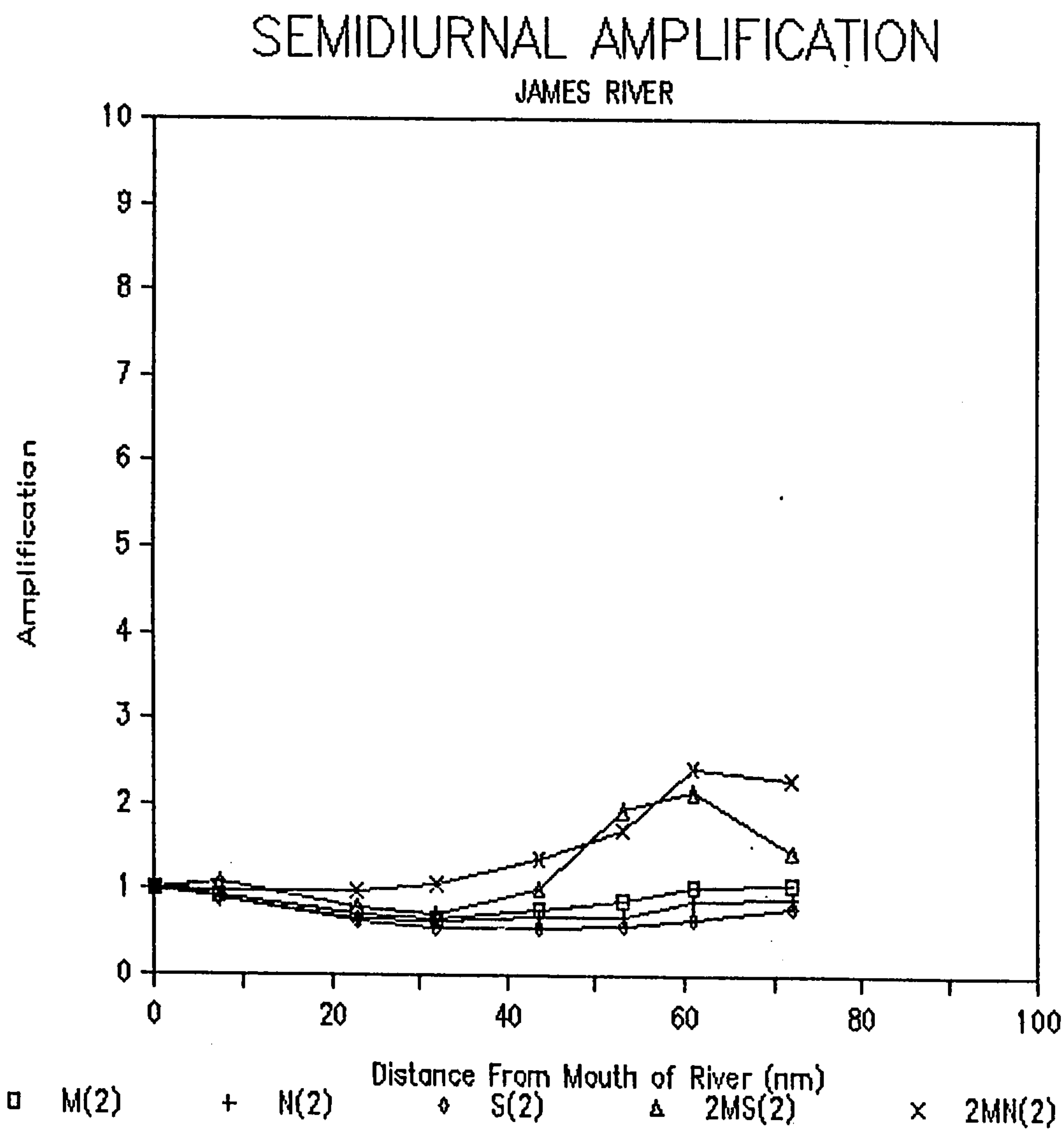
SEMIDIURNAL AMPLIFICATION
JAMES RIVER
Amplification
10
9
8
7
6
5
4
3
2
1
0
0
20
40
60
80
100
Distance From Mouth of River (nm)
M(2)
N(2)
S(2)
2MS(2)
2MN(2)

Figure 48. Amplification of the principal semidiurnal tidal constituents in the Rappahannock River.

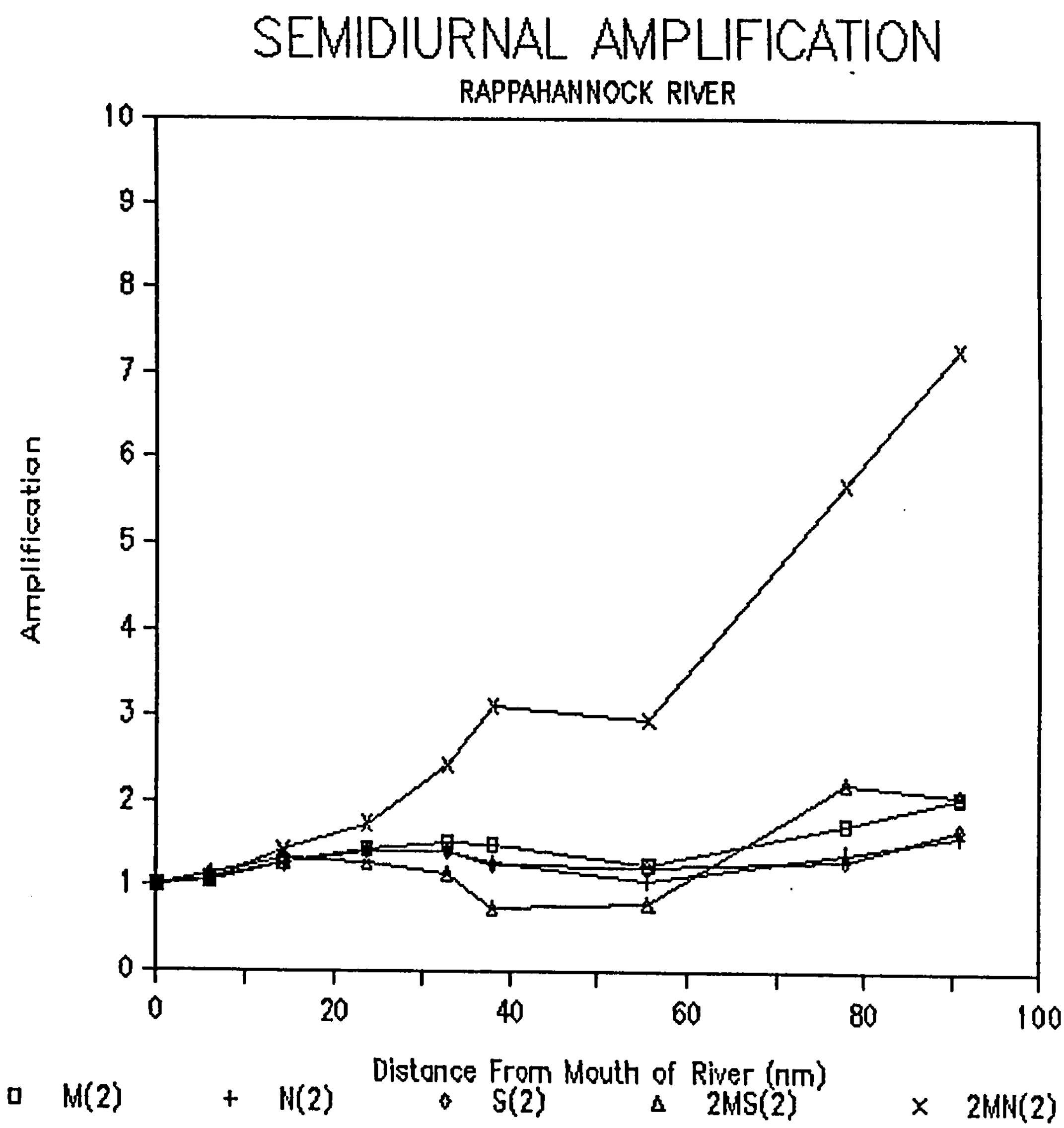
SEMIDIURNAL AMPLIFICATION
RAPPAHANNOCK RIVER
Amplification
0
1
2
3
4
5
6
7
8
9
10
0
20
40
60
80
100
Distance From Mouth of River (nm)
M(2)
N(2)
S(2)
2MS(2)
2MN(2)

Figure 49. Amplification of the principal semidiurnal tidal constituents in the Potomac River.

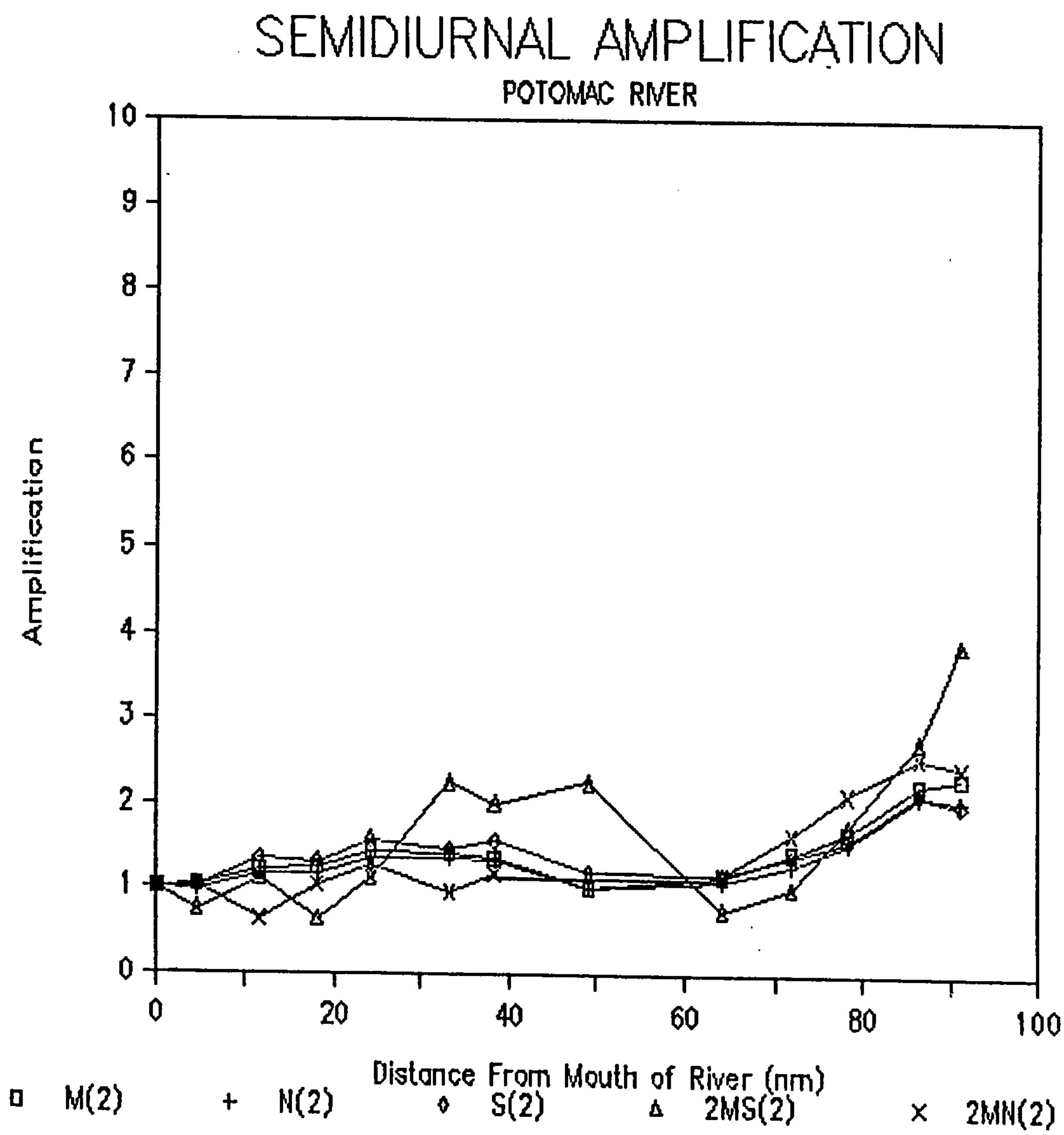
SEMIDIURNAL AMPLIFICATION
POTOMAC RIVER
Amplification
10
9
8
7
6
5
4
3
2
1
0
0
20
40
60
80
100
Distance From Mouth of River (nm)
M(2)
N(2)
S(2)
2MS(2)
2MN(2)

distance of about 10 nautical miles. Then, it increases again to a maximum of 3.88 at Washington, DC. The observed minimum may indicate the quasinode of the $2MS_2$ tidal wave. The compound constituent $2MN_2$ is the next most amplified semidiurnal constituent in the Potomac River, but its amplification is only slightly greater than that of the elementary constituents.

Both $2MS_2$ and $2MN_2$ are amplified much more than the semidiurnal elementary constituents in the James River, but the amount of amplification is somewhat less than observed in the other tributaries. In comparison, Parker observed that $2MS_2$ is amplified sixfold and $2MN_2$ is amplified fivefold in the Delaware River and Bay by the time these constituent waves reach Trenton, NJ. This amplification is greater than that observed in the James and Potomac rivers, but agrees fairly well with the amplification of $2MN_2$ observed in the Rappahannock River. He determined that the quadratic frictional resistance term in the equations of motion provides the mechanism to generate these compound tides.

Amplification of the terdiurnal compound constituents MK_3 and $2MK_3$ in the major tributaries is shown in Figures 50, 51, and 52. The amplification curves for MK_3 and $2MK_3$ are nearly identical in any specific tributary. Both constituents are amplified about sixfold in the James and Rappahannock rivers. The amplification of the terdiurnal constituents in the Potomac river is significantly larger, and not nearly as identical. The ratio for MK_3 increases to 9.5 at Washington, DC and the ratio for $2MK_3$ increases to 8.4. In each amplification curve for the Potomac River there is a discernable secondary maximum in amplification located approximately 35 nautical miles from the mouth.

Figure 50. Amplification of the principal terdiurnal tidal constituents in the James River.

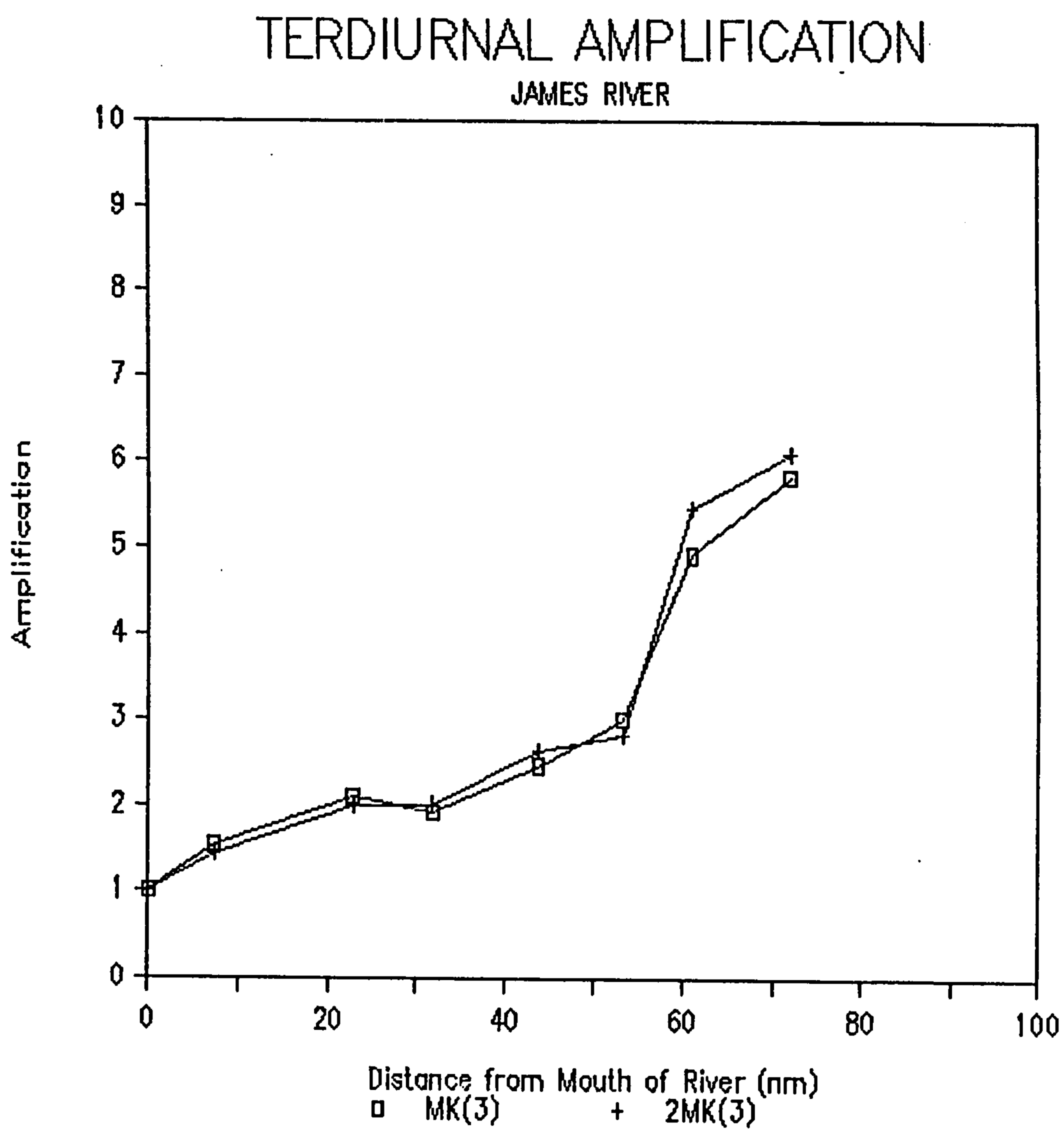
TERDIURNAL AMPLIFICATION
JAMES RIVER
Amplification
0
1
2
3
4
5
6
7
8
9
10
0
20
40
60
80
100
Distance from Mouth of River (nm)
MK(3)
2MK(3)

Figure 51. Amplification of the principal terdiurnal tidal constituents in the Rappahannock River.

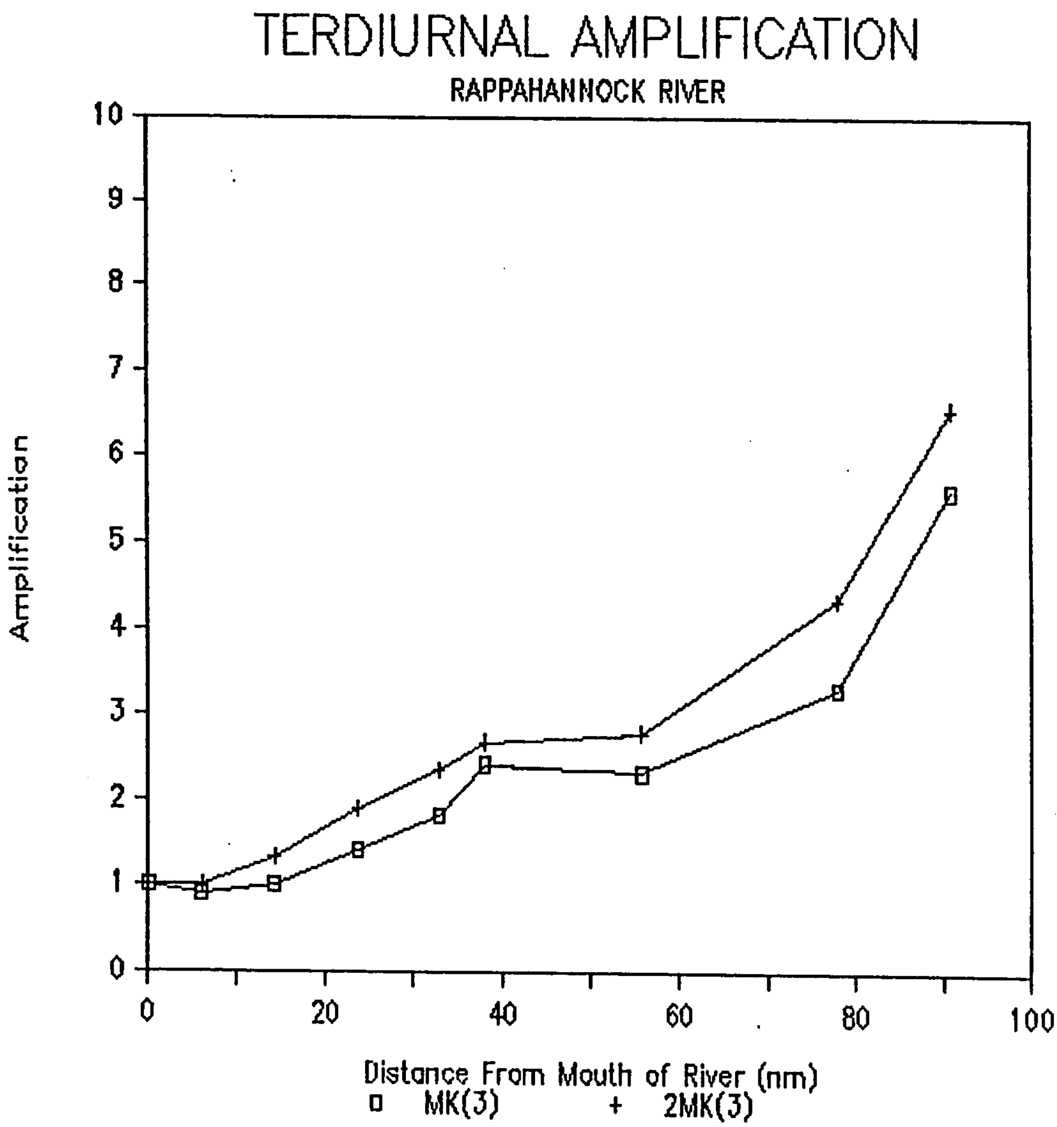

TERDIURNAL AMPLIFICATION
RAPPAHANNOCK RIVER
Amplification
0
1
2
3
4
5
6
7
8
9
10
0
20
40
60
80
100
Distance From Mouth of River (nm)
MK(3)
2MK(3)

Figure 52. Amplification of the principal terdiurnal tidal constituents in the Potomac River.

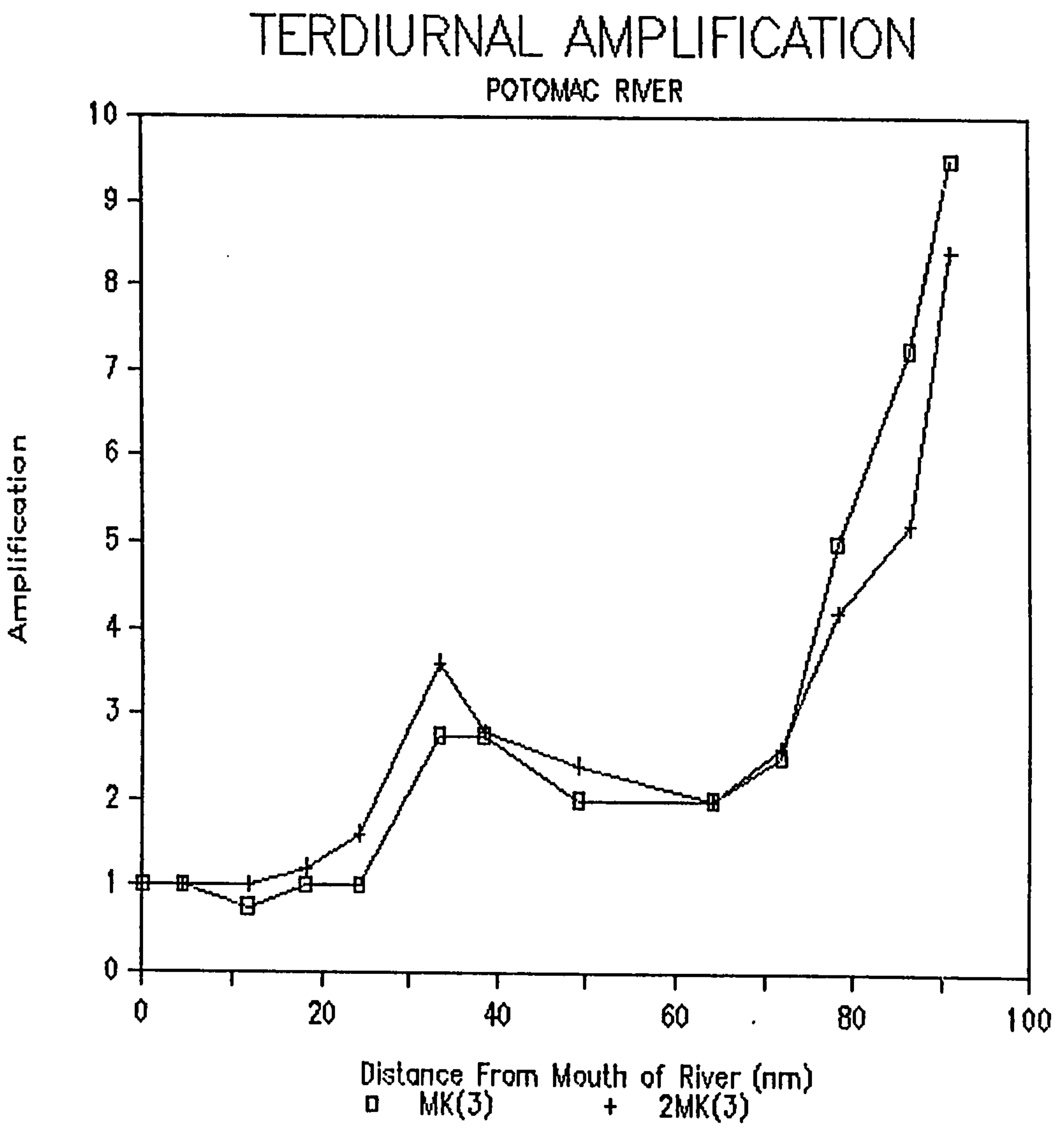
TERDIURNAL AMPLIFICATION
POTOMAC RIVER
Amplification
0
1
2
3
4
5
6
7
8
9
10
0
20
40
60
80
100
Distance From Mouth of River (nm)
MK(3)
2MK(3)

There may also be a minimum located about 80 nautical miles from the mouth. This maximum and possible minimum may indicate the locations of the antinode and quasinode of each constituent wave. Again, Parker has shown that the quadratic frictional resistance term and the elevation effect on the frictional momentum loss term in the equations of motion, as well as the nonlinear term in the continuity equation, all provide the mechanism to generate terdiurnal compound tides.

Amplification of the quarterdiurnal shallow water tides in the major tributaries is shown in Figures 53, 54, and 55. These plots indicate the amplification curve for the M_4 overtide agrees very well with the quarterdiurnal compound tides, MN_4 and MS_4. The greatest amplification again occurs in the Potomac River. The amplification of all three constituents increases gradually from the mouth to a location about 78 nautical miles upriver where the ratios for M_4, MN_4, and MS_4 are 2.33, 2.60, and 3.67, respectively. Continuing up the river, the amplification of all three constituents increases rapidly. Maximum amplification occurs at Washington, DC where the ratios are 11.92, 11.00, and 13.00, respectively.

In the James River, M_4 is amplified more than the quarterdiurnal compound constituents, with a maximum amplification of 9.36 at Richmond. Both MN_4 and MS_4 are amplified fivefold from the mouth to the limit of tide, and their amplification curves are nearly identical. The amplification of the quarterdiurnal compound tides tends to differ more in the Rappahannock River. The MN_4 and MS_4 ratios increase gradually to 2.50 and 3.17, respectively, from the mouth to a location about 38 nautical miles upriver, then decrease slightly during the next 40 nautical miles, and finally increase rapidly to 4.75 and 6.83 at Massaponax.

Figure 53. Amplification of the principal quarterdiurnal tidal constituents in the James River.

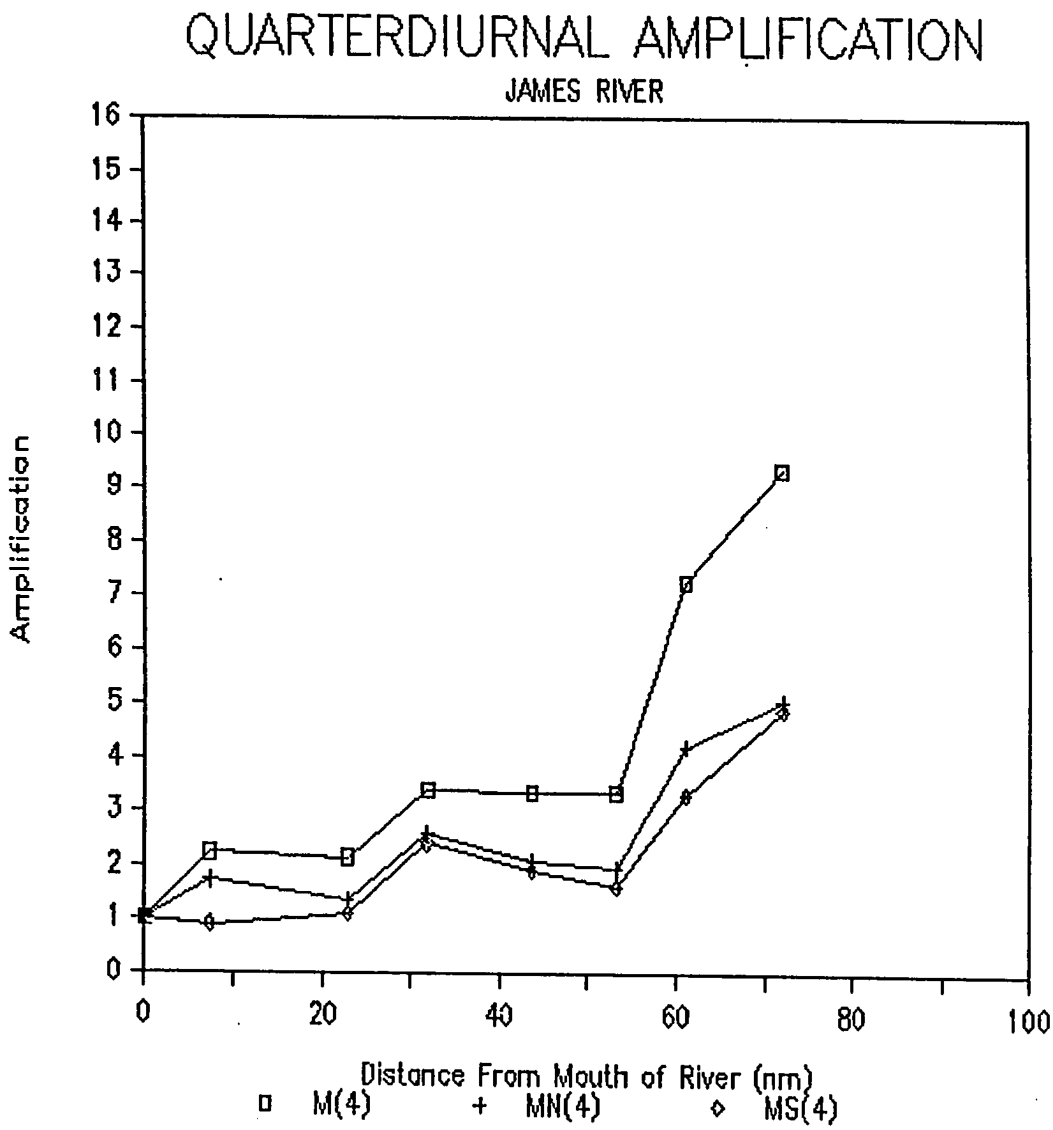

QUARTERDIURNAL AMPLIFICATION
JAMES RIVER
Amplification
16
15
14
13
12
11
10
9
8
7
6
5
4
3
2
1
0
0
20
40
60
80
100
Distance From Mouth of River (nm)
M(4)
MN(4)
MS(4)

Figure 54. Amplification of the principal quarterdiurnal tidal constituents in the Rappahannock River.

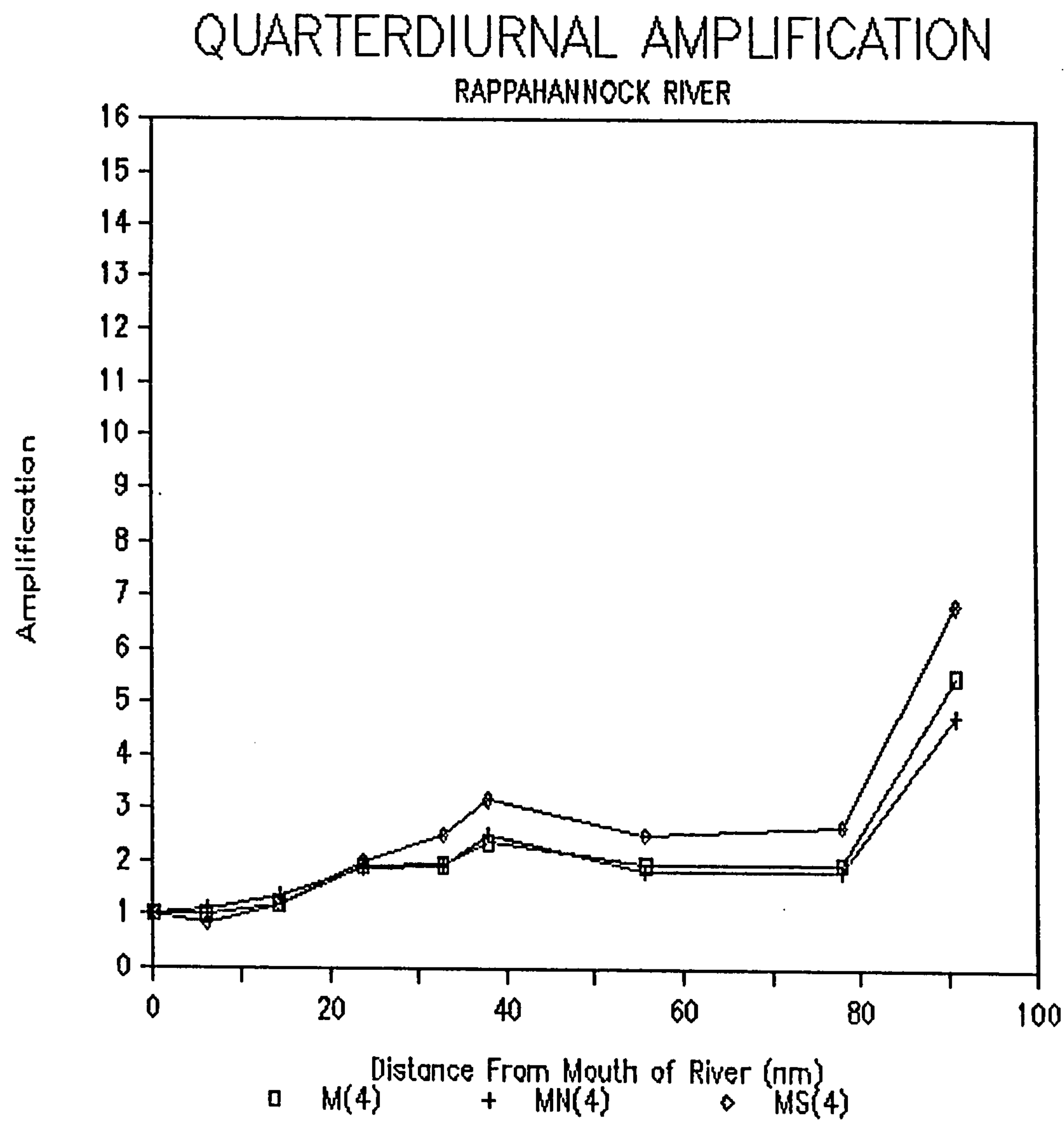
QUARTERDIURNAL AMPLIFICATION
RAPPAHANNOCK RIVER
Amplification
16
15
14
13
12
11
10
9
8
7
6
5
4
3
2
1
0
0
20
40
60
80
100
Distance From Mouth of River (nm)
M(4)
MN(4)
MS(4)

Figure 55. Amplification of the principal quarterdiurnal tidal constituents in the Potomac River.

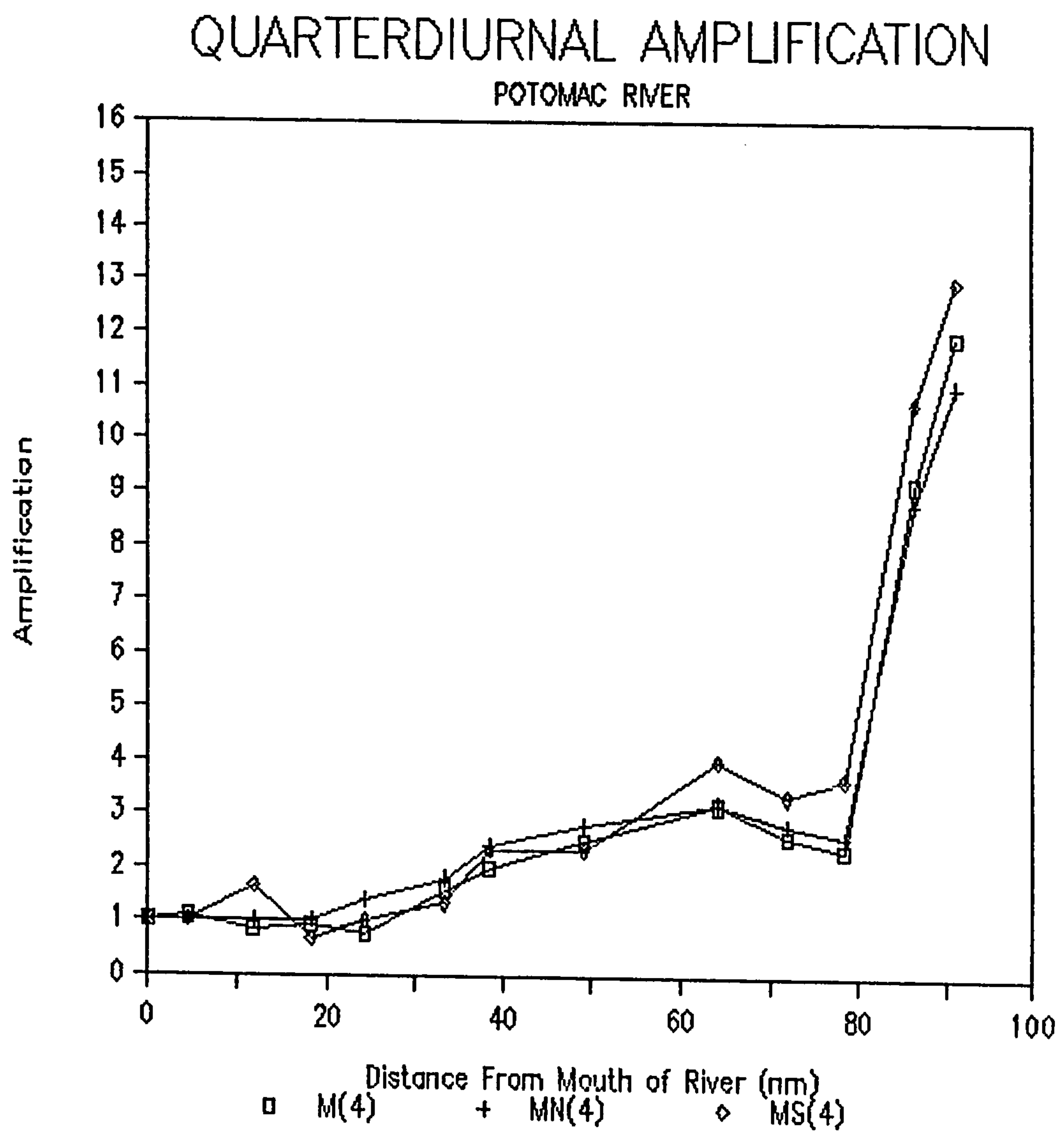
QUARTERDIURNAL AMPLIFICATION
POTOMAC RIVER
Amplification
16
15
14
13
12
11
10
9
8
7
6
5
4
3
2
1
0
0
20
40
60
80
100
Distance From Mouth of River (nm)
M(4)
MN(4)
MS(4)

In this case, Parker has shown that the nonlinear term in the continuity equation and the frictional momentum loss term in the equations of motion provide the mechanisms to generate even harmonic overtides and quarterdiurnal compound tides.

CHAPTER 6

SUMMARY AND RECOMMENDATIONS

This study has shown that the physical dimensions of Chesapeake Bay and its major tributaries strongly affect its tidal circulation. The height of tide and speed of tidal current at any location, as well as time of occurrence, are directly related to the length, width, and depth of each basin. In addition, amplification of tidal constituents occurs in the major tributaries, primarily due to the nonlinear effects of friction as well as resonance in each basin.

Since the lower bay is of sufficient width to be affected by Coriolis force, its tidal circulation is shown to be a frictionally damped Kelvin wave. In comparison, the upper bay and the major tributaries are much narrower so the Coriolis effect can be considered negligible, and the tide in these waterways is a simple frictionally damped tidal wave. A one dimensional analytic model of a frictionally damped reflected tidal wave, the Redfield model, has been used to determine that reflection does occur in each waterway, the most likely location where the wave is reflected, and the amount of frictional damping per tidal cycle.

It has been observed that the tide is nearly a pure standing wave in the vicinity of the point of reflection in each tributary. In fact, standing wave characteristics were observed over a considerable distance downriver from the point of reflection in the James and Rappahannock rivers. In comparison, the tide is observed to be a more progressive wave in the vicinity of the mouths of these tributaries and in Chesapeake Bay Entrance. Frictional damping almost totally attenuates a tidal wave by the time it is reflected back to the river mouth or bay entrance. The frictional damping coefficient varies from 2.1 to 3.5 in the major tributaries indicating an 88 percent to 97 percent attenuation of the tide per tidal cycle. In comparison, the frictional damping coefficient for the lower bay is estimated to be on the order of 1.0 indicating the tide is only attenuated about 63 percent.

The coamplitude and cophase charts of the M_2 and K_1 tidal constituents were used, in conjunction with the one dimensional analytic model, to indicate the location of the quasinodes and antinodes of the constituent tidal waves in each waterway. These constituent tidal waves were then used to explain the interaction of the semidiurnal and diurnal tides with respect to whether the observed tide is classified completely semidiurnal or mixed, mainly semidiurnal.

The amplification of the major diurnal, semidiurnal, terdiurnal and quarterdiurnal tidal constituents, as well as higher harmonics of M_2, was determined. This amplification was explained in terms of tidal hydrodynamics and the nonlinear effects of friction. It was shown that there is little amplification of the elementary constituents, but there is significant amplification of the shallow water constituents near the limit of tide in the major tributaries.

The cophase chart of the M_2 tidal constituent was compared to the cophase chart of the M_2 tidal current constituent to determine the relationship of the tide and tidal current throughout the bay. This comparison indicated the observed data agreed well with simple reflected wave theory. It was shown that the M_2 tide and M_2 tidal current are nearly in phase in Chesapeake Bay Entrance, which is to be expected since the tidal wave is known to be nearly progressive there. In comparison, the M_2 tide lags the current by 48° near the head of bay. This also agrees well with reflected wave theory since the tide is expected to be more like a standing wave in the vicinity of the point of reflection.

The cospeed chart of the M_2 tidal current constituent was used as an approximate description of the maximum flood current pattern in the Bay Proper. It clearly showed two major inflows in Chesapeake Bay Entrance, and that the currents are strongly affected by bottom topography throughout the bay.

In summary, this study has shown that the tide in the upper bay and the major tributaries can be effectively modeled with a one dimensional frictionally damped analytic model such as the Redfield model. This model can be used to explain the tidal hydrodynamics of these waterways and to compute tidal amplitudes and tidal current speeds for any specified location at any time. It has also been shown that the tide in the lower bay cannot be modeled properly with a one dimensional analytic model because of its width. A two dimensional frictionally damped analytic model was considered which produced a cotidal line pattern that is very similar to the cotidal and coamplitude lines observed in the lower bay. This pattern appears to be amphidromic but displaced significantly to the west due to friction. A virtual amphidrome would be located west of Chesapeake Bay on the peninsula between the Rappahannock and Potomac rivers.

However, the mechanism for reflection of the Kelvin wave in the lower bay is not clearly understood. Perhaps the incident Kelvin wave becomes a more one dimensional wave as it enters the narrower upper bay. This study has shown that the tidal wave is clearly reflected at the head of bay. Then the reflected wave would travel back down to the lower bay where the increased width would cause it to become a Kelvin wave again that would travel in the direction opposite to that of the incident Kelvin wave. If this were so, then the two dimensional analytic model needs to be modified to account for the phase difference which occurs between the time the incident Kelvin wave leaves the lower bay and the reflected wave returns to the lower bay to become a Kelvin wave again.

The possibility of an added oscillation across the narrows located just north of the lower bay, which would reflect the incident Kelvin wave, was also considered, but no cross channel oscillations were observed at this location during this study. These oscillations may be present in the current meter data, but were not detected by the types of analyses used. It is recommended that future analysis of this current meter data include analysis techniques which would detect oscillations at frequencies other than tidal frequencies.

This study has not accounted for any loss of tidal energy from the bay into its tributaries, or from the tributaries into smaller tributaries thereof. The loss of tidal energy was not included in either the one dimensional or two dimensional analytic model. However, these energy losses can be accounted for in the development of the one dimensional analytic model if the amount of energy loss at each side channel is known. It may be too complicated a process to develop a two dimensional analytic model that accounts for loss of tidal energy, and numerical modeling techniques may be required. It is recommended that the tidal energy loss at each tributary be determined and used to modify these analytic models, if possible.

Since there were few offshore tide stations deployed in the bay or tributaries during this study, it was difficult to determine how to draw the cotidal lines in offshore waters. Future cotidal charts can be significantly improved if tide observations can be obtained at more offshore locations.

In addition, it was not possible to construct cocurrent charts of the observed tidal current during this study because the Greenwich mean lunitidal intervals and maximum flood current speeds had not been determined. It is recommended that cocurrent charts of the observed tidal current be constructed once the required lunitidal intervals and speeds have been determined by the National Ocean Service.

Finally, this study did not address any tidal current circulation in the bay other than near the surface. During the tide and current survey which was the source of data for this study, additional current meters were deployed near the bottom and at mid-depth, where water depth permitted. The data from these meters should be analyzed in conjunction with the CTD data which was observed at the same time, and used to describe the tidal circulation at depth in Chesapeake Bay also.

BIBLIOGRAPHY

Amin, M. 1986. On the conditions for classification of tides, International Hydrographic Review, 118(1):161-174.

Boicourt, W. C. 1981. Circulation in the Chesapeake Bay Entrance region: estuary-shelf interaction, In: Chesapeake Bay Plume Study, Superflux 1980. NASA Conference Publication 2188. 515 pp.

Brown, P. J. 1972. Kelvin wave reflection in a semi-infinite canal, Jour. of Marine Research, 31(1):1-10.

Courtier, A. 1938. Marees, Service Hydrographique de la Marine. Paris, France. p 149-159.

Defant, A. 1961. Physical Oceanography, Vol. 2. Pergamon Press, New York, NY. 598 pp.

Dennis, R. E. and E. E. Long. 1971. A user's guide to a computer program for harmonic analysis of data at tidal frequencies, NOAA Technical Report, NOS 41. U.S. National Ocean Survey, Rockville, MD. 31 pp.

Dietrich, G. 1944. Die schwingungssysteme der halb-und eintagigen tiden in den oceanen, Veroff. Inst. Meerest., Univ. Berlin, N. F. A., No. 41.

Doodson, A. T. and H. D. Warburg. 1941. Admiralty Manual of Tides. Hydrographic Department, Admiralty. London, England. 270 pp.

Dyer, K. R. 1973. Estuaries: A Physical Introduction. John Wiley and Sons, London, England. 140 pp.

Fjeldstad, J. E. 1929. Contribution to the dynamics of free progressive tidal waves, the Norwegian North Polar Expedition with the MAUD, 1918-1925, Scientific Results, 4(3), Geofysisk Institute, Bergen, Norway. 80 pp.

Gallagher, B. S. and W. H. Munk. 1971. Tides in shallow water: spectroscopy, Tellus, 23:346-363.

Haight, F. J., H. E. Finnegan and G. L. Anderson. 1930. Tides and currents in Chesapeake Bay and tributaries, Special Publication No. 162. U.S. Coast and Geodetic Survey, Washington, DC. 143 pp.

BIBLIOGRAPHY (CONTINUED)

Harris, D. L., N. A. Pore and R. Cummings. 1963. The application of high speed computers to practical tidal problems, Abstracts of Papers 6:16, IAPO, Thirteenth General Assembly, IUGG, Berkeley, CA.

Harris, D. L. 1981. Tides and tidal datums in the United States, Special Report No. 7. Coastal Engineering Research Center, U.S. Army Corps of Engineers, Fort Belvoir, VA. 382 pp.

Harris, R. A. 1907. Currents, shallow water tides, meteorological tides and miscellaneous matters, Manual of Tides, Appendix 6, Chapter 6:357, Annual Report for 1907. U.S. Coast and Geodetic Survey, Washington, DC.

Hendershott, M. C. and A. Speranza. 1971. Cooscillating tides in long, narrow bays; the Taylor problem revisited, Deep-Sea Research, 18:959-980.

Hicks, S. D. 1964. Tidal wave characteristics of Chesapeake Bay, Chesapeake Science, 5(3):103-113.

Hicks, S. D. 1984. Tide and Current Glossary. U.S. National Ocean Service, Washington, DC. 28 pp.

Hilder, F. A. 1980. Surface circulation and horizontal diffusion processes of the lower Chesapeake Bay, Ph.D. Dissertation, Old Dominion University, Norfolk, VA. 189 pp.

Houlder, R. A. and W. M. Dunston. 1982. Memorandum of understanding between the NOAA Atlantic Marine Center and the Department of Oceanography, Old Dominion University (unpublished). 3pp.

Ippen, A. T. and D. R. F. Harleman. 1966. Tidal dynamics in estuaries. In: Estuary and Coastline Hydrodynamics, A. T. Ippen [ed], p 493-545. McGraw-Hill, New York, NY.

Kabbaj, A. and C. LeProvost. 1980. Nonlinear tidal waves in channels: a perturbation method adopted to the importance of quadratic bottom friction, Tellus, 9(1):143-163.

LeBlond, P. H. 1978. On tidal propagation in shallow rivers, Jour. Geophysical Research, 83(C9):4717-4721.

Long, E. E. 1983. Program TABLE 14-15, a computer program for the harmonic analysis of uniformly spaced and semi-random tidal data. National Ocean Service, Washington, DC.

Marmer, H. A. 1951. Tidal Datum Planes, Special Publication No. 135. U.S. Coast and Geodetic Survey, Washington, DC. 142 pp.

BIBLIOGRAPHY (CONTINUED)

Parker, B. B. 1977. Tidal hydrodynamics in the Strait of Juan de Fuca - Strait of Georgia, NOAA Technical Report NOS 69, National Ocean Survey, Washington, DC.

Parker, B. B. 1980. The attenuation of tidal waves in a long, narrow semi-enclosed basin, EOS, 61(17):273.

Parker, B. B. 1984. Frictional effects on the tidal dynamics of a shallow estuary, Ph.D. Dissertation, Johns Hopkins University, Baltimore, MD. 292 pp.

Patchen, R. C. 1975. The computer program ELLIPSE. U.S. National Ocean Survey, Washington, DC.

Pedlosky, J. 1979. Geophysical Fluid Dynamics. Springer-Verlag, New York, NY. 624 pp.

Pritchard, D. W. 1952. Salinity distribution and circulation in the Chesapeake Bay estuarine system, Jour. Marine Science, 11:106-123.

Redfield, A. C. 1950. The analysis of tidal phenomena in narrow embayments, Papers in Physical Oceanography and Meteorology, 11(4):1-37. Massachusetts Institute of Technology and Woods Hole Oceanographic Institution.

Ruzecki, E. P. 1976. The effects of tropical storm Agnes on the Chesapeake Bay estuarine system, hydrographic effects, CRC Publication No. 54, p 1-12. Chesapeake Bay Research Constortium, Washington, DC.

Schureman, P. 1958. Manual of Harmonic Analysis and Prediction of Tides, Special Publication No. 98. U.S. Coast and Geodetic Survey, Washington, DC. 317 pp.

Swanson, R. L. 1971. Some aspects of currents in Long Island Sound, Ph.D. Dissertation. Oregon State University, Corvallis, OR. 86 pp.

Stok, Van Der. 1897. Wind, Weather, Currents, Tides, and Tidal Streams of the East Indian Archipelago. Batavia.

Taylor, G. I. 1920. Tidal oscillations in gulfs and rectangular basins, Proc. London Math. Soc., 20(2):148-181.

U.S. Coast and Geodetic Survey. 1950 (Supplement 1961). Manual of Current Observations, Special Publication No. 215. U.S. Coast and Geodetic Survey, Washington, DC. 87 pp.

BIBLIOGRAPHY (CONTINUED)

U.S. Coast and Geodetic Survey. 1952. Manual of Harmonic Constant Reductions, Special Publication No. 260. U.S. Coast and Geodetic Survey, Washington, DC. 74 pp.

U.S. Coast and Geodetic Survey. 1965. Manual of Tide Observations, Publication No. 30-1. U.S. Coast and Geodetic Survey, Washington, DC. 72 pp.

U.S. National Ocean Survey. 1973. Upper Chesapeake Bay Tidal Current Charts, Second Edition. U.S. National Ocean Survey, Rockville, MD. 13 pp

U.S. National Ocean Survey. 1983a. Tidal Current Tables, Atlantic Coast of North America. U.S. National Ocean Survey, Rockville, MD. 234 pp (each).

U.S. National Ocean Survey. 1983b. Tide Tables, East Coast of North and South America. U.S. National Ocean Survey, Rockville, MD. 285 pp (each).

APPENDIX A

SUMMARY OF TIDE STATIONS

SUMMARY OF TIDE STATIONS

Station Number	Station Name	Latitude (N)	Longitude (W)	Installed	Removed	*Greenwich Int. HWI(Hr)	LWI(Hr)	*Mean Range(Ft)	**NGVD-MSL(Ft)
8571073	DN2, SMITH IS, MD	37/58.3	75/59.1	04/27/77	12/18/77	5.39	11.91	1.73	
8571091	CRISFIELD, MD	37/58.6	75/51.8	04/23/77 09/01/81	12/19/77 10/20/81	5.20	11.78	1.88	
8571181	COLBOURN CK, MD	38/02.9	75/48.2	10/19/81	11/30/81	5.62	12.32	1.94	
8571214	HOLLAND BAR LT, MD	38/04.1	76/05.8	08/30/81	12/01/81	5.54	11.98	1.40	
8571266	RUMBLEY, MD	38/05.5	75/51.7	10/21/81	11/30/81	5.61	12.23	1.92	
8571289	LT6, L DEAL IS, MD	38/07.5	75/56.8	04/25/77	12/20/77	6.01	0.17	1.97	
8571351	CHANCE, MD	38/10.3	75/56.7	07/25/72	07/12/74	6.12	0.37	1.94	-0.09
8571402	HOOPER ST LH, MD	38/13.6	76/04.6	10/22/81	12/01/81	6.07	0.27	1.48	
8571477	NANTICOKE, MD	38/16.2	75/54.8	10/21/81	12/03/81	6.42	0.77	2.10	
8571519	MIDHOOPERS IS, MD	38/17.8	76/12.3	06/23/71	11/27/74	6.82	1.06	1.49	-0.21
8571559	MCCREADYS CK, MD	38/18.0	76/00.4	10/19/81	12/02/81	6.56	0.97	2.09	
8571752	TAYLORS IS, MD	38/28.0	76/17.7	07/18/72	10/09/73	8.56	2.50	1.22	-0.24
8571773	VIENNA, MD	38/29.0	75/49.1	07/24/72	10/09/73	9.28	3.26	2.21	-0.22
8571890	CAMBRIDGE, MD	38/34.5	76/04.3	10/21/80	NO	8.96	3.10	1.55	-0.18
8571901	AVALON, MD	38/42.6	76/20.1	09/28/83	12/08/83	8.67	2.73	1.32	
8571944	DOVER BRIDGE, MD	38/45.4	75/59.9	07/17/72	10/09/73	11.32	5.01	1.62	-0.26
8571979	FERRY COVE, MD	38/46.0	76/19.5	07/14/83	10/13/83	9.04	3.11	1.14	
8572342	ST MICHAELS, MD	38/47.2	76/13.3	07/27/83	09/09/83	9.33	3.66	1.39	
8572458	BLOODY PT. BAR LIGHT, MD	38/50.0	76/23.5	UNKNOWN	UNKNOWN	9.00	3.05	1.11	
8572770	MATAPEAKE, MD	38/57.5	76/21.3	07/13/72	08/24/84	10.21	3.99	0.99	-0.27
8572955	LOVE PT, MD	39/01.9	76/18.1	06/29/71 07/13/83	01/01/73 09/09/83	11.21	5.04	1.17	-0.31

* BASED ON 1960-78 EPOCH
** BASED ON 1941-59 EPOCH

SUMMARY OF TIDE STATIONS

Station Number	Station Name	Latitude (N)	Longitude (W)	Installed	Removed	*Greenwich Int. HWI(Hr)	LWI(Hr)	*Mean Range(Ft)	**NGVD-MSL(Ft)
8573137	CLIFFS WHARF, MD	39/06.6	76/08.3	06/22/71 07/13/83	11/26/74 08/24/83	11.68	5.56	1.54	-0.35
8573343	CHESTERTOWN, MD	39/12.4	76/03.8	06/23/71	07/10/72	12.43	6.16	1.83	-0.40
8573364	TOLCHESTER, MD	39/12.8	76/14.7	06/24/71 03/19/83 06/07/83	08/29/74 04/28/83 09/16/83	12.15	5.99	1.18	-0.33
8573704	BETTERTON, MD	39/22.3	76/03.8	06/24/71 05/05/83	07/10/72 07/21/83	1.85	8.04	1.50	-0.52
8573903	TOWN PT WHARF, MD	39/30.2	75/55.0	10/17/72 03/17/83	05/06/80 06/21/83	2.56	8.78	2.06	-0.39
8573927	CHESAPEAKE CITY, MD	39/31.6	75/48.6	11/15/72 06/07/84	06/22/83 NO	3.16	9.58	2.74	-0.40
8574008	PORT DEPOSIT, MD	39/36.2	76/06.8	05/04/83	06/23/83	2.50	9.54	1.74	
8574070	HAVRE DE GRACE, MD	39/32.2	76/05.4	11/17/72	NO	2.49	9.29	1.79	-0.64
8574561	BACK RIVER, MD	39/18.0	76/28.9	05/04/78	09/14/78	0.23	6.46	1.10	
8574680	BALTIMORE, MD	39/16.0	76/34.7	07/01/02	NO	11.70	5.78	1.11	-0.38
8574821	HAWKINS PT, MD	39/12.5	76/32.0	08/12/76	11/11/76	11.74	5.79	1.10	
8574857	NORTH PT, MD	39/11.8	76/26.7	06/28/71 06/06/83	11/11/76 08/31/83	11.72	5.69	1.04	-0.35
8574931	STONY CK, MD	39/09.8	76/31.6	11/05/76	11/11/76	11.74	4.68	1.05	
8575024	BODKIN CK, MD	39/07.5	76/27.0	11/12/75	01/21/76	11.40	5.63	0.95	
8575109	CORNFIELD CK, MD	39/06.0	76/26.7	11/01/75	12/01/75	11.08	4.86	0.97	
8575510	ANNAPOLIS, MD	38/59.1	76/29.2	08/07/28	01/17/80	(SEE STATION 8575512)			
8575512	ANNAPOLIS, MD	38/59.0	76/28.8	09/14/78	NO	10.06	3.97	0.93	
8575550	GINGERVILLE CK, MD	38/57.5	76/33.3	10/04/66	04/24/79	9.77	3.66	1.00	-0.34
8575787	RHODE RIVER, MD	38/53.2	76/32.4	06/30/71	05/27/77	9.77	3.43	0.95	-0.30

* BASED ON 1960-78 EPOCH
** BASED ON 1941-59 EPOCH

SUMMARY OF TIDE STATIONS

Station Number	Station Name	Latitude (N)	Longitude (W)	Installed	Removed	*Greenwich Int. HWI(Hr)	LWI(Hr)	*Mean Range(Ft)	**NGVD-MSL(Ft)
8576363	CHESAPEAKE BCH, MD	38/41.0	76/32.0	06/27/72 08/15/83	12/18/75 12/01/83	8.68	2.65	1.00	
8577123	BROOMES IS, MD	38/24.9	76/32.7	06/19/72	10/11/73	7.51	1.53	1.31	
8577188	COVE PT, MD	38/23.1	76/22.9	07/06/72 10/12/83	07/23/74 12/02/83	7.38	1.18	0.98	
8577330	SOLOMONS IS, MD	38/19.0	76/27.2	11/05/37	NO	6.95	0.92	1.18	-0.23
8577381	CEDAR PT, MD	38/17.9	76/22.2	05/15/79	06/07/79	6.67	0.50	1.14	
8577385	NAVY SEAPLANE BASIN BOATHOUSE, MD	38/16.3	76/23.8	08/28/81	12/03/81	6.70	0.71	1.12	
8577940	CORNFIELD HBR, MD	38/03.7	76/21.4	10/30/71	02/24/72	5.93	12.34	1.20	-0.17
8578002	PT LOOKOUT, MD	38/02.4	76/19.4	10/05/81	12/04/81	6.26	0.17	1.21	-0.17
8578240	PINEY PT, MD	38/08.0	76/32.0	11/21/58	12/13/77	6.39	0.23	1.40	-0.17
8578465	COLTON PT, MD	38/13.4	76/44.9	07/17/69	10/15/69	6.99	0.78	1.80	-0.34
8578693	LOWER CEDAR PT, MD	38/20.5	76/58.6	UNKNOWN	UNKNOWN	7.71	1.68	1.50	
8578769	PORT TOBACCO, MD	38/27.2	77/03.2	09/30/71	07/11/72	8.16	2.39	1.42	-0.29
8578853	RIVERSIDE, MD	38/23.2	77/08.7	07/16/69	10/11/72	8.91	3.09	1.24	-0.30
8578981	SMITH PT, MD	38/24.8	77/16.0	UNKNOWN	UNKNOWN	10.73	4.86	1.03	
8578984	LIVERPOOL PT, MD	38/27.6	77/16.2	UNKNOWN	UNKNOWN	10.67	4.96	0.81	
8579135	BENEDICT, MD	38/30.8	76/40.2	06/14/72	11/15/73	7.84	1.98	1.55	
8579381	INDIAN HEAD, MD	38/36.1	77/11.1	10/30/70	10/10/72	12.10	5.95	1.75	-0.29
8579542	LOWER MARLBORO, MD	38/39.3	76/41.0	07/10/72	10/11/73	8.85	2.84	1.77	
8579629	MARSHALL HALL, MD	38/41.2	76/06.1	10/30/70	10/10/72	12.09	6.58	2.18	-0.37
8594900	WASHINGTON, DC	38/52.5	77/01.4	11/10/24	NO	0.37	7.51	2.77	-0.52

* BASED ON 1960-78 EPOCH
** BASED ON 1941-59 EPOCH

SUMMARY OF TIDE STATIONS

Station Number	Station Name	Latitude (N)	Longitude (W)	Installed	Removed	*Greenwich Int. HWI(Hr)	LWI(Hr)	*Mean Range(Ft)	**NGVD-MSL(Ft)
8632065	FISHERMANS IS SOUTH, VA	37/05.1	75/57.9	06/20/77 05/12/80	01/04/78 09/26/80	0.77	6.88	3.27	
8632085	FISHERMANS IS, VA	37/05.8	75/59.0	06/21/77 03/16/82	01/04/78 11/22/82	0.82	7.07	2.98	
8632200	KIPTOPEAKE, VA	37/10.0	75/59.3	08/22/51	NO	0.99	7.41	2.68	0.06
8632366	CAPE CHARLES HARBOR, VA	37/15.8	76/01.2	06/25/47 03/16/82	11/07/52 07/12/82	1.45	7.94	2.33	
8632599	MATTAWOMAN CK, VA	37/23.3	75/57.8	03/16/82	12/09/82	2.17	9.12	1.94	
8632869	GASKIN PT, VA	37/33.4	75/55.0	08/01/72 07/12/82	07/18/74 09/02/82	3.46	10.28	1.70	0.11
8632974	RAPPAHANNOCK SHOAL, VA	37/35.6	76/01.9	06/24/83	10/31/83	3.34	9.79	1.45	
8633091	HARBORTON, VA	37/40.0	75/50.0	01/28/76	06/24/77	3.85	10.45	1.81	
8633362	SCHOONER BAY, VA	37/45.8	75/46.4	06/10/75	09/04/75	4.41	10.90	2.00	
8633451	WATTS IS, VA	37/47.9	75/53.8	04/12/61	05/05/61	4.65	11.06	1.61	
8633532	TANGIER IS, VA	37/49.7	75/59.5	08/08/79 08/27/81 10/06/82	05/29/80 10/30/81 11/17/82	4.62	11.22	1.48	
8633596	GUARDSHORE, VA	37/51.0	75/42.0	08/02/72	07/18/74	4.67	11.58	2.28	-0.12
8634214	ALEXANDRIA, VA	38/48.3	77/02.3	05/16/74	07/16/75	12.37	7.44	2.72	-0.52
8634437	MT VERNON, VA	38/42.3	77/05.3	09/13/74	11/19/74	0.09	6.81	2.14	
8634489	WHITESTONE PT, VA	38/40.6	77/08.1	09/11/74	11/22/74	12.39	6.55	1.94	
8634689	QUANTICO, VA	38/31.2	77/17.2	10/04/71	12/19/72	11.47	5.43	1.36	-0.36
8634858	AQUIA CK, VA	38/25.1	77/21.2	11/01/70	09/07/72	10.78	4.98	1.18	-0.32
8634892	MATHIAS PT, VA	38/23.9	77/03.2	07/06/62	10/15/62	8.44	2.70	1.13	

* BASED ON 1960-78 EPOCH
** BASED ON 1941-59 EPOCH

SUMMARY OF TIDE STATIONS

Station Number	Station Name	Latitude (N)	Longitude (W)	Installed	Removed	*Greenwich Int. HWI(Hr)	LWI(Hr)	*Mean Range(Ft)	**NGVD-MSL(Ft)
8634951	METONKIN PT, VA	38/21.8	77/08.6	08/07/62	10/15/62	9.76	3.95	0.85	
8635027	DAHLGREN, VA	38/19.2	77/02.2	04/09/70	02/23/72	7.50	1.66	1.60	-0.28
8635150	COLONIAL BCH, VA	38/15.2	76/57.7	01/07/72	NO	7.33	1.31	1.66	-0.28
8635154	MASSAPONAX SAND & GRAVEL, VA	38/15.3	77/24.6	02/15/71	02/24/72	11.72	6.85	2.47	-0.71
8635171	HOPYARD LNDG, VA	38/14.6	77/13.6	01/15/71	02/23/72	11.24	5.57	2.11	-0.64
8635485	COLES NECK, VA	38/08.5	76/36.8	10/05/71	01/19/72	6.81	0.58	1.52	-0.37
8635554	SAUNDERS WHARF, VA	38/05.4	77/02.0	01/15/71	04/04/72	8.48	2.84	1.52	-0.43
8635750	LEWISETTA, VA	37/59.8	76/27.8	10/20/70	NO	6.19	0.08	1.26	-0.19
8635881	TAPPAHANNOCK, VA	37/55.8	76/51.4	06/29/70	12/17/74	6.10	0.62	1.74	-0.26
8635961	SMITH PT, VA	37/53.3	76/14.5	08/26/81 10/06/82	10/17/81 11/22/82	6.21	12.30	0.90	
8635985	WARES WHARF, VA	37/52.4	76/47.0	01/12/71	04/03/72	5.55	12.24	1.75	-0.34
8636128	FLEET PT, VA	37/48.8	76/16.5	10/21/70	01/18/72	4.59	10.99	1.12	-0.11
8636142	GT WICOMICO RIVER LIGHTHOUSE, VA	37/48.3	76/16.1	10/12/54	08/22/55	4.63	11.08	1.06	
8636261	BAYPORT, VA	37/45.3	76/40.4	01/14/71	04/03/72	4.80	11.60	1.63	-0.28
8636522	URBANNA, VA	37/39.0	76/34.5	01/07/71	02/22/72	4.26	10.90	1.43	-0.16
8636580	WINDMILL PT MARINA, VA	37/36.7	76/16.5	06/24/70 03/10/82 04/21/83	03/18/75 09/29/82 10/31/83	3.49	10.19	1.17	-0.02
8636654	NEW MILL CK, VA	37/35.0	76/25.1	06/29/70	04/07/78	3.89	10.44	1.26	-0.03
8636735	DELTAVILLE, VA	37/32.9	76/19.9	05/17/72	10/04/73	3.03	9.81	1.18	-0.03
8636769	WEST POINT, VA	37/32.1	76/47.6	12/29/70	12/20/74	3.61	10.39	2.78	-0.02

* BASED ON 1960-78 EPOCH
** BASED ON 1941-59 EPOCH

SUMMARY OF TIDE STATIONS

Station Number	Station Name	Latitude (N)	Longitude (W)	Installed	Removed	*Greenwich Int. HWI(Hr)	LWI(Hr)	*Mean Range(Ft)	**NGVD-MSL(Ft)
8636831	DIXIE, VA	37/30.4	76/25.0	05/11/72	10/04/72	2.99	9.98	1.31	-0.09
8636912	PT BREEZE, VA	37/28.3	76/16.9	06/23/53	09/02/53	3.08	10.07	1.09	
8636969	ROANE PT, VA	37/26.8	76/42.5	05/18/72	11/15/73	3.18	9.59	2.77	
8637072	BELLEVILLE, VA	37/24.7	76/26.3	07/27/71	07/22/72	1.33	7.74	2.48	-0.06
8637144	WOLF TRAP LH, VA	37/23.4	76/11.4	04/29/53	10/16/53	1.51	8.36	1.58	
8637199	MOBJACK, VA	37/22.4	76/20.8	07/15/52	10/15/52	1.26	7.86	2.36	
8637289	NEW POINT, VA	37/20.8	76/16.4	04/16/53 03/09/82	06/22/53 11/24/82	1.44	8.12	1.70	
8637444	BROWNS BAY, VA	37/18.0	76/24.0	04/28/47	05/22/47	1.30	7.75	2.37	
8637472	CHEATHAM ANNEX, VA	37/17.5	76/35.2	05/09/72	11/14/73	2.23	8.40	2.45	0.05
8637589	NEW PT COMFORT SHOAL, VA	37/15.4	76/13.3	05/29/81	09/10/81	1.32	7.72	2.09	
8637624	GLOUCESTER PT, VA	37/14.8	76/30.0	05/16/50	NO	1.82	8.04	2.41	0.05
8637663	TUE MARSHES LH, VA	37/14.1	76/23.1	01/22/71	05/01/71	1.55	7.81	2.13	0.09
8637686	YORKTOWN,VA	37/13.8	76/26.2	01/01/72 06/07/82	12/03/73 07/27/82	1.65	8.07	2.31	0.09
8638051	MESSICK PT, VA	37/06.5	76/19.1	06/25/47 06/05/82	08/14/47 07/12/82	1.40	7.87	2.34	
8638288	OLD PT COMFORT, VA	37/00.2	76/18.9	08/09/71	07/17/74	1.44	7.59	2.52	0.03
8638401	HUNTINGTON PK, VA	37/00.8	76/27.5	06/17/71	11/01/72	2.18	8.48	2.65	0.04
8638409	HOLLIDAYS PT, VA	36/50.3	76/33.0	08/13/71	11/02/72	2.36	8.66	2.97	0.00
8638421	BURWELL BAY, VA	37/03.4	76/40.1	07/01/71	09/07/72	2.84	9.48	2.45	-0.06
8638433	SCOTLAND, VA	37/11.1	76/47.0	01/07/72	09/12/72	4.37	11.16	1.90	-0.11
8638442	FERRY PT, VA	37/15.8	76/52.6	07/26/70	04/26/76	5.44	12.18	1.90	-0.17

* BASED ON 1960-78 EPOCH
** BASED ON 1941-59 EPOCH

SUMMARY OF TIDE STATIONS

Station Number	Station Name	Latitude (N)	Longitude (W)	Installed	Removed	*Greenwich Int. HWI(Hr)	LWI(Hr)	*Mean Range(Ft)	**NGVD-MSL(Ft)
8638449	CLAREMONT, VA	37/13.9	76/56.9	07/24/70	11/19/74	5.48	12.33	1.84	-0.19
8638464	WILCOX WHARF, VA	37/18.9	77/05.9	07/01/71	09/12/72	6.93	1.15	2.15	-0.23
8638481	HOPEWELL, VA	37/18.8	77/16.3	06/09/71	10/01/72	7.95	2.22	2.46	-0.34
8638489	PUDDLEDOCK SAND & GRAVEL, VA	37/16.0	77/22.3	02/08/78	10/06/78	8.94	3.47	2.32	
8638491	CHESTER, VA	37/23.0	77/22.7	06/03/71	09/13/72	8.71	3.55	2.91	-0.51
8638495	RICHMOND, VA	37/31.5	77/25.2	02/21/71	06/19/72	9.09	4.10	3.15	
8638610	HAMPTON ROADS, VA	36/56.8	76/19.9	07/01/27	NO	1.63	7.91	2.47	0.03
8638660	PORTSMOUTH, VA	36/49.3	76/17.6	04/09/35	NO	1.75	8.07	2.80	0.05
8638863	CHESAPEAKE BAY BRIDGE TUNNEL	36/58.0	76/06.8	01/26/76	NO	0.68	6.84	2.61	
8638905	LYNNHAVEN FISHING PIER, VA	36/55.0	76/04.7	01/10/75	01/25/79	0.49	6.70	2.77	
8639168	VIRGINIA BEACH, VA	36/50.6	75/58.3	(01/01/68)	(12/31/68)	0.06	6.32	3.34	
2600000	CHESAPEAKE LIGHT	36/54.3	75/42.8	06/24/76	11/12/80	0.04	6.30	3.55	

* BASED ON 1960-78 EPOCH
** BASED ON 1941-59 EPOCH

APPENDIX B

SUMMARY OF HARMONIC CONSTANTS FOR TIDES

SUMMARY OF HARMONIC CONSTANTS FOR TIDES

Station No.	8571073		8571090		8571181		
Name	DM NO.2, SMITH IS., MD		CRISFIELD, MD		COLBOURN CK, MD		
Lat. (N)	37/58.3		37/58.6		38/02.9		
Long. (W)	75/59.1		75/51.8		75/48.2		
Series Beg.	04/29/77		07/09/77		10/20/81		
Length of Analysis (Days)	81		149		42		
Corrected Using Sta. No.	8638863		8638863		8635750		
Constituents	Amp (Ft)	Phase* (Deg)	Amp (Ft)	Phase* (Deg)	Amp (Ft)	Phase* (Deg)	Constituents
M(2)	.853	011.7	.890	006.9	.932	019.6	M(2)
S(2)	.149	033.0	.144	024.0	.176	037.6	S(2)
N(2)	.157	357.1	.190	353.3	.175	000.3	N(2)
K(1)	.162	189.8	.137	196.5	.134	183.7	K(1)
M(4)	.028	283.4	.028	277.2	.043	305.7	M(4)
O(1)	.110	204.5	.105	204.1	.149	236.3	O(1)
M(6)	.008	117.5	.011	123.1	.013	150.3	M(6)
MK(3)	.035	011.1	.015	132.8	.020	176.2	MK(3)
S(4)			.010	236.7			S(4)
MN(4)	.007	283.2	.010	223.7	.014	297.6	MN(4)
NU(2)			.045	346.3			NU(2)
S(6)			.003	100.9			S(6)
MU(2)	.013	008.1	.030	034.5	.006	321.5	MU(2)
2N(2)			.024	022.6			2N(2)
OO(1)			.008	295.2			OO(1)
LAM(2)			.016	082.4			LAM(2)
S(1)							S(1)
M(1)			.007	195.7			M(1)
J(1)							J(1)
Mm			.064	208.1			Mm
MSf			.049	296.5			MSf
Mf			.101	222.0			Mf
RHO(1)			.010	147.9			RHO(1)
Q(1)			.018	208.6			Q(1)
T(2)							T(2)
R(2)							R(2)
2Q(1)			.009	239.8			2Q(1)
P(1)			.076	191.4			P(1)
2SM(2)			.008	347.2			2SM(2)
M(3)	.004	028.7	.010	356.7	.003	091.6	M(3)
L(2)	.036	005.7	.042	024.4	.051	030.9	L(2)
2MK(3)	.007	000.1	.004	054.9	.020	007.3	2MK(3)
K(2)			.060	016.7			K(2)
M(8)	.002	034.4	.001	141.5	.001	095.3	M(8)
MS(4)	.007	000.3	.007	339.3	.007	295.3	MS(4)

(K1+O1)/(M2+S2) = .271   (K1+O1)/(M2+S2) = .234   (K1+O1)/(M2+S2) = .255

* Kappa prime at Longitude 75° W.

SUMMARY OF HARMONIC CONSTANTS FOR TIDES

Station No.	8571214	8571266	8571289
Name	HOLLAND BAR LT, MD	RUMBLEY, MD	CH LT 6, LITTLE DEAL IS, MD
Lat. (N)	38/04.1	38/05.5	38/07.5
Long. (W)	76/05.8	75/51.7	75/56.8
Series Beg.	08/31/81	10/22/81	09/17/77
Length of Analysis (Days)	92	40	76
Corrected Using Sta. No.	8635750	8635750	8638863

Constituents	Amp (Ft)	Phase* (Deg)	Amp (Ft)	Phase* (Deg)	Amp (Ft)	Phase* (Deg)	Constituents
M(2)	.665	013.6	.921	018.7	.763	047.6	M(2)
S(2)	.104	033.1	.175	038.3	.117	073.9	S(2)
N(2)	.129	354.3	.183	357.5	.143	029.0	N(2)
K(1)	.119	188.6	.131	185.3	.125	199.9	K(1)
M(4)	.015	264.2	.039	308.1	.102	309.2	M(4)
O(1)	.080	220.6	.148	242.1	.091	219.9	O(1)
M(6)	.009	124.2	.011	157.5	.025	255.5	M(6)
MK(3)	.003	048.4	.020	192.6	.016	175.5	MK(3)
S(4)							S(4)
MN(4)	.006	249.3	.014	303.1	.064	306.0	MN(4)
NU(2)							NU(2)
S(6)							S(6)
MU(2)	.008	320.0	.008	321.7	.067	247.1	MU(2)
2N(2)							2N(2)
OO(1)							OO(1)
LAM(2)							LAM(2)
S(1)							S(1)
M(1)							M(1)
J(1)							J(1)
Mm							Mm
MSf							MSf
Mf							Mf
RHO(1)							RHO(1)
Q(1)							Q(1)
T(2)							T(2)
R(2)							R(2)
2Q(1)							2Q(1)
P(1)							P(1)
2SM(2)							2SM(2)
M(3)	.006	019.7	.002	074.6	.012	286.4	M(3)
L(2)	.040	024.5	.065	045.6	.026	356.9	L(2)
2MK(3)	.012	021.2	.013	347.8	.011	170.6	2MK(3)
K(2)							K(2)
M(8)	.001	004.0	.001	103.1	.004	098.1	M(8)
MS(4)	.004	334.6	.006	299.9	.020	341.2	MS(4)

(K1+O1)/(M2+S2) = .259 (K1+O1)/(M2+S2) = .255 (K1+O1)/(M2+S2) = .253

* Kappa prime at Longitude 75° W.

SUMMARY OF HARMONIC CONSTANTS FOR TIDES

Station No.	8571351	8571402	8571477
Name	CHANCE, MD	HOOPER STRAIT LH, MD	NANTICOKE, MD
Lat. (N)	38/10.3	38/13.6	38/16.2
Long. (W)	75/56.7	76/04.6	75/54.8
Series Beg.	10/11/73	10/23/81	10/22/81
Length of Analysis (Days)	82	39	42
Corrected Using Sta. No.	8572770	8635750	8635750

Constituents	Amp (Ft)	Phase* (Deg)	Amp (Ft)	Phase* (Deg)	Amp (Ft)	Phase* (Deg)	Constituents
M(2)	.816	039.4	.711	030.5	1.009	046.5	M(2)
S(2)	.113	060.8	.118	051.2	.195	068.7	S(2)
N(2)	.192	022.1	.143	006.5	.201	025.6	N(2)
K(1)	.101	196.7	.103	204.7	.135	201.4	K(1)
M(4)	.040	266.2	.030	333.0	.051	004.3	M(4)
O(1)	.074	208.3	.107	257.2	.134	261.1	O(1)
M(6)	.008	213.5	.014	185.7	.014	312.5	M(6)
MK(3)	.019	055.8			.040	195.7	MK(3)
S(4)							S(4)
MN(4)	.013	270.6	.010	307.0	.017	351.2	MN(4)
NU(2)							NU(2)
S(6)							S(6)
MU(2)	.041	073.4	.009	340.3	.005	329.6	MU(2)
2N(2)							2N(2)
OO(1)							OO(1)
LAM(2)							LAM(2)
S(1)							S(1)
M(1)							M(1)
J(1)							J(1)
Mm							Mm
MSf							MSf
Mf							Mf
RHO(1)							RHO(1)
Q(1)							Q(1)
T(2)							T(2)
R(2)							R(2)
2Q(1)							2Q(1)
P(1)							P(1)
2SM(2)							2SM(2)
M(3)	.003	056.0	.003	059.7	.007	071.5	M(3)
L(2)	.034	138.0	.047	052.8	.085	074.6	L(2)
2MK(3)	.024	094.3	.009	037.4	.020	016.8	2MK(3)
K(2)							K(2)
M(8)	.001	244.1	.001	093.1			M(8)
MS(4)	.010	337.1	.006	352.1	.008	346.8	MS(4)

(K1+O1)/(M2+S2) = .188 (K1+O1)/(M2+S2) = .253 (K1+O1)/(M2+S2) = .223

* Kappa prime at Longitude 75° W.

SUMMARY OF HARMONIC CONSTANTS FOR TIDES

Station No.	8571519	8571559	8571752
Name	MID HOOPERS IS, MD	MCCREADY'S CK, MD	TAYLORS IS, MD
Lat. (N)	38/17.8	38/18.0	38/28.0
Long. (W)	76/12.3	76/00.4	76/17.7
Series Beg.	12/18/72	10/20/81	08/01/72
Length of Analysis (Days)	147	43	365
Corrected Using Sta. No.	8572770	8635750	

Constituents	Amp (Ft)	Phase* (Deg)	Amp (Ft)	Phase* (Deg)	Amp (Ft)	Phase* (Deg)	Constituents
M(2)	.753	044.7	1.014	048.0	.586	096.2	M(2)
S(2)	.118	069.7	.184	074.1	.089	124.8	S(2)
N(2)	.175	024.7	.197	029.1	.117	075.1	N(2)
K(1)	.121	209.0	.138	201.5	.133	263.9	K(1)
M(4)	.052	348.6	.056	015.8	.020	060.1	M(4)
O(1)	.087	237.6	.129	260.4	.108	276.3	O(1)
M(6)	.013	256.2	.006	302.4	.010	340.9	M(6)
MK(3)	.011	080.6	.019	171.7	.011	167.3	MK(3)
S(4)	.007	237.4			.002	338.0	S(4)
MN(4)	.019	319.5	.018	020.9	.009	030.7	MN(4)
NU(2)	.036	046.1			.028	046.4	NU(2)
S(6)	.001	313.2			.001	349.9	S(6)
MU(2)	.028	077.1	.005	340.9	.006	214.7	MU(2)
2N(2)	.034	011.3			.016	024.6	2N(2)
OO(1)	.008	349.8			.007	298.4	OO(1)
LAM(2)	.036	065.7			.006	102.1	LAM(2)
S(1)					.038	216.9	S(1)
M(1)	.003	127.9			.007	131.4	M(1)
J(1)	.006	237.7			.005	262.7	J(1)
Mm	.164	224.8			.101	253.5	Mm
MSf	.200	175.3			.067	185.2	MSf
Mf	.128	300.9			.075	301.7	Mf
RHO(1)	.019	025.7			.010	018.2	RHO(1)
Q(1)	.015	274.2			.010	265.2	Q(1)
T(2)					.010	117.8	T(2)
R(2)					.008	285.4	R(2)
2Q(1)	.003	302.2			.008	220.6	2Q(1)
P(1)	.030	241.8			.044	266.8	P(1)
2SM(2)	.001	232.0			.006	338.4	2SM(2)
M(3)	.014	043.0	.006	070.7	.004	063.8	M(3)
L(2)	.044	061.2	.068	062.9	.038	116.8	L(2)
2MK(3)	.021	076.1			.010	177.8	2MK(3)
K(2)	.052	048.4			.020	118.7	K(2)
M(8)	.003	193.5	.001	262.5	.001	235.1	M(8)
MS(4)	.019	039.2	.014	002.7	.007	106.8	MS(4)

(K1+O1)/(M2+S2) = .239 (K1+O1)/(M2+S2) = .223 (K1+O1)/(M2+S2) = .357

* Kappa prime at Longitude 75° W.

SUMMARY OF HARMONIC CONSTANTS FOR TIDES

Station No.	8571773	8571890	8571901
Name	VIENNA, MD	CAMBRIDGE, MD	AVALON, MD
Lat. (N)	38/29.0	38/34.5	38/42.6
Long. (W)	75/49.1	76/04.3	76/20.1
Series Beg.	7/26/72	01/01/80	09/29/83
Length of Analysis (Days)	347	366	61
Corrected Using Sta. No.			8572770

Constituents	Amp (Ft)	Phase* (Deg)	Amp (Ft)	Phase* (Deg)	Amp (Ft)	Phase* (Deg)	Constituents
M(2)	.978	115.2	.758	114.7	.663	102.8	M(2)
S(2)	.154	148.5	.106	139.0	.099	126.2	S(2)
N(2)	.178	095.2	.144	094.0	.136	081.8	N(2)
K(1)	.153	240.1	.169	269.4	.141	263.7	K(1)
M(4)	.081	077.8	.030	153.5	.018	097.2	M(4)
O(1)	.099	263.1	.148	270.1	.124	277.3	O(1)
M(6)	.043	026.0	.007	107.5	.005	001.8	M(6)
MK(3)	.039	176.0	.015	227.2	.010	215.1	MK(3)
S(4)	.004	096.5	.004	080.2			S(4)
MN(4)	.037	068.1	.014	116.6	.007	084.9	MN(4)
NU(2)	.037	088.3	.029	065.5			NU(2)
S(6)	.001	326.6	.001	040.5			S(6)
MU(2)	.031	241.2	.013	228.7	.003	146.0	MU(2)
2N(2)	.029	073.8	.003	101.5			2N(2)
OO(1)			.024	281.5			OO(1)
LAM(2)	.039	118.1	.016	124.0			LAM(2)
S(1)			.057	219.6			S(1)
M(1)	.005	043.2	.003	246.6			M(1)
J(1)	.005	225.3	.016	163.1			J(1)
Mm	.054	264.8	.076	268.6			Mm
MSF	.034	212.1	.049	235.8			MSF
Mf	.074	285.6	.045	261.6			Mf
RHO(1)	.010	006.5	.014	333.7			RHO(1)
Q(1)	.017	269.7	.022	269.7			Q(1)
T(2)			.011	122.5			T(2)
R(2)			.007	108.4			R(2)
2Q(1)	.008	166.4	.002	131.6			2Q(1)
P(1)	.045	251.1	.061	271.6			P(1)
2SM(2)	.010	345.1	.012	092.5			2SM(2)
M(3)	.005	156.7	.004	306.5			M(3)
L(2)	.066	119.0	.066	146.6	.032	142.2	L(2)
2MK(3)	.038	190.2	.020	216.7	.010	225.1	2MK(3)
K(2)	.044	155.1	.034	145.8			K(2)
M(8)	.004	351.7	.002	098.9			M(8)
MS(4)	.026	120.4	.008	193.2	.009	141.2	MS(4)

(K1+O1)/(M2+S2) = .223 (K1+O1)/(M2+S2) = .367 (K1+O1)/(M2+S2) = .348

* Kappa prime at Longitude 75° W.

SUMMARY OF HARMONIC CONSTANTS FOR TIDES

Station No.	8571944		8571979		8572342		
Name	DOVER BRIDGE, MD		FERRY COVE, MD		ST MICHAELS, MD		
Lat. (N)	38/45.4		38/46.0		38/47.2		
Long. (W)	75/59.8		76/19.5		76/13.3		
Series Beg.	08/01/72		07/15/83		07/28/83		
Length of Analysis (Days)	365		90		43		
Corrected Using Sta. No.			8572770		857770		
Constituents	Amp (Ft)	Phase* (Deg)	Amp (Ft)	Phase* (Deg)	Amp (Ft)	Phase* (Deg)	
M(2)	.792	165.9	.524	116.0	.654	126.4	M(2)
S(2)	.117	193.8	.079	137.1	.102	150.1	S(2)
N(2)	.148	138.6	.114	093.8	.143	106.6	N(2)
K(1)	.166	293.7	.174	271.2	.186	275.3	K(1)
M(4)	.025	181.6	.010	121.2	.040	177.5	M(4)
O(1)	.136	300.4	.139	282.9	.154	225.2	O(1)
M(6)	.024	185.9	.006	009.9	.007	155.1	M(6)
MK(3)	.023	270.9	.011	227.9	.017	254.7	MK(3)
S(4)	.003	142.6					S(4)
MN(4)	.013	154.6	.005	107.4	.017	154.8	MN(4)
NU(2)	.035	132.3					NU(2)
S(6)	.001	098.4					S(6)
MU(2)	.023	302.5	.003	170.4	.004	169.0	MU(2)
2N(2)	.029	114.7					2N(2)
OO(1)	.003	041.7					OO(1)
LAM(2)	.019	166.8					LAM(2)
S(1)	.042	236.7					S(1)
M(1)	.009	131.9					M(1)
J(1)	.009	268.6					J(1)
Mm	.067	255.2					Mm
MSf	.043	192.3					MSf
Mf	.087	298.4					Mf
RHO(1)	.013	005.6					RHO(1)
Q(1)	.014	298.8					Q(1)
T(2)	.012	135.0					T(2)
R(2)	.009	015.6					R(2)
2Q(1)	.011	226.5					2Q(1)
P(1)	.061	295.5					P(1)
2SM(2)	.004	034.3					2SM(2)
M(3)	.005	144.3	.003	177.2	.008	230.5	M(3)
L(2)	.055	191.6	.033	146.7	.038	153.0	L(2)
2MK(3)	.022	273.4	.008	203.7	.015	241.0	2MK(3)
K(2)	.032	199.2					K(2)
M(8)	.002	184.1					M(8)
MS(4)	.008	240.2	.006	167.1	.020	219.0	MS(4)
	(K1+O1)/(M2+S2) = .332		(K1+O1)/(M2+S2) = .519		(K1+O1)/(M2+S2) = .450		

* Kappa prime at Longitude 75° W.

SUMMARY OF HARMONIC CONSTANTS FOR TIDES

Station No.	8572770	8572955	8573137
Name	MATAPEAKE, MD	LOVE POINT, MD	CLIFFS POINT WHARF, MD
Lat. (N)	38/57.5	39/02.2	39/06.6
Long. (W)	76/21.3	76/18.2	76/08.3
Series Beg.	01/01/83	01/01/72	01/01/72
Length of Analysis (Days)	365	365	366
Corrected Using Sta. No.			

Constituents	Amp (Ft)	Phase* (Deg)	Amp (Ft)	Phase* (Deg)	Amp (Ft)	Phase* (Deg)	Constituents
M(2)	.463	146.8	.527	177.9	.704	192.0	M(2)
S(2)	.076	169.1	.091	204.1	.120	220.3	S(2)
N(2)	.102	126.4	.115	154.2	.153	168.9	N(2)
K(1)	.194	276.2	.221	280.5	.238	286.4	K(1)
M(4)	.010	100.8	.004	320.1	.003	214.8	M(4)
O(1)	.154	288.8	.183	298.1	.196	303.2	O(1)
M(6)	.005	047.5	.001	086.5	.007	174.8	M(6)
MK(3)	.008	259.9	.014	306.5	.024	331.3	MK(3)
S(4)	.001	100.4	.001	169.0	.003	236.8	S(4)
MN(4)	.004	083.2	.004	276.0	.002	299.1	MN(4)
NU(2)	.028	126.2	.020	151.6	.026	161.1	NU(2)
S(6)	.001	162.0					S(6)
MU(2)	.003	182.8	.010	139.3	.007	160.6	MU(2)
2N(2)	.018	121.8	.011	119.9	.016	131.4	2N(2)
OO(1)	.013	269.6	.011	304.9	.009	308.5	OO(1)
LAM(2)	.005	184.1	.013	170.6	.015	182.5	LAM(2)
S(1)	.071	212.3	.048	219.7	.049	224.4	S(1)
M(1)	.004	068.8	.005	341.8	.003	351.7	M(1)
J(1)	.004	092.9	.008	223.2	.008	214.4	J(1)
Mm	.046	188.7	.068	114.2	.072	120.7	Mm
MSf	.068	077.9	.113	049.1	.112	051.3	MSf
Mf	.062	101.3	.071	345.7	.063	349.8	Mf
RHO(1)	.004	242.6	.019	122.3	.017	136.1	RHO(1)
Q(1)	.030	281.3	.031	233.2	.031	242.5	Q(1)
T(2)	.005	149.4	.007	167.1	.007	173.5	T(2)
R(2)	.004	285.6	.008	003.5	.011	008.7	R(2)
2Q(1)	.021	325.5	.014	266.0	.008	264.1	2Q(1)
P(1)	.063	265.8	.070	278.6	.077	284.0	P(1)
2SM(2)	.002	251.8	.002	084.6	.002	071.5	2SM(2)
M(3)	.004	197.4	.002	293.1	.005	323.4	M(3)
L(2)	.025	175.7	.026	201.8	.036	208.1	L(2)
2MK(3)	.011	252.7	.015	298.4	.027	325.1	2MK(3)
K(2)	.027	172.6	.030	198.5	.039	210.5	K(2)
M(8)			.002	169.9			M(8)
MS(4)	.004	141.4	.002	031.0	.002	152.1	MS(4)
	(K1+O1)/(M2+S2) = .646		(K1+O1)/(M2+S2) = .654		(K1+O1)/(M2+S2) = .527		

* Kappa prime at Longitude 75° W.

SUMMARY OF HARMONIC CONSTANTS FOR TIDES

Station No.	8573343	8573364	8573704
Name	CHESTERTOWN, MD	TOLCHESTER BEACH, MD	BETTERTON, MD
Lat. (N)	39/12.4	39/12.8	39/22.3
Long. (W)	76/03.8	76/14.7	76/03.8
Series Beg.	07/01/71	10/01/71	07/01/71
Length of Analysis (Days)	365	365	365
Corrected Using Sta. No.			

Constituents	Amp (Ft)	Phase* (Deg)	Amp (Ft)	Phase* (Deg)	Amp (Ft)	Phase* (Deg)	Constituents
M(2)	.892	209.0	.542	202.7	.730	260.7	M(2)
S(2)	.141	239.7	.084	227.4	.101	294.8	S(2)
N(2)	.177	185.6	.114	176.0	.143	231.3	N(2)
K(1)	.243	295.6	.221	287.9	.248	302.6	K(1)
M(4)	.019	199.3	.012	292.2	.007	345.9	M(4)
O(1)	.227	313.5	.210	303.9	.224	318.8	O(1)
M(6)	.004	322.9	.003	262.0	.005	070.7	M(6)
MK(3)	.032	347.4	.012	319.3	.017	092.8	MK(3)
S(4)	.003	358.6	.002	164.5	.002	299.8	S(4)
MN(4)	.004	167.6	.006	264.0	.004	328.8	MN(4)
NU(2)	.045	188.2	.020	181.0	.033	248.0	NU(2)
S(6)	.001	261.4	.002	210.7	.001	340.6	S(6)
MU(2)	.010	248.4	.004	145.5	.011	050.3	MU(2)
2N(2)	.012	203.4	.012	160.6	.005	269.6	2N(2)
OO(1)	.013	319.2	.007	295.0	.009	318.3	OO(1)
LAM(2)	.026	212.7	.010	199.4	.023	280.6	LAM(2)
S(1)	.061	245.3	.041	217.5	.022	237.3	S(1)
M(1)	.009	346.0	.005	317.4	.008	340.5	M(1)
J(1)	.017	300.4	.010	289.9	.020	306.6	J(1)
Mm	.071	142.7	.063	164.4	.088	148.8	Mm
MSf	.098	032.1	.147	013.4	.113	026.4	MSf
RHO(1)	.012	150.1	.014	117.5	.007	169.7	RHO(1)
Q(1)	.043	253.5	.037	240.3	.042	258.1	Q(1)
T(2)	.011	185.5	.015	178.9	.022	244.0	T(2)
R(2)	.011	305.0	.006	029.4	.004	206.2	R(2)
2Q(1)	.013	321.5	.004	321.5	.007	317.3	2Q(1)
P(1)	.079	284.3	.072	282.8	.076	287.1	P(1)
2SM(2)	.005	009.2	.004	319.6	.008	049.8	2SM(2)
M(3)	.009	005.5	.003	300.0	.002	119.5	M(3)
L(2)	.055	209.0	.036	231.9	.064	279.4	L(2)
2MK(3)	.036	349.7	.012	330.0	.018	096.9	2MK(3)
K(2)	.051	230.3	.031	216.0	.042	280.2	K(2)
M(8)	.003	019.8	.001	189.6	.001	117.5	M(8)
MS(4)	.008	197.5	.005	337.8	.003	035.6	MS(4)

(K1+O1)/(M2+S2) = .455 (K1+O1)/(M2+S2) = .688 (K1+O1)/(M2+S2) = .568

* Kappa prime at Longitude 75° W.

SUMMARY OF HARMONIC CONSTANTS FOR TIDES

Station No.	8573903	8573927	8574008
Name	TOWN POINT WHARF, MD	CHESAPEAKE CITY, MD	PORT DEPOSIT, MD
Lat. (N)	39/30.2	39/31.6	39/36.2
Long. (W)	75/55.0	75/48.6	76/06.8
Series Beg.	01/01/79	01/01/73	05/05/83
Length of Analysis (Days)	365	365	49
Corrected Using Sta. No.			8574070

Constituents	Amp (Ft)	Phase* (Deg)	Amp (Ft)	Phase* (Deg)	Amp (Ft)	Phase* (Deg)	Constituents
M(2)	.936	290.7	1.373	306.3	.841	288.0	M(2)
S(2)	.129	329.0	.197	341.0	.164	322.9	S(2)
N(2)	.174	265.6	.241	284.7	.172	258.7	N(2)
K(1)	.221	311.2	.116	288.9	.291	318.9	K(1)
M(4)	.037	212.6	.068	222.1	.056	114.6	M(4)
O(1)	.141	315.3	.057	293.6	.177	321.9	O(1)
M(6)	.011	135.4	.024	028.4	.008	199.5	M(6)
MK(3)	.020	091.4	.024	079.5	.045	136.3	MK(3)
S(4)	.005	311.0	.001	002.0			S(4)
MN(4)	.011	188.4	.029	209.5	.020	090.9	MN(4)
NU(2)	.049	261.0	.084	284.2			NU(2)
S(6)			.001	167.6			S(6)
MU(2)	.023	074.5	.047	068.1	.028	089.0	MU(2)
2N(2)	.022	287.8	.045	260.6			2N(2)
OO(1)	.004	062.3	.006	003.6			OO(1)
LAM(2)	.019	326.1	.047	323.6			LAM(2)
S(1)	.031	289.8	.048	130.1			S(1)
M(1)	.020	009.7	.008	321.6			M(1)
J(1)	.022	189.7	.021	275.6			J(1)
Mm	.133	026.6	.080	302.2			Mm
MSf	.058	332.5	.055	032.1			MSf
Mf	.080	275.7	.026	181.2			Mf
RHO(1)	.019	197.3	.017	343.3			RHO(1)
Q(1)	.035	320.8	.013	348.9			Q(1)
T(2)	.016	324.9	.028	320.2			T(2)
R(2)	.011	160.2	.012	353.8			R(2)
2Q(1)	.016	208.3	.004	029.6			2Q(1)
P(1)	.058	324.0	.043	286.6			P(1)
2SM(2)	.011	173.8	.005	165.3			2SM(2)
M(3)	.008	164.9	.008	036.2	.017	040.4	M(3)
L(2)	.068	332.2	.106	329.5			L(2)
2MK(3)	.030	087.6	.026	054.4	.039	130.4	2MK(3)
K(2)	.037	352.0	.061	338.8			K(2)
M(8)	.002	350.9	.008	250.0	.002	137.4	M(8)
MS(4)	.012	256.5	.028	249.6	.019	131.4	MS(4)

(K1+O1)/(M2+S2) = .340   (K1+O1)/(M2+S2) = .110   (K1+O1)/(M2+S2) = .466

* Kappa prime at Longitude 75° W.

SUMMARY OF HARMONIC CONSTANTS FOR TIDES

Station No.	8574070	8574680	8574821
Name	HAVRE DE GRACE	BALTIMORE, MD	HAWKINS PT, MD
Lat. (N)	39/32.2	39/16.0	39/12.5
Long. (W)	76/05.4	76/34.7	76/32.0
Series Beg.	01/01/83	02/01/75	09/03/75
Length of Analysis (Days)	365	365	137
Corrected Using Sta. No.			8574680

Constituents	Amp (Ft)	Phase* (Deg)	Amp (Ft)	Phase* (Deg)	Amp (Ft)	Phase* (Deg)	Constituents
M(2)	.850	286.0	.509	193.9	.501	194.7	M(2)
S(2)	.147	322.2	.079	213.4	.079	217.9	S(2)
N(2)	.166	260.1	.114	173.4	.110	178.2	N(2)
K(1)	.275	311.7	.219	296.6	.223	297.2	K(1)
M(4)	.051	114.7	.023	318.9	.021	319.9	M(4)
O(1)	.188	319.5	.156	298.5	.158	297.8	O(1)
M(6)	.008	191.0	.009	294.6	.009	300.6	M(6)
MK(3)	.040	135.4	.017	327.6	.017	323.3	MK(3)
S(4)	.002	177.4	.003	130.0	.002	125.9	S(4)
MN(4)	.019	087.3	.011	295.5	.009	292.3	MN(4)
NU(2)	.069	270.1	.028	181.2	.031	172.3	NU(2)
S(6)	.002	335.8	.001	292.4	.001	239.2	S(6)
MU(2)	.025	089.4	.005	174.6	.009	138.8	MU(2)
2N(2)	.035	283.5	.019	151.3	.015	148.0	2N(2)
OO(1)	.016	311.4	.020	291.3	.026	281.2	OO(1)
LAM(2)	.024	313.7	.011	253.9	.012	240.4	LAM(2)
S(1)	.017	169.1	.049	214.7			S(1)
M(1)	.008	096.7	.012	007.3	.013	016.6	M(1)
J(1)	.005	107.6	.015	222.9	.012	245.0	J(1)
Mm	.059	200.2	.114	273.5	.105	280.3	Mm
MSF	.045	075.2	.020	099.8	.021	095.4	MSf
Mf	.091	097.6	.039	157.9	.033	154.4	Mf
RHO(1)	.004	076.3	.003	084.4	.002	046.0	RHO(1)
Q(1)	.031	289.7	.020	253.3	.025	238.2	Q(1)
T(2)	.037	305.5	.002	265.4			T(2)
R(2)	.018	159.2	.005	357.4			R(2)
2Q(1)	.019	321.2	.034	343.4	.037	345.8	2Q(1)
P(1)	.061	309.8	.073	288.7	.072	281.6	P(1)
2SM(2)	.013	011.4	.002	296.8	.001	237.1	2SM(2)
M(3)	.012	030.5	.006	222.7	.015	219.0	M(3)
L(2)	.065	321.3	.034	212.1	.031	205.0	L(2)
2MK(3)	.038	124.0	.012	313.0	.010	307.7	2MK(3)
K(2)	.036	304.9	.032	218.7	.037	213.5	K(2)
M(8)	.002	326.7	.003	013.3	.004	031.6	M(8)
MS(4)	.019	135.6	.009	354.4	.008	356.1	MS(4)
	(K1+O1)/(M2+S2) = .464		(K1+O1)/(M2+S2) = .638		(K1+O1)/(M2+S2) = .657		

* Kappa prime at Longitude 75° W.

SUMMARY OF HARMONIC CONSTANTS FOR TIDES

Station No.	8574857	8575512	8575550
Name	NORTH POINT, MD	ANNAPOLIS, MD	GINGERVILLE CK, MD
Lat. (N)	39/11.8	38/59.0	38/57.5
Long. (W)	76/26.7	76/28.8	76/33.3
Series Beg.	07/01/71	01/01/81	01/01/74
Length of Analysis (Days)	365	365	365
Corrected Using Sta. No.			

Constituents	Amp (Ft)	Phase* (Deg)	Amp (Ft)	Phase* (Deg)	Amp (Ft)	Phase* (Deg)	Constituents
M(2)	.450	191.7	.416	147.2	.457	131.6	M(2)
S(2)	.077	215.5	.070	175.0	.076	157.3	S(2)
N(2)	.096	167.2	.081	126.0	.099	109.1	N(2)
K(1)	.207	289.6	.179	283.3	.173	277.5	K(1)
M(4)	.018	326.0	.011	130.5	.018	123.6	M(4)
O(1)	.201	307.9	.155	294.1	.138	288.2	O(1)
M(6)	.002	244.4	.009	095.2	.012	035.1	M(6)
MK(3)	.015	315.4	.009	261.4	.008	241.2	MK(3)
S(4)	.001	122.8	.003	094.2	.004	095.1	S(4)
MN(4)	.008	272.5	.006	105.8	.009	096.2	MN(4)
NU(2)	.022	171.4	.020	135.8	.022	096.2	NU(2)
S(6)	.001	072.5	.001	307.4	.001	277.6	S(6)
MU(2)	.006	172.6	.001	302.2	.009	185.2	MU(2)
2N(2)	.010	159.8	.006	108.9	.016	099.7	2N(2)
OO(1)	.011	303.8	.008	239.2	.015	281.1	OO(1)
LAM(2)	.013	209.2	.006	189.2	.010	150.0	LAM(2)
S(1)	.052	227.4	.051	210.9	.040	188.4	S(1)
M(1)	.009	342.2	.007	015.3	.007	340.6	M(1)
J(1)	.015	299.3	.007	311.3	.009	268.3	J(1)
Mm	.090	154.1	.067	191.6	.135	065.8	Mm
MSf	.107	016.8	.163	094.9	.066	244.1	MSf
Mf	.085	039.5	.028	059.7	.048	290.8	Mf
RHO(1)	.010	154.1	.002	075.0	.013	331.1	RHO(1)
Q(1)	.038	252.9	.020	252.5	.025	237.2	Q(1)
T(2)	.005	160.6	.004	157.2	.010	126.8	T(2)
R(2)	.005	320.5	.003	333.9	.003	304.3	R(2)
2Q(1)	.007	292.4	.009	339.8	.006	188.9	2Q(1)
P(1)	.067	282.6	.045	279.0	.065	268.4	P(1)
2SM(2)	.003	352.2	.002	028.9	.002	255.2	2SM(2)
M(3)	.004	341.5	.001	241.9	.004	175.4	M(3)
L(2)	.027	216.4	.033	163.5	.031	164.8	L(2)
2MK(3)	.014	323.4	.009	266.5	.009	243.4	2MK(3)
K(2)	.029	206.8	.023	170.3	.020	149.2	K(2)
M(8)	.001	104.6	.001	285.5	.005	097.9	M(8)
MS(4)	.006	350.7	.004	171.9	.006	163.5	MS(4)
	(K1+O1)/(M2+S2) = .774		(K1+O1)/(M2+S2) = .688		(K1+O1)/(M2+S2) = .583		

* Kappa prime at Longitude 75° W.

SUMMARY OF HARMONIC CONSTANTS FOR TIDES

Station No.	8575787	8576363	8577123
Name	RHODE RIVER, MD	CHESAPEAKE BEACH, MD	BROOMES IS, MD
Lat. (N)	38/58.2	38/41.4	38/24.9
Long. (W)	76/32.4	76/31.9	76/32.7
Series Beg.	01/01/74	01/01/74	08/01/72
Length of Analysis (Days)	365	365	365
Corrected Using Sta. No.			

Constituents	Amp (Ft)	Phase* (Deg)	Amp (Ft)	Phase* (Deg)	Amp (Ft)	Phase* (Deg)	Constituents
M(2)	.434	129.8	.457	103.9	.645	064.3	M(2)
S(2)	.071	155.1	.070	130.5	.103	087.9	S(2)
N(2)	.093	106.9	.096	079.4	.135	041.5	N(2)
K(1)	.170	278.2	.146	271.4	.090	245.2	K(1)
M(4)	.015	121.8	.007	083.4	.022	028.3	M(4)
O(1)	.133	288.8	.118	282.3	.082	265.4	O(1)
M(6)	.008	035.6	.003	357.7	.010	284.4	M(6)
MK(3)	.007	234.1	.005	184.2	.012	125.8	MK(3)
S(4)	.002	084.0	.001	038.0	.004	326.3	S(4)
MN(4)	.006	094.0	.002	044.0	.011	013.0	MN(4)
NU(2)	.022	099.9	.025	074.7	.032	039.2	NU(2)
S(6)	.001	262.5			.001	205.5	S(6)
MU(2)	.008	190.3	.009	196.1	.003	261.8	MU(2)
2N(2)	.017	100.0	.018	075.3	.018	018.7	2N(2)
OO(1)	.013	287.1	.011	287.4	.004	225.0	OO(1)
LAM(2)	.011	135.0	.013	116.2	.005	075.2	LAM(2)
S(1)	.042	196.9	.039	201.3	.028	216.5	S(1)
M(1)	.008	319.5	.005	315.0	.006	255.3	M(1)
J(1)	.008	266.4	.008	250.5	.006	235.2	J(1)
Mm	.140	064.7	.089	325.3	.179	277.6	Mm
MSf	.065	239.6	.021	357.5	.074	222.4	MSf
Mf	.043	289.9	.019	155.6	.054	289.0	Mf
RHO(1)	.014	332.8	.015	329.7	.003	274.1	RHO(1)
Q(1)	.024	238.2	.024	236.6	.016	275.6	Q(1)
T(2)	.007	113.1	.012	099.7	.006	088.1	T(2)
R(2)	.004	324.6	.002	346.5	.001	087.7	R(2)
2Q(1)	.006	197.3	.004	198.7	.002	285.6	2Q(1)
P(1)	.066	269.5	.057	261.8	.030	252.2	P(1)
2SM(2)	.001	264.5			.005	301.3	2SM(2)
M(3)	.004	175.4	.003	169.7	.004	035.5	M(3)
L(2)	.026	159.7	.032	144.9	.036	096.7	L(2)
2MK(3)	.008	233.9	.005	203.9	.010	130.2	2MK(3)
K(2)	.018	149.1	.017	118.6	.028	087.5	K(2)
M(8)	.002	045.4			.001	220.6	M(8)
MS(4)	.005	164.9	.002	120.8	.007	083.5	MS(4)

(K1+O1)/(M2+S2) = .600 (K1+O1)/(M2+S2) = .501 (K1+O1)/(M2+S2) = .230

* Kappa prime at Longitude 75°.

SUMMARY OF HARMONIC CONSTANTS FOR TIDES

Station No.	8577188		8577330		8577385		
Name	COVE POINT, MD		SOLOMONS IS, MD		NAVY SEAPLANE BASIN BOATHOUSE, MD		
Lat. (N)	38/23.1		38/19.0		38/16.3		
Long. (W)	76/22.9		76/27.2		76/23.8		
Series Beg.	10/13/83		01/01/80		08/29/81		
Length of Analysis (Days)	49		366		55		
Corrected Using Sta. No.	8577330				8577330		
Constituents	Amp (Ft)	Phase* (Deg)	Amp (Ft)	Phase* (Deg)	Amp (Ft)	Phase* (Deg)	Constituents
M(2)	.478	063.4	.537	054.2	.491	043.3	M(2)
S(2)	.075	082.7	.077	070.5	.075	064.5	S(2)
N(2)	.105	035.9	.106	032.4	.101	019.6	N(2)
K(1)	.105	244.9	.090	243.7	.074	233.5	K(1)
M(4)	.016	328.9	.017	344.2	.014	312.8	M(4)
O(1)	.072	261.4	.094	252.5	.070	256.6	O(1)
M(6)	.008	233.7	.010	222.0	.011	195.3	M(6)
MK(3)	.012	104.7	.011	118.8	.007	127.6	MK(3)
S(4)			.003	283.2			S(4)
MN(4)	.009	307.2	.008	305.9	.010	296.3	MN(4)
NU(2)			.018	020.6			NU(2)
S(6)			.001	186.7			S(6)
MU(2)	.002	256.1	.002	219.5	.013	316.5	MU(2)
2N(2)			.004	329.2			2N(2)
OO(1)			.014	277.8			OO(1)
LAM(2)			.015	055.5			LAM(2)
S(1)			.035	215.7			S(1)
M(1)			.003	239.4			M(1)
J(1)			.002	140.8			J(1)
Mm			.081	253.9			Mm
MSf			.066	245.1			MSf
Mf			.059	271.0			Mf
RHO(1)			.008	280.0			RHO(1)
Q(1)			.010	223.5			Q(1)
T(2)			.007	073.9			T(2)
R(2)			.006	008.9			R(2)
2Q(1)			.009	185.6			2Q(1)
P(1)			.039	252.5			P(1)
2SM(2)			.003	076.4			2SM(2)
M(3)	.002	183.5	.004	148.8	.005	129.7	M(3)
L(2)			.039	103.6	.045	061.9	L(2)
2MK(3)	.002	038.7	.012	120.9	.008	084.1	2MK(3)
K(2)			.021	073.6			K(2)
M(8)			.001	191.8	.001	166.2	M(8)
MS(4)	.007	346.5	.004	048.9	.006	015.3	MS(4)
	(K1+O1)/(M2+S2) = .320		(K1+O1)/(M2+S2) = .299		(K1+O1)/(M2+S2) = .254		

* Kappa prime at Longitude 75° W.

SUMMARY OF HARMONIC CONSTANTS FOR TIDES

Station No.	8578002	8578240	0578465
Name	POINT LOOKOUT, MD	PINEY POINT, MD	COLTON POINT, MD
Lat. (N)	38/02.4	38/08.0	38/13.4
Long. (W)	76/19.4	76/32.0	76/44.9
Series Beg.	10/06/81	01/01/60	12/29/70
Length of Analysis (Days)	59	365	101
Corrected Using Sta. No.	8635750		8635750

Constituents	Amp (Ft)	Phase* (Deg)	Amp (Ft)	Phase* (Deg)	Amp (Ft)	Phase* (Deg)	Constituents
M(2)	.562	024.4	.678	040.6	.812	055.3	M(2)
S(2)	.087	043.3	.117	058.3	.137	078.6	S(2)
N(2)	.119	357.3	.138	022.1	.160	030.6	N(2)
K(1)	.075	198.3	.075	205.8	.081	201.2	K(1)
M(4)	.012	270.2	.010	263.3	.009	344.8	M(4)
O(1)	.059	229.4	.058	229.6	.070	241.6	O(1)
M(6)	.010	172.9	.012	238.8	.013	274.1	M(6)
MK(3)	.004	140.6	.002	094.6	.004	158.2	MK(3)
S(4)			.001	357.9			S(4)
MN(4)	.002	050.6	.005	209.1	.007	292.5	MN(4)
NU(2)			.032	020.4			NU(2)
S(6)							S(6)
MU(2)	.008	335.0	.009	057.1	.009	042.5	MU(2)
2N(2)			.019	000.7			2N(2)
OO(1)			.009	084.7			OO(1)
LAM(2)			.012	051.4			LAM(2)
S(1)			.019	212.4			S(1)
M(1)			.003	225.3			M(1)
J(1)			.008	229.3			J(1)
Mm			.034	175.4			Mm
MSf			.090	027.8			MSf
Mf			.096	285.9			Mf
RHO(1)			.006	144.9			RHO(1)
Q(1)			.018	212.6			Q(1)
T(2)			.007	058.3			T(2)
R(2)			.008	254.8			R(2)
2Q(1)			.011	120.0			2Q(1)
P(1)			.034	209.6			P(1)
2SM(2)			.003	258.5			2SM(2)
M(3)	.006	254.8	.001	343.3	.007	108.1	M(3)
L(2)	.044	048.3	.028	056.2	.056	094.3	L(2)
2MK(3)	.005	063.9	.005	159.5	.008	173.3	2MK(3)
K(2)			.024	049.9			K(2)
M(8)			.001	259.3			M(8)
MS(4)	.003	345.6	.005	333.4	.003	065.5	MS(4)
	(K1+O1)/(M2+S2) = .206		(K1+O1)/(M2+S2) = .167		(K1+O1)/(M2+S2) = .159		

* Kappa prime at Longitude 75° W.

SUMMARY OF HARMONIC CONSTANTS FOR TIDES

Station No.	8578769	8578853	8579135
Name	PORT TOBACCO, MD	RIVERSIDE, MD	BENEDICT, MD
Lat. (N)	38/27.2	38/25.0	38/30.8
Long. (W)	77/03.2	77/08.5	76/40/2
Series Beg.	11/05/71	01/01/71	08/01/72
Length of Analysis (Days)	249	365	365
Corrected Using Sta. No.			

Constituents	Amp (Ft)	Phase* (Deg)	Amp (Ft)	Phase* (Deg)	Amp (Ft)	Phase* (Deg)	Constituents
M(2)	.659	091.8	.563	110.4	.754	076.6	M(2)
S(2)	.127	120.4	.103	132.5	.118	103.3	S(2)
N(2)	.146	069.3	.121	085.3	.153	051.5	N(2)
K(1)	.102	219.4	.104	235.3	.092	251.1	K(1)
M(4)	.033	088.5	.030	100.2	.039	055.2	M(4)
O(1)	.086	256.8	.086	267.1	.082	269.1	O(1)
M(6)	.024	062.2	.029	083.6	.014	348.7	M(6)
MK(3)	.014	173.6	.008	190.6	.019	146.5	MK(3)
S(4)	.006	072.3	.002	062.6	.007	012.1	S(4)
MN(4)	.015	061.1	.014	066.6	.019	025.8	MN(4)
NU(2)	.026	062.9	.023	088.6	.040	040.7	NU(2)
S(6)			.002	277.0			S(6)
MU(2)	.020	055.2	.018	076.5	.005	259.6	MU(2)
2N(2)	.020	064.1	.016	060.2	.025	036.5	2N(2)
OO(1)	.008	229.3	.004	203.5	.003	282.7	OO(1)
LAM(2)	.015	092.0	.004	120.6	.013	101.6	LAM(2)
S(1)			.042	221.9	.030	211.2	S(1)
M(1)	.003	352.4	.006	251.3	.002	179.0	M(1)
J(1)	.014	226.5	.007	219.4	.005	212.8	J(1)
Mm	.186	141.5	.024	054.4	.092	258.9	Mm
MSf	.207	006.5	.007	237.9	.069	189.5	MSf
Mf	.152	027.2	.075	029.9	.087	297.1	Mf
RHO(1)	.011	225.9	.003	280.8	.002	095.4	RHO(1)
Q(1)	.018	217.7	.017	282.9	.014	266.5	Q(1)
T(2)			.006	132.7	.016	087.9	T(2)
R(2)			.001	132.3	.009	279.4	R(2)
2Q(1)	.011	221.4	.002	298.9	.011	225.0	2Q(1)
P(1)	.021	276.3	.034	235.7	.029	263.5	P(1)
2SM(2)	.003	181.5	.006	200.7	.005	325.5	2SM(2)
M(3)	.006	174.9	.003	214.8	.005	057.6	M(3)
L(2)	.019	118.8	.016	135.4	.045	112.1	L(2)
2MK(3)	.017	203.9	.012	208.2	.014	153.5	2MK(3)
K(2)	.040	116.8	.034	140.1	.034	089.9	K(2)
M(8)	.006	069.1	.006	056.5	.002	337.2	M(8)
MS(4)	.011	131.1	.007	125.8	.011	111.4	MS(4)

(K1+O1)/(M2+S2) = .239 (K1+O1)/(M2+S2) = .285 (K1+O1)/(M2+S2) = .200

* Kappa prime at Longitude 75° W.

SUMMARY OF HARMONIC CONSTANTS FOR TIDES

Station No.	8579381	8579542	8579629
Name	INDIAN HEAD, MD	LOWER MARLBORO, MD	MARSHALL HALL, MD
Lat. (N)	38/36.1	38/39.3	38/41.2
Long. (W)	77/11.1	76/41.0	77/06.1
Series Beg.	01/01/71	08/01/72	03/01/71
Length of Analysis (Days)	365	365	366
Corrected Using Sta. No.			

Constituents	Amp (Ft)	Phase* (Deg)	Amp (Ft)	Phase* (Deg)	Amp (Ft)	Phase* (Deg)	Constituents
M(2)	.796	199.6	.853	106.3	.934	218.1	M(2)
S(2)	.119	223.8	.128	134.0	.137	249.9	S(2)
N(2)	.151	171.5	.161	085.1	.183	197.4	N(2)
K(1)	.133	262.4	.096	262.7	.141	270.8	K(1)
M(4)	.031	236.3	.041	078.2	.028	014.9	M(4)
O(1)	.106	294.7	.080	282.2	.115	298.7	O(1)
M(6)	.034	297.6	.021	058.8	.028	328.3	M(6)
MK(3)	.010	316.5	.023	180.0	.020	009.2	MK(3)
S(4)	.003	243.4	.006	078.0	.001	318.0	S(4)
MN(4)	.014	210.0	.020	067.2	.013	333.5	MN(4)
NU(2)	.035	186.1	.033	069.5	.058	225.9	NU(2)
S(6)	.001	331.6			.001	024.9	S(6)
MU(2)	.008	331.2	.022	246.7	.014	282.7	MU(2)
2N(2)	.013	157.5	.032	067.8	.022	211.3	2N(2)
OO(1)	.010	327.7	.003	297.7	.006	285.2	OO(1)
LAM(2)	.018	232.1	.022	083.6	.026	317.7	LAM(2)
S(1)	.046	242.5	.033	215.4	.055	255.3	S(1)
M(1)	.007	025.0	.005	093.4	.010	023.4	M(1)
J(1)	.009	230.9	.005	266.6	.013	245.2	J(1)
Mm	.021	060.2	.127	279.6	.079	097.0	Mm
MSf	.011	295.7	.079	212.9	.058	017.1	MSf
Mf	.079	033.7	.099	284.2	.106	017.0	Mf
RHO(1)	.013	288.6	.002	192.4	.019	325.0	RHO(1)
Q(1)	.022	285.7	.016	290.5	.021	280.6	Q(1)
T(2)	.006	162.5	.011	111.9	.022	132.9	T(2)
R(2)	.009	239.3	.010	338.6	.014	136.7	R(2)
2Q(1)	.007	306.0	.019	217.6	.013	300.3	2Q(1)
P(1)	.029	299.8	.029	276.3	.024	298.4	P(1)
2SM(2)	.005	352.2	.005	265.3	.014	007.5	2SM(2)
M(3)	.003	317.4	.003	077.4	.003	057.8	M(3)
L(2)	.072	219.6	.055	132.2	.093	276.8	L(2)
2MK(3)	.013	340.8	.020	193.6	.021	041.6	2MK(3)
K(2)	.039	228.5	.036	134.4	.035	240.4	K(2)
M(8)	.002	357.7	.003	053.4	.007	075.7	M(8)
MS(4)	.010	278.4	.013	120.8	.011	044.9	MS(4)

(K1+O1)/(M2+S2) = .261   (K1+O1)/(M2+S2) = .179   (K1+O1)/(M2+S2) = .239

* Kappa prime at Longitude 75° W.

SUMMARY OF HARMONIC CONSTANTS FOR TIDES

Station No.	8594900	8632085	8632200
Name	WASHINGTON, D C	FISHERMANS IS, VA	KIPTOPEKE BCH, VA
Lat. (N)	38/52.5	37/05.8	37/10.0
Long. (W)	77/01.4	75/59.0	75/59.3
Series Beg.	09/01/79	03/19/82	01/01/81
Length of Analysis (Days)	366	248	365
Corrected Using Sta. No.			

Constituents	Amp (Ft)	Phase* (Deg)	Amp (Ft)	Phase* (Deg)	Amp (Ft)	Phase* (Deg)	Constituents
M(2)	1.302	233.8	1.416	239.5	1.241	247.9	M(2)
S(2)	.174	268.5	.246	258.6	.228	270.8	S(2)
N(2)	.242	214.4	.330	221.2	.271	229.2	N(2)
K(1)	.149	281.7	.199	111.4	.196	119.3	K(1)
M(4)	.143	029.2	.057	299.1	.016	021.3	M(4)
O(1)	.089	308.2	.153	138.2	.162	144.5	O(1)
M(6)	.040	121.4	.016	225.3	.015	226.8	M(6)
MK(3)	.038	043.0	.012	183.9	.012	212.6	MK(3)
S(4)	.001	294.7	.015	320.8	.012	009.5	S(4)
MN(4)	.055	005.3	.027	284.4	.009	010.5	MN(4)
NU(2)	.048	193.1	.077	207.9	.061	234.1	NU(2)
S(6)	.001	359.9	.002	091.8	.004	125.6	S(6)
MU(2)	.031	338.4	.041	224.2	.029	241.5	MU(2)
2N(2)	.026	263.3	.046	210.9	.038	219.7	2N(2)
OO(1)	.013	344.0	.016	098.6	.008	128.4	OO(1)
LAM(2)	.033	244.6	.018	343.8	.007	301.5	LAM(2)
S(1)	.054	250.7			.020	051.8	S(1)
M(1)	.004	082.3	.006	098.1	.005	137.9	M(1)
J(1)	.012	092.0	.007	174.8	.011	111.7	J(1)
Mm	.112	326.7	.144	228.4	.028	249.2	Mm
MSf	.025	118.5	.040	146.3	.161	072.2	MSf
Mf	.063	283.9	.120	246.9	.136	085.7	Mf
RHO(1)			.011	109.2	.016	155.0	RHO(1)
Q(1)	.006	211.9	.028	143.3	.035	128.9	Q(1)
T(2)	.017	324.8			.023	249.3	T(2)
R(2)	.009	202.3			.009	179.4	R(2)
2Q(1)	.011	300.1	.005	158.6	.022	115.7	2Q(1)
P(1)	.040	301.2	.063	113.4	.059	128.8	P(1)
2SM(2)	.019	117.5	.006	200.2	.004	203.0	2SM(2)
M(3)	.013	122.4	.015	199.2	.009	248.1	M(3)
L(2)	.107	279.3	.046	279.8	.059	271.2	L(2)
2MK(3)	.042	049.5	.017	212.5	.015	236.4	2MK(3)
K(2)	.041	289.4	.072	256.3	.062	283.7	K(2)
M(8)	.013	250.2	.004	137.5	.001	146.7	M(8)
MS(4)	.039	065.2	.014	261.3	.007	210.1	MS(4)

(K1+O1)/(M2+S2) = .161 (K1+O1)/(M2+S2) = .212 (K1+O1)/(M2+S2) = .243

* Kappa prime at Longitude 75° W.

SUMMARY OF HARMONIC CONSTANTS FOR TIDES

Station No.	8632366	8632599	8632869
Name	CAPE CHARLES HBR, VA	MATTAWOMAN CK, VA	GASKINS PT, VA
Lat. (N)	37/15.8	37/23.3	37/33.4
Long. (W)	76/01.2	75/57.8	75/55.0
Series Beg.	03/17/82	03/17/82	01/01/73
Length of Analysis (Days)	117	266	365
Corrected Using Sta. No.	8632200		

Constituents	Amp (Ft)	Phase* (Deg)	Amp (Ft)	Phase* (Deg)	Amp (Ft)	Phase* (Deg)	Constituents
M(2)	1.096	260.9	.917	286.3	.806	315.1	M(2)
S(2)	.198	279.7	.161	308.5	.143	339.5	S(2)
N(2)	.258	241.6	.208	270.0	.182	299.6	N(2)
K(1)	.173	126.8	.146	140.0	.142	156.8	K(1)
M(4)	.026	037.8	.071	124.7	.055	170.1	M(4)
O(1)	.124	148.3	.112	164.0	.112	181.5	O(1)
M(6)	.010	253.0	.015	324.1	.008	082.5	M(6)
MK(3)	.017	234.4	.019	298.6	.012	324.7	MK(3)
S(4)			.010	087.9	.006	140.8	S(4)
MN(4)	.020	019.6	.034	107.7	.026	150.8	MN(4)
NU(2)			.046	266.4	.042	295.3	NU(2)
S(6)			.001	201.2	.001	353.4	S(6)
MU(2)	.036	256.2	.014	288.4	.018	322.1	MU(2)
2N(2)			.029	238.6	.026	280.6	2N(2)
OO(1)			.015	177.9	.003	174.6	OO(1)
LAM(2)			.013	304.7	.017	335.6	LAM(2)
S(1)					.022	241.1	S(1)
M(1)			.005	040.8	.002	103.2	M(1)
J(1)			.005	152.3	.009	111.0	J(1)
Mm			.088	212.7	.084	288.0	Mm
MSf			.016	130.0	.029	121.6	MSf
Mf			.130	249.9	.039	121.7	Mf
RHO(1)			.011	139.9	.005	148.5	RHO(1)
Q(1)			.032	139.6	.025	172.5	Q(1)
T(2)					.024	327.7	T(2)
R(2)					.002	314.4	R(2)
2Q(1)			.006	008.4	.001	102.4	2Q(1)
P(1)			.050	154.3	.041	154.6	P(1)
2SM(2)			.008	298.4	.004	309.3	2SM(2)
M(3)	.010	226.6	.012	277.9	.007	288.1	M(3)
L(2)	.047	301.8	.038	314.3	.036	328.4	L(2)
2MK(3)	.015	263.2	.015	319.8	.012	332.8	2MK(3)
K(2)			.042	320.8	.042	333.3	K(2)
M(8)	.001	265.8	.003	298.3	.003	064.3	M(8)
MS(4)	.002	148.3	.022	164.9	.016	223.0	MS(4)

(K1+O1)/(M2+S2) = .230 (K1+O1)/(M2+S2) = .239 (K1+O1)/(M2+S2) = .267

* Kappa prime at Longitude 75° W.

SUMMARY OF HARMONIC CONSTANTS FOR TIDES

Station No.	8632974	8633091	8633362
Name	RAPPAHANNOCK SHOAL, VA	HARBORTON, VA	SCHOONER BAY, VA
Lat. (N)	37/35.6	37/40.0	37/45.8
Long. (W)	76/01.9	75/50.0	75/46.4
Series Beg.	06/25/83	02/12/76	06/19/75
Length of Analysis (Days)	129	315	75
Corrected Using Sta. No.	8638863		8635750

Constituents	Amp (Ft)	Phase* (Deg)	Amp (Ft)	Phase* (Deg)	Amp (Ft)	Phase* (Deg)	Constituents
M(2)	.708	311.2	.843	328.0	.894	343.5	M(2)
S(2)	.126	329.4	.151	344.3	.169	001.5	S(2)
N(2)	.169	291.7	.190	311.3	.192	327.6	N(2)
K(1)	.107	161.4	.140	161.3	.129	165.6	K(1)
M(4)	.029	112.9	.034	178.3	.035	212.0	M(4)
O(1)	.101	173.8	.106	184.5	.144	198.8	O(1)
M(6)	.013	005.1	.022	042.2	.015	060.1	M(6)
MK(3)	.012	301.2	.017	334.5	.008	299.3	MK(3)
S(4)			.008	160.0			S(4)
MN(4)	.021	105.9	.015	148.6	.016	204.8	MN(4)
NU(2)			.037	304.1			NU(2)
S(6)			.001	322.5			S(6)
MU(2)	.017	288.2	.012	339.2	.022	202.6	MU(2)
2N(2)			.019	283.4			2N(2)
OO(1)			.027	103.5			OO(1)
LAM(2)			.013	321.5			LAM(2)
S(1)							S(1)
M(1)			.004	127.1			M(1)
J(1)			.012	161.6			J(1)
Mm			.028	182.3			Mm
MSf			.053	295.9			MSf
Mf			.058	333.8			Mf
RHO(1)			.010	178.0			RHO(1)
Q(1)			.022	187.9			Q(1)
T(2)							T(2)
R(2)							R(2)
2Q(1)			.006	241.5			2Q(1)
P(1)			.049	178.6			P(1)
2SM(2)			.008	290.3			2SM(2)
M(3)	.011	266.2	.006	306.0	.020	142.4	M(3)
L(2)	.028	350.9	.047	336.8	.094	000.6	L(2)
2MK(3)	.015	322.8	.009	347.9			2MK(3)
K(2)			.048	343.4			K(2)
M(8)	.001	115.0	.003	230.6			M(8)
MS(4)	.009	135.2	.006	251.0	.002	290.6	MS(4)
	(K1+O1)/(M2+S2) = .249		K1+O1)/(M2+S2) = .247		(K1+O1)/(M2+S2) = .257		

* Kappa prime at Longitude 75° W.

SUMMARY OF HARMONIC CONSTANTS FOR TIDES

Station No.	8633532	8633596	8634214
Name	TANGIER IS, VA	GUARDSHORE, VA	ALEXANDRIA, VA
Lat. (N)	37/49.7	37/51.0	38/48.3
Long. (W)	75/59.5	75/42.0	77/02.3
Series Beg.	08/28/81	06/25/75	07/01/74
Length of Analysis (Days)	64	70	365
Corrected Using Sta. No.	8635750	8635750	

Constituents	Amp (Ft)	Phase* (Deg)	Amp (Ft)	Phase* (Deg)	Amp (Ft)	Phase* (Deg)	Constituents
M(2)	.696	347.5	1.061	359.3	1.248	230.1	M(2)
S(2)	.111	005.5	.194	018.0	.185	260.9	S(2)
N(2)	.133	331.3	.242	344.5	.250	206.7	N(2)
K(1)	.132	166.6	.144	179.0	.139	279.8	K(1)
M(4)	.022	247.1	.075	261.9	.110	028.3	M(4)
O(1)	.086	197.9	.137	201.2	.088	304.8	O(1)
M(6)	.012	068.3	.026	160.8	.025	103.5	M(6)
MK(3)	.005	058.2	.010	320.5	.029	026.1	MK(3)
S(4)					.001	097.7	S(4)
MN(4)	.010	257.3	.045	278.2	.044	002.0	MN(4)
NU(2)					.048	208.8	NU(2)
S(6)					.001	105.1	S(6)
MU(2)	.009	319.0	.016	017.3	.022	334.2	MU(2)
2N(2)					.023	195.0	2N(2)
OO(1)					.014	170.3	OO(1)
LAM(2)					.039	261.0	LAM(2)
S(1)					.036	269.5	S(1)
M(1)					.015	011.1	M(1)
J(1)					.029	272.8	J(1)
Mm					.115	336.7	Mm
MSf					.029	030.3	MSf
Mf					.041	147.7	Mf
RHO(1)					.009	016.5	RHO(1)
Q(1)					.021	270.0	Q(1)
T(2)					.018	216.2	T(2)
R(2)					.010	270.2	R(2)
2Q(1)					.013	258.0	2Q(1)
P(1)					.041	290.0	P(1)
2SM(2)					.007	108.0	2SM(2)
M(3)	.008	227.3			.013	334.2	M(3)
L(2)	.032	344.8	.073	006.5	.112	260.5	L(2)
2MK(3)	.009	033.9	.023	113.7	.026	043.3	2MK(3)
K(2)					.065	260.0	K(2)
M(8)	.001	287.5	.011	190.6	.005	228.8	M(8)
MS(4)	.005	248.6	.023	294.7	.032	068.6	MS(4)

(K1+O1)/(M2+S2) = .270 (K1+O1)/(M2+S2) = .224 (K1+O1)/(M2+S2) = .158

* Kappa prime at Longitude 75° W.

SUMMARY OF HARMONIC CONSTANTS FOR TIDES

Station No.	8634689	8634858	8635027
Name	QUANTICO, VA	AQUIA CREEK, VA	DAHLGREN, VA
Lat. (N)	38/31.2	38/25.1	38/19.2
Long. (W)	77/17/2	77/21.2	77/02.2
Series Beg.	02/12/71	01/01/71	01/01/71
Length of Analysis (Days)	254	365	365
Corrected Using Sta. No.			

Constituents	Amp (Ft)	Phase* (Deg)	Amp (Ft)	Phase* (Deg)	Amp (Ft)	Phase* (Deg)	Constituents
M(2)	.639	186.6	.510	168.9	.757	074.3	M(2)
S(2)	.100	211.2	.084	189.2	.135	100.8	S(2)
N(2)	.129	160.2	.102	141.4	.159	052.1	N(2)
K(1)	.146	255.2	.113	255.7	.095	217.7	K(1)
M(4)	.038	211.1	.048	207.6	.024	063.1	M(4)
O(1)	.095	285.5	.096	288.5	.082	252.3	O(1)
M(6)	.012	226.7	.036	173.7	.012	019.7	M(6)
MK(3)	.008	280.8	.009	246.2	.011	174.2	MK(3)
S(4)	.004	236.8	.002	168.5	.004	062.1	S(4)
MN(4)	.016	189.5	.019	182.4	.012	035.1	MN(4)
NU(2)	.022	166.9	.019	153.3	.031	055.0	NU(2)
S(6)			.001	200.2	.001	299.0	S(6)
MU(2)	.006	062.9	.006	088.0	.016	077.5	MU(2)
2N(2)	.012	133.0	.011	123.1	.021	029.9	2N(2)
OO(1)	.008	330.0	.010	296.8	.004	183.1	OO(1)
LAM(2)	.011	223.6	.008	203.5	.005	086.6	LAM(2)
S(1)			.043	233.2	.035	210.9	S(1)
M(1)	.009	001.3	.006	021.2	.006	235.0	M(1)
J(1)	.009	217.5	.010	241.6	.006	200.5	J(1)
Mm	.169	003.0	.030	061.5	.025	058.9	Mm
MSF	.039	084.0	.011	291.6	.006	246.0	MSF
MF	.102	017.3	.082	029.9	.074	028.0	MF
RHO(1)	.014	318.0	.012	261.4	.003	267.2	RHO(1)
Q(1)	.020	291.0	.020	287.4	.016	269.6	Q(1)
T(2)			.004	143.3	.008	101.0	T(2)
R(2)			.005	174.7	.001	100.6	R(2)
2Q(1)	.010	344.9	.008	304.7	.002	286.9	2Q(1)
P(1)	.047	281.9	.030	293.1	.031	218.1	P(1)
2SM(2)	.004	293.2	.002	282.0	.009	180.7	2SM(2)
M(3)	.005	294.9	.005	253.0	.005	172.7	M(3)
L(2)	.051	220.7	.031	197.9	.051	073.0	L(2)
2MK(3)	.010	303.2	.012	273.3	.014	193.3	2MK(3)
K(2)	.029	205.9	.025	194.1	.042	106.2	K(2)
M(8)	.003	227.9	.005	299.3	.002	094.1	M(8)
MS(4)	.012	251.7	.014	242.0	.007	116.7	MS(4)

(K1+O1)/(M2+S2) = .326 (K1+O1)/(M2+S2) = .352 (K1+O1)/(M2+S2) = .198

* Kappa prime at 75° W.

SUMMARY OF HARMONIC CONSTANTS FOR TIDES

Station No.	8635150	8635154	8635171
Name	COLONIAL BEACH, VA	MASSAPONAX S&G, VA	HOPYARD LANDING, VA
Lat. (N)	38/15.2	38/15.3	38/14.6
Long. (W)	76/57.7	77/24.6	77/13.6
Series Beg.	01/01/80	02/01/71	02/01/71
Length of Analysis (Days)	366	365	365
Corrected Using Sta. No.			

Constituents	Amp (Ft)	Phase* (Deg)	Amp (Ft)	Phase* (Deg)	Amp (Ft)	Phase* (Deg)	Constituents
M(2)	.793	069.1	1.129	190.2	.954	178.2	M(2)
S(2)	.127	097.9	.175	237.5	.136	210.2	S(2)
N(2)	.161	051.8	.189	163.7	.165	156.9	N(2)
K(1)	.098	219.0	.132	076.9	.136	250.2	K(1)
M(4)	.019	043.3	.154	279.2	.055	223.7	M(4)
O(1)	.084	241.9	.094	098.7	.099	281.6	O(1)
M(6)	.009	356.6	.060	323.0	.057	224.1	M(6)
MK(3)	.011	187.6	.056	128.7	.033	276.9	MK(3)
S(4)	.003	016.5	.010	003.8	.006	249.6	S(4)
MN(4)	.009	014.3	.057	248.9	.022	198.6	MN(4)
NU(2)	.031	028.3	.054	148.3	.048	150.7	NU(2)
S(6)	.001	319.0	.003	343.0	.003	188.3	S(6)
MU(2)	.018	093.6	.031	283.4	.033	282.4	MU(2)
2N(2)	.013	042.6	.016	004.1	.022	135.5	2N(2)
OO(1)	.013	254.0	.003	039.3	.004	218.8	OO(1)
LAM(2)	.015	064.3	.031	180.8	.007	193.1	LAM(2)
S(1)	.028	211.6	.056	056.2	.046	226.1	S(1)
M(1)	.002	005.3	.012	183.5	.007	265.9	M(1)
J(1)	.005	028.3	.004	126.5	.008	234.5	J(1)
Mm	.082	257.0	.034	013.1	.048	034.6	Mm
MSf	.077	248.7	.081	207.8	.013	127.2	MSf
Mf	.062	264.9	.123	008.4	.106	022.4	Mf
RHO(1)	.009	272.8	.023	139.2	.004	295.1	RHO(1)
Q(1)	.008	207.9	.007	004.9	.019	297.2	Q(1)
T(2)	.008	127.8	.009	165.5	.008	210.4	T(2)
R(2)	.013	057.4	.018	216.5	.001	209.9	R(2)
2Q(1)	.018	251.3	.012	249.8	.003	313.0	2Q(1)
P(1)	.036	241.3	.022	164.9	.045	250.6	P(1)
2SM(2)	.005	348.5	.036	336.6	.016	313.9	2SM(2)
M(3)	.004	241.5	.014	221.5	.009	351.4	M(3)
L(2)	.042	084.6	.138	190.5	.108	179.6	L(2)
2MK(3)	.018	184.2	.059	140.6	.039	303.4	2MK(3)
K(2)	.043	104.0	.051	252.8	.040	215.7	K(2)
M(8)	.001	200.1	.016	036.0	.016	281.5	M(8)
MS(4)	.004	099.5	.041	324.0	.016	248.1	MS(4)
	(K1+O1)/(M2+S2) = .198		(K1+O1)/(M2+S2) = .173		(K1+O1)/(M2+S2) = .216		

* Kappa prime at Longitude 75° W.

SUMMARY OF HARMONIC CONSTANTS FOR TIDES

Station No.	8635485	8635554	8635750
Name	COLES NECK, VA	SAUNDERS WHARF, VA	LEWISETTA, VA
Lat. (N)	38/08.5	38/05.4	37/59.8
Long. (W)	76/36.8	77/02.0	76/27.8
Series Beg.	03/10/71	02/01/71	01/01/81
Length of Analysis (Days)	314	365	365
Corrected Using Sta. No.			

Constituents	Amp (Ft)	Phase* (Deg)	Amp (Ft)	Phase* (Deg)	Amp (Ft)	Phase* (Deg)	Constituents
M(2)	.696	042.8	.693	097.9	.575	033.8	M(2)
S(2)	.114	064.8	.117	123.2	.087	054.7	S(2)
N(2)	.140	017.4	.125	074.8	.116	007.6	N(2)
K(1)	.076	203.2	.120	216.3	.073	205.0	K(1)
M(4)	.011	259.9	.054	072.8	.013	277.5	M(4)
O(1)	.071	234.4	.089	249.9	.057	230.2	O(1)
M(6)	.012	227.7	.043	008.2	.010	196.1	M(6)
MK(3)	.004	139.7	.023	159.3	.004	126.5	MK(3)
S(4)	.004	258.7	.006	094.6	.003	244.0	S(4)
MN(4)	.005	225.9	.022	045.4	.005	266.6	MN(4)
NU(2)	.029	019.9	.031	078.7	.028	028.6	NU(2)
S(6)	.001	110.3	.003	327.2	.001	175.9	S(6)
MU(2)	.005	025.4	.012	204.9	.006	341.3	MU(2)
2N(2)	.017	003.3	.006	353.4	.016	344.9	2N(2)
OO(1)	.010	249.0	.004	223.2	.001	193.1	OO(1)
LAM(2)	.014	041.8	.015	091.9	.003	053.0	LAM(2)
S(1)			.033	198.8	.018	194.2	S(1)
M(1)	.002	003.4	.003	352.2	.002	067.0	M(1)
J(1)	.011	204.9	.006	222.6	.006	234.5	J(1)
Mm	.027	110.3	.068	021.5	.037	212.1	Mm
MSf	.020	161.6	.021	035.5	.170	085.3	MSf
Mf	.062	031.6	.092	029.8	.079	081.2	Mf
RHO(1)	.007	214.2	.017	299.9	.006	221.1	RHO(1)
Q(1)	.012	220.8	.010	229.6	.022	192.4	Q(1)
T(2)			.009	062.0	.005	025.8	T(2)
R(2)			.008	065.3	.003	207.7	R(2)
2Q(1)	.012	268.2			.012	144.0	2Q(1)
P(1)	.031	213.4	.015	251.4	.034	222.7	P(1)
2SM(2)	.008	164.7	.004	253.4	.003	274.1	2SM(2)
M(3)	.003	114.4	.009	207.2	.002	076.0	M(3)
L(2)	.045	061.5	.056	110.0	.043	050.6	L(2)
2MK(3)	.006	164.2	.025	188.0	.005	073.2	2MK(3)
K(2)	.034	069.5	.038	120.1	.024	045.7	K(2)
M(8)	.001	006.6	.011	354.3	.001	039.7	M(8)
MS(4)	.002	258.6	.015	105.6	.003	000.1	MS(4)

(K1+O1)/(M2+S2) = .181   (K1+O1)/(M2+S2) = .261   (K1+O1)/(M2+S2) = .196

* Kappa prime at Longitude 75° W.

SUMMARY OF HARMONIC CONSTANTS FOR TIDES

Station No.	8635881	8635961	8635985
Name	TAPPAHANNOCK, VA	SMITH POINT, VA	WARES WHARF, VA
Lat. (N)	37/55.8	37/53.3	37/52.4
Long. (W)	76/51.4	76/14.5	76/47.0
Series Beg.	01/01/71	08/27/81	03/01/71
Length of Analysis (Days)	365	51	365
Corrected Using Sta. No.		8635750	

Constituents	Amp (Ft)	Phase* (Deg)	Amp (Ft)	Phase* (Deg)	Amp (Ft)	Phase* (Deg)	Constituents
M(2)	.819	039.3	.397	029.2	.834	021.1	M(2)
S(2)	.130	064.0	.053	056.7	.148	042.2	S(2)
N(2)	.152	017.8	.073	012.9	.167	000.4	N(2)
K(1)	.119	186.1	.062	199.1	.124	173.0	K(1)
M(4)	.066	336.0	.008	076.0	.054	297.1	M(4)
O(1)	.083	218.0	.052	238.0	.094	203.0	O(1)
M(6)	.009	204.6	.006	108.0	.001	155.2	M(6)
MK(3)	.024	085.1	.003	328.8	.018	066.9	MK(3)
S(4)	.008	011.5			.007	308.2	S(4)
MN(4)	.030	313.5	.005	025.3	.023	271.6	MN(4)
NU(2)	.035	018.4			.035	002.5	NU(2)
S(6)	.005	092.5			.001	180.0	S(6)
MU(2)	.011	082.0	.002	313.2	.017	028.7	MU(2)
2N(2)	.012	339.8			.013	323.6	2N(2)
OO(1)	.003	269.0			.006	240.5	OO(1)
LAM(2)	.011	043.0			.010	344.5	LAM(2)
S(1)	.025	184.2			.014	172.8	S(1)
M(1)	.001	101.5			.003	234.4	M(1)
J(1)	.008	158.2			.010	184.4	J(1)
Mm	.031	038.5			.040	042.7	Mm
MSf	.004	270.2			.049	045.7	MSf
Mf	.067	024.6			.094	012.2	Mf
RHO(1)	.007	214.4			.010	258.4	RHO(1)
Q(1)	.016	199.2			.012	174.4	Q(1)
T(2)	.018	335.5			.021	346.8	T(2)
R(2)	.003	292.8			.003	288.0	R(2)
2Q(1)	.007	290.8			.007	257.9	2Q(1)
P(1)	.019	190.6			.018	184.9	P(1)
2SM(2)	.003	267.4			.003	139.3	2SM(2)
M(3)	.011	134.5	.003	066.2	.009	101.9	M(3)
L(2)	.059	053.8	.020	037.4	.046	041.2	L(2)
2MK(3)	.024	120.2	.005	032.4	.021	103.4	2MK(3)
K(2)	.043	073.8			.044	045.2	K(2)
M(8)	.005	061.8			.002	038.5	M(8)
MS(4)	.019	004.1	.003	050.3	.015	330.6	MS(4)
	(K1+O1)/(M2+S2) = .213		(K1+O1)/(M2+S2) = .253		(K1+O1)/(M2+S2) = .222		

* Kappa prime at Longitude 75° W.

SUMMARY OF HARMONIC CONSTANTS FOR TIDES

Station No.	8636128	8636261	8636522
Name	FLEET PT, VA	BAYPORT, VA	URBANNA, VA
Lat. (N)	37/48.8	37/45.3	37/39.0
Long. (W)	76/16.5	76/40.0	76/34.5
Series Beg.	01/01/71	02/01/71	02/01/71
Length of Analysis (Days)	365	365	365
Corrected Using Sta. No.			

Constituents	Amp (Ft)	Phase* (Deg)	Amp (Ft)	Phase* (Deg)	Amp (Ft)	Phase* (Deg)	Constituents
M(2)	.518	346.6	.795	000.2	.699	343.2	M(2)
S(2)	.093	002.0	.147	019.8	.132	001.8	S(2)
N(2)	.112	322.4	.167	338.2	.152	322.6	N(2)
K(1)	.084	164.8	.118	161.5	.111	155.5	K(1)
M(4)	.025	197.1	.053	257.1	.033	220.6	M(4)
O(1)	.071	200.1	.091	194.6	.089	188.4	O(1)
M(6)	.018	057.3	.012	157.7	.010	109.1	M(6)
MK(3)	.008	000.3	.014	040.3	.010	008.3	MK(3)
S(4)	.003	158.0	.007	258.5	.006	216.6	S(4)
MN(4)	.011	174.1	.022	229.2	.016	189.1	MN(4)
NU(2)	.022	325.6	.035	334.6	.029	318.9	NU(2)
S(6)	.001	355.1	.002	110.5	.001	003.9	S(6)
MU(2)	.011	301.8	.019	347.5	.020	332.4	MU(2)
2N(2)	.015	298.1	.018	303.5	.018	297.9	2N(2)
OO(1)	.003	129.5	.007	237.9	.007	240.8	OO(1)
LAM(2)	.004	353.8	.008	337.2	.006	318.0	LAM(2)
S(1)	.013	225.5	.009	177.0	.001	223.9	S(1)
M(1)	.005	182.4	.001	189.8	.002	168.9	M(1)
J(1)	.006	147.1	.010	157.6	.009	156.1	J(1)
Mm	.038	017.2	.074	013.7	.053	016.2	Mm
MSf	.016	070.0	.035	012.8	.014	013.1	MSf
Mf	.058	010.9	.059	033.2	.074	016.8	Mf
RHO(1)	.003	215.2	.009	214.0	.007	181.0	RHO(1)
Q(1)	.014	217.7	.018	164.0	.015	160.3	Q(1)
T(2)	.005	002.3	.019	343.5	.016	331.4	T(2)
R(2)	.001	001.8	.003	265.0	.003	200.7	R(2)
2Q(1)	.002	235.3	.004	317.5	.003	272.6	2Q(1)
P(1)	.028	165.2	.024	171.4	.025	164.9	P(1)
2SM(2)	.002	154.7	.003	159.8	.003	162.6	2SM(2)
M(3)	.004	000.9	.008	060.5	.006	023.5	M(3)
L(2)	.015	010.9	.033	029.3	.027	017.5	L(2)
2MK(3)	.007	027.9	.017	078.2	.012	050.0	2MK(3)
K(2)	.025	001.6	.043	024.8	.038	005.6	K(2)
M(8)	.001	330.5					M(8)
MS(4)	.006	267.3	.012	299.4	.007	272.0	MS(4)
	(K1+O1)/(M2+S2) = .254		(K1+O1)/(M2+S2) = .222		(K1+O1)/(M2+S2) = .241		

* Kappa Prime at Longitude 75° W.

SUMMARY OF HARMONIC CONSTANTS FOR TIDES

Station No.	8636580	8636654	8636735
Name	WINDMILL PT, VA	NEW MILL CREEK, VA	DELTAVILLE, VA
Lat. (N)	37/36.7	37/35.0	37/32.9
Long. (W)	76/16.5	76/25.1	76/19.9
Series Beg.	01/01/71	01/01/71	02/21/73
Length of Analysis (Days)	365	365	225
Corrected Using Sta. No.			

Constituents	Amp (Ft)	Phase* (Deg)	Amp (Ft)	Phase* (Deg)	Amp (Ft)	Phase* (Deg)	Constituents
M(2)	.552	317.3	.589	328.9	.550	308.6	M(2)
S(2)	.105	334.0	.110	346.0	.095	327.8	S(2)
N(2)	.119	297.2	.128	307.2	.121	291.1	N(2)
K(1)	.097	148.7	.102	152.3	.102	143.4	K(1)
M(4)	.028	156.6	.028	174.5	.043	135.0	M(4)
O(1)	.078	181.8	.080	184.9	.077	176.2	O(1)
M(6)	.011	020.7	.009	043.6	.013	026.1	M(6)
MK(3)	.010	322.8	.009	339.5	.012	299.2	MK(3)
S(4)	.004	132.3	.004	156.1	.005	144.7	S(4)
MN(4)	.012	128.1	.013	143.9	.019	113.0	MN(4)
NU(2)	.028	301.4	.027	309.7	.024	291.4	NU(2)
S(6)	.001	298.9	.001	325.3	.001	290.5	S(6)
MU(2)	.015	306.4	.017	315.7	.013	289.8	MU(2)
2N(2)	.013	281.7	.016	289.2	.017	263.8	2N(2)
OO(1)	.006	224.9	.007	237.0	.007	170.5	OO(1)
LAM(2)	.003	332.3	.004	339.5	.008	319.8	LAM(2)
S(1)	.006	253.3	.004	302.7			S(1)
M(1)	.001	160.9			.002	327.9	M(1)
J(1)	.008	141.4	.009	142.2	.012	124.8	J(1)
Mm	.039	019.9	.034	022.0	.226	280.5	Mm
MSf	.017	067.8	.019	080.7	.115	167.0	MSf
Mf	.059	012.0	.062	011.4	.040	348.9	Mf
RHO(1)	.009	174.1	.008	181.6	.012	134.9	RHO(1)
Q(1)	.016	157.0	.015	153.2	.019	174.6	Q(1)
T(2)	.011	305.1	.010	324.5			T(2)
R(2)	.001	223.4	.001	292.1			R(2)
2Q(1)	.004	296.3	.005	317.5	.004	234.9	2Q(1)
P(1)	.032	160.9	.028	164.8	.025	151.8	P(1)
2SM(2)	.003	195.5	.003	198.3	.003	277.6	2SM(2)
M(3)	.006	346.3	.007	001.2	.007	282.1	M(3)
L(2)	.019	348.7	.020	005.4	.021	327.7	L(2)
2MK(3)	.009	359.1	.009	014.6	.011	310.3	2MK(3)
K(2)	.032	340.9	.032	349.2	.026	327.9	K(2)
M(8)	.001	097.2			.001	011.3	M(8)
MS(4)	.006	215.9	.005	226.1	.010	186.4	MS(4)

(K1+O1)/(M2+S2) = .266   (K1+O1)/(M2+S2) = .260   (K1+O1)/(M2+S2) = .278

* Kappa prime at Longitude 75° W.

SUMMARY OF HARMONIC CONSTANTS FOR TIDES

Station No.	8636769	8636831	8636969
Name	WEST POINT, VA	DIXIE, VA	ROANE POINT, VA
Lat. (N)	37/31.9	37/30.4	37/26.8
Long. (W)	76/47.5	76/25.0	76/42.5
Series Beg.	01/01/71	10/01/72	06/01/72
Length of Analysis (Days)	365	365	365
Corrected Using Sta. No.			

Constituents	Amp (Ft)	Phase* (Deg)	Amp (Ft)	Phase* (Deg)	Amp (Ft)	Phase* (Deg)	Constituents
M(2)	1.295	323.9	.602	313.5	1.354	306.7	M(2)
S(2)	.227	345.5	.111	331.5	.257	331.5	S(2)
N(2)	.243	302.2	.132	295.1	.305	284.5	N(2)
K(1)	.163	154.4	.106	145.6	.171	142.5	K(1)
M(4)	.113	189.4	.054	151.7	.055	180.4	M(4)
O(1)	.128	182.2	.078	178.4	.124	169.8	O(1)
M(6)	.027	314.3	.017	065.8	.012	219.9	M(6)
MK(3)	.031	338.5	.011	306.1	.021	276.2	MK(3)
S(4)	.019	214.7	.011	132.1	.021	194.9	S(4)
MN(4)	.053	173.8	.025	132.7	.031	161.4	MN(4)
NU(2)	.059	311.4	.028	290.9	.062	285.1	NU(2)
S(6)	.005	055.2	.002	312.2	.003	355.6	S(6)
MU(2)	.022	024.7	.016	292.6	.037	309.5	MU(2)
2N(2)	.015	255.5	.018	264.9	.039	252.7	2N(2)
OO(1)	.002	139.5	.006	205.9	.013	192.0	OO(1)
LAM(2)	.035	311.1	.012	352.4	.040	302.5	LAM(2)
S(1)	.027	085.0	.011	293.0	.029	047.2	S(1)
M(1)	.002	133.2	.007	154.1	.016	236.7	M(1)
J(1)	.014	171.3	.006	112.7	.005	200.7	J(1)
Mm	.067	033.8	.132	277.1	.120	238.3	Mm
MSf	.042	055.9	.100	156.3	.083	199.3	MSf
Mf	.087	020.3	.049	339.8	.066	282.8	Mf
RHO(1)	.011	260.2	.005	136.1	.010	198.3	RHO(1)
Q(1)	.029	145.7	.015	188.4	.013	190.3	Q(1)
T(2)	.012	319.2	.011	318.4	.038	304.2	T(2)
R(2)	.009	018.6	.007	183.4	.017	067.9	R(2)
2Q(1)	.009	159.3	.002	351.0	.015	045.8	2Q(1)
P(1)	.025	166.0	.031	148.6	.061	129.6	P(1)
2SM(2)	.004	061.7	.002	348.3	.011	280.3	2SM(2)
M(3)	.015	038.7	.009	282.6	.010	315.4	M(3)
L(2)	.087	334.5	.021	328.8	.060	309.6	L(2)
2MK(3)	.031	359.7	.014	325.5	.018	304.7	2MK(3)
K(2)	.066	345.2	.028	329.8	.064	322.7	K(2)
M(8)	.008	220.6	.001	096.3	.004	128.1	M(8)
MS(4)	.020	190.1	.014	205.2	.006	094.5	MS(4)

(K1+O1)/(M2+S2) = .191 (K1+O1)/(M2+S2) = .257 (K1+O1)/(M2+S2) = .183

* Kappa prime at Longitude 75° W.

SUMMARY OF HARMONIC CONSTANTS FOR TIDES

Station No.	8637072	8637289	8637444
Name	BELLEVILLE, VA	NEW POINT, VA	BROWN'S BAY, VA
Lat. (N)	37/24.7	37/20.8	37/18.0
Long. (W)	76/26.3	76/16.4	76/24.0
Series Beg.	01/01/71	03/10/82	06/09/82
Length of Analysis (Days)	365	260	41
Corrected Using Sta. No.			8637624

Constituents	Amp (Ft)	Phase* (Deg)	Amp (Ft)	Phase* (Deg)	Amp (Ft)	Phase* (Deg)	Constituents
M(2)	1.142	258.8	.801	262.7	1.072	257.2	M(2)
S(2)	.219	280.2	.141	283.2	.216	280.2	S(2)
N(2)	.233	242.3	.186	247.1	.234	236.9	N(2)
K(1)	.152	122.0	.127	120.3	.156	121.2	K(1)
M(4)	.061	107.0	.049	091.6	.049	102.9	M(4)
O(1)	.119	149.8	.084	149.1	.103	147.0	O(1)
M(6)	.040	354.3	.009	283.3	.021	299.4	M(6)
MK(3)	.013	262.2	.016	268.7	.017	254.9	MK(3)
S(4)	.022	072.2	.013	053.0			S(4)
MN(4)	.036	070.1	.023	069.0	.030	079.9	MN(4)
NU(2)	.051	243.9	.046	245.1			NU(2)
S(6)	.008	244.4	.001	234.9			S(6)
MU(2)	.037	273.7	.025	271.9	.021	264.3	MU(2)
2N(2)	.021	226.1	.022	219.9			2N(2)
OO(1)	.004	168.0	.008	078.1			OO(1)
LAM(2)	.021	233.1	.015	272.5			LAM(2)
S(1)	.030	056.1					S(1)
M(1)	.004	126.4	.005	054.2			M(1)
J(1)	.012	114.8	.009	148.5			J(1)
Mm	.040	001.8	.128	214.5			Mm
MSf	.015	070.6	.043	142.3			MSf
Mf	.060	021.4	.120	249.7			Mf
RHO(1)	.004	081.8	.007	125.2			RHO(1)
Q(1)	.028	129.1	.027	152.0			Q(1)
T(2)	.012	262.0					T(2)
R(2)	.003	228.5					R(2)
2Q(1)	.004	062.5	.005	054.9			2Q(1)
P(1)	.042	120.2	.031	115.6			P(1)
2SM(2)	.004	270.8	.004	300.2			2SM(2)
M(3)	.011	285.0	.012	244.2	.014	221.1	M(3)
L(2)	.034	246.1	.031	284.0	.039	307.7	L(2)
2MK(3)	.015	289.9	.013	290.0	.011	266.3	2MK(3)
K(2)	.063	281.3	.043	280.5			K(2)
M(8)	.003	060.6	.001	264.2	.001	097.9	M(8)
MS(4)	.020	220.3	.013	145.5	.025	190.4	MS(4)

(K1+O1)/(M2+S2) = .199 (K1+O1)/(M2+S2) = .224 (K1+O1)/(M2+S2) = .216

* Kappa prime at Longitude 75° W.

SUMMARY OF HARMONIC CONSTANTS FOR TIDES

Station No.	8637472	8637589	8637624
Name	CHEATHAM ANNEX, VA	NEW PT COMFORT SHOAL, VA	GLOUCESTER PT, VA
Lat. (N)	37/17.5	37/15.4	37/14.8
Long. (W)	76/35.2	76/13.3	76/30.0
Series Beg.	06/01/72	05/30/81	01/01/71
Length of Analysis (Days)	365	103	365
Corrected Using Sta. No.		8638863	

Constituents	Amp (Ft)	Phase* (Deg)	Amp (Ft)	Phase* (Deg)	Amp (Ft)	Phase* (Deg)	Constituents
M(2)	1.185	280.6	.998	256.1	1.155	268.3	M(2)
S(2)	.238	304.7	.181	278.5	.220	288.7	S(2)
N(2)	.282	260.3	.220	238.1	.239	250.9	N(2)
K(1)	.171	127.1	.147	124.2	.159	125.6	K(1)
M(4)	.019	164.4	.025	071.4	.016	137.0	M(4)
O(1)	.124	156.1	.120	149.3	.126	152.2	O(1)
M(6)	.020	038.9	.011	266.4	.013	000.5	M(6)
MK(3)	.015	258.0	.008	303.3	.011	271.9	MK(3)
S(4)	.013	106.3			.012	086.6	S(4)
MN(4)	.011	109.5	.008	067.6	.013	077.0	MN(4)
NU(2)	.047	256.4			.054	250.0	NU(2)
S(6)	.003	289.7			.002	215.0	S(6)
MU(2)	.035	272.1	.035	270.8	.038	280.0	MU(2)
2N(2)	.038	234.7			.024	239.0	2N(2)
OO(1)	.008	181.6			.005	193.0	OO(1)
LAM(2)	.011	311.6			.021	254.7	LAM(2)
S(1)	.023	035.8			.030	040.3	S(1)
M(1)	.008	134.2			.002	130.0	M(1)
J(1)	.009	156.0			.011	116.9	J(1)
Mm	.121	257.9			.048	018.3	Mm
MSf	.104	210.9			.024	078.5	MSf
Mf	.048	326.5			.066	015.7	Mf
RHO(1)	.002	211.0			.003	098.3	RHO(1)
Q(1)	.020	161.5			.029	129.4	Q(1)
T(2)	.029	276.6			.012	270.0	T(2)
R(2)	.011	089.8			.004	215.2	R(2)
2Q(1)	.005	022.3			.006	058.3	2Q(1)
P(1)	.052	125.3			.040	119.8	P(1)
2SM(2)	.004	207.1			.004	268.8	2SM(2)
M(3)	.013	297.7	.010	291.5	.010	294.9	M(3)
L(2)	.039	291.9	.050	266.1	.038	266.2	L(2)
2MK(3)	.014	299.0	.010	245.4	.012	302.1	2MK(3)
K(2)	.060	300.1			.065	289.7	K(2)
M(8)	.003	039.8	.001	207.5	.002	339.3	M(8)
MS(4)	.012	308.8	.012	230.5	.013	272.9	MS(4)

(K1+O1)/(M2+S2) = .207 (K1+O1)/(M2+S2) = .226 (K1+O1)/(M2+S2) = .207

* Kappa prime at Longitude 75° W.

SUMMARY OF HARMONIC CONSTANTS FOR TIDES

Station No.	8637663	8637686	8638051
Name	TUE MARSH LT, VA	YORKTOWN, VA	MESSICK PT, VA
Lat. (N)	37/14.1	37/13.8	37/06.5
Long. (W)	76/23.1	76/26.2	76/19.1
Series Beg.	01/23/71	06/08/82	06/06/82
Length of Analysis (Days)	104	49	36
Corrected Using Sta. No.	8637624	8637624	8638863

Constituents	Amp (Ft)	Phase* (Deg)	Amp (Ft)	Phase* (Deg)	Amp (Ft)	Phase* (Deg)	Constituents
M(2)	1.124	261.1	1.067	265.8	1.101	258.0	M(2)
S(2)	.199	283.0	.201	287.1	.194	275.4	S(2)
N(2)	.225	242.4	.238	249.8	.254	239.6	N(2)
K(1)	.150	124.3	.152	123.9	.145	120.1	K(1)
M(4)	.020	124.3	.025	105.5	.035	063.4	M(4)
O(1)	.124	151.5	.109	147.9	.105	138.6	O(1)
M(6)	.012	306.2	.009	351.4	.010	331.7	M(6)
MK(3)	.008	264.0	.014	261.3			MK(3)
S(4)							S(4)
MN(4)	.014	058.5	.017	072.8	.018	001.5	MN(4)
NU(2)							NU(2)
S(6)							S(6)
MU(2)	.035	271.9	.028	267.7	.035	244.4	MU(2)
2N(2)							2N(2)
OO(1)							OO(1)
LAM(2)							LAM(2)
S(1)							S(1)
M(1)							M(1)
J(1)							J(1)
Mm							Mm
MSf							MSf
Mf							Mf
RHO(1)							RHO(1)
Q(1)							Q(1)
T(2)							T(2)
R(2)							R(2)
2Q(1)							2Q(1)
P(1)							P(1)
2SM(2)							2SM(2)
M(3)	.010	281.8	.013	244.3			M(3)
L(2)	.032	262.9	.039	292.1	.044	280.2	L(2)
2MK(3)	.008	299.8	.012	271.1	.023	216.3	2MK(3)
K(2)							K(2)
M(8)	.006	338.7	.001	345.1	.002	286.1	M(8)
MS(4)	.013	249.2			.004	275.9	MS(4)

(K1+O1)/(M2+S2) = .207 (K1+O1)/(M2+S2) = .206 (K1+O1)/(M2+S2) = .193

* Kappa prime at Longitude 75^{o} W.

SUMMARY OF HARMONIC CONSTANTS FOR TIDES

Station No.	8638288	8638401	8638409
Name	OLD PT COMFORT, VA	HUNTINGTON PARK, VA	HOLLIDAY'S PT, VA
Lat. (N)	37/00.2	37/00.8	36/50.3
Long. (W)	76/18.9	76/27.5	76/33.0
Series Beg.	07/01/71	01/19/72	09/01/71
Length of Analysis (Days)	365	80	365
Corrected Using Sta. No.		8638610	

Constituents	Amp (Ft)	Phase* (Deg)	Amp (Ft)	Phase* (Deg)	Amp (Ft)	Phase* (Deg)	Constituents
M(2)	1.188	255.7	1.250	278.1	1.387	284.6	M(2)
S(2)	.230	276.5	.227	301.2	.258	313.9	S(2)
N(2)	.265	236.5	.264	260.9	.304	267.2	N(2)
K(1)	.170	119.0	.176	131.1	.181	135.8	K(1)
M(4)	.012	271.2	.022	062.2	.059	081.0	M(4)
O(1)	.146	146.4	.147	159.0	.153	160.7	O(1)
M(6)	.009	255.2	.005	281.5	.008	182.0	M(6)
MK(3)	.008	177.2	.011	215.4	.027	234.8	MK(3)
S(4)	.008	022.0			.011	133.3	S(4)
MN(4)	.007	301.7	.014	080.0	.032	068.6	MN(4)
NU(2)	.051	240.3			.050	267.2	NU(2)
S(6)	.003	123.6			.003	281.3	S(6)
MU(2)	.041	266.4	.028	315.5	.050	341.0	MU(2)
2N(2)	.032	224.9			.026	246.1	2N(2)
OO(1)	.008	116.7			.006	093.7	OO(1)
LAM(2)	.023	239.1			.020	237.9	LAM(2)
S(1)	.038	044.7			.057	056.4	S(1)
M(1)	.006	140.3			.009	169.4	M(1)
J(1)	.012	119.8			.004	137.0	J(1)
Mm	.070	174.6			.111	195.6	Mm
MSf	.111	352.1			.123	338.4	MSf
Mf	.089	027.4			.099	042.2	Mf
RHO(1)	.004	304.7			.017	291.0	RHO(1)
Q(1)	.020	105.9			.017	102.5	Q(1)
T(2)	.011	245.8			.011	269.6	T(2)
R(2)	.003	014.8			.007	108.4	R(2)
2Q(1)	.012	162.8			.005	161.8	2Q(1)
P(1)	.048	115.5			.046	131.3	P(1)
2SM(2)	.009	306.6			.006	063.7	2SM(2)
M(3)	.010	238.6	.017	253.4	.021	303.1	M(3)
L(2)	.033	262.2	.053	272.1	.049	268.7	L(2)
2MK(3)	.007	232.0	.011	275.6	.023	259.7	2MK(3)
K(2)	.059	266.8			.062	302.6	K(2)
M(8)	.002	220.3	.001	217.3	.005	288.1	M(8)
MS(4)	.015	270.8	.010	000.0	.017	068.5	MS(4)

(K1+O1)/(M2+S2) = .223 (K1+O1)/(M2+S2) = .219 (K1+O1)/(M2+S2) = .203

* Kappa prime at Longitude 75° W.

SUMMARY OF HARMONIC CONSTANTS FOR TIDES

Station No.	8638421	8638433	8638442
Name	BURWELL BAY, VA	SCOTLAND, VA	FERRY PT, VA
Lat. (N)	37/03.4	37/11.1	37/15.8
Long. (W)	76/40.1	76/47.0	76/52.6
Series Beg.	07/01/71	07/01/71	06/14/71
Length of Analysis (Days)	364	365	216
Corrected Using Sta. No.			8638433

Constituents	Amp (Ft)	Phase* (Deg)	Amp (Ft)	Phase* (Deg)	Amp (Ft)	Phase* (Deg)	Constituents
M(2)	1.164	299.4	.884	341.5	.874	007.6	M(2)
S(2)	.201	323.2	.143	006.1	.127	034.8	S(2)
N(2)	.237	279.9	.170	324.2	.160	349.4	N(2)
K(1)	.168	147.0	.156	178.4	.165	191.9	K(1)
M(4)	.049	142.3	.047	241.3	.056	287.4	M(4)
O(1)	.144	173.6	.136	203.3	.145	217.4	O(1)
M(6)	.023	299.0	.028	050.4	.052	122.0	M(6)
MK(3)	.017	286.2	.023	353.1	.025	025.1	MK(3)
S(4)	.009	145.3	.006	237.4	.004	315.8	S(4)
MN(4)	.024	125.0	.019	217.2	.024	263.7	MN(4)
NU(2)	.058	278.5	.042	319.7	.037	345.8	NU(2)
S(6)	.001	311.4					S(6)
MU(2)	.030	342.5	.022	069.3	.022	093.0	MU(2)
2N(2)	.015	251.3	.012	299.7	.010	293.1	2N(2)
OO(1)	.007	137.3	.004	168.5	.005	172.1	OO(1)
LAM(2)	.033	302.6	.026	338.2	.029	001.6	LAM(2)
S(1)	.043	086.1	.043	128.3			S(1)
M(1)	.005	205.1	.009	248.3	.013	261.1	M(1)
J(1)	.004	143.1	.002	090.3	.003	106.3	J(1)
Mm	.067	162.6	.044	170.2	.066	287.3	Mm
MSf	.150	351.3	.174	356.9	.068	358.2	MSf
Mf	.097	030.8	.100	026.3	.061	011.7	Mf
RHO(1)	.006	324.7	.008	011.9	.002	124.6	RHO(1)
Q(1)	.014	133.5	.011	161.3	.013	180.7	Q(1)
T(2)	.012	292.9	.005	311.0			T(2)
R(2)	.005	357.8	.006	069.4			R(2)
2Q(1)	.011	195.9	.014	217.9	.010	222.8	2Q(1)
P(1)	.039	137.2	.031	159.6	.027	158.3	P(1)
2SM(2)	.006	041.6	.006	075.9	.005	112.3	2SM(2)
M(3)	.011	323.2	.009	027.7	.013	083.7	M(3)
L(2)	.052	292.5	.052	325.5	.071	360.7	L(2)
2MK(3)	.016	317.2	.022	011.1	.031	040.4	2MK(3)
K(2)	.054	312.1	.043	351.2	.040	020.7	K(2)
M(8)	.004	937.9	.005	248.5	.004	013.6	M(8)
MS(4)	.009	175.3	.011	281.2	.015	328.2	MS(4)
	(K1+O1)/(M2+S2) = .229		(K1+O1)/(M2+S2) = .284		(K1+O1)/(M2+S2) = .310		

* Kappa prime at Longitude 75° W.

SUMMARY OF HARMONIC CONSTANTS FOR TIDES

Station No.	8638449	8638464	8638481
Name	CLAREMONT, VA	WILLCOX WHARF, VA	HOPEWELL, VA
Lat. (N)	37/13.9	37/18.9	37/18.8
Long. (W)	76/56.9	77/05.9	77/16.3
Series Beg.	07/01/72	07/01/71	02/08/78
Length of Analysis (Days)	365	365	230
Corrected Using Sta. No.			

Constituents	Amp (Ft)	Phase* (Deg)	Amp (Ft)	Phase* (Deg)	Amp (Ft)	Phase* (Deg)	Constituents
M(2)	.819	011.8	.958	056.7	1.096	87.8	M(2)
S(2)	.128	040.6	.126	085.8	.130	124.9	S(2)
N(2)	.166	355.0	.178	037.3	.181	077.0	N(2)
K(1)	.169	193.8	.180	207.9	.195	212.7	K(1)
M(4)	.075	280.7	.074	331.7	.074	042.8	M(4)
O(1)	.133	218.7	.160	231.1	.166	254.6	O(1)
M(6)	.047	122.2	.033	217.3	.041	314.1	M(6)
MK(3)	.021	032.5	.027	094.2	.033	150.1	MK(3)
S(4)	.004	272.4	.006	012.2			S(4)
MN(4)	.036	263.9	.029	314.6	.027	029.1	MN(4)
NU(2)	.036	342.1	.047	044.4	.054	075.0	NU(2)
S(6)	.001	082.1	.001	309.9			S(6)
MU(2)	.020	114.0	.028	179.0	.054	192.5	MU(2)
2N(2)	.024	319.0	.010	297.9	.027	074.5	2N(2)
OO(1)	.006	243.3	.007	200.5	.004	065.8	OO(1)
LAM(2)	.018	017.1	.029	057.4	.034	097.7	LAM(2)
S(1)	.028	137.9	.058	147.6			S(1)
M(1)	.008	357.7	.011	277.5	.023	340.7	M(1)
J(1)	.005	252.4	.001	296.2	.022	043.1	J(1)
Mm	.124	290.4	.065	167.2	.122	063.7	Mm
MSf	.024	186.9	.196	350.1	.089	091.2	MSf
Mf	.057	329.5	.098	034.8	.172	162.6	Mf
RHO(1)	.005	296.8	.009	023.6	.008	268.7	RHO(1)
Q(1)	.020	237.3	.011	202.6	.018	267.8	Q(1)
T(2)	.021	021.7	.008	356.9			T(2)
R(2)	.006	226.9	.011	166.9			R(2)
2Q(1)	.005	049.0	.013	260.5	.007	160.7	2Q(1)
P(1)	.039	195.0	.024	195.6	.075	197.2	P(1)
2SM(2)	.006	253.6	.006	148.1	.008	288.8	2SM(2)
M(3)	.005	060.9	.008	138.3	.010	216.1	M(3)
L(2)	.056	017.9	.071	050.8	.090	101.3	L(2)
2MK(3)	.022	046.2	.029	113.0	.031	158.4	2MK(3)
K(2)	.032	036.3	.040	064.9	.058	102.0	K(2)
M(8)	.008	032.4	.008	135.5	.012	272.0	M(8)
MS(4)	.024	320.9	.019	020.6	.016	092.0	MS(4)

(K1+O1)/(M2+S2) = .319   (K1+O1)/(M2+S2) = .314   (K1+O1)/(M2+S2) = .294

* Kappa prime at Longitude 75° W.

SUMMARY OF HARMONIC CONSTANTS FOR TIDES

Station No.	8638489	8638491	8638495
Name	PUDDLEDOCK S&G, VA	CHESTER, VA	RICHMOND, VA
Lat. (N)	37/16.0	37/23.0	37/31.5
Long. (W)	77/22.3	77/22.7	77/25.2
Series Beg.	02/09/78	07/01/71	06/01/71
Length of Analysis (Days)	81	365	365
Corrected Using Sta. No.	8638863		

Constituents	Amp (Ft)	Phase* (Deg)	Amp (Ft)	Phase* (Deg)	Amp (Ft)	Phase* (Deg)	Constituents
M(2)	1.071	113.9	1.302	117.1	1.323	123.0	M(2)
S(2)	.123	131.1	.148	154.4	.178	155.5	S(2)
N(2)	.176	113.2	.227	101.9	.239	107.0	N(2)
K(1)	.181	230.3	.197	233.9	.207	238.9	K(1)
M(4)	.103	105.4	.160	129.5	.206	139.8	M(4)
O(1)	.162	268.8	.173	255.5	.158	257.3	O(1)
M(6)	.072	026.7	.036	077.0	.076	099.0	M(6)
MK(3)	.023	194.8	.054	198.6	.064	206.9	MK(3)
S(4)			.005	194.3	.003	229.6	S(4)
MN(4)	.029	086.4	.059	114.5	.071	123.5	MN(4)
NU(2)			.072	096.7	.054	108.1	NU(2)
S(6)			.002	267.4	.002	041.5	S(6)
MU(2)	.145	145.5	.056	219.7	.040	230.5	MU(2)
2N(2)			.033	022.9	.046	350.9	2N(2)
OO(1)			.006	231.8	.012	212.7	OO(1)
LAM(2)			.049	106.1	.059	120.1	LAM(2)
S(1)			.072	176.4	.065	184.2	S(1)
M(1)			.014	307.1	.012	342.8	M(1)
J(1)			.007	033.0	.014	059.4	J(1)
Mm			.034	087.8	.112	153.1	Mm
MSf			.169	358.2	.039	298.2	MSf
Mf			.133	013.1	.319	350.7	Mf
RHO(1)			.008	029.2	.018	058.0	RHO(1)
Q(1)			.008	242.1	.015	301.2	Q(1)
T(2)			.005	345.3	.016	291.2	T(2)
R(2)			.029	197.8	.045	188.8	R(2)
2Q(1)			.013	280.6	.012	219.7	2Q(1)
P(1)			.024	219.1	.021	250.1	P(1)
2SM(2)			.011	269.0	.026	284.2	2SM(2)
M(3)	.007	245.2	.016	274.5	.020	295.8	M(3)
L(2)	.078	140.1	.128	104.7	.121	117.2	L(2)
2MK(3)	.026	185.8	.060	214.1	.067	224.3	2MK(3)
K(2)			.047	137.0	.041	166.3	K(2)
M(8)	.015	027.8	.008	054.1	.044	114.6	M(8)
MS(4)	.022	087.0	.033	168.9	.049	175.0	MS(4)
	(K1+O1)/(M2+S2) = .287		(K1+O1)/(M2+S2) = .255		(K1+O1)/(M2+S2) = .243		

* Kappa prime at Longitude 75^{o} W.

SUMMARY OF HARMONIC CONSTANTS FOR TIDES

Station No.	8638610	8638660	8638863
Name	HAMPTON ROADS, VA	PORTSMOUTH, VA	CHES BAY BR TUNNEL, VA
Lat. (N)	36/56.8	36/49.3	36/58.0
Long. (W)	76/19.9	76/17.6	76/06.8
Series Beg.	01/01/81	01/01/80	01/01/80
Length of Analysis (Days)	365	366	366
Corrected Using Sta. No.			

Constituents	Amp (Ft)	Phase* (Deg)	Amp (Ft)	Phase* (Deg)	Amp (Ft)	Phase* (Deg)	Constituents
M(2)	1.169	263.3	1.304	268.7	1.239	235.3	M(2)
S(2)	.210	287.4	.232	293.7	.228	255.9	S(2)
N(2)	.251	246.0	.288	252.3	.280	218.1	N(2)
K(1)	.170	127.9	.186	125.5	.196	109.1	K(1)
M(4)	.010	035.8	.025	092.6	.015	273.1	M(4)
O(1)	.145	152.8	.134	154.0	.143	135.8	O(1)
M(6)	.007	281.3	.011	009.6	.021	215.2	M(6)
MK(3)	.010	214.3	.013	225.8	.005	138.6	MK(3)
S(4)	.009	046.2	.015	060.7	.011	335.6	S(4)
MN(4)	.006	038.2	.018	051.2	.011	279.7	MN(4)
NU(2)	.058	247.0	.050	239.1	.055	210.0	NU(2)
S(6)	.003	196.9	.008	269.7	.006	118.6	S(6)
MU(2)	.026	288.6	.036	288.9	.043	234.9	MU(2)
2N(2)	.028	235.1	.021	260.2	.031	212.8	2N(2)
OO(1)	.009	111.9	.022	090.7	.022	077.9	OO(1)
LAM(2)	.021	269.1	.019	283.7	.015	242.9	LAM(2)
S(1)	.029	034.7	.039	022.7	.033	011.2	S(1)
M(1)	.008	151.1	.003	055.9	.005	063.3	M(1)
J(1)	.012	143.3	.014	150.2	.013	129.8	J(1)
Mm	.030	286.8	.094	205.1	.092	211.0	Mm
MSf	.195	069.7	.064	305.8	.057	302.2	MSf
Mf	.164	089:6	.126	245.5	.125	245.3	Mf
RHO(1)	.014	159.2	.004	116.3	.007	118.2	RHO(1)
Q(1)	.031	145.4	.031	150.9	.034	127.0	Q(1)
T(2)	.025	282.3	.026	268.6	.021	227.7	T(2)
R(2)	.007	120.8	.017	203.0	.011	148.0	R(2)
2Q(1)	.016	122.2	.007	329.3	.005	003.7	2Q(1)
P(1)	.043	131.2	.055	121.1	.061	108.1	P(1)
2SM(2)	.001	186.7	.006	263.0	.007	247.9	2SM(2)
M(3)	.010	280.9	.012	295.5	.009	227.4	M(3)
L(2)	.055	261.2	.056	278.2	.030	258.8	L(2)
2MK(3)	.014	242.5	.012	269.6	.005	270.1	2MK(3)
K(2)	.054	285.2	.066	294.9	.061	258.0	K(2)
M(8)	.001	256.8			.002	154.3	M(8)
MS(4)	.006	262.0	.006	250.3	.011	205.8	MS(4)

(K1+O1)/(M2+S2) = .228 (K1+O1)/(M2+S2) = .208 (K1+O1)/(M2+S2) = .231

* Kappa prime at Longitude 75° W.

SUMMARY OF HARMONIC CONSTANTS FOR TIDES

Station No.	8638905	8639168	2600000
Name	LYNNHAVEN FISH PIER, VA	VIRGINIA BEACH, VA	CHESAPEAKE LT
Lat. (N)	36/55.0	36/50.6	36/54.3
Long. (W)	76/04.7	75/58.3	75/42.8
Series Beg.	01/01/76	01/01/68	09/01/76
Length of Analysis (Days)	235	366	114
Corrected Using Sta. No.			8638863

Constituents	Amp (Ft)	Phase* (Deg)	Amp (Ft)	Phase* (Deg)	Amp (Ft)	Phase* (Deg)	Constituents
M(2)	1.308	232.1	1.588	218.5	1.651	230.5	M(2)
S(2)	.259	253.9	.319	237.2	.313	244.8	S(2)
N(2)	.318	218.3	.385	203.8	.423	215.2	N(2)
K(1)	.179	101.2	.240	100.4	.234	109.7	K(1)
M(4)	.020	283.8	.018	298.2	.018	317.8	M(4)
O(1)	.162	139.4	.189	132.1	.190	133.6	O(1)
M(6)	.013	224.2	.021	210.0	.010	249.3	M(6)
MK(3)	.007	110.7	.002	206.0	.006	145.4	MK(3)
S(4)	.008	346.5	.017	294.1			S(4)
MN(4)	.013	271.6	.014	261.4	.010	233.5	MN(4)
NU(2)	.053	203.7	.073	202.6			NU(2)
S(6)	.003	114.0	.007	015.7			S(6)
MU(2)	.051	235.4	.061	212.5	.081	210.3	MU(2)
2N(2)	.042	208.1	.054	194.8			2N(2)
OO(1)	.017	095.3	.009	119.5			OO(1)
LAM(2)	.007	162.3	.010	207.1			LAM(2)
S(1)			.026	023.0			S(1)
M(1)	.012	108.6	.014	131.4			M(1)
J(1)	.020	150.8	.022	114.4			J(1)
Mm	.136	255.0	.094	182.1			Mm
MSf	.051	294.1	.081	047.5			MSf
Mf	.079	305.3	.071	178.8			Mf
RHO(1)	.022	129.4	.015	136.4			RHO(1)
Q(1)	.041	117.0	.041	120.6			Q(1)
T(2)			.032	211.0			T(2)
R(2)			.010	102.6			R(2)
2Q(1)	.008	145.6	.010	216.6			2Q(1)
P(1)	.065	115.6	.084	106.2			P(1)
2SM(2)	.010	294.9	.008	235.7			2SM(2)
M(3)	.012	213.7	.015	189.3	.025	217.6	M(3)
L(2)	.054	210.7	.039	189.4	.062	224.6	L(2)
2MK(3)	.005	188.8	.004	077.3			2MK(3)
K(2)	.076	246.7	.084	233.8			K(2)
M(8)	.001	193.2			.004	136.7	M(8)
MS(4)	.014	206.0	.014	165.9	.018	171.3	MS(4)

(K1+O1)/(M2+S2) = .218 (K1+O1)/(M2+S2) = .224 (K1+O1)/(M2+S2) = .216

* Kappa prime at Longitude 75° W.

APPENDIX C

SUMMARY OF CURRENT METER STATIONS

SUMMARY OF CURRENT METER STATIONS

Sta No.	Location Lat (N)	Location Long (W)	Depth at MLW (ft)	Meter Ht Above Bottom (ft)	Meter Ht/Dpth Ratio	Series Begins (date)	Length of Series (days)	Harmonic Analysis (days)
1	37-53.23	76-11.90	11.6	5	.43	09/09/81	15	15
2	37-52.75	76-09.12	73.0	58	.79	09/09/81	34	29
2	37-52.63	76-09.08	73.6	58	.78	10/13/81	34	29
3	37-52.65	76-07.08	38.6	24	.63	09/09/81	34	29
4	37-52.67	76-05.30	29.5	15	.51	09/08/81	14	None
5	37-52.83	76-02.65	10.9	5	.46	09/08/81	16	15
6	37-54.50	75-57.42	94.5	80	.85	09/09/81	36	29
6	37-54.07	75-57.50	94.9	79	.83	10/14/82	19	15
7	37-54.87	75-47.92	11.5	5	.43	09/02/81	27	15
8	37-58.12	76-23.50	15.4	5	.32	09/24/81	20	15
9	37-59.87	76-21.75	37.9	24	.62	09/23/81	35	29
10	38-00.80	76-20.62	52.5	38	.72	09/08/81	69	29
10	38-00.80	76-20.62	52.5	38	.72	10/14/82	34	29
11	38-01.25	76-19.45	47.8	33	.68	09/23/81	34	29
12	38-02.30	76-17.50	36.0	19	.53	11/16/81	16	15
13	38-00.88	76-12.12	63.5	48	.76	10/13/81	17	15
13	38-00.88	76-12.12	64.0	48	.75	11/16/81	15	15
14	38-00.45	76-07.28	37.0	19	.51	10/13/81	17	15
15	38-00.05	75-54.52	97.9	83	.85	09/09/81	21	15
16	38-03.45	76-01.93	14.8	5	.34	09/25/81	19	15
17	38-02.93	75-51.45	17.5	5	.29	11/12/81	19	15
18	38-05.82	75-53.48	25.3	5	.20	11/12/81	16	15
19	38-08.43	76-18.13	22.6	5	.22	10/29/81	15	15
20	38-08.38	76-15.67	44.0	29	.66	10/14/81	30	29
21	38-08.13	76-13.75	97.0	82	.84	10/14/81	30	29
22	38-08.38	76-09.80	26.0	10	.38	11/13/81	17	15
23	38-08.67	76-06.87	17.8	5	.28	11/03/81	10	None
24	38-08.45	75-58.33	47.3	32	.68	10/30/81	32	29
25	38-13.05	76-03.83	21.0	7	.33	11/13/81	17	15
27	38-12.80	75-54.02	14.8	5	.34	11/12/81	18	15
28	38-13.48	75-59.37	24.7	10	.40	11/12/81	18	15
29	38-15.80	75-55.43	42.3	24	.57	11/12/81	18	15
31	38-13.25	76-06.20	22.9	8	.35	10/29/81	15	15
36	38-18.73	76-18.75	56.9	40	.70	06/17/83	171	29*
37	37-04.85	75-58.83	24.7	10	.40	05/12/82	12	None
38	37-03.37	75-58.33	33.3	17	.51	05/12/82	22	15
39	37-01.40	75-59.55	19.9	5	.26	05/12/82	34	29
40	36-58.77	75-59.98	42.0	27	.64	03/29/82	330	330 & 29**

* Harmonic analysis of 29 day series beginning 06/17/83 is most representative of 171 day period.

** Harmonic analysis of 29 day series beginning 12/17/83 is most representative of 330 day period.

SUMMARY OF CURRENT METER STATIONS

Sta No.	Location Lat (N)	Long (W)	Depth at MLW (ft)	Meter Ht Above Bottom (ft)	Meter Ht/Dpth Ratio	Series Begins (date)	Length of Series (days)	Harmonic Analysis (days)
41	36-57.53	76-00.68	61.8	47	.76	05/12/82	34	29
42	36-56.33	75-59.98	46.1	31	.67	05/12/82	22	15
43	37-06.10	76-00.33	29.8	14	.47	05/11/82	22	15
44	37-03.73	76-05.58	46.5	28	.60	11/03/82	15	15
45	36-58.73	76-07.57	53.2	38	.71	05/11/82	22	15
47	36-56.05	76-10.60	23.1	8	.36	05/12/82	21	15
48	37-00.32	76-13.60	51.4	36	.70	06/02/82	16	15
49	37-00.12	76-17.72	94.0	81	.86	06/02/82	16	15
50	36-59.42	76-18.23	51.9	37	.71	06/16/82	20	15
52	36-57.03	76-20.32	50.3	37	.74	06/16/82	14	None
55	37-07.38	76-09.20	40.5	27	.67	06/02/82	34	29
56	37-09.37	76-01.60	22.9	9	.39	06/17/82	19	15
57	37-15.95	76-05.95	101.3	87	.86	04/26/82	15	15
57	37-15.87	76-05.62	102.5	86	.84	11/08/82	22	15
58	37-17.40	76-11.45	41.5	26	.63	04/26/82	15	15
59	37-13.55	76-18.47	37.9	23	.61	06/15/82	15	15
59	37-13.55	76-18.47	37.0	23	.62	07/22/82	18	15
60	37-14.80	76-23.28	53.9	40	.75	06/14/82	37	29
61	37-14.28	76-24.13	36.5	22	.60	07/06/82	15	15
62	37-17.70	76-19.25	24.5	9	.37	06/15/82	15	15
63	37-25.00	76-12.90	18.5	5	.32	07/21/82	19	15
64	37-24.67	76-10.90	32.3	17	.53	04/27/82	13	None
64	37-24.67	76-10.57	31.3	16	.51	07/07/82	33	29
65	37-24.80	76-07.40	41.2	26	.63	02/24/83	286	29*
66	37-24.50	76-04.80	72.3	56	.77	04/08/82	32	None
66	37-24.50	76-05.00	71.2	56	.79	07/07/82	33	29
67	37-24.50	76-03.83	37.4	23	.61	07/07/82	33	29
68	37-24.20	76-00.78	20.6	5	.25	07/07/82	33	29
69	37-29.97	75-59.37	21.2	8	.38	07/21/82	20	15
70	37-29.90	76-06.40	37.0	23	.62	06/01/82	70	29
71	37-30.03	76-14.70	21.6	6	.28	07/21/82	20	15
73	37-34.53	76-17.08	28.2	8	.28	08/09/82	16	15
74	37-36.00	76-17.50	43.8	28	.64	04/09/82	32	29
75	37-35.30	76-11.50	43.3	29	.67	08/10/82	15	15
76	37-34.60	76-03.80	41.2	27	.66	08/10/82	15	15
77	37-35.45	75-58.10	25.5	9	.35	08/10/82	15	15
79	37-39.85	76-00.52	45.9	33	.72	08/11/82	15	15
80	37-40.70	76-12.25	41.4	28	.68	08/10/82	15	15
80	37-40.70	76-12.25	43.4	28	.65	10/13/82	19	15

* Harmonic analysis of 29 day series beginning 06/20/83 most representative of 286 day period.

SUMMARY OF CURRENT METER STATIONS

Sta No.	Location Lat (N)	Long (W)	Depth at MLW (ft)	Meter Ht Above Bottom (ft)	Meter Ht/Dpth Ratio	Series Begins (date)	Length of Series (days)	Harmonic Analysis (days)
81	37-39.70	76-17.98	25.4	11	.43	08/10/82	15	15
83	37-47.00	76-11.50	100.7	87	.86	10/13/82	34	29
84	37-47.03	76-05.68	36.0	21	.58	11/01/82	16	15
86	37-47.25	75-57.83	102.4	86	.84	10/14/82	34	29
88	37-47.85	75-50.67	90.7	66	.73	10/14/82	21	15
89	37-49.33	76-18.07	20.4	8	.39	08/11/82	15	15
90	39-00.32	76-22.80	47.7	33	.69	07/19/83	50	29
100	38-22.88	76-21.62	47.7	32	.67	10/07/83	31	29
100	38-22.88	76-21.62	47.7	32	.67	11/19/83	16	15
101	38-22.80	76-19.52	102.7	88	.86	10/20/83	39	29
102	38-38.70	76-29.23	32.6	18	.55	09/20/83	16	15
103	38-38.63	76-26.88	39.1	22	.56	09/20/83	16	15
103	38-38.63	76-26.88	39.5	22	.56	11/08/83	20	15
104	38-38.60	76-25.22	82.5	65	.79	10/03/83	17	15
105	38-36.43	76-20.88	31.7	12	.38	09/20/83	16	15
106	38-30.83	76-18.75	50.1	35	.70	10/06/83	40	29
107	38-37.70	76-09.10	28.8	12	.42	10/05/83	20	15
108	38-34.78	76-03.67	40.3	22	.55	10/25/83	16	15
111	38-45.10	76-29.93	24.7	10	.40	09/21/83	15	15
112	38-44.98	76-26.73	52.9	38	.72	09/21/83	15	15
113	38-45.37	76-25.77	97.2	83	.85	09/08/83	40	29
114	38-50.33	76-20.25	38.9	24	.62	08/04/83	35	29
115	38-50.57	76-18.13	23.4	10	.43	08/22/83	17	15
116	38-52.50	76-15.08	41.6	27	.65	08/04/83	35	29
119	38-53.88	76-28.23	16.9	5	.30	07/19/83	12	None
120	38-53.62	76-25.83	38.4	22	.57	07/19/83	16	15
121	38-53.75	76-23.28	78.5	57	.73	11/09/82	198	29*
122	38-57.63	76-27.05	20.3	5	.25	07/20/83	15	15
123	39-02.05	76-16.07	20.5	5	.24	07/19/83	50	29
124	39-00.63	76-10.95	44.9	29	.65	07/19/83	15	15
127	39-05.68	76-23.58	42.0	24	.57	07/19/83	31	29
128	39-06.48	76-18.32	31.8	18	.57	07/19/83	31	29
129	39-08.85	76-19.48	32.2	14	.43	06/30/83	34	29
130	39-10.70	76-26.65	20.3	5	.25	06/15/83	33	29
137	39-13.03	76-14.90	39.4	25	.63	06/15/83	33	29
138	39-14.78	76-17.80	20.7	6	.29	06/15/83	33	29
139	39-18.70	76-13.03	24.8	8	.32	06/15/83	33	29
140	39-22.23	76-07.80	31.1	16	.51	05/13/83	18	15
143	39-23.78	76-03.02	23.3	9	.39	05/13/83	31	29
144	39-26.60	76-02.03	14.0	5	.36	05/11/83	14	None

* Harmonic analysis of 29 day series beginning 05/02/83.

SUMMARY OF CURRENT METER STATIONS

Sta No.	Location Lat (N)	Location Long (W)	Depth at MLW (ft)	Meter Ht Above Bottom (ft)	Meter Ht/Dpth Ratio	Series Begins (date)	Length of Series (days)	Harmonic Analysis (days)
145	39-30.08	76-05.00	14.7	5	.35	05/10/83	30	29
146	39-32.33	76-04.80	15.0	5	.33	04/13/83	42	29
151	39-30.23	75-55.12	38.4	21	.55	04/12/83	55	29
152	39-31.67	75-51.97	34.0	26	.76	05/12/83	19	15
153	39-33.17	75-39.00	43.0	25	.58	04/12/83	14	None
154	39-33.62	75-34.20	42.6	24	.56	04/12/83	15	None
154	39-33.62	75-34.20	37.8	28	.74	09/07/83	15	None
155	39-33.05	75-32.58	48.7	32	.66	04/26/83	49	None
159	39-30.88	75-32.97	43.3	30	.69	05/11/83	34	None
160	39-34.37	75-33.27	36.2	20	.55	04/26/83	28	None
161	39-32.55	75-42.15	42.6	26	.61	04/12/83	30	None
162	39-31.67	75-48.43	46.3	20	.43	04/12/83	30	None
163	39-29.30	75-59.85	13.7	5	.36	05/12/83	13	None
164	39-11.47	76-15.95	27.9	13	.47	06/29/83	19	None
165	39-11.57	76-17.22	20.3	5	.25	06/15/83	27	15
166	39-10.95	76-16.87	35.1	18	.51	06/15/83	33	29
167	38-37.63	76-08.15	35.9	18	.50	10/25/83	13	None
168	38-36.23	76-06.87	12.3	5	.41	09/20/83	35	None
169	38-28.03	76-22.60	71.6	57	.79	10/07/83	31	29
170	38-22.52	76-17.92	20.7	5	.24	10/20/83	39	29
171	38-19.08	76-24.07	46.4	33	.73	10/07/83	31	29
172	39-09.78	76-23.38	21.7	8	.37	06/15/83	15	15
173	39-16.97	76-13.57	21.8	6	.28	06/15/83	33	15*
174	38-40.43	76-15.45	19.1	5	.26	09/21/83	15	15
175	39-00.22	76-20.93	45.6	31	.68	06/29/83	36	29
176	39-02.42	76-22.67	42.6	28	.66	07/19/83	15	15

* Harmonic analysis of 15 day series beginning 06/29/83.

APPENDIX D

SUMMARY OF PRINCIPAL HARMONIC CONSTANTS FOR TIDAL CURRENTS

SUMMARY OF PRINCIPAL HARMONIC CONSTANTS FOR TIDAL CURRENTS

	M_2					S_2					N_2					K_1					O_1				
Sta No.	Major Dir (°T)	Speed (cm/sec) Major	Speed (cm/sec) Minor	Major Phase (°)	Rot	Major Dir (°T)	Speed (cm/sec) Major	Speed (cm/sec) Minor	Major Phase (°)	Rot	Major Dir (°T)	Speed (cm/sec) Major	Speed (cm/sec) Minor	Major Phase (°)	Rot	Major Dir (°T)	Speed (cm/sec) Major	Speed (cm/sec) Minor	Major Phase (°)	Rot	Major Dir (°T)	Speed (cm/sec) Major	Speed (cm/sec) Minor	Major Phase (°)	Rot
1	359	39.397	0.567	318	C	354	7.902	0.221	342	C	359	7.643	0.137	304	C	002	16.390	0.621	181	CC	004	11.189	0.056	153	C
2	347	28.326	1.824	001	CC	335	4.533	0.480	013	CC	349	6.004	1.450	339	CC	351	9.314	0.105	214	CC	351	8.930	0.508	196	C
2	355	29.492	2.418	001	CC	351	4.702	1.027	014	CC	353	5.901	1.798	352	CC	351	9.122	0.217	221	C	359	7.649	0.261	197	C
3	348	26.501	1.512	355	CC	351	3.262	0.190	022	CC	345	4.851	0.055	349	CC	344	7.950	0.228	211	C	348	6.862	0.035	195	CC
5	356	17.607	1.690	315	CC	355	3.499	0.152	327	CC	357	3.411	0.377	309	CC	348	6.235	0.323	180	C	354	4.973	0.234	145	CC
6	349	32.105	0.482	344	CC	347	5.062	0.159	006	C	346	6.262	0.214	314	CC	351	5.727	0.430	170	CC	344	5.758	0.207	170	CC
6	352	35.984	1.579	347	CC	350	7.890	0.014	007	CC	353	6.973	0.455	336	CC	346	5.057	1.024	187	CC	358	4.241	1.218	132	CC
7	027	15.900	1.789	282	CC	028	3.445	0.213	307	CC	026	3.074	0.433	268	CC	036	1.423	0.334	109	C	051	1.380	0.042	106	CC
8	291	4.680	0.315	313	CC	295	1.245	0.088	333	C	290	0.902	0.122	303	CC	275	1.617	0.930	311	C	306	1.180	0.155	034	CC
9	297	17.695	2.244	352	C	303	3.056	0.631	014	C	294	3.365	0.301	312	C	321	2.217	0.114	172	CC	297	1.937	0.050	179	CC
10	297	21.266	0.407	356	C	284	4.272	0.467	019	CC	296	3.633	1.423	342	CC	325	2.936	0.613	152	CC	301	2.842	0.890	150	C
10	301	18.990	1.338	356	C	292	4.395	0.458	016	C	303	2.725	0.497	342	CC	271	1.890	1.140	044	C	342	2.172	1.028	137	C
11	284	27.145	3.474	335	C	278	4.942	0.488	350	C	284	5.041	0.956	308	C	314	2.615	0.352	203	CC	317	2.227	0.145	192	C
12	345	11.236	8.564	037	C	000	2.319	1.205	069	CC	339	2.215	1.614	023	C	002	7.373	0.610	189	C	001	6.279	1.538	200	C
13	341	21.477	0.348	007	C	339	3.057	0.234	043	CC	341	4.159	0.256	348	C	343	10.157	0.111	201	CC	349	6.074	0.188	174	C
13	339	22.918	1.680	016	CC	328	3.188	0.072	045	CC	339	4.435	0.458	001	CC	339	6.962	0.027	202	CC	339	6.153	0.109	211	CC
14	010	22.920	1.775	332	CC	009	4.257	0.032	011	C	009	4.429	0.527	311	CC	007	4.141	0.350	159	C	015	3.504	0.110	138	C
15	007	34.333	0.461	346	CC	002	5.941	0.104	014	C	006	6.651	0.374	330	CC	013	6.636	1.555	175	C	011	5.776	0.179	344	CC
16	093	35.311	0.638	278	C	096	5.243	0.225	304	C	094	6.851	0.104	264	C	092	6.727	0.365	040	C	102	3.116	0.281	031	CC
17	077	14.432	0.263	305	CC	094	3.004	0.380	333	C	079	2.768	0.421	290	CC	091	0.964	0.115	137	CC	083	1.623	0.082	155	C
18	013	18.951	0.606	322	CC	009	2.856	0.446	323	CC	013	3.674	0.185	322	C	012	0.808	0.279	155	C	019	2.719	0.092	139	C
19	355	19.145	0.128	017	C	343	2.450	0.223	047	CC	355	3.713	0.097	002	C	004	6.540	0.007	185	C	356	6.990	0.515	200	C
20	345	17.513	0.734	036	CC	342	2.883	0.317	052	CC	336	3.477	0.394	021	C	346	8.098	0.113	204	C	355	6.583	0.209	207	C
21	350	14.284	1.660	038	CC	343	2.306	0.359	063	CC	006	3.163	0.669	005	CC	355	6.011	0.331	215	CC	351	5.523	0.270	220	CC
22	345	14.207	4.206	014	CC	329	2.301	1.024	049	CC	345	2.755	0.822	000	CC	349	5.017	0.259	191	C	345	4.044	0.679	222	C
24	000	33.207	1.279	345	CC	000	4.407	0.122	005	CC	000	7.174	0.866	321	CC	359	3.274	0.088	145	C	355	2.720	0.003	167	CC
25	102	38.881	1.410	286	C	101	7.485	0.093	317	C	102	7.539	0.365	269	C	107	3.413	0.168	038	C	103	3.774	0.501	049	C
27	074	33.797	0.410	346	C	070	3.865	0.542	358	C	074	6.552	0.270	338	CC	074	1.686	0.080	138	CC	074	1.739	0.503	149	C
28	315	23.495	4.335	008	CC	311	3.797	0.822	018	CC	315	4.572	0.762	004	CC	312	2.670	0.132	169	CC	305	2.531	0.526	183	CC
29	359	47.960	0.989	005	CC	358	7.496	0.338	006	CC	000	9.303	0.234	005	CC	000	3.642	0.090	151	CC	002	3.917	0.281	169	C
31	044	27.779	3.863	305	CC	052	4.598	0.651	322	CC	044	5.392	0.730	295	CC	067	2.690	0.291	049	CC	067	2.149	0.657	070	CC
36	351	24.775	0.919	066	C	000	3.544	0.263	078	CC	341	5.703	0.689	046	CC	335	10.825	0.134	214	CC	333	6.739	0.556	235	C
38	304	61.567	3.655	229	C	295	11.416	1.390	210	C	304	11.964	0.164	238	C	312	8.361	0.789	098	C	305	5.313	0.242	118	C
39	314	33.398	2.079	223	C	310	8.093	1.830	249	C	317	8.878	0.731	198	C	305	5.360	0.828	100	CC	307	4.083	0.017	141	CC
40*	300	50.3	4.9	243	CC	300	10.7	0.3	255	C	300	12.6	1.5	219	CC	300	7.0	0.4	114	CC	300	5.4	0.6	136	CC
40**	301	48.721	1.393	241	CC	303	11.217	0.779	249	C	300	11.478	0.265	225	C	299	6.861	0.648	124	C	298	3.645	1.189	128	CC
41	292	56.747	2.540	258	C	281	12.137	0.535	011	C	288	17.100	0.201	230	C	284	13.731	0.481	135	CC	294	10.089	1.939	159	CC
42	294	68.181	4.190	249	C	292	13.116	0.542	271	C	294	13.336	0.933	237	C	295	14.559	0.969	137	C	309	10.482	1.554	118	C
43	337	64.548	3.087	234	CC	331	9.448	1.991	235	C	338	12.370	2.039	231	CC	342	9.329	0.531	102	CC	336	7.260	0.264	134	CC
44	328	58.036	8.848	256	C	329	8.863	1.644	280	C	327	11.290	1.497	243	C	327	1.735	0.143	162	C	330	9.294	0.406	135	CC
45	304	49.531	5.094	249	C	293	12.328	1.710	269	C	304	9.639	0.636	236	C	289	13.511	0.777	167	C	300	12.315	3.164	141	C
47	277	21.508	0.979	210	C	277	10.571	1.103	124	CC	275	4.154	0.437	255	C	257	3.304	0.175	165	CC	255	4.413	0.027	114	C
48	294	48.349	12.37	245	C	286	10.367	2.003	257	C	294	9.380	2.398	236	C	291	6.084	1.659	080	C	286	7.753	1.764	109	C
49	235	77.642	11.91	217	C	241	14.479	0.081	270	CC	236	14.814	3.574	188	C	236	6.983	0.937	072	C	233	5.375	0.697	107	CC
50	248	79.215	0.302	211	CC	262	12.739	1.628	185	CC	249	15.242	1.960	222	C	244	4.730	0.542	056	C	258	3.844	0.595	076	C
55	343	50.026	15.16	275	C	337	8.773	1.421	287	C	324	11.541	3.517	245	C	352	8.170	0.412	136	C	349	6.360	0.589	180	C
56	346	44.040	1.160	248	CC	351	5.657	2.799	255	C	350	8.394	1.610	243	CC	339	5.398	0.760	114	CC	325	6.160	0.341	134	CC
57	003	49.849	6.432	288	C	000	9.533	1.695	310	C	005	9.688	1.106	279	C	353	14.841	1.622	130	CC	015	7.811	2.136	117	C
57	002	44.427	4.593	291	C	004	4.463	0.485	308	C	001	8.616	0.922	281	C	012	2.338	0.160	148	C	357	9.576	0.944	128	CC
58	020	46.723	13.79	297	C	032	11.957	1.607	308	C	015	8.832	3.363	291	C	018	10.777	0.117	151	CC	025	4.354	1.491	099	C
59	300	27.779	6.196	219	C	300	3.990	0.362	229	C	298	5.297	1.557	213	C	330	1.323	0.075	054	C	310	3.145	0.955	084	C
59	298	26.573	6.988	218	C	304	3.784	0.517	248	C	297	5.054	1.696	202	C	021	0.717	0.035	095	CC	332	2.224	0.172	105	C

* See expanded list of tidal constituents in Appendix E (based on harmonic analysis of 300 day series beginning 03/30/82).

** Result of harmonic analysis of 29 day series beginning 12/17/81.

SUMMARY OF PRINICPAL HARMONIC CONSTANTS FOR TIDAL CURRENTS

Sta	M_2					S_2					N_2					K_1					O_1				
No.	Major Dir (°T)	Speed (cm/sec) Major	Speed (cm/sec) Minor	Major Phase (°)	Rot	Major Dir (°T)	Speed (cm/sec) Major	Speed (cm/sec) Minor	Major Phase (°)	Rot	Major Dir (°T)	Speed (cm/sec) Major	Speed (cm/sec) Minor	Major Phase (°)	Rot	Major Dir (°T)	Speed (cm/sec) Major	Speed (cm/sec) Minor	Major Phase (°)	Rot	Major Dir (°T)	Speed (cm/sec) Major	Speed (cm/sec) Minor	Major Phase (°)	Rot
60	262	33.074	0.357	232	C	256	6.690	0.685	264	C	261	6.777	0.047	212	C	251	2.559	0.572	054	CC	262	3.482	0.016	098	CC
61	251	35.652	0.377	239	CC	257	5.407	0.023	260	CC	251	6.916	0.090	227	CC	228	1.960	0.649	068	CC	227	2.201	0.194	079	CC
62	313	23.124	0.973	174	CC	304	2.303	0.474	195	CC	313	4.484	0.231	165	C	327	2.399	0.295	352	C	331	1.917	0.160	057	C
63	349	28.774	2.533	260	C	346	4.673	0.960	271	C	348	5.596	0.305	254	C	025	3.473	0.412	107	CC	024	3.112	1.938	124	CC
64	000	53.119	2.097	293	C	349	5.672	0.177	307	C	354	10.951	0.803	269	C	000	10.132	2.446	154	CC	005	8.582	1.006	186	CC
65	004	53.482	6.774	308	C	012	9.230	0.631	337	CC	009	11.576	1.254	279	C	012	9.492	1.720	153	CC	024	5.531	1.258	178	C
66	009	57.404	9.435	308	C	021	6.911	0.035	323	CC	014	12.986	2.457	282	C	355	8.598	2.428	168	CC	357	9.055	0.146	185	CC
67	010	53.787	7.882	304	C	014	7.401	0.177	329	CC	015	11.621	2.312	273	C	003	6.150	2.202	153	CC	350	5.289	0.114	169	CC
68	358	25.592	2.732	275	CC	013	2.809	1.097	288	CC	002	5.251	0.980	269	CC	340	2.337	1.342	135	CC	359	2.442	0.578	135	CC
69	355	31.696	2.920	293	CC	010	6.851	2.311	291	CC	353	6.173	0.143	291	CC	340	4.988	2.889	161	CC	335	6.468	2.703	174	CC
70	358	47.065	4.142	311	C	010	6.680	0.843	323	CC	004	9.082	0.411	276	CC	010	9.020	0.015	144	C	000	6.791	0.430	188	CC
71	333	25.236	3.558	272	CC	339	5.308	0	272	C	334	4.832	1.049	273	CC	353	2.851	1.490	082	CC	339	3.579	0.529	123	CC
73	298	21.464	0.558	256	CC	317	4.264	0.096	280	CC	298	4.164	0.124	242	CC	276	1.423	0.403	019	C	261	2.108	0.237	020	C
74	286	28.910	1.778	288	CC	279	5.932	0.322	315	CC	279	7.683	0.242	278	CC	263	3.786	0.952	101	C	283	2.377	0.407	131	C
75	354	37.427	0.809	315	C	007	4.613	0.389	335	CC	001	7.221	0.775	304	CC	351	6.857	1.053	183	CC	353	6.237	0.561	204	CC
76	001	43.795	5.457	319	C	002	6.480	0.666	346	C	000	8.495	1.066	305	C	023	7.513	1.916	141	CC	002	3.833	0.665	181	C
77	017	31.460	5.566	287	CC	010	2.295	1.297	313	CC	019	6.190	0.323	274	CC	027	2.324	0.236	135	CC	027	2.418	0.558	138	CC
79	024	30.122	4.276	308	CC	034	4.565	0.459	323	CC	024	5.816	1.004	300	CC	019	4.872	1.350	143	CC	024	3.212	0.850	143	CC
80	357	23.752	3.150	077	C	356	3.578	0.146	137	C	000	4.601	0.662	045	CC	021	4.982	0.024	220	C	000	3.181	1.161	224	CC
80	359	23.397	2.351	325	C	003	4.493	0.630	347	C	357	4.544	0.402	313	C	353	5.396	0.648	214	C	345	3.721	1.221	138	CC
81	324	5.156	0.165	264	C	312	1.980	0.392	281	C	324	0.999	0.051	252	CC	316	2.771	0.944	303	C	353	0.346	0.304	204	C
83	005	24.091	0.647	342	C	003	3.307	0.340	349	C	009	6.010	0.696	327	CC	015	6.456	1.633	222	C	009	4.097	0.324	188	CC
84	356	29.381	3.318	344	CC	358	4.319	0.629	006	CC	356	5.706	0.593	333	CC	351	7.305	0.247	227	C	353	7.456	0.574	174	CC
86	019	46.562	2.943	315	CC	021	9.494	0.479	328	CC	028	8.326	1.333	294	CC	013	4.286	0.147	147	CC	023	4.587	0.502	142	CC
88	028	45.990	1.173	298	CC	031	9.711	0.220	317	C	028	8.922	0.249	288	CC	023	5.125	0.683	118	CC	017	4.035	0.578	101	CC
89	344	9.134	0.063	259	CC	341	1.980	0.012	283	CC	344	1.772	0.014	246	CC	357	1.138	0.312	001	CC	332	0.332	0.015	088	CC
90	027	43.216	1.824	146	CC	019	6.523	2.048	170	CC	040	5.844	0.973	132	CC	017	14.190	1.025	185	CC	019	8.492	0.297	191	CC
100	347	29.986	0.616	069	C	348	5.284	0.322	082	C	344	7.526	0.364	038	C	351	12.368	0.671	224	CC	345	10.978	0.065	219	CC
100	344	30.790	0.216	064	C	339	5.827	0.314	082	CC	344	5.970	0.200	054	C	342	7.784	0.081	234	CC	342	7.097	0.512	209	C
101	347	27.448	0.633	068	C	349	4.263	0.153	086	C	351	5.311	0.221	041	C	349	13.445	0.249	222	CC	344	7.087	0.335	220	C
102	352	16.441	0.009	097	CC	001	3.901	0.042	124	C	359	3.160	0.430	082	CC	349	9.378	0.188	188	CC	356	3.680	0.228	209	CC
103	358	17.910	0.375	099	C	008	3.442	0.126	121	CC	359	3.472	0.149	087	CC	002	11.772	0.208	189	CC	003	4.305	0.336	222	CC
103	002	17.613	0.320	101	C	354	3.023	0.097	124	CC	359	3.416	0.104	089	C	006	7.358	0.358	227	C	005	1.953	0.307	190	CC
104	000	17.544	1.809	101	CC	005	2.738	0.320	112	CC	358	3.406	0.329	095	CC	358	7.943	0.051	237	CC	001	6.007	0.372	228	CC
105	031	31.202	1.933	053	CC	033	6.125	0.127	091	CC	031	6.043	0.510	032	CC	032	9.501	0.383	155	CC	038	3.865	0.266	179	CC
106	057	26.311	1.274	033	CC	058	4.374	0.278	042	CC	056	5.887	0.701	351	CC	053	2.229	0.171	187	C	051	2.652	0.069	184	CC
107	146	20.913	0.976	048	CC	149	3.325	0.455	037	CC	146	4.061	0.022	053	C	144	4.148	0.670	210	CC	133	3.765	0.155	205	CC
108	136	16.014	0.201	075	C	142	1.473	0.145	117	CC	136	3.098	0.229	052	C	141	1.648	0.091	232	CC	139	2.218	0.106	240	CC
111	358	12.366	0.509	106	CC	351	2.157	0.370	127	CC	358	2.399	0.101	097	CC	348	6.490	1.323	198	CC	353	3.009	0.071	213	C
112	003	20.430	0.258	119	C	010	3.583	0.154	136	CC	002	3.962	0.100	110	C	009	11.207	0.994	190	CC	000	3.685	0.106	231	C
113	001	23.663	0.328	125	CC	004	3.508	0.297	138	CC	008	6.318	0.563	105	C	007	12.483	1.384	207	CC	006	5.507	0.068	208	CC
114	046	17.577	1.051	052	CC	047	2.937	0.464	075	CC	056	3.612	0.654	025	CC	030	3.349	1.018	207	CC	032	2.623	0.399	221	C
115	041	16.016	2.197	043	CC	041	3.460	0.375	085	CC	041	3.100	0.473	020	CC	060	2.040	0.678	197	CC	021	1.833	0.340	218	C
116	105	13.714	1.957	342	CC	072	2.009	0.583	336	C	342	5.729	0.395	230	C	100	3.193	0.347	144	C	099	1.648	0.766	144	CC
120	020	40.588	1.361	132	CC	020	9.542	0.236	179	CC	020	7.873	0.299	106	CC	008	11.179	2.648	185	CC	352	6.150	0.523	225	C
121	009	23.573	0.546	138	CC	016	5.044	0.603	172	C	000	5.674	0.458	113	CC	012	6.985	0.413	206	C	007	7.223	0.617	251	C
122	338	7.716	0.433	075	CC	341	1.081	0.454	080	CC	338	1.491	0.160	072	C	246	3.043	0.314	225	CC	193	2.964	1.528	276	CC
123	182	15.808	1.133	113	C	179	3.036	0.391	145	C	173	2.924	0.937	092	C	186	4.976	0.047	184	CC	187	3.437	0.510	227	C
124	354	21.171	1.181	125	CC	019	3.892	0.066	149	C	005	4.103	0.289	111	CC	000	5.294	0.592	206	C	004	2.222	0.375	231	CC
127	002	24.967	2.762	157	CC	346	3.234	0.010	212	C	351	5.183	0.349	142	C	355	7.212	0.210	216	CC	349	3.987	0.682	234	CC
128	359	20.389	1.970	159	CC	358	2.538	0.068	191	CC	008	2.872	1.168	140	CC	002	4.559	1.662	213	C	005	3.644	0.939	225	C

SUMMARY OF PRINCIPAL HARMONIC CONSTANTS FOR TIDAL CURRENTS

	M_2					S_2					N_2					K_1					O_1				
Sta No.	Major Dir (°T)	Speed (cm/sec) Major	Speed (cm/sec) Minor	Major Phase (°)	Rot	Major Dir (°T)	Speed (cm/sec) Major	Speed (cm/sec) Minor	Major Phase (°)	Rot	Major Dir (°T)	Speed (cm/sec) Major	Speed (cm/sec) Minor	Major Phase (°)	Rot	Major Dir (°T)	Speed (cm/sec) Major	Speed (cm/sec) Minor	Major Phase (°)	Rot	Major Dir (°T)	Speed (cm/sec) Major	Speed (cm/sec) Minor	Major Phase (°)	Rot
129	015	30.149	2.774	168	CC	001	3.856	1.037	205	C	020	6.213	1.915	136	CC	000	7.38[illegible]	0.236	226	C	356	4.995	1.197	230	CC
130	314	6.235	0.069	138	CC	259	1.033	0.015	173	CC	293	1.663	0.030	115	C	306	4.04[illegible]	0.391	253	C	302	3.053	0.182	275	CC
137	019	44.475	0.688	183	C	020	4.819	0.893	216	C	018	9.529	0.349	156	CC	020	9.248	0.312	226	C	018	6.460	0.050	228	C
138	050	29.228	4.477	180	C	053	2.451	0.003	234	CC	050	5.897	0.808	157	C	048	5.696	0.065	216	C	042	3.291	0.027	231	C
139	027	43.258	2.718	196	CC	021	5.371	0.437	235	C	626	8.576	0.136	174	CC	022	7.309	0.238	232	CC	019	4.486	0.660	236	CC
140	054	44.590	0.084	200	C	055	6.591	0.194	228	CC	054	8.649	0.162	185	C	050	4.457	0.450	243	C	053	5.876	0.208	265	C
143	033	33.917	1.538	209	CC	034	4.161	0.047	220	C	034	5.676	0.290	199	CC	036	4.570	0.146	247	CC	028	2.768	0.195	297	CC
145	005	16.137	1.079	234	C	003	2.570	0.178	209	C	007	2.976	0.239	244	C	006	9.129	0.157	236	C	009	2.574	0.194	281	C
146	008	3.513	0.246	238	C	003	0.917	0.164	183	C	010	0.492	0.005	184	C	004	3.032	0.034	209	C	008	0.881	0.141	317	C
151	058	53.006	0.496	195	C	059	7.040	0.114	213	C	058	7.405	0.008	163	CC	058	8.148	0.958	332	C	058	7.949	0.781	348	C
152	062	65.563	0.519	195	CC	063	13.904	0.564	256	C	062	12.712	0.442	163	CC	064	12.638	0.037	355	C	062	16.265	0.222	000	C
165	029	29.727	1.426	173	C	036	5.766	0.769	201	C	029	5.773	0.059	159	C	040	4.593	1.020	223	C	034	4.807	1.346	221	C
166	034	40.625	3.983	167	C	068	2.139	0.974	238	C	035	8.012	1.782	135	CC	039	7.826	0.987	209	C	040	5.375	0.229	200	C
169	334	26.568	0.935	073	CC	340	4.731	0.299	087	CC	331	5.632	0.215	038	CC	337	11.785	0.243	224	CC	332	8.786	0.241	220	CC
170	347	16.812	0.173	036	CC	349	2.978	0.057	057	CC	356	3.552	0.128	013	C	349	4.874	0.164	177	C	342	2.278	0.032	177	C
171	254	16.672	1.223	350	C	263	2.246	0.445	019	C	254	2.740	0.258	265	C	284	0.918	0.447	169	CC	269	1.353	0.266	193	CC
172	004	16.911	5.083	149	CC	020	2.669	0.371	143	CC	354	3.293	0.946	154	CC	315	3.890	0.805	227	CC	295	3.945	0.860	241	CC
173	022	45.127	4.587	193	CC	022	3.909	0.291	197	C	020	8.639	1.675	192	CC	023	6.972	0.026	228	C	012	2.847	0.227	245	CC
174	083	8.726	0.120	041	CC	081	1.928	0.218	065	CC	083	1.693	0.032	029	C	092	2.055	0.390	204	CC	067	1.323	0.039	227	CC
175	020	36.804	0.698	154	C	024	4.177	0.039	184	CC	017	5.827	1.717	126	CC	020	12.875	0.292	216	CC	020	7.239	0.201	230	CC
176	359	36.417	1.141	153	C	349	6.721	0.095	188	CC	000	7.063	0.275	133	CC	352	14.612	0.990	193	C	001	6.288	0.779	201	CC

APPENDIX E

SUMMARY OF HARMONIC CONSTANTS FOR LONG TERM CURRENT STATION 40

SUMMARY OF HARMONIC CONSTANTS FOR LONG-TERM CURRENT STATION 40*

Major Direction of Observed Current is 300° T

Constituent	Major Axis Speed (cm/sec)	Major Axis Phase (°)	Minor Axis Speed (cm/sec)	Minor Axis Phase (°)
M_2	50.3	243	4.9	210
S_2	10.7	255	0.3	316
N_2	12.6	219	1.5	216
K_1	7.0	114	0.4	295
M_4	3.7	004	1.0	014
O_1	5.4	136	0.6	028
M_6	0.7	258	0.4	277
MK_3	0.9	215	0.2	144
S_4	0.5	337	0.2	348
MN_4	2.0	341	0.4	323
Nu_2	2.9	213	0.5	184
S_6	0.4	116	0.1	154
Mu_2	2.5	192	0.8	266
$2N_2$	1.8	192	0.2	218
OO_1	0.5	115	0.1	321
Lam_2	0.8	348	0.5	148
S_1	2.3	153	1.3	297
M_1	0.3	321	0.4	181
J_1	1.0	077	0.3	135
Mm	1.8	187	0.9	199
MSf	1.6	202	1.1	190
Mf	0.9	120	0.6	078
Rho_1	0.3	154	0.3	335
Q_1	0.8	107	0.2	057
T_2	1.1	219	0.6	306
R_2	0.7	121	0.5	003
$2Q_1$	0.4	197	0.3	107
P_1	2.8	122	0.1	228
$2MS_2$	0.2	111	0.2	059
M_3	0.9	209	0.3	029
L_2	1.0	319	0.4	182
$2MK_3$	1.1	229	0.4	225
K_2	2.3	263	0.7	144
M_8	0.2	243	0.1	112
MS_4	0.7	022	0.2	354

* Based on a least square harmonic analysis of a 330 day series beginning on 03/29/82.

AUTOBIOGRAPHICAL STATEMENT

Carl W. Fisher

Born:

April 12, 1942 in Canandaigua, New York.

Education:

BS (Meteorology and Oceanography) and Third Mate's License (Oceans Unlimited), State University of New York Maritime College - June 1965.

MS (Physical Oceanography), Oregon State University, Sept. 1969.

Honors:

Phi Kappa Phi, 1984.

Sigma Xi, 1984.

Appointments and Positions:

Commissioned as an Ensign in the National Oceanic and Atmospheric Administration in July 1965, and am presently a Captain in the NOAA Officer Corps.

I have served in the following key assignments in NOAA:
Staff Assistant, National Advisory Committee on Oceans and Atmosphere, 1972.
Chief, Oceanographic Division, National Ocean Service, 1973-1976.
Commanding Officer, NOAA Ship PEIRCE, 1977-1978.
Chief, Operations Division, NOAA Atlantic Marine Center, 1979-1981.
Commanding Officer, NOAA Ship RAINIER, 1985-present.

Publications:

"A Statistical Study of the Relationship of Temperature and Winds During Oregon Coastal Upwelling," MS Thesis, Oregon State University. 1969.

"Tides and Tidal Currents," American Practical Navigator, Defense Mapping Agency Hydrographic Center, Washington, DC. rev. 1977.

"The NOAA Ocean Service Center Concept," Proceedings of the 1984 Annual Marine Technology/IEEE Conference, Washington, DC, 1984.